

**Production of Biofuels and Biodegradable Plastics from Common Waste
Substrates in Engineered *Ralstonia eutropha***

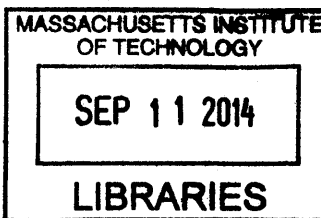
by

Jingnan Lu

B.Sc., Chemistry

State University of New York-College of Environmental Science and Forestry in
Association with Syracuse University, 2009

ARCHIVES



Submitted to the Department of Chemistry
in Partial Fulfillment of the Requirements for the Degree of

Doctor of Philosophy in Biological Chemistry

at the

MASSACHUSETTS INSTITUTE OF TECHNOLOGY

September 2014

© 2014 Massachusetts Institute of Technology
All rights reserved

Signature redacted

Signature of Author

Department of Chemistry
July 28th, 2014

Signature redacted

Certified by

Professor Anthony J. Sinskey
Professor of Biology, Health Science & Technology, and Engineering Systems
Thesis Supervisor

Signature redacted

Accepted by

Professor Robert W. Field
Haslam and Dewey Professor of Chemistry
Chairman, Department Committee on Graduate Studies

A Committee of the Department of Chemistry and Biology as follows has examined this doctoral thesis.

Signature redacted

Professor Barbara Imperiali
Class of 1922 Professor of Chemistry and Professor of Biology
Thesis Committee Chair

Signature redacted

Professor Anthony J. Sinsky
Professor of Biology, Health Science & Technology, and Engineering Systems
Thesis Supervisor

Signature redacted

Professor Alexander M. Klibanov
Novartis Professor of Chemistry and Bioengineering
Thesis Committee Member

**To my mother, for encouraging me to dream
big, fail often, and be resilient.**

Production of Biofuels and Biodegradable Plastics from Common Waste Substrates in Engineered *Ralstonia eutropha*

by

Jingnan Lu

Submitted to the Department of Chemistry on July 28th, 2014 in Partial Fulfillment of the Requirements for the Degree of Doctor of Philosophy

ABSTRACT

Ralstonia eutropha, a Gram-negative proteobacterium, is capable of utilizing a plethora of simple and complex carbon sources derived from common waste streams. When experiencing nutrient stress in the presence of high carbons, *R. eutropha* can store carbon and energy in the form of polyhydroxyalkanoates (PHAs), a biodegradable and biocompatible plastic. In this thesis, the native carbon storage system was genetically disabled and the carbons redirected to produce biofuels. Key enzymes involved in *R. eutropha* CO₂, oil, and branched-chain amino acid metabolism were evaluated for the production of biofuels and bioplastics.

R. eutropha valine biosynthesis pathway was modified, so its intermediate 2-ketoisovalerate can be converted to isobutanol, a drop-in biofuel that can directly substitute for fossil-based fuels and be employed within the current transportation infrastructure. Challenges facing large production of isobutanol include the tightly regulated biosynthetic pathway and product toxicity to the cells. Modification of both the pathway enzyme for reduced-feedback inhibition, in addition to genotypic adaptation to exogenous isobutanol stress produced insights that will allow for further improvements on isobutanol production. Furthermore, strains of *R. eutropha* were also engineered to produce isopropanol, another biofuel.

Growth on carbon dioxide requires carefully balanced intercellular pH and ion transport. Four *R. eutropha* carbonic anhydrases were identified to play individual and non-complementary roles in CO₂ metabolism. An extracellular lipase and its chaperone were identified and characterized in *R. eutropha*. This lipase is crucial for growth on plant oil and when overexpressed, not only reduced the growth lag phase, but also eliminated the use of supplemental surfactants. Production of PHAs was achieved by using palm oil, one of the world's most abundant plant oils, as well as vinasse, a byproduct of ethanol fermentation. Metabolic versatility and genetic tractability combined with its ability to store a variety of carbons make *R. eutropha* an excellent platform organism for the production of value-added compounds. Demonstrated in this thesis are the production of biofuels and bioplastics from fructose, CO₂, oils, and mixed-organic acids.

Thesis Supervisor: Anthony J. Sinskey

Title: Professor of Biology, Health Science & Technology, and Engineering Systems

ACKNOWLEDGEMENTS

I am incredibly fortunate to have many people in my life, who continuously encourage, help, and support me on all my dreams and goals. The past five years at MIT, I have faced many disappointments, challenges, and hardships; however I was never alone in these situations and could always count on these incredible people around me. I honestly could not have accomplished anything without them, so I would like to take a moment to thank each and every one of my professors, colleagues, friends, and families for being by my side and getting me here.

Foremost, I am extremely grateful to my advisor, Anthony Sinskey, who has not only helped me becoming a good strategic scientist, but also encouraged me to stay true to myself, and being an honest and kind person. Tony, I admire your passion towards science and life. You are extremely kind and caring towards everyone around you. You are patient with me and always spoke what's on your mind. You are particularly considerate of my feelings. Any constructive criticisms, you made sure to inform me in person with no others around. I love how you always ask me what I have learned that day; because what's important, is not how much time I spent in lab, but what I have learned from a day's research and classes, and how I have bettered myself in the process. You always encourage me to learn, not only things that are related to my research, but also things that could make me a well-rounded person. You are proud when I take classes in business and engineering, participate in club activities, and intern with companies. Thank you for allowing me the freedom to learn and explore. Your motto of "keep it moving" will stay with me for the rest of my life and I am sure I can overcome all challenges if I just keep on trying.

Thank you Professor ChoKyun Rha, for sharing with me your stories as a student at MIT and for embracing me in the Rha-Sinskey family. Professor Barbara Imperiali, my thesis committee chair, thank you for giving me the opportunity to participate in the Chemical Biology Interface Program, which has led me to the Sinskey lab, and for caring about me, the progress of my projects, and my future endeavor. I want to also thank my thesis committee member, Professor Alex Klibanov, for making sure I had a good biochemistry background and teaching me to become a concise scientist and presenter. Professor John Essigmann, I was so lucky to have met you and Ellen on my undergraduate research trip at Chulabhorn Research Institute in Thailand. I learned a great deal from you and had tons of fun working with you as a TA for 5.07 and a GRT at Simmons Hall. Professor Cathy Drennan, it is so kind of you for always looking out for me and supporting me. You are honest, caring, and easy to talk to. Thank you for being such an amazing role model to all the female scientists. I will always remember your advice on "be prepared, because you will never know when an opportunity presents itself". Professor JoAnne Stubbe, words cannot describe how much I have learned from you and how much you have influenced my way of scientific thinking. Your enzymology and 5.07 classes, although challenging, were my favorite here at MIT. Professor Sarah O'Connor, I am incredibly thankful for your guidance, even before I came to MIT. I am appreciative to Professor Liz Nolan, who has taught me to be organized and design well thought-out experiments.

To my college advisors, Professor Chris Nomura and David Kieber, you have always seen the potential in me and encouraged me to reach high. I am forever grateful for everything you have taught me, for helping me get into graduate school, and for continuously supporting me through my Ph.D. career. I wish to also thank the following people who have taken the time to help me with projects, career and professional developments: Professor Sean Elliott, Professor Jason Sello, Professor Andrey Zarur, Emily Reichert, and Siamak Kia.

I greatly appreciate the following funding sources: U.S. Department of Energy-Advanced Research Projects Agency-Energy, Malaysian Palm Oil Board, NIH Chemical Biology Interface Training Grant, MIT Chaplin Fellowship, MISTI-France and MISTI-Brazil funds. Thanks also to all my collaborators: Worden Lab at Michigan State University, Way and Silver labs at Harvard Wyss Institute and Harvard Medical School, Guillouet Lab at INSA-Toulouse, and Aragao Lab at University of Federal de Santa Catarina.

To all the former and current Sinskey lab members, you are like family to me. Because of you, I am happy and excited of coming into lab each and every day. Chris Brigham, I am extremely grateful to have you as a mentor. You have literally taught me everything from molecular biology to publishing. I laugh really hard whenever I recall you taking pictures of cell growth and telling the flasks to “work it”. I agree with you that the best thing to go with a glass of wine is a manuscript. You have taught me to work hard, but also have fun in the process. I am thankful to Charles Budde, who has guided me through my very first project and article here at MIT. John Quimby, you are the glue that keeps all lab members together. You are always eager to learn and ready to help. Your 24-hour turn around on manuscript edits is unbeatable. Thank you for bringing in wine and snacks every Friday, so everyone can sit around and chat about science, innovation, arts, music, and just about anything. I will truly miss all these intellectually stimulating conversations. I am very thankful to have Fen Tung as an amazing administrative assistance and the best trainer at MIT. Fen, thank you for keeping everything in line for the lab, in addition to helping me stay healthy, fit, and stress-free. I appreciate all the help and guidance from Dan MacEachran, Jens Plassmeier, and Tony DeBono. Sebastian Riedel, Jens and Jenny Plassmeier, Claudia Gai, Daan Septh, Amanda Bernardi, Aidan Smith, Jose Laser, Esther Reimer, Travis Neuenhaus, Caio Alves, Till Olfers, Anna Harikrishna, Sandra Wewetzer, Estelle Grousseau, and Lucie Crepin; thank you for all the fun times we shared after long hours in lab. I will miss our trips to the beach, dancing till 2 am at the Phoenix, cruising through Boston, building snowman on a freezing snowy day, Wednesday chicken wings at the Muddy Charles, Halloween parties, poker nights, MIT Galas, culture exchange parties, and best of it all, watching Germany finally won the World Cup. Sebastian, my best buddy in lab, thank you for being such a fun labmate and making all the late night working hours memorable. Sophia Li, thanks for inviting me to all your MITSO concerts and for benge visiting all the museums at Toulouse and Paris with me.

I would also like to thank members of the Sinskey, Rha, and Nomura labs, of whom I have published with: Christopher Brigham, Sebastian Riedel, Charles Budde, Claudia Gai,

Sohpia Li, Daan Sph, Estelle Grousseau, Amanda Bernardi, Qiang Fei, Rongzhan Fu, Alison Mahan, Ryan Tapple, Nathalie Gorret, and Jens Plassmeier.

Thanks also to members of the Rha, Imperiali, O'Connor, Dreanan, Stubbe, and King labs: Sam, Robert, Cassie, Sarah, Ken, Choi, Vinita, Elizabeth, Michelle, Joris, Carsten, Austin, Julie, Kasper, Brenda, Wesley, John, Rachael, Mimi, Michael, Marcus, Peter, Christina, Marco, Jeremy, Tsehai, Elizabeth, Allena, Nozomi, Daniel, Oksana, and Camie. My WIC mentor Stephanie Lam, thank you for being such a great listener in the past five years.

Thanks also to the entire Simmons Hall community: John and Ellen Essigmann, Steven Hall, Josh Gozalez, Nika Hollingsworth, GRTs, residential scholars, and students for caring about me when I'm sick, supporting me through my insane number of interviews, and distracting me with entertaining activities at all hours. Thanks to Women in Chemistry and ChemREFS. It was a pleasure to have worked with you and for all the fun events and supports you offered me with. I am grateful to the Consulting Club at MIT, for providing me with opportunities to work on real projects, network with companies, and meet people who share the same passion as me. Will Herbert, Ben Lai, Jeremy Curuksu, Shila Ray, Kerry Wei, Amrit Jalan, Vivian Tu, Christy Lin and Jen Nwankwo, thank you for spending hundreds of hours with me preparing for business case interviews and supporting me through all 30+ interviews.

Michael Funk and Christina Hasan, you two have been with me through all the ups and downs at MIT. I am very fortunate to have you two as my best friends. I will miss our Christmas karaoke specials, stories when the truth box gets opened, and countless conversations over CBC nachos and beers. Vinita Lukose, I am very certain I won't last a month at MIT without your support. You are so wise and mature. I know I can always count on you. Thank you for embracing my craziness, having my back, and 'fighting so many battles' with me. I am thankful to my roommates Amy Adams and Katya Vinogradova. Amy, you are like a big sister to me. You are full of positive energy and have taught me so many life lessons. The always well-dressed Katya, I will miss our girl talks, shopping trips, and dressup moments. I am thankful to have the continuous support and love from friends: Kenric Tam, Tom Baldwin, Retsina Meyer, Andrew Eastham, Scott Anderson, Qin Wang, Yuyan Yang, Brittany Gowan, Han Pham, Azusa Tojo, Matt Martino, Alex Mueller, Leah Flynn Gallant, Mark and Liz Woodford.

Most importantly, I am grateful to my family, for all the love, encouragement, support, and optimism. Thank you for everything you have done and sacrificed to help me reach my goals. You have made me the person I am today and I wouldn't be here without you. I love you.

TABLE OF CONTENTS

ABSTRACT.....	5
ACKNOWLEDGEMENTS.....	6
LIST OF FIGURES	12
LIST OF TABLES.....	14
CHAPTER 1	15
<i>Ralstonia eutropha</i> H16 as a platform for the production of biodegradable plastics, biofuels, and fine chemicals from diverse carbon resources	15
INTRODUCTION	15
ADVANTAGES IN SUBSTRATE AND METABOLITE DIVERSITY AND FLEXIBILITY	16
DIVERSE PATHWAYS FOR BIOSYNTHESIS OF VALUE-ADDED COMPOUNDS	29
SUMMARY	34
REFERENCES	35
CHAPTER 2	43
Branched-chain alcohols production in engineered <i>Ralstonia eutropha</i>	43
INTRODUCTION	43
MATERIALS AND METHODS.....	45
RESULTS	50
DISCUSSION	62
REFERENCES	65
APPENDIX.....	70
CHAPTER 3	75
Production of branched-chain alcohols by engineered <i>Ralstonia eutropha</i> in fed-batch fermentation	75
INTRODUCTION	75
MATERIALS AND METHODS.....	77
RESULTS	79
DISCUSSION	84
REFERENCES	86
CHAPTER 4	89
Characterization and modification of enzymes in the 2-ketoisovalerate biosynthesis pathway of <i>Ralstonia eutropha</i> H16.....	89
INTRODUCTION	89
MATERIALS AND METHODS.....	92
RESULTS	96
DISCUSSION	103
REFERENCES	107
APPENDIX.....	112

CHAPTER 5	119
Experimental evolution and gene knockout studies revealed an ArcA-mediated isobutanol tolerance in <i>Ralstonia eutropha</i>	119
INTRODUCTION	119
MATERIALS AND METHODS.....	120
RESULTS	124
DISCUSSION	129
REFERENCES	131
CHAPTER 6	135
Insights into bacterial fitness revealed by the characterization of carbonic anhydrases in <i>Ralstonia eutropha</i> H16	135
INTRODUCTION	135
MATERIALS AND METHODS.....	136
RESULTS	140
DISCUSSION	146
REFERENCES	149
APPENDIX.....	152
CHAPTER 7	157
Isopropanol production in engineered <i>Ralstonia eutropha</i>	157
INTRODUCTION	157
MATERIALS AND METHODS.....	159
RESULTS	163
DISCUSSION.....	169
APPENDIX.....	177
CHAPTER 8	185
Characterization of an extracellular lipase and its chaperone from <i>Ralstonia eutropha</i> H16	185
INTRODUCTION	185
MATERIALS AND METHODS.....	186
RESULTS	189
DISCUSSION.....	198
REFERENCES	201
APPENDIX.....	206
CHAPTER 9	209
Production of biopolymer from common waste materials in <i>Ralstonia eutropha</i>	209
INTRODUCTION	209
MATERIALS AND METHODS.....	211
RESULTS	213
DISCUSSION.....	221
REFERENCES	224
CHAPTER 10	229
Conclusions and future work	229
SUMMARY OF AIMS AND ACHIEVEMENTS	229

OPPORTUNITIES FOR FUTURE WORK 232
FINAL THOUGHTS 238
REFERENCES 241
CURRICULUM VITAE..... 243

LIST OF FIGURES

Figure 1.1: Proposed roles of carbonic anhydrases (CAs) in <i>R. eutropha</i> .	17
Figure 1.2: Carbon-concentrating mechanism of the carboxysome.	19
Figure 1.3: Depiction of <i>R. eutropha</i> lithoautotrophic growth.	21
Figure 1.4: Pathway mediating between C3 and C4 intermediates.	27
Figure 1.5: Engineered <i>R. eutropha</i> for the production of copolymers.	30
Figure 1.6: Synthesis and degradation of poly-3-hydroxybutyrate.	33
Figure 2.1: Schematic of isobutanol and 3-methyl-1-butanol production pathways.	44
Figure 2.2: Production of isobutanol in strain Re2061/pJL23.	52
Figure 2.3: Mutations in the upstream nucleotide sequences of <i>adh</i> .	53
Figure 2.4: Isobutyraldehyde dehydrogenase activity and production of isobutanol.	54
Figure 2.5: Activities of isobutanol production pathway enzymes.	56
Figure 2.6: Effect of nitrogen concentrations on the production of isobutanol.	58
Figure 2.7: Improvement of branched-chain alcohols yield by elimination of carbon sinks	60
Figure 2.8: Semi-continuous flask culture.	61
Figure 3.1: Time profile of cell dry weight, residual carbon, and total alcohol production.	80
Figure 3.2: Time profile of cell growth of Re2410/pBBR1MCS-2.	82
Figure 3.3: Time profile of cell growth and alcohol production by Re2410/pJL26.	83
Figure 3.4: Concentration and compositions of alcohols produced by Re2410/pJL26.	84
Figure 4.1: Schematic of the branched-chain amino acid biosynthesis pathway.	91
Figure 4.2: SDS-PAGE gel images of His-tag purified IlvB, IlvH, IlvC, and IlvD.	97
Figure 4.3: Specific activities of AHAS in the presence of inhibitors.	101
Figure 4.4: Growth rate of <i>R. eutropha</i> H16 compared to mutant strain on valine.	102
Figure 4.5: Influence of valine, leucine, and isoleucine on mutant AHAS.	103
Figure 5.1: Result of isobutanol tolerance growth and survival assays.	124
Figure 5.2: Agarose gel on <i>acrA</i> .	126
Figure 5.3: Survival assay viable cell counts.	127
Figure 5.4: Isobutanol consumption.	127
Figure 5.5: Isobutanol production by engineered strains.	128
Figure 6.1: Reaction mechanism of carbonic anhydrase.	135
Figure 6.2: Specific activity of purified, His-tagged carbonic anhydrase enzymes.	141
Figure 6.3: Growth, PHB production, and activity of CA overexpression strains.	142
Figure 6.4: Growth of wild type <i>R. eutropha</i> and CA deletion strains.	143
Figure 6.5: Growth of complemented strains.	144
Figure 6.6: Substrate specificity of CAs.	145
Figure 6.7: Schematic depiction of the role of CAs in <i>R. eutropha</i> metabolism.	148
Figure 7.1: Engineered isopropanol production pathway in <i>R. eutropha</i> .	158
Figure 7.2: Schematic of constructed isopropanol production pathways.	160
Figure 7.3: Time point in which maximum isopropanol concentration was produced.	164
Figure 7.4: Carbon distribution in Cmol.L^{-1} of the products.	165
Figure 7.5: THL activity vs copy number and ADH activity vs promoter distance.	167
Figure 7.6: Evaluation of substrate and products over cultivation time of Re2133/pEG7c.	169
Figure 8.1: TLC analysis of supernatants taken from the palm oil cultures.	190
Figure 8.2: TLC analysis on overexpression of <i>lipA</i> in palm oil cultures.	191
Figure 8.3: Growth and lipase activities of <i>R. eutropha</i> H16, Re2313, and Re2318.	193

Figure 8.4: Growth and lipase activity of <i>R. eutropha lipA</i> overexpression strain.	194
Figure 8.5: Viable colony counts of H16/pBBR1MCS-2 and H16/pCJB201.	195
Figure 8.6: Effect of temperature and pH on LipA lipase activity.	197
Figure 8.7: Metal ion alleviation of LipA lipase activity inhibition by chelators.	198
Figure 9.1: Structure of PHA with various monomer units and P3HB- <i>co</i> -3HHx.	212
Figure 9.2: Cell dry weight profile of strains on 4% palm oil.	216
Figure 9.3: PHA production profile.	217
Figure 9.4: Lipase activities of <i>R. eutropha</i> strains in 4% palm oil fermentation cultures.	218
Figure 9.5: Production of PHA by <i>R. eutropha</i> H16 with vinasse.	220
Figure 9.6: Fructose utilization profile.	221
Figure 9.7: Sucrose utilization profile.	221
Figure 9.8: Lactose utilization profile.	222
Figure 9.9: Glycerol utilization profile.	222
Figure 9.10: Acetate utilization profile.	223
Figure 9.11: Ethanol utilization profile.	223
Figure 10.1: Schemes for alteration of NADH/NADPH pool size in <i>R. eutropha</i> .	235
Figure 10.2: Concentration of NADP ⁺ , NADPH, NAD ⁺ , and NADH in pM per colony.	236
Figure 10.3: Schematic of the construction of synthetic metabolon.	237
Figure 10.4: Expression plasmid addiction system.	238
Figure 10.5: Rare codons identified in wild type <i>R. eutropha</i> .	239
Figure 10.6: Site-directed mutagenesis on native tRNA.	240
Figure 10.7: The two possible usages of rare tRNA overexpression systems.	240
Figure 10.8: Schematic demonstrating <i>R. eutropha</i> 's metabolic versatility.	241

LIST OF TABLES

Table 2.1: Strains used in this work.	46
Table 2.2: Plasmids used in this work.	46
Table 2.3: Physiologic difference between wild type <i>R. eutropha</i> and Re2061.	51
Table 2.4: Isobutanol tolerance of <i>R. eutropha</i> strains.	57
Table 3.1: Specification comparison of biofuels and fossil fuels.	75
Table 3.2: Effect of the nitrogen concentration on cell growth and alcohol production.	79
Table 3.3: Fed-batch cultures of Re2410/pBBR1MCS-2.	81
Table 4.1: Strains used in this work.	92
Table 4.2: Plasmids used in this work.	93
Table 4.3: Reconstitution of AHAS holoenzyme.	98
Table 4.4: Kinetic parameters of AHAS, AHAIR, and DHAD.	99
Table 4.5: Specificity constant of AHAS.	99
Table 4.6: Influence of valine, leucine, and isoleucine on AHAS, AHAIR, and DHAD	100
Table 5.1: Strains used in this work.	120
Table 5.2: Plasmids used in this study.	121
Table 5.3: potential gene related to isobutanol tolerance.	122
Table 5.4: Primers used in this work.	122
Table 6.1: Bacterial strains used in this study.	137
Table 6.2: Plasmids used in this study.	137
Table 7.1: Comparison of isopropanol production.	171
Table 8.1: Strains used in this study.	186
Table 8.2: Plasmids used in this study.	187
Table 8.3: Effect of carbon sources on lipase production.	195
Table 8.4: Effect of various metal ions or chelating agents on lipase activity.	198
Table 8.5: Effect of detergents on lipase activity.	199
Table 9.1: Strains used in this study.	213
Table 9.2: Carbon and nitrogen source composition and concentration in vinasse liquid.	219
Table 9.3: Growth of <i>R. eutropha</i> H16 in minimal media with vinasse.	220

CHAPTER 1

***Ralstonia eutropha* H16 as a platform for the production of biodegradable plastics, biofuels, and fine chemicals from diverse carbon resources**

(This chapter was modified from a book chapter in preparation for publication in *Biotechnologies for Biofuel Production and Optimization*, 2014 Chapter 12: '*Ralstonia eutropha* H16 as a platform for the production of biofuels, fine chemicals, and biodegradable plastics from diverse carbon resources' Jingnan Lu, Christopher Brigham, Sophia Li, and Anthony Siskey © Elsevier and a review published in *Applied Microbiology and Biotechnology*, 2014 'Lipid and fatty acid metabolism in *Ralstonia eutropha*: relevance for the biotechnological production of value-added products' Sebastian Riedel, Jingnan Lu, Ulf Stahl, and Christopher Brigham © Springer-Verlag)

INTRODUCTION

The Gram-negative betaproteobacterium *Ralstonia eutropha* is found in soil and freshwater environments. It has been previously named and renamed *Hydrogenomonas eutropha*, *Alcaligenes eutrophus*, and *Wautersia eutropha*, in part due to its ability to utilize many different compounds as sources of nutrients and energy. The current official name of the organism is *Cupriavidus necator*, which was a result of genome sequence comparison with other *C. necator* strains (Vandamme and Coenye 2004). However, many prominent researchers in the field have opted to continue using the *R. eutropha* name for the sake of continuity.

Given the ability of *R. eutropha* to grow autotrophically in the presence of hydrogen, carbon dioxide, and oxygen, it was originally examined for the application of CO₂ mitigation for astronauts in space flight (Schlegel and Lafferty 1971), as well as single-cell protein for animals (Calloway and Kumar 1969; Waslien and Calloway 1969). For the past three decades, *R. eutropha* has been studied globally as a model industrial organism for the production of polyhydroxyalkanoate (PHA) bioplastic. Mechanisms for intracellular PHA homeostasis have been largely elucidated in *R. eutropha* strains, revealing a complex physiological pathway.

R. eutropha can grow and produce PHA from a wide variety of carbon substrates, from sugars (Cramm 2009), short chain organic acids and other compounds (Yan et al. 2003), fatty acids and lipids (Budde et al. 2011; Lu et al. 2013), CO₂ (Brigham et al. 2013; Jeffke et al. 1999). Because it is capable of metabolizing such diverse carbon sources, it is an excellent platform organism for the production of value-added compounds. First and foremost, PHA has been synthesized by wild type and engineered *R. eutropha* strains on a variety of carbon compounds in the laboratory and at pilot manufacturing scale. Due to the genetic tractability of the organism, the availability of genetic tools and the advent of metabolic engineering, the range of compounds *R. eutropha* can produce is being expanded to include molecules like fatty acids, alcohols, and esters. This chapter discusses the biomanufacturing capabilities of *R. eutropha*, including the current state of the research in value-added product biosynthesis.

ADVANTAGES IN SUBSTRATE AND METABOLITE DIVERSITY AND FLEXIBILITY

Lithoautotrophic metabolism

R. eutropha assimilates CO₂ as a carbon source through the Calvin-Benson-Bassham (CBB) cycle. As a facultative chemoautotroph, *R. eutropha* is able to induce the CBB cycle when needed, even under heterotrophic conditions (Bowien and Kusian 2002; Friedrich et al. 1981). Carbon fixation enzymes in the CBB cycle are encoded in two *ccb* operons located on chromosome 2 and on the megaplasmid pHG1 (Bowien and Kusian 2002). A LysR-type transcriptional regulator CbbR on chromosome 2 activates both operons, while the metabolite phosphoenolpyruvate (PEP) acts as a negative effector of the operon (Bowien and Kusian 2002). While the mechanism of the *ccb* operon in *R. eutropha* has been well-studied, the regulator of the *ccb* operon and the reduced metabolite that acts as a positive effector remain to be identified.

Two important carbon fixation enzymes, carbonic anhydrase (CA) and ribulose-1,5-bisphosphate carboxylase/oxygenase (RuBisCO) are found in *R. eutropha*. Carbonic anhydrase interconverts carbon dioxide and bicarbonate, and also has a role in controlling intracellular pH. These carbonic anhydrases operate through a zinc-dependent mechanism and are classified into five different classes (α , β , γ , δ , and ζ), which have evolved convergently (Smith and Ferry 2000). *R. eutropha* has four CA enzymes that are necessary for proper function. Can and Can2 encode β -CAs, Caa encodes a periplasmic α -CA, and Cag encodes a γ -CA (Pohlmann et al. 2006). Each CA has a different role in *R. eutropha* (Figure 1.1). Can is required for growth under atmospheric CO₂ levels, and supplies CO₂ to RuBisCO (Gai et al. 2014; Kusian et al. 2002). Caa differs from the other CA enzymes by its location, in the periplasm, and its preference for CO₂ as a substrate (Gai et al. 2014). These differences are necessary for Caa's role in converting CO₂ that has diffused through the membrane to the more soluble bicarbonate, effectively trapping the carbon inside the cell. The roles of Cag and Can2 are less clear, but Cag may also provide CO₂ to RuBisCO, while Can2 has a possible role in pH homeostasis (Gai et al. 2014) (Figure 1.1). More research is required to elucidate the exact roles of these four CAs in the metabolism of CO₂.

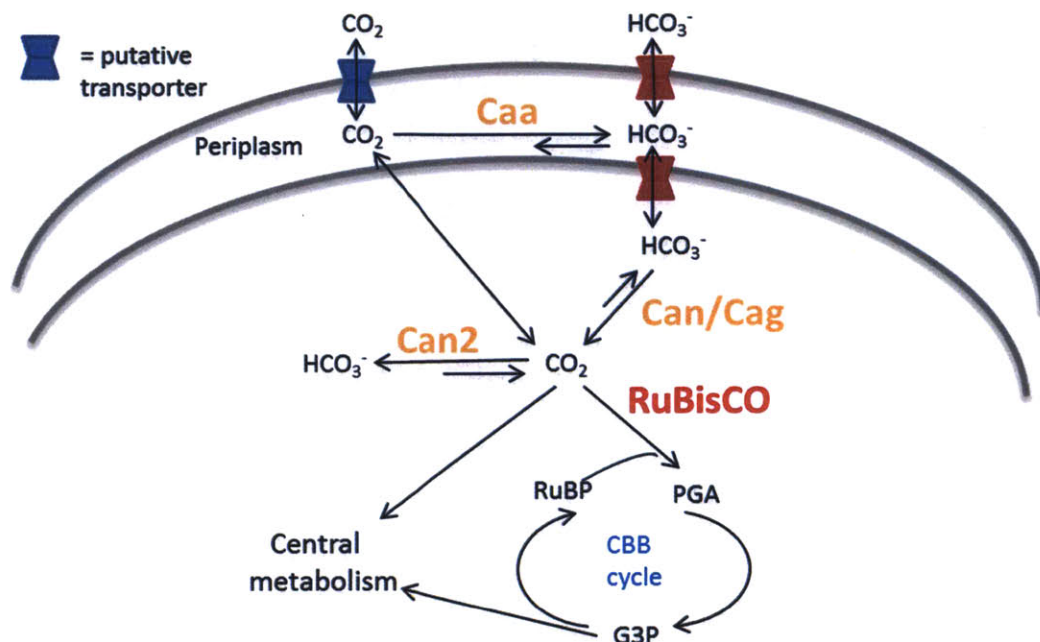


Figure 1.1: Proposed roles of carbonic anhydrases (CAs) in *R. eutropha*. Periplasmic Caa preferentially converts CO_2 into bicarbonate. Cytosolic Can supplies CO_2 to RuBisCO in the Calvin-Benson-Bassham (CBB) cycle. The roles of Cag and Can2 are less clear; however Cag could play a similar role to Can, while Can2 could be involved with intracellular pH homeostasis. Abbreviations: Ribulose-1,5-bisphosphate carboxylase oxygenase (RuBisCO), ribulose-1,5-bisphosphate (RuBP), 3-phosphoglycerate (PGA), glyceraldehyde 3-phosphate (G3P).

RuBisCO, the second key enzyme, is responsible for the carbon fixation step where ribulose-1,5-bisphosphate is carboxylated with CO_2 to form two molecules of 3-phosphoglycerate. *R. eutropha*, similar to many other facultative autotrophs, has Form 1C of RuBisCO, which is more suited to O_2 -containing environments with medium to high levels of CO_2 (Badger and Bek 2008). RuBisCO, however, is an inefficient enzyme with a slow catalytic turnover rate, a low affinity for carbon dioxide, and O_2 acts as a competing substrate (Badger and Bek 2008). The oxygenation reaction results in the formation of toxic phosphoglycolate, further inhibiting carbon fixation (Yeates et al. 2008). The efficiency of RuBisCO is a challenge to be addressed when maximizing the efficiency of carbon fixation.

Improvements on carbon fixation

Improving carbon fixation in *R. eutropha* is an active area of research. A metabolic model of *R. eutropha* H16 has been used to study the effect of different feeding ratios of H_2 , O_2 , and CO_2 on lithoautotrophic growth (Park et al. 2011). Electricity has also been used to reduce CO_2 to formate, providing the reducing equivalents needed for carbon fixation, growth, and biofuel production in *R. eutropha* (Brigham et al. 2013; Li et al. 2012). However, few studies have attempted to improve the efficiency of carbon metabolism and the CBB cycle in *R. eutropha*.

There has been an increasing interest in the engineering of CBB cycle genes, alternative carbon fixation pathways, and carbon-concentrating mechanisms in bacteria in order to promote

carbon fixation (Ducat and Silver 2012). The *cbb* operon from *R. eutropha* H16 has been expressed in *E. coli*, leading to an increase in 2-phosphoglycolate phosphatase and transketolase activities in the normally heterotrophic bacteria (Schäferjohann et al. 1993). However growth of *E. coli* on CO₂ has not been successful to date. Attempts have been made to engineer RuBisCO with limited success, since improvements in velocity often decrease the selectivity of the enzyme (Tcherkez et al. 2006). The 3-hydroxypropionate (3-HOP) CO₂ fixation cycle in the phototrophic bacterium *Chloroflexus aurantiacus* may be an advantageous alternative pathway, since its RuBisCO enzyme incorporate bicarbonate, instead of CO₂, as a substrate, and have no known oxygenation side reactions (Zarzycki et al. 2009). Finally, the expression of the carbon-concentrating mechanism of carboxysomes in nonnative hosts may maximize RuBisCO's efficiency and improve carbon fixation (Yeates et al. 2008). Functional carboxysomes have been expressed and assembled heterologously in *E. coli* (Bonacci et al. 2012), demonstrating the applicability of these bacterial microcompartments in nonnative hosts. However, carboxysomes have not yet been demonstrated in *R. eutropha*.

A carboxysome is a bacterial microcompartment, similar to a synthetic organelle, where an icosahedral protein shell encases the enzymes carbonic anhydrase and RuBisCO (Figure 1.2) (Frank et al. 2013). Carboxysomes are natively found in cyanobacteria and some chemoautotrophic bacteria (Price and Badger 1991). These bacteria often grow in environments with CO₂ concentrations lower than that of the K_M of RuBisCO, but they are still able to fix CO₂ efficiently by concentrating it (Cannon et al. 2001). It has been hypothesized that the carboxysome increases the efficiency of carbon fixation through two main mechanisms: saturating RuBisCO with CO₂ and blocking RuBisCO from taking O₂ as a substrate for the production of wasteful byproducts (Yeates et al. 2008). In native organisms, bicarbonate is able to diffuse through pores in the protein shell into the carboxysome, where carbonic anhydrase converts it to CO₂ (Figure 1.2). The proximity of carbonic anhydrase and RuBisCO and the trapping of CO₂ inside the carboxysome increase the specificity and efficiency of RuBisCO. The protein shell also shields RuBisCO from O₂, minimizing the substrate competition between O₂ and CO₂ for RuBisCO and decreasing the amount of the toxic side product phosphoglycolate in the cytoplasm (Yeates et al. 2008). Through these two mechanisms (Cannon et al. 2001; Rae et al. 2013), the carboxysome allows the bacteria to more efficiently fix CO₂ to form 3-phosphoglycerate, a precursor for cell growth and the production of valuable products.

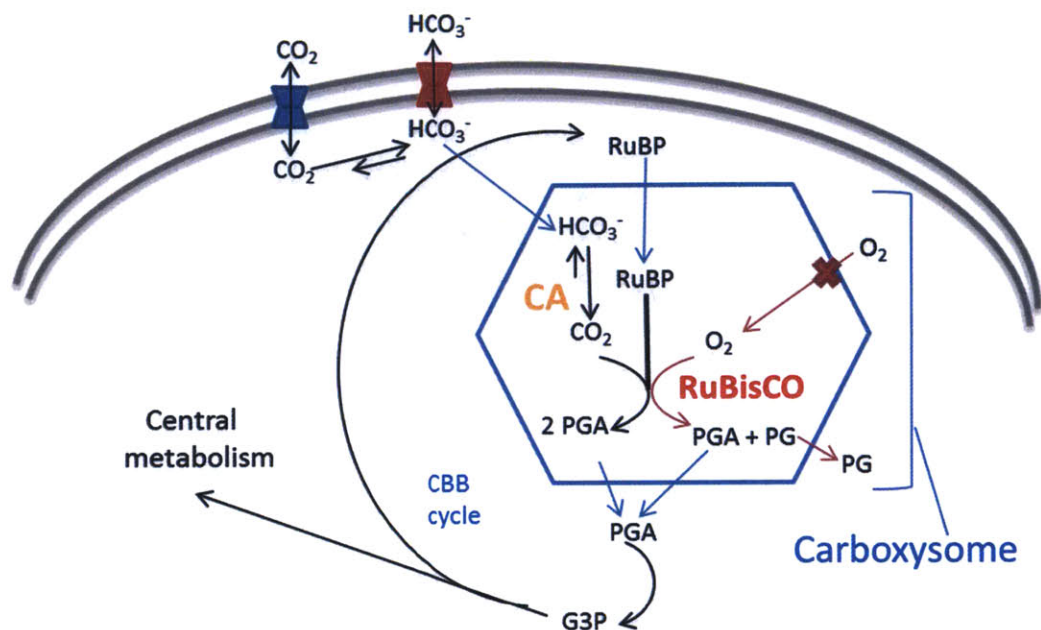


Figure 1.2: Carbon-concentrating mechanism of the carboxysome. Carbonic anhydrase (CA) and ribulose-1,5-bisphosphate carboxylase oxygenase (RuBisCO) are inside the protein shell of the carboxysome. Bicarbonate enters the carboxysome through pores and is converted to CO_2 . RuBisCO then catalyzes the carbon fixation reaction where ribulose-1,5-bisphosphate (RuBP) and CO_2 are converted to two molecules of 3-phosphoglycerate (PGA). The carboxysome shell restricts oxygen from entering and interacting with RuBisCO to form the toxic side product, phosphoglycolate (PG). Abbreviation: Calvin-Benson-Bassham cycle (CBB cycle).

Improving *R. eutropha*'s ability to utilize CO_2 as a substrate has become an attractive way to address problems associated with rising CO_2 emissions, but many challenges lie ahead. While the general roles of *R. eutropha*'s various carbonic anhydrases (Gai et al. 2014), and the genetics and regulation of the CBB cycle have been studied (Bowien and Kusian 2002), the exact mechanisms and regulation of carbon fixation in *R. eutropha* need to be elucidated. Expressing a more efficient natural variant of RuBisCO, implementing a carbon-concentrating mechanism through carboxysomes, engineering alternative carbon fixation pathways, and finding novel ways to supply the reducing power required for the CBB cycle are all future directions to explore in improving carbon fixation in this lithoautotrophic organism.

Oxygen-tolerant hydrogenases

R. eutropha is capable of growing on an explosive gas mixture of 70% H_2 , 10% CO_2 , and 20% O_2 (Bowien and Kusian 2002; Schäferjohann et al. 1993). Cellular metabolism relies entirely on CO_2 fixation, which is an extremely energy intensive process. In order to keep up with the energy supply via oxidation of H_2 , *R. eutropha* possesses three hydrogenases (Bowien and Kusian 2002; Cramm 2009). The membrane-bound hydrogenase (MBH), soluble hydrogenase (SH), and regulatory hydrogenase (RH) all belong to the [NiFe] hydrogenase family. [NiFe] hydrogenase catalyzes the reversible conversion of molecular hydrogen to protons and electrons (Burgdorf et al. 2005a; Lenz et al. 2010). Besides the [NiFe] cofactor, this type of

hydrogenase also contains [FeS] clusters $\sim 14\text{\AA}$ apart from [NiFe] active site, which facilitate electron transfers. Both MBH and SH produce energy from the reducing equivalents harvested via H_2 oxidation to support cell growth under autotrophic condition. In most organisms, oxygen and carbon monoxide can bind at the [NiFe] active site, and inhibit or inactivate the hydrogenase. All three *R. eutropha* hydrogenases functions differently, but are tolerant to oxygen and carbon monoxide, which makes *R. eutropha* the model organism for the study of mechanism of tolerance (Buhrke et al. 2005; Burgdorf et al. 2005a).

The MBH is a heterotrimer consisting of HoxG, HoxK, and HoxZ subunits for H_2 catalysis, electron transfer, and cytoplasmic membrane localization respectively. Besides the [NiFe] active site, it also contains two [4Fe-4S] clusters and one [3Fe-4S] cluster, in addition to two *b*-type hemes. The heterotrimer of MBH is fused with a cytochrome *b*, which transfers electrons from H_2 oxidation into the electron transport chain for the production of ATP (Figure 1.3). It allows *R. eutropha* to grow aerobically using H_2 as an energy source and O_2 as the terminal electron acceptor. MBH is considered a slow oxidase and possesses a strong bias towards H_2 oxidation (Burgdorf et al. 2005a; Lenz et al. 2010). The active site and proximal cluster surrounding the active site of MBH are significantly different from other [NiFe] hydrogenases. As revealed by biochemical and spectroscopic studies, six Cysteine residues coordinate the [4Fe-4S] cluster instead of only four found in other [NiFe] hydrogenases. Mutation of the two extra Cysteine residues to Glycines abolished the MBH's ability to tolerate O_2 and caused lithoautotrophic growth retardation. Such finding suggests that the two additional Cysteine residues located around the [4Fe-4S] cluster of MBH allow for two sequential one-electron transfers during hydrogenase reactivation in O_2 -containing atmosphere (Saggu et al. 2009). An O_2 -sensitive hydrogenase from *Desulfovibrio gigas* cannot be engineered to tolerate O_2 by mutating the two Glycine residues to Cysteine, indicating that other factors in concert contribute to O_2 tolerance in *R. eutropha* MBH (Fritsch et al. 2011; Lenz et al. 2010; Saggu et al. 2009).

SH is a bidirectional cytoplasmic hydrogenase and acts as a redox valve to prevent overreduction of the electron transport chain. SH consists of a heterodimer with subunits HoxH and HoxY. HoxH contains the [NiFe] catalysis site, while HoxY contains one [4Fe-4S] site and one FMN cofactor for electron transfer. The HoxHY heterodimer is bound to a diaphorase dimer HoxF and HoxU, which contains two [4Fe-4S] clusters, one on each subunit, two [2Fe-2S] on HoxU, and a FMN and NAD^+ binding site on HoxF. A homodimer of HoxI subunit is bound to HoxY and contains the NADP^+ binding pocket. Such complex structure allows first for the oxidation of H_2 , then harvest of electron potential into the reduction of NAD^+ to NADH, and lastly the subsequential reduction of NADP^+ to NADPH (Burgdorf et al. 2005b; Linden et al. 2004). The ATP generated via the MBH, in addition to the NADPH reducing equivalents generated through SH, together support the high energy-demanding carbon fixation that occurs with the CBB cycle (Figure 1.3). The presence of a hydrophobic gas channel into the active site of SH allows it to favor H_2 entrance over O_2 , thus reducing inhibition due to O_2 exposure. Furthermore, the [NiFe] active site of SH contains two extra CN ligands coordinated to Ni; removal of such CN groups resulted in a hydrogenase that is sensitive to O_2 (Burgdorf et al. 2005b; Lenz et al. 2010; Linden et al. 2004).

RH of *R. eutropha* is based on a bacterial two-component regulatory system. The RH complex exists in a dimeric state. Each holoenzyme contains a H_2 -sensing HoxBC unit, which contains the [NiFe] active site in addition to a [4Fe-4S] cluster (Figure 1.3). The H_2 -signaling cascade, HoxA, is similar to a NtrC response regulator. HoxA is inactive in the phosphorylated

form and phosphorylation is mediated by HoxJ, a Histidine–protein kinase. Non-phosphorylated HoxA is capable of initiating transcription of both MBH and SH genes. It was hypothesized that in an environment with H₂, HoxBC oxidizes H₂ and passes along the electrons as a signal to the HoxJ transmitter, which can dephosphorylate the Aspartate 55 of HoxA. The dephosphorylated-HoxA then activates transcription of MBH and SH genes and maturation proteins (Burgdorf et al. 2005b; Kleihues et al. 2000; Lenz et al. 2010). In wild type *R. eutropha* H16, the expression of MBH and SH solely depends on the global energy status of the cell. An increase in expression is independent of H₂ availability, but solely occurs under energy-limiting conditions.

Studies revealed that the H₂ sensor protein in H16 was silenced as a result of a single residue mutation in HoxJ. When such mutation is repaired, SH is capable of responding to both a global energy signal and H₂ accessibility (Kleihues et al. 2000). Such silencing and inactivation of the regulatory cascade of SH could be explained by evolutionary adaptation under low and unsteady availability of H₂ in the environment. The transcription, translation, and maturation of MBH and SH take time; therefore in order to not miss the opportunity to access H₂ and survive under limited and unreliable amounts of H₂, *R. eutropha* adapted to dismiss the H₂-sensing signal transduction chain and instead expresses both hydrogenases under low energy state.

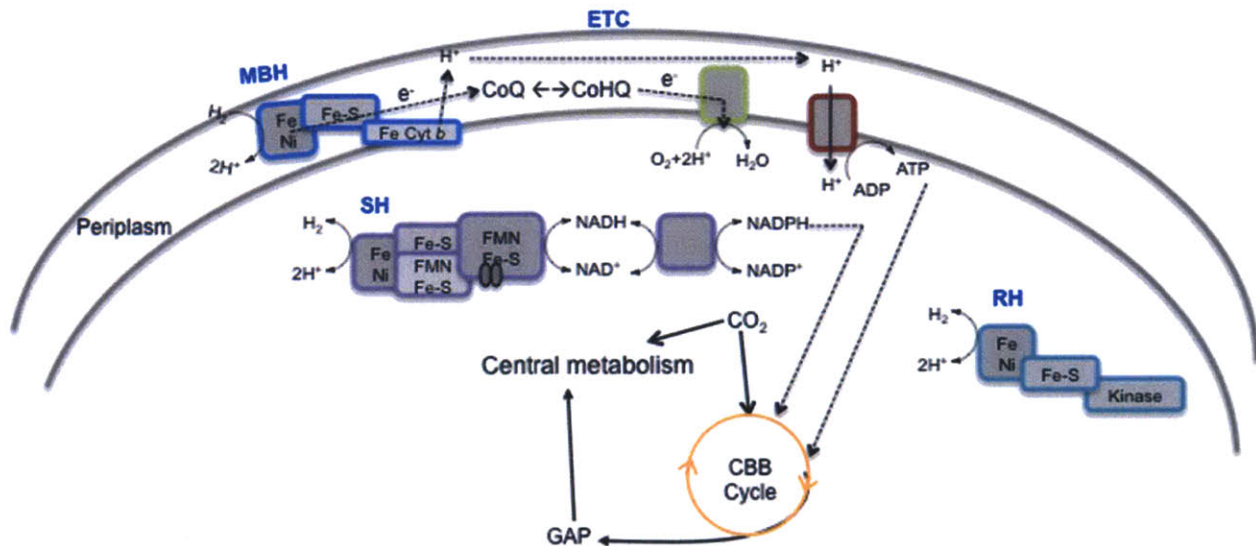


Figure 1.3: Depiction of *R. eutropha* lithoautotrophic growth. The membrane-bound hydrogenase (MBH) complex transfers electrons from hydrogen (H₂) oxidation to coenzyme Q and subsequently passes to cytochrome *a* oxidase of the electron transport chain (ETC), which results in the reduction of molecular O₂ to H₂O. Protons are translocated to the periplasm as electrons pass through the ETC and return into the cell by the ATPase to produce ATP. The soluble hydrogenase (SH) catalyzes H₂ oxidation and transfers electron potential to the production of NADH. The presence of a transhydrogenase can subsequently reduce NADP⁺ to NADPH via NADH oxidation. The ATP and NADPH generated through hydrogen oxidation by MBH and SH are utilized in the Calvin-Benson-Bassham cycle for carbon fixation. Regulatory hydrogenase (RH) could activate transcription of hydrogenase genes through phosphorylation, but is inactivated in wild type *R. eutropha* H16.

O₂-tolerance is critical for the survival of cells under aerobic lithoautotrophic growth mode. Recently, additional structural model analysis and mutant comparisons support a multipartite approach to combat O₂ in both MBH and SH of *R. eutropha*. The diverse factors are summarized here: 1) specific chaperone proteins are produced to shield the active site [NiFe]

from O₂-inactivation during hydrogenase maturation process; 2) the presence of hydrophobic cavities into the [NiFe] active sites limit O₂ passage and allows only H₂ to enter the active site; 3) rapid and spontaneous reactivation of the active site to its EPR Ni-B ready state when exposed to O₂; 4) [NiFe] active site nearby [4Fe-4S] cluster is distorted with a distal Fe, which can assist [NiFe] site reactivation; 5) two additional Cysteine residues located around the [4Fe-4S] cluster of O₂-tolerant hydrogenases that are Glycines in O₂-sensitive hydrogenases allow two sequential one-electron transfers during reactivation, thus eliminates the formation of reactive oxygen species and reduces O₂ rapidly to H₂O (Buhrke et al. 2005; Fritsch et al. 2011a, Fritsch et al. 2011b; Lenz et al. 2010; Linden et al. 2004; Saggiu et al. 2009). *R. eutropha* hydrogenases' ability to overcome O₂ toxicity is very complex, unique, and still not well understood.

Hydrogenase-based technologies

R. eutropha oxygen-tolerant hydrogenases not only play crucial roles in microbial energy metabolism, but also hold significant potential in H₂-based biotechnological applications. Recent developments with *R. eutropha* hydrogenases include the platinum-free hydrogenase electrodes for fuel cells and light-driven H₂ production. Platinum-based fuel cell presents three major drawbacks, which includes the high cost and low availability of platinum electrocatalysts, significant and irreversible inhibition by CO and H₂S impurities, and unspecific selectivity towards both H₂ oxidation and O₂ reduction. Electrocatalysis by hydrogenase is an alternative to platinum-based fuel cell. Hydrogenase enzyme can be immobilized on an electrode and serve as an electrocatalyst for hydrogen oxidation. Since the *R. eutropha* hydrogenase is renewable, able to tolerate CO, and is highly selective towards H₂ oxidation, energy conversion was able to reach 100% theoretical yield in neutral media (Kim and Kim 2011; Winkler et al. 2011). The second promising-technology is the photosynthetic conversion of sunlight and water directly into H₂ and O₂, which bypasses the current natural gas-based H₂ generation. Such solar H₂ production has been achieved by coupling photosystem I (PS I) with a hydrogenase. In one study, *R. eutropha* hydrogenase subunit HoxK was directly coupled to PS I as a protein fusion. Unfortunately H₂ production from solar energy by this protein fusion system is incredibly low and inefficient. Studies to improve efficiency included the addition of a gold electroplate *in vitro* to the fusion system and chemically linking electron transfer [Fe-S] clusters. *R. eutropha* hydrogenases are highly valued because both MBH and SH are capable of H₂ production in the presence of O₂. Additionally, such a system is renewable and carbon-neutral (Ihara et al. 2006; Winkler et al. 2011). Efficiency and sustainability are challenges faced by both hydrogenase-based technologies. In the case of hydrogenase fuel cells, it is difficult to achieve hydrogen equilibrium, especially in a fuel cell setting. On the other hand, the solar H₂ production system is limited because proton reduction at low potential is not favored and H₂ is a potent inhibitor of MBH-mediated H₂ production.

Lithoorganotrophic metabolism

Formate (HCO₂⁻) acts both as a carbon and energy source to support cell growth under organoautotrophic conditions. Once inside the cell, formate is irreversibly broken down to CO₂ and enters the central metabolism via the CBB cycle. The electrons from this oxidation are transferred to quinol and into the electron transport chain or utilized for the reduction of NAD⁺ (Bowien and Kusian 2002; Schwartz et al. 2009). *R. eutropha* processes two types of formate

dehydrogenases, the soluble formate dehydrogenase (S-FDH) and the membrane-bound formate dehydrogenase (M-FDH). S-FDH is Molybdenum (Mo)-dependent with subunits FdsGBACD encoded on chromosome 1. Transcription of S-FDH genes is controlled by formate concentration, although studies have shown oxalate can also induce S-FDH gene transcription. FdsA is the catalytic subunit, which contains Mo and four [4Fe-4S] electron transfer sites. Surprisingly, unlike other S-FDH, tungsten (W) cannot replace the Mo cofactor. Electrons released from formate oxidation are transferred to FdsB via the iron-sulfur clusters and FMN. NAD⁺ on FdsB then gets reduced to NADH. Other subunits FdsG, FdsC, and FdsD all facilitate the transfer of electrons. *R. eutropha* was hypothesized to contain one Mo-dependent M-FDH and two W-dependent M-FDHs. The expression of M-FDH is constitutive and well understood, since FDH activity was detected at various growth conditions. The M-FDH also contains a catalytic subunit and various iron-sulfur clusters, in addition to a transmembrane cytochrome *b* subunit that transfers the electrons to quinone and lastly the reduction of NAD⁺ to NADH (Cramm 2009; Lee et al. 2006; Oh and Bowien 1999).

Study of autotrophic growth on CO₂ can be challenging, since it requires an exact control of CO₂, O₂, and H₂ gas compositions. The mixture of H₂ and O₂ is considered unsafe, even though preventative strategies for mixed-gas explosion do exist. Utilization of formate to study autotrophic growth and production in *R. eutropha* has been routinely utilized as a safe alternative (Brigham et al. 2013). The downside of formate utilization is that formate can be toxic to the cells at concentrations as low as 0.2 g/L. A recent study combined stoichiometric-modeling data with well-controlled fermentation cultivation to achieve up to 85% theoretical yield of biomass in a formate-limited continuous fermentation culture. The maximum growth capacities can also be reached in a chemostat or a pH-controlled fed-batch culture at null residual formic acid concentration to avoid toxic effect.

Since the soluble formate dehydrogenase is capable of catalyzing the reversible conversion of formate to CO₂, various research has focused on production of formate from CO₂. One group was able to use electrochemical conversion for the production of formate, and subsequently bioconvert it into branched-chain alcohol biofuel in engineered *R. eutropha* (Li et al. 2012). Another idea includes coupling formate dehydrogenase with photosystem I, so the energy harvested from sunlight could be utilized for the conversion of CO₂ to formate. The main challenge facing all these engineered systems is energy balance. In other words, the energy output should outweigh the energy input.

Respiratory metabolism

R. eutropha transitions between heterotrophic and lithotrophic growth conditions due to environmental variations, therefore its energetic metabolism is capable of rapid adaptation to carbon source fluctuations. The respiratory chain is highly flexible in terms of sources and destinations of electrons. NADH dehydrogenases (NDH-1 and NDH-2) transfer electrons from NADH to the membrane-soluble transporters, ubiquinone or menaquinone, and then subsequently pass on the electrons, one at a time, to Cytochrome *c* oxydoreductase (complex bc₁). Electron paramagnetic resonance spectroscopy analysis identified three [FeS] clusters in NDH-1, and that NDH-2 contains a FAD, both of which assist in the transfer of electrons. Electrons can also enter the electron transport chain via oxidation of succinate by succinate dehydrogenase (Cramm 2009; Schwartz et al. 2009).

Proteomic analysis, redox titration, in addition to inhibition studies by HQNO, antimycin A, rotenone, and myxothiazol revealed at least three different oxidases in both lithotrophic and heterotrophic growth conditions. Two oxidases belong to the heme-copper oxidase family, which contains a binuclear heme a_3 -copper center and an additional heme a_3 subunit II with Cu_A . The third oxidase is a quinol oxidase, which does not contain heme or Cu_A , nor does it pump protons (Cramm 2009). The abundance of high-affinity oxidases increases during lithoautotrophic growth conditions, which can be explained by the low availability of O_2 inside the cell during H_2 oxidation. Oxidative phosphorylation coupled with various substrates resulted in H^+/O (number of protons pumped across the membrane per each oxygen molecule reduced) ratio of 6 and 8 under lithoautotrophic and heterotrophic growth settings respectively. The Chemiosmotic Theory suggests that approximately three protons are required to generate the chemical energy to make a single ATP. Therefore, the *R. eutropha* phosphorylation coefficient (P/O), also known as the number of ATP per oxygen can be determined from the H^+/O ratio. For NADH under lithoautotrophic growth condition 2 ATPs are generated, while close to 3 ATPs per NADH are made during heterotrophic growth (Grousseau et al. 2013).

R. eutropha is capable of anaerobic metabolism by reducing nitrogen compounds instead of oxygen. Four reductase enzymes carry out this denitrification process. Nitrate (NO_3^-) is sequentially reduced to nitrite (NO_2^-), nitric oxide (NO), and nitrous oxide (N_2O) respectively by nitrate reductase (NAR), nitrite reductase (NIR), nitric oxide reductase (NOR), and nitrous oxide reductase (NOS) (Bernhard et al. 2000; Kohlmann et al. 2011; Ye and Thomas 2001). All four enzymes are encoded on the megaplasmid (pHG1), which is required for anaerobic growth on nitrate, even though a second copy of genes encoding for all key denitrification enzymes were also found on chromosome 2. Stoichiometric-modeling indicates that 1.42 ATP is produced per NADH and 0.75 ATP per $FADH_2$ when nitrate is used as the terminal electron acceptor (Grousseau et al. 2013).

The genome sequence of *R. eutropha* strain H16 revealed various genes encoding an ArsR-type transcription regulator, sulfur dehydrogenase, sulfur-chelating/binding complex, thiosulfate-oxidizing complex, and sulfate thioesterase (Pohlmann et al. 2006; Schwartz et al. 2003). These enzymes make up a sulfur reduction pathway and suggest *R. eutropha* could use sulfur as an alternative terminal electron acceptor during anaerobic growth. Although the isolated sulfur dehydrogenase is active, growth on sulfur has not been established to date. Additional research is needed to elucidate the expression of sulfur reduction genes, cofactor requirements, and growth conditions.

The presence of alternative electron accepting pathways improves *R. eutropha*'s likelihood to survive under harsh environmental growth conditions. It also presents an alternative strategy to eliminate O_2 -induced metabolic inhibition in industrial production settings. Lastly, growth on CO_2 , H_2 , and an alternative electron acceptor could be utilized to allow for safe and easy fermentations, since the use of nitrate or sulfur eliminates the possibility of explosion caused by the interaction of H_2 and O_2 , in addition to difficulties associated with gas diffusion.

Growth of *R. eutropha* on C2-C3 waste carbon substrates

Lactate is often produced in anaerobic treatment of waste carbon, and is a suitable carbon source for fermentations to synthesize value-added products. PHA production in fed batch culture using lactate and acetate as carbon sources has been studied using a novel carbon

substrate feeding technique. Since lactate and acetate are both acids and could potentially play a role in culture pH regulation, feedstock supply was linked to pH-stat control (Tsuge et al. 2001). Fed batch co-culture of *R. eutropha* and *Lactobacillus plantarum* has been attempted, and lactate concentration (produced by *L. plantarum*) in the culture plays a key role in PHA productivity (Patnaik 2008). Furthermore, lactate-containing PHA copolymers have been produced in engineered *R. eutropha* with 3-hydroxybutyrate (3HB) as the co-monomer (Park et al. 2013). Like lactate, the C2 α -hydroxy acid glyoxylate can be used as a carbon source. Recently, glycolate and other 2-hydroxyalkanoic acids have been incorporated into PHA in *E. coli* (Matsumoto and Taguchi 2013). Similar polymers have yet to be produced in *R. eutropha*, but a broad-specificity propionate CoA-transferase has been characterized in *R. eutropha* that could be used to produce the precursor molecule, glycolyl-CoA, although relative activity is low with this substrate compared to propionate (Volodina et al. 2014). Glyoxylate has not been demonstrated as an extracellular carbon source, but *R. eutropha* expresses glyoxylate bypass enzymes malate synthase and isocitrate lyase. A functional glyoxylate bypass has been shown to be of importance in *R. eutropha*, especially during growth on acetate and compounds that are metabolized to an acetyl-CoA intermediate, such as fatty acids (Brigham et al. 2010a; Wang et al. 2003). Disruption of the glyoxylate bypass has been shown to severely inhibit growth on acetate as the main carbon source (Brigham et al. 2010b).

Wild type *R. eutropha* is not capable of producing ethanol or utilizing it as a carbon source. Engineered strains have been constructed that are capable of synthesizing short chain alcohols on a variety of substrates, including CO₂ and H₂. *R. eutropha* harbors multiple alcohol dehydrogenase genes in its genome. The constitutive activity of one particular alcohol dehydrogenase gene, *adh*, in *R. eutropha* resulted in its ability to grow on alcohols like ethanol or 2,3-butanediol (Jendrossek et al. 1988; Jendrossek et al. 1990). PHA could be produced by these strains from ethanol in co-culture with the brewer's yeast *Saccharomyces cerevisiae*.

Pure glycerol is an important industrial feedstock in the food, drug, and cosmetic industries; however crude glycerol, the main byproduct of biodiesel production from the transesterification of plant or animal fats and oils, has very low value due to the presence of methanol, salt, and fatty acid impurities (Bormann and Roth 1999). Crude glycerol treatment involves filtration, addition of chemicals, and fractional vacuum distillation, which can be very costly and time-consuming. There is a high incentive to redirect these waste crude glycerols into other industries (Solaiman et al. 2006). Cellular utilization of glycerol can be achieved by the conversion of glycerol into glyceraldehyde 3-phosphate via glycerol kinase, glycerol-3-phosphate dehydrogenase, and triosephosphate isomerase. Glyceraldehyde 3-phosphate then enters the central metabolism via the Entner-Doudoroff pathway and can be converted to acetyl-CoA for energy and growth. Since *R. eutropha* is able to tolerate growth conditions with high salts, in addition to utilizing glycerol, methanol, and fatty acids for growth, 1.5 g/L/h PHA productivity has been achieved using unprocessed crude glycerol directly from biodiesel production (Bormann and Roth 1999; Cavalheiro et al. 2009; Solaiman et al. 2006). Such a process can be directly coupled with biodiesel production and achieve environmentally friendly coproduction of two high value products.

Growth of *R. eutropha* on organic acids

In many industries, carbon-rich waste streams are produced, which require treatment to mitigate Chemical Oxygen Demand and Biological Oxygen Demand. Agricultural and

municipal waste streams are often treated by anaerobic digestion, resulting in high concentrations of mixed organic acids, containing compounds like acetate, propionate, lactate, and butyrate (Hassan and Nelson 2012). These carbon substrates, if suitably purified, can serve as feedstocks for *R. eutropha* growth and production.

Innovative processes have been investigated to utilize organic acids in *R. eutropha* growth media. Since these organic acids are toxic and inhibitory to the bacterium, the mixed acids concentration is kept at a low level (Du et al. 2001; Yan et al. 2003; Yang et al. 2010). Organic acids can penetrate freely through the cell membrane, so therefore dissociate and acidify the cytoplasm. In order to maintain intracellular pH and proton gradient, cells must rapidly pump out protons, which results in an increase in the release of free energy via ATPase (Jian Yu 2009). Such a process decouples the energy production and electron transport system, and therefore affects the overall wellness of *R. eutropha*, including organic acid utilization, growth, and PHA production. Various mixture analysis models were implemented to study the effect of mixed organic acids ratio on cell growth, PHA production, and PHA monomer composition (Jian Yu 2009; Yang et al. 2010). These studies have demonstrated *R. eutropha* utilizing short chain organic acids for PHA production. Upon feeding different mixtures of acetic, propionic and butyric acids, carbon flux was studied in *R. eutropha* during growth and PHA biosynthesis. With acetate, a C2 carbon source, present in the growth media, *R. eutropha* can produce polyhydroxybutyrate (PHB). When propionic acid (C3) is present in the growth medium, the biopolymer poly(hydroxybutyrate-co-hydroxyvalerate) [P(HB-co-HV)] is produced. Flux analysis demonstrates that, even in the presence of propionate, the majority of the carbon that is routed to PHA in *R. eutropha* is going to the hydroxybutyrate (HB) monomer (Yu and Si 2004).

Organic acids from treated oil palm milling waste have been used to produce P(HB-co-HV) (Ali Hassan et al. 1996; Hassan et al. 2002). Organic acid solutions made to simulate treated waste streams have also been used for demonstrating optimal acid mixtures for PHB and P(HB-co-HV) production (Yang et al. 2010). Valerate (C5) has also been supplemented to *R. eutropha* growth media to achieve increased HV monomer content in P(HB-co-HV) copolymer. Recently, the incorporation of 3-hydroxypropionate into *R. eutropha* PHA has been investigated. For production of a poly(hydroxybutyrate-co-hydroxypropionate) [P(HB-co-HP)] copolymer from fructose and other unrelated carbon source, portions of the 3-hydroxypropionate cycle from *Chloroflexus auranticus* were inserted into *R. eutropha* (Fukui et al. 2009). At the current time, P(HB-co-HP) has not been produced from propionate in engineered *R. eutropha*.

R. eutropha is also capable of utilizing organic acids such as fumarate, succinate, aspartate, malate, and glutamate, from the TCA (tricarboxylic acid) cycle by mediating between C3 and C4 molecules. Proteomic studies revealed active TCA cycle enzymes in both autotrophically and heterotrophically grown bacteria (Bruland et al. 2010). Additionally, three enzymes, phosphoenolpyruvate (PEP) carboxykinase, malic enzyme (malate dehydrogenase or NAD-malic enzyme), and PEP synthase were found to be active under heterotrophic growth conditions on organic carbon sources. These enzymes allow for the flow of metabolites between the Entner-Doudoroff pathway and the TCA cycle. In PHA production phase, the gene encoding malic enzyme became upregulated. Malic enzyme catalyzes the reversible conversion of malate to pyruvate and is part of a metabolic shunt for the production of NADPH (Bruland et al. 2010; Jian Yu 2009). Since *R. eutropha* does not contain 6-phosphogluconate dehydrogenase, an important enzyme in the pentose-phosphate pathway, production of NADPH for cellular metabolism and PHA production could be from this malic shunt (Figure 1.4).

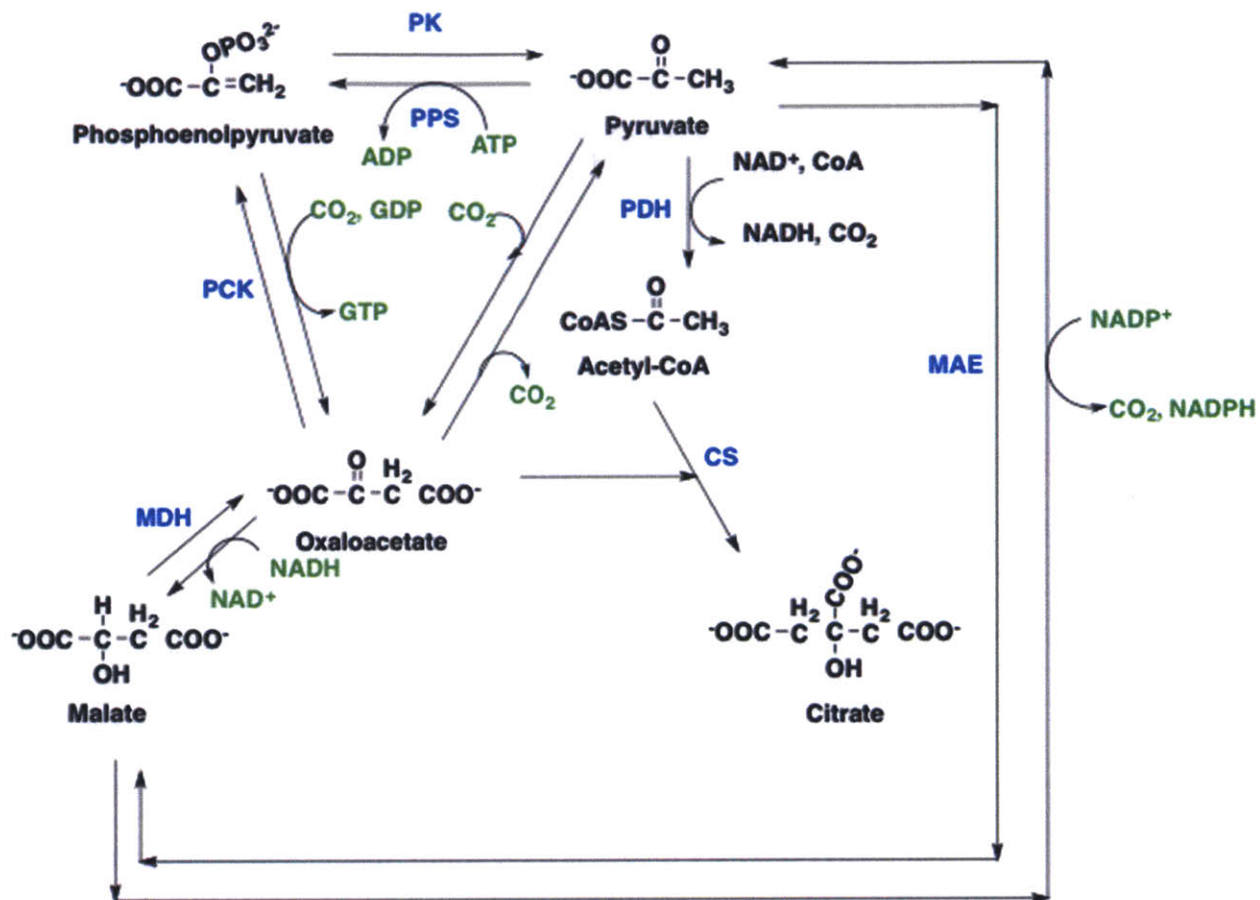


Figure 1.4: Pathway mediating between C3 and C4 intermediates. Malic enzyme (MAE) produces NADPH at the expense of ATP and NADH. Abbreviations: pyruvate kinase (PK), phosphoenolpyruvate synthase (PPS), pyruvate dehydrogenase (PDH), citrate synthase (CS), malate dehydrogenase (MDH), phosphoenolpyruvate carboxykinase (PCK).

Carbohydrate utilization

Unlike many commensal and pathogenic microorganisms, *R. eutropha* does not express a wide variety of glycohydrolases and sugar degrading enzymes and thus is unable to metabolize many different carbohydrates. In physiological studies of the bacterium, fructose (Grousseau et al. 2013) and gluconate (Brandt et al. 2012) are often used as carbon sources. It has also been shown that *R. eutropha* can grow on xylose and *N*-acetyl-D-glucosamine (NAG), although fructose is a more preferred carbon source (Holder et al. 2011). A wild type strain of *R. eutropha* H16, is not able to utilize glucose as a main carbon source. However, glucose-utilizing variants have been engineered (Raberg et al. 2012). Also, other glucose-utilizing *R. eutropha* strains have been uncovered in nature. The addition of molasses has been shown to enhance PHB production in solid-state fermentations featuring *R. eutropha* (Oliveira et al. 2007), however it has not been characterized whether the specific strain utilized both glucose and fructose from the crude carbon source. PHB has also been synthesized by *R. eutropha* from a crude sugar solution extracted from oil palm fronds. In this study, both glucose and fructose were shown to be consumed (Mohd Zahari et al. 2012).

Cellulosic biomass utilization

R. eutropha is also able to utilize cellulosic biomass, a renewable feedstock, to generate products. PHB has been produced from wheat-based feedstock streams, where wheat was converted into glucose-rich wheat hydrolysate and nitrogen-rich fungal extract (Koutinas et al. 2007). *R. eutropha* grown on levulinic acid, a chemical made from refining cellulosic biomass, produced P(HB-co-HV) (Wang et al. 2013) and a terpolyester comprising 3-hydroxybutyrate and 3-hydroxyvalerate as major monomers, and 4-hydroxyvalerate as the minor monomer (Yu et al. 2009). Fed-batch cultivation on hydrolysed sago starch led to PHA production (Syamsu et al. 2006), and up to 57% cell dry weight PHA was produced from pretreated sugarcane bagasse (Yu and Stahl 2008), further demonstrating *R. eutropha*'s substrate diversity.

Aromatics utilization

R. eutropha is also unique in its ability to use aromatic compounds such as benzoate and phenol as sole carbon and energy sources (Johnson and Stanier 1971). The catabolism of these aromatic compounds is inducible, and is achieved through various pathways. *R. eutropha* consumes phenols through the meta pathway encoded in chromosome 1 (Pohlmann et al. 2006), where catechol-2,3-oxygenase catalyzes the first reaction (Johnson and Stanier 1971). *R. eutropha* strain E2 has a phenol hydroxylase that allows phenol to be converted to catechol (Hino et al. 1998). p-nitrophenol, a pollutant from pesticide and explosives production (Spain 1995), is degraded by *R. eutropha* JMP134 through 3-nitrophenol nitroreductase (Schenzle et al. 1997). JMP134 can also degrade substituted aromatic pollutants such as 2,4-dichlorophenoxyacetic acid (2,4-D) through *tfd* genes on plasmid pJP4 (Trefault et al. 2004) and is chemotactic toward 2,4-D (Hawkins and Harwood 2002). Lastly, benzoate is degraded through the beta-ketoadipate pathway (Johnson and Stanier 1971), and phenol catabolism is repressed when this pathway is activated (Ampe et al. 1998). The ability of *R. eutropha* to utilize aromatics, a large source of environmental pollutants, demonstrates its potential for bioremediation applications.

Utilization of lipids and fats

Fatty acids and lipids pack in more energy per mole of carbon than any other carbon source; therefore, they are a more efficient group of carbon source for growth and production of value-added products such as PHAs (Riedel et al. 2014). Increasing research has been focused on utilizing plant oil or animal fats in *R. eutropha* fermentations. Triacylglycerols in plant oils and animal fats consist of glycerol triesters of fatty acids. The length and saturation of fatty acids may vary depending on the source of triacylglycerol, whether it is plant oil or animal fats. Triacylglycerols cannot be utilized directly by the cells and must be broken down to free fatty acids by the digestive enzyme, lipase. *R. eutropha* has one extracellular lipase, LipA that is responsible for the breaking down of triacylglycerols. LipA is a non-specific lipase, which is able to completely digest triacylglycerols into glycerols and free fatty acids. Triacylglycerols are water insoluble, whereas lipases are water soluble, so digestion of triacylglycerol takes place at the lipid water interface. The rate of LipA catalysis depends on the surface area of the interface, which increases up to 500% with enhancement of interfacial surface (Lu et al. 2013). In various fermentation settings, surfactants were used to emulsify oils and fatty acids, in order to increase

the interfacial surface area and allowing fatty acids to be uptake by cells (Budde et al. 2012). Free fatty acids released from LipA catalyzed triacylglycerol breakdown can act as natural surfactants to emulsify the lipids and fatty acids in *R. eutropha* growth culture, thus increasing the bioavailability of the fatty acids (Riedel et al. 2014).

Once inside the cells, fatty acids are broken down two carbons at a time in a cyclic manner to produce one molecule each of acetyl-CoA, FADH₂, and NADH. FADH₂ and NADH are reoxidized by electron-transport chain through the intermediacy of a series of electron-transfer reactions to produce ATP. Genome sequencing of *R. eutropha* indicated the presence of two sets of β -oxidation pathway genes. A previous study also revealed that both β -oxidation pathways are active and essential for growth on oils and fats (Brigham et al. 2010b). Fatty acyl-CoA intermediates from the β -oxidation pathway can serve as PHA precursors. Expression of a gene encoding for enoyl-CoA hydratase (*phaJ*) from *Pseudomonas aeruginosa* in *R. eutropha* allowed for conversion of enoyl-CoA to (*R*)-3-hydroxyacyl-CoA, a PHA precursor. Similarly, 3-hydroxyacyl-ACP:CoA transferase gene (*phaG*) from *P. putida* when expressed in *R. eutropha* is capable of redirecting 3-ketoacyl-ACP from the fatty acid biosynthesis pathway to (*R*)-3-hydroxyacyl-CoA. Expression of either *phaJ* or *phaG* gene allowed for the production of copolymer poly(3-hydroxybutyrate-co-hydroxyhexanoate) (Budde et al. 2011; Riedel et al. 2014).

DIVERSE PATHWAYS FOR BIOSYNTHESIS OF VALUE-ADDED COMPOUNDS

R. eutropha PHA production

As mentioned, *R. eutropha* was proposed to be used as single cell protein (SCP) for animals feeds. However, the large amounts of intracellular PHA that are synthesized under nitrogen limiting conditions were demonstrated to be poorly digestible by rats (Waslien and Calloway 1969). PHA is produced by *R. eutropha* under stress conditions, such as non-carbon nutrient starvation. PHA synthesis as a stress response has been demonstrated to be regulated in part by the bacterial stringent response (Brigham et al. 2012a). In the last couple of decades, utility for PHA was indeed firmly established as a biodegradable, biocompatible replacement for petroleum-based polymer. Many applications for PHA have been suggested, including disposable household products (Philip et al. 2007), packaging (Chen 2009), agricultural (Voinova et al. 2009), and waste treatment (Sudesh et al. 2011). However, the most successful application for PHA to date is in medical devices and consumable items, including sutures, implants, surgical meshes, scaffolds, and timed-release drug delivery devices (Brigham and Sinskey 2012). In particular, sutures and surgical meshes have been marketed and are being produced and used today.

A schematic of native and engineered PHA biosynthesis pathways in *R. eutropha* is shown in Figure 1.5. PHA can be synthesized enzymatically or chemically by incorporating many different monomer types. In nature, short chain length (*scl*) PHA is a polymerization of C3-C5 monomers, with the primary example being the PHB homopolymer, which is comprised of C4 monomers. Medium chain length (*mcl*) PHA incorporates C6-C12 monomers, and is typically produced by members of the genus *Pseudomonas*, among some others. Some bacteria can produce PHA containing a combination of *scl* and *mcl* monomers (i.e., *scl-co-mcl* PHA). The PHA synthase from these microbes, such as *Aeromonas caviae* and *Rhodococcus*

aetherivorans, are highly sought after for *R. eutropha* strain engineering to produce biodegradable polymer with characteristics very similar to petroleum-based plastics. The versatile metabolism and genetic tractability of *R. eutropha* allows for this organism to be used to produce many different types of PHA biopolymer, each with different thermal and mechanical properties. Wild type *R. eutropha* is capable of producing *scl*-PHA, typically PHB on most carbon sources. Odd-chain length (C3 or C5) precursors must be fed, in order to synthesize the copolymer P(HB-*co*-HV).

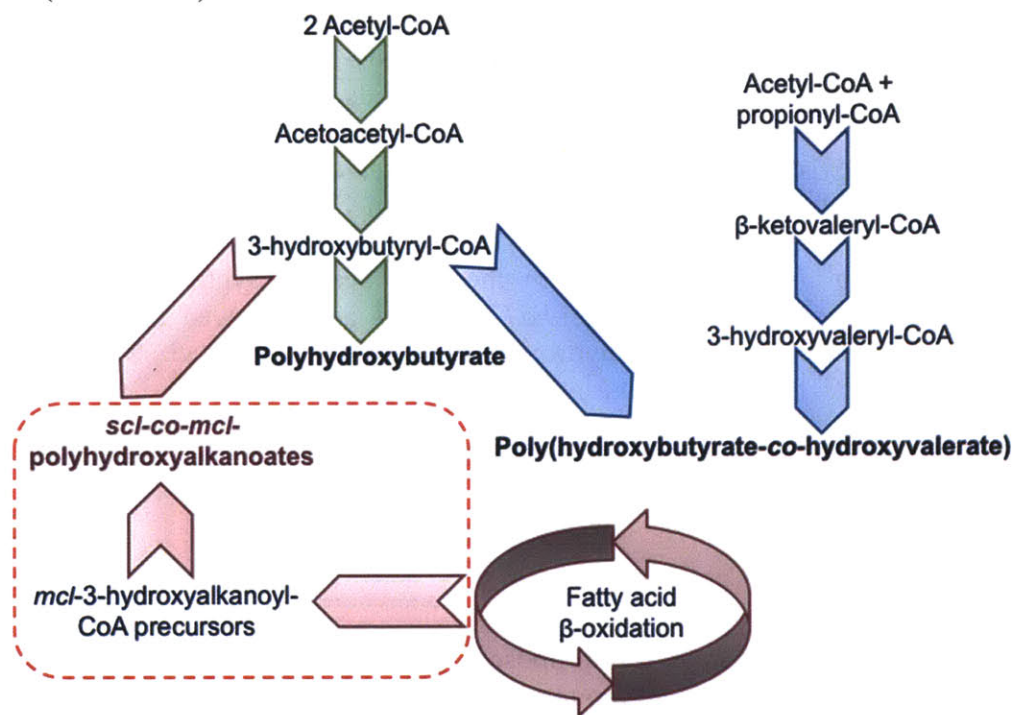


Figure 1.5: Wild type *R. eutropha* produces polyhydroxybutyrate from condensation of two acetyl-CoA molecules. When the cells are fed with odd-chain length precursors, poly(hydroxybutyrate-*co*-hydroxyvalerate) can be produced. Engineered *R. eutropha* can incorporate hydroxyalkanoyl-CoA precursors from β -oxidation of fatty acids and produce PHA copolymers with both SCL and MCL monomers.

Given their advantageous properties, *scl-co-mcl* PHAs are often the goal of production. This requires strain engineering of *R. eutropha* to confer the capability of synthesizing and polymerizing *mcl* 3-hydroxyacyl-CoA (*mcl*-3HA-CoA) precursor molecules. The *mcl*-3HA-CoA precursors can be produced via intermediates of fatty acid metabolism. Typically, fatty acid β -oxidation intermediates are employed to synthesize these precursors using an (*R*)-specific-enoyl-CoA reductase enzyme, PhaJ (Brigham et al. 2012b). In most strain engineering studies available in the literature, the *phaJ* gene from *Pseudomonas* is expressed in *R. eutropha* heterologously (Davis et al. 2008). However, *phaJ* homologs have been characterized in *R. eutropha* (Kawashima et al. 2012).

R. eutropha is considered to be the model organism of PHA homeostasis. It can produce up to 90% of its cell dry weight as polymer (Brigham et al. 2012b), its PHB biosynthetic enzymes were among the first to be studied extensively (Budde et al. 2010), and many different PHA granule-associated proteins (GAPs) have been initially characterized in *R. eutropha*. Pilot

scale PHA production operations have been established in areas around the world using *R. eutropha* as the biocatalyst. This bacterium is efficient at moving carbon from feedstock to product and is often considered in many biotechnological applications.

Polythioesters (PTEs) is another group of bio-based polymers. PTEs, although non-biodegradable in nature, are thought to be a durable, bio-based alternative to petrochemical plastics. The main difference between PTEs and PHAs is the thioester group in the backbone, resulting in the polymer's non-biodegradability. *R. eutropha* was first demonstrated to produce a PTE copolymer of poly(3-hydroxybutyrate-co-3-mercaptopropionate) [P(HB-co-3MP)], when 3MP was fed to cells. Other PTE copolymers could be synthesized by *R. eutropha* if the corresponding mercapto-acid (MA) was presented in the growth media. Other precursor substrates that promote PTE biosynthesis in *R. eutropha* are 3,3'-dithiodipropionic acid (DTDP) and 3,3'-thiodipropionic acid (TDP). The feeding of the TDP and DTDP precursors to *R. eutropha* cells resulted in synthesis of P(HB-co-3MP) with >50 mole% 3MP monomer content. The main issue with production of PTEs is that specialized precursors are needed, and many potential thiol-containing precursors are toxic to the cells (Lütke-Eversloh and Steinbüchel 2003). PTEs have been examined for their thermal and mechanical properties, and have been found to be generally more heat stable than PHAs. Also, the exact characteristics observed depended on the chain length of the MA monomer incorporated into the PTE (Kawada et al. 2003).

Biofuel production by *R. eutropha*

R. eutropha has also been examined for biosynthesis of non-alcohol fuel molecules. PHA can be converted by an acid-catalyzed hydrolysis to produce biofuel molecules, *i.e.*, methyl esters (Chen 2009). Engineered strains have been constructed to produce free fatty acids (Torella et al. 2013), which can also be converted to methyl esters. A strain of *R. eutropha* with inactivated PHB biosynthesis and fatty acid β -oxidation pathways also produced free fatty acids. This strain, however, also produced methyl ketones, which are another potential biofuel molecule. The addition of a heterologous methyl ketone biosynthesis pathway to this strain resulted in a strain with even higher ketone production capabilities (Müller et al. 2013). It should be noted that these biofuel molecules could be synthesized from most of the carbon feedstocks discussed in this chapter, including CO₂.

Isobutanol, *n*-butanol, and isopropanol have attracted research and industrial attentions as promising next generation alcohol biofuel alternatives to ethanol and biodiesel. Each alcohol has a similar research octane number as gasoline and a higher energy density than ethanol. Most importantly, each alcohol can be used directly in the current fuel delivery infrastructure due to its low vapor pressure, low hygroscopicity, and low water solubility (Connor and Atsumi 2010; Lan and Liao 2013). When the native PHA production genes were eliminated from *R. eutropha*, the bacteria secrete large amounts of pyruvate and stored more energy in the form of NADH than wild type (Brigham et al. 2013; Lu et al. 2012). The secreted pyruvate and extra energy in these PHA-negative strains were redirected for the production of isobutanol and isopropanol. Production of isobutanol relies on the valine biosynthesis pathway, in which the intermediate 2-ketoisovalerate is decarboxylated and reduced to form isobutanol. Expression of heterologous ketoisovalerate decarboxylase from *Lactococcus lactis* in a mutant *R. eutropha* strain with constitutively expressed alcohol dehydrogenase enabled the cells to produce isobutanol. Two studies utilizing *R. eutropha* native or heterologous valine biosynthesis enzymes in addition to

ketoisovalerate decarboxylase and alcohol dehydrogenase were able to produce isobutanol from fructose, formate, and CO₂ in *R. eutropha* (Li et al. 2012; Lu et al. 2012). Another study redirected acetoacetyl-CoA, the precursor for the production of polyhydroxybutyrate, for the production of isopropanol via expression of acetoacetate decarboxylase and alcohol dehydrogenase from *Clostridium* (Grousseau et al. 2014). Since the production of isopropanol and polyhydroxybutyrate share common precursors, isopropanol production titer reached near theoretical maximum in fed-batch fermentation. Although the *de novo* production of *n*-butanol has not been demonstrated in *R. eutropha*, one study utilized genes from the *R. eutropha* polyhydroxybutyrate production pathway for *n*-butanol production in *E. coli* (Bond-Watts et al. 2011).

Production of fine-chemicals and pharmaceutical precursors

Hydroxyalkanoate monomers incorporated into PHA polymers are all chiral molecules. Each monomer has a chiral center on the carbon with the hydroxyl group and possesses the (*R*)-configuration (Figure 6). These chiral molecules also contain two functional groups, a hydroxyl group and a carboxyl group, which promote further modification to produce fine chemicals such as antibiotics, vitamins, perfumes, and pheromones (Gao et al. 2011). The most widely produced polymer by *R. eutropha*, PHB, contains monomer units of (*R*)-3-hydroxybutyric acid, which is an important precursor for the production of 4-acetoxyazetidinone for carbapenem antibiotics. (*R*)-3-hydroxybutyric acid has also shown medical potential for the activation of Ca ion channels and memory enhancement. Production of (*R*)-hydroxyalkanoates can be achieved through chemical synthesis or chemical hydrolysis, although both methods are very complicated and expensive. As discussed above, *R. eutropha* naturally produces PHAs as a way to store excess carbon. When the cells undergo starvation, PHA depolymerases are capable of breaking down PHAs into (*R*)-hydroxyalkanoate monomers. This is a well-controlled and utilized process for *R. eutropha* to reserve and reuse excess carbon and energy sources. *R. eutropha* has seven identified PHA depolymerases, and in carbon-limited cultivation condition, these depolymerases are able to hydrolyze PHB to (*R*)-3-hydroxybutyric acid monomers (Figure 6). This allows for the production of (*R*)-hydroxyalkanoates without any *in vitro* hydrolysis step (Lee and Lee 2003; Shiraki et al. 2006). Since engineered *R. eutropha* is capable of producing PHAs with various monomer lengths, a variety of (*R*)-hydroxyalkanoates chiral compounds can be produced. Additionally, the gene encoding the PHA synthase can be eliminated from the *R. eutropha* genome, which could potentially allow for the accumulation and direct isolation of (*R*)-hydroxyalkanoates precursors.

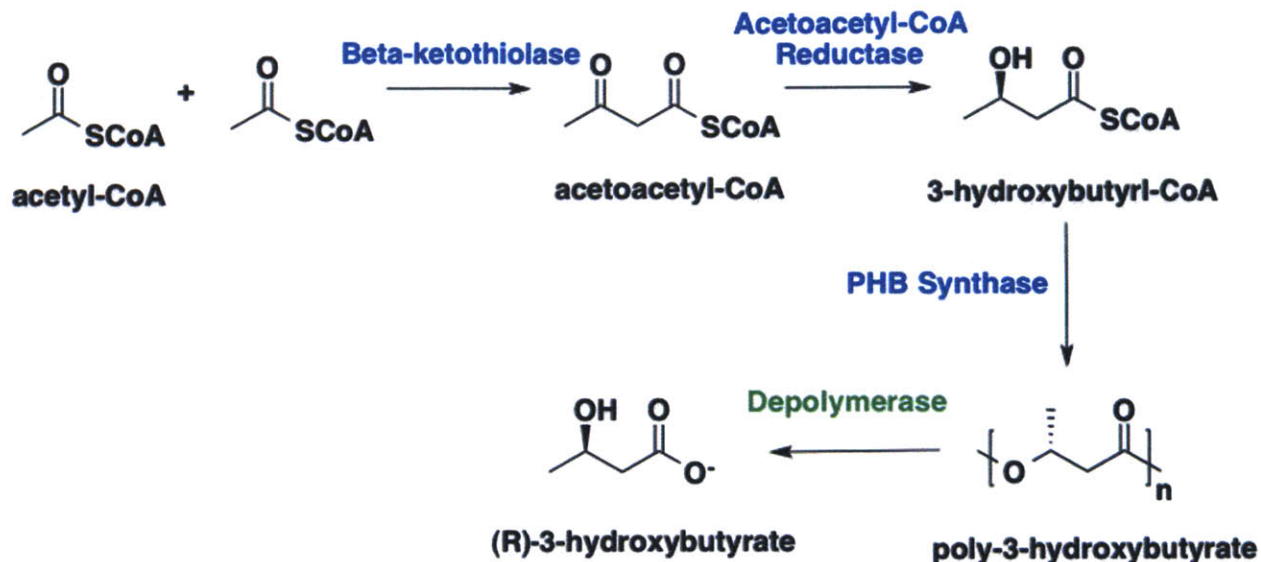


Figure 1.6: Synthesis and degradation of poly-3-hydroxybutyrate. (*R*)-3-hydroxybutyrate, the chiral molecule that can be used as pharmaceutical precursors can be generated from depolymerization of poly-3-hydroxybutyrate.

R. eutropha has also been engineered to produce (*R*)-1,2-propanediol, a pharmaceutical precursor for the production of antibacterial agents. Alcohol dehydrogenase from *Kluyveromyces lactis* was used to convert hydroxyacetone, the product from reduction and dehydration of glycerol, to (*R*)-1,2-propanediol (Oda et al. 2013). This study coupled hydrogen oxidation as the reduction energy source with the synthesis of (*R*)-1,2-propanediol, which increased production yield and minimized carbon dioxide generation.

Recombinant protein expression system

R. eutropha has been engineered to harbor an efficient recombinant protein expression system. This recombinant protein expression system contains a T7 RNA polymerase under the control of *R. eutropha phaP* inducible promoter. As a proof of principle, organophosphohydrolase, a protein that is prone to form inclusion bodies in *E. coli* overexpression systems, was overexpressed in this *R. eutropha* system. Using this novel expression system, *R. eutropha* produced greater than 10 g/L soluble and active organophosphohydrolase (Barnard et al. 2005; Schmidt 2004; Srinivasan et al. 2002), which is 200 times higher yield than *E. coli*. *R. eutropha* recombinant protein expression system has great potential in the expression and production of commodity enzymes, therapeutic proteins, vaccines, and peptides.

Application in bioremediation

The metabolically versatile *R. eutropha* is capable of surviving in harsh environmental conditions. It is tolerant to various environmental pollutants including aromatics and heavy metals. As described earlier, *R. eutropha* can break down aromatic compounds and utilize them for growth. Soils contaminated with p-nitrophenol or 2,4-dichlorophenoxyacetic acid can be cleaned up using *R. eutropha* (Chen et al. 2004; Watanabe 2001). A study also demonstrated

that heavy metal-polluted soil had decreased toxic effect on plants when pre-innoculated with *R. eutropha*, which suggests that *R. eutropha* also contains a detoxification machinery for heavy metal bioremediation (Pandey and Jain 2002; Watanabe 2001).

SUMMARY

R. eutropha is capable of utilizing a plethora of simple and complex carbon-containing compounds. When experiencing unbalanced growth conditions high in carbon source and limited in other nutrient such as nitrogen or phosphorus, *R. eutropha* can store carbon and energy in the form of polyhydroxyalkanoates (PHA), a biodegradable and biocompatible plastic. The monomer composition of PHAs can be a direct result of the carbon source. Wild type *R. eutropha* can be engineered to harbor broad substrate reductase and polymerase enzymes for the production of copolymers with a variety of properties. The native depolymerase is capable of hydrolyze these polymers into valuable chiral molecules. The native PHA carbon storage system can be genetically disabled and the carbons redirected to produce biofuels and pharmaceutical precursors. The metabolic versatility and genetic tractability combined with its ability to store a variety of carbons makes *R. eutropha* an excellent platform organism for the production of value-added compounds from common waste resources. In the upcoming chapters, the production of biofuels and bioplastics from fructose, CO₂, oils, and mixed-organic acids will be described in detail, along with the characterization of enzymes involved in the CO₂ and lipid metabolism.

REFERENCES

- Ampe F, Léonard D, and Lindley ND (1998) Repression of phenol catabolism by organic acids in *Ralstonia eutropha*. *Appl. Environ. Microbiol.* 64: 1–6
- Badger MR, and Bek EJ (2008) Multiple Rubisco forms in proteobacteria: their functional significance in relation to CO₂ acquisition by the CBB cycle. *J Exp Bot* 59: 1525–1541
- Barnard GC, McCool JD, Wood DW, and Gerngross TU (2005) Integrated Recombinant Protein Expression and Purification Platform Based on *Ralstonia eutropha*. *Appl Environ Microbiol* 71: 5735–5742
- Bernhard M, Friedrich B, and Siddiqui RA (2000) *Ralstonia eutropha* TF93 Is Blocked in Tat-Mediated Protein Export. *J Bacteriol* 182: 581–588
- Bonacci W, Teng PK, Afonso B, Niederholtmeyer H, Grob P, Silver PA, and Savage DF (2012) Modularity of a carbon-fixing protein organelle. *Proc Natl Acad Sci USA* 109: 478–483
- Bond-Watts BB, Bellerose RJ, and Chang MCY (2011) Enzyme mechanism as a kinetic control element for designing synthetic biofuel pathways. *Nat Chem Biol* 7: 222–227
- Bormann EJ, and Roth M (1999) The production of polyhydroxybutyrate by *Methylobacterium rhodesianum* and *Ralstonia eutropha* in media containing glycerol and casein hydrolysates. *Biotechnol Lett* 21: 1059–1063
- Bowien B, and Kusian B (2002) Genetics and control of CO₂ assimilation in the chemoautotroph *Ralstonia eutropha*. *Arch Microbiol* 178: 85–93
- Brandt U, Raberg M, Voigt B, Hecker M, and Steinbüchel A (2012) Elevated poly(3-hydroxybutyrate) synthesis in mutants of *Ralstonia eutropha* H16 defective in lipopolysaccharide biosynthesis. *Appl Microbiol Biotechnol* 95: 471–483
- Brigham CJ, and Sinskey AJ (2012) Applications of polyhydroxyalkanoates in the medical industry. *Int J Biotechnol Wellness Ind* 1: 52–60
- Brigham CJ, Budde CF, Holder JW, Zeng Q, Mahan AE, Rha C, and Sinskey AJ (2010a) Elucidation of β -Oxidation Pathways in *Ralstonia eutropha* H16 by Examination of Global Gene Expression. *J Bacteriol* 192: 5454–5464
- Brigham CJ, Budde CF, Holder JW, Zeng Q, Mahan AE, Rha C, and Sinskey AJ (2010b) Elucidation of beta-oxidation pathways in *Ralstonia eutropha* H16 by examination of global gene expression. *J Bacteriol* 192, 5454–5464
- Brigham CJ, Speth DR, Rha C, and Sinskey AJ (2012a) Whole-genome microarray and gene deletion studies reveal regulation of the polyhydroxyalkanoate production cycle by the stringent response in *Ralstonia eutropha* H16. *Appl Environ Microbiol* 78: 8033–8044
- Brigham CJ, Zhila N, Shishatskaya E, Volova, TG, and Sinskey AJ (2012b) Manipulation of *Ralstonia eutropha* Carbon Storage Pathways to Produce Useful Bio-Based Products. In *Reprogramming Microbial Metabolic Pathways*, X Wang, J Chen, and P Quinn. (Springer Netherlands), pp. 343–366

Brigham CJ, Gai CS, Lu J, Speth DR, Worden RM, and Sinskey AJ (2013) Engineering *Ralstonia eutropha* for Production of Isobutanol from CO₂, H₂, and O₂. In *Advanced Biofuels and Bioproducts*, JW Lee (Springer New York), pp. 1065–1090

Bruland N, Voß I, Brämer C, and Steinbüchel A (2010) Unravelling the C3/C4 carbon metabolism in *Ralstonia eutropha* H16. *J Appl Microbiol* 109, 79–90

Budde CF, Riedel SL, Willis LB, Rha C, and Sinskey AJ (2011) Production of Poly(3-Hydroxybutyrate-co-3-Hydroxyhexanoate) from Plant Oil by Engineered *Ralstonia eutropha* Strains. *Appl Environ Microbiol* 77: 2847–2854

Buhrke T, Lenz O, Krauss N, and Friedrich B (2005) Oxygen Tolerance of the H₂-sensing [NiFe] Hydrogenase from *Ralstonia eutropha* H16 Is Based on Limited Access of Oxygen to the Active Site. *J Biol Chem* 280, 23791–23796

Burgdorf T, Lenz O, Buhrke T, van der Linden E, Jones AK, Albracht SPJ, and Friedrich B (2005a) [NiFe]-Hydrogenases of *Ralstonia eutropha* H16: Modular Enzymes for Oxygen-Tolerant Biological Hydrogen Oxidation. *J Mol Microbiol Biotechnol* 10: 181–196

Burgdorf T, Linden E van der, Bernhard M, Yin QY, Back JW, Hartog AF, Muijsers AO, Koster CG, de Albracht SPJ, and Friedrich B (2005b) The Soluble NAD⁺-Reducing [NiFe]-Hydrogenase from *Ralstonia eutropha* H16 Consists of Six Subunits and Can Be Specifically Activated by NADPH. *J Bacteriol* 187: 3122–3132

Calloway DH, and Kumar AM (1969) Protein quality of the bacterium *Hydrogenomonas eutropha*. *Appl Microbiol* 17: 176–178

Cannon GC, Bradburne CE, Aldrich HC, Baker SH, Heinhorst S, and Shively JM (2001) Microcompartments in prokaryotes: carboxysomes and related polyhedra. *Appl Environ Microbiol* 67: 5351–5361

Cavalheiro JMBT, de Almeida MCMD, Grandfils C, and da Fonseca MMR (2009) Poly(3-hydroxybutyrate) production by *Cupriavidus necator* using waste glycerol. *Process Biochem* 44: 509–515

Chen GQ (2009) A microbial polyhydroxyalkanoates (PHA) based bio- and materials industry. *Chem Soc Rev* 38, 2434–2446

Chen WM, Chang JS, Wu CH, and Chang SC (2004) Characterization of phenol and trichloroethene degradation by the rhizobium *Ralstonia taiwanensis*. *Res Microbiol* 155: 672–680

Connor MR, and Atsumi S (2010) Synthetic Biology Guides Biofuel Production. *J Biomed Biotechnol*

Cramm R (2009) Genomic View of Energy Metabolism in *Ralstonia eutropha* H16. *J Mol Microbiol Biotechnol*. 16: 38–52

Davis R, Chandrashekar A, and Shamala TR (2008) Role of (R)-specific enoyl coenzyme A hydratases of *Pseudomonas sp* in the production of polyhydroxyalkanoates. *Antonie Van Leeuwenhoek* 93: 285–296

Du G, Si Y, and Yu J (2001) Inhibitory effect of medium-chain-length fatty acids on synthesis of polyhydroxyalkanoates from volatile fatty acids by *Ralstonia eutropha*. *Biotechnol. Lett.* 23: 1613–1617

- Ducat DC, and Silver PA (2012) Improving carbon fixation pathways. *Curr Opin Chem Biol* 16, 337–344
- Frank S, Lawrence AD, Prentice MB, and Warren MJ (2013) Bacterial microcompartments moving into a synthetic biological world. *J Biotechnol* 163, 273–279
- Friedrich CG, Friedrich B, Bowien B (1981) Formation of enzymes of autotrophic metabolism during heterotrophic growth of *Alcaligenes eutrophus*. *J Gen Microbiol* 122: 69–78
- Fritsch J, Lenz O, and Friedrich B (2011) The Maturation Factors HoxR and HoxT Contribute to Oxygen Tolerance of Membrane-Bound [NiFe] Hydrogenase in *Ralstonia eutropha* H16. *J. Bacteriol.* 193: 2487–2497
- Fukui T, Suzuki M, Tsuge T, and Nakamura S (2009) Microbial synthesis of poly((R)-3-hydroxybutyrate-co-3-hydroxypropionate) from unrelated carbon sources by engineered *Cupriavidus necator*. *Biomacromolecules* 10: 700–706
- Gai CS, Lu J, Brigham CJ, Bernardi AC, and Sinskey AJ (2014) Insights into bacterial CO₂ metabolism revealed by the characterization of four carbonic anhydrases in *Ralstonia eutropha* H16. *AMB Express* 4: 2
- Gao X, Chen JC, Wu Q, and Chen GQ (2011) Polyhydroxyalkanoates as a source of chemicals, polymers, and biofuels. *Curr Opin Biotechnol* 22: 768–774
- Grousseau E, Blanchet E, Délérís S, Albuquerque MGE, Paul E, and Uribelarrea JL (2013) Impact of sustaining a controlled residual growth on polyhydroxybutyrate yield and production kinetics in *Cupriavidus necator*. *Bioresour Technol* 148: 30–38
- Grousseau E, Lu J, Gorret N, Guillouet SE, and Sinskey AJ (2014) Isopropanol production with engineered *Cupriavidus necator* as bioproduction platform. *Appl Microbiol Biotechnol* 98: 4277–4290
- Hassan AN, and Nelson BK (2012) Invited review: Anaerobic fermentation of dairy food wastewater. *J Dairy Sci* 95: 6188–6203
- Hassan MA, Nawata O, Shirai Y, Rahman NAA, Yee PL, Ariff AB, and Karim MIA (2002) A Proposal for Zero Emission from Palm Oil Industry Incorporating the Production of Polyhydroxyalkanoates from Palm Oil Mill Effluent. *J Chem Eng Jpn* 35: 9–14
- Ali Hassan M, Shirai Y, Kusubayashi N, Ismail Abdul Karim M, Nakanishi K, and Hashimoto K (1996) Effect of organic acid profiles during anaerobic treatment of palm oil mill effluent on the production of polyhydroxyalkanoates by *Rhodobacter sphaeroides*. *J Ferment Bioeng* 82: 151–156
- Hawkins AC, and Harwood CS (2002) Chemotaxis of *Ralstonia eutropha* JMP134(pJP4) to the herbicide 2,4-dichlorophenoxyacetate. *Appl Environ Microbiol* 68: 968–972
- Hino S, Watanabe K, and Takahashi N (1998) Phenol hydroxylase cloned from *Ralstonia eutropha* strain E2 exhibits novel kinetic properties. *Microbiol Read Engl* 144: 1765–1772
- Holder JW, Ulrich JC, DeBono AC, Godfrey PA, Desjardins CA, Zucker J, Zeng Q, Leach ALB, Ghiviriga I, Dancel C (2011) Comparative and functional genomics of *Rhodococcus opacus* PD630 for biofuels development. *PLoS Genet* 7: e1002219

- Ihara M, Nishihara H, Yoon KS, Lenz O, Friedrich B, Nakamoto H, Kojima K, Honma D, Kamachi T, and Okura I (2006) Light-driven Hydrogen Production by a Hybrid Complex of a [NiFe]-Hydrogenase and the Cyanobacterial Photosystem I. *Photochem Photobiol* 82: 676–682
- Jeffke T, Gropp NH, Kaiser C, Grzeszik C, Kusian B, and Bowien B (1999) Mutational analysis of the *cbb* operon (CO₂ assimilation) promoter of *Ralstonia eutropha*. *J Bacteriol* 181: 4374–4380
- Jendrossek D, Steinbüchel A, and Schlegel HG (1988) Alcohol dehydrogenase gene from *Alcaligenes eutrophus*: subcloning, heterologous expression in *Escherichia coli*, sequencing, and location of Tn5 insertions. *J Bacteriol* 170: 5248–5256
- Jendrossek D, Krüger N, and Steinbüchel A (1990) Characterization of alcohol dehydrogenase genes of derepressible wild-type *Alcaligenes eutrophus* H16 and constitutive mutants. *J Bacteriol* 172: 4844–4851
- Jian Yu LXLC (2009) Biopolyester Synthesis and Protein Regulations in *Ralstonia eutropha* on Levulinic Acid and Its Derivatives from Biomass Refining. *J Biobased Mater Bioenergy* 3: 113–122
- Johnson BF, and Stanier RY (1971) Dissimilation of aromatic compounds by *Alcaligenes eutrophus*. *J Bacteriol* 107: 468–475
- Kawada J, Lütke-Eversloh T, Steinbüchel A, and Marchessault RH (2003) Physical properties of microbial polythioesters: characterization of poly(3-mercaptoalkanoates) synthesized by engineered *Escherichia coli*. *Biomacromolecules* 4: 1698–1702
- Kawashima Y, Cheng W, Mifune J, Orita I, Nakamura S, and Fukui T (2012) Characterization and functional analyses of R-specific enoyl coenzyme A hydratases in polyhydroxyalkanoate-producing *Ralstonia eutropha*. *Appl Environ Microbiol* 78: 493–502
- Kim DH, and Kim MS (2011) Hydrogenases for biological hydrogen production. *Bioresour Technol* 102: 8423–8431
- Kleihues L, Lenz O, Bernhard M, Buhrke T, and Friedrich B (2000) The H₂ Sensor of *Ralstonia eutropha* Is a Member of the Subclass of Regulatory [NiFe] Hydrogenases. *J Bacteriol* 182: 2716–2724
- Kohlmann Y, Pohlmann A, Otto A, Becher D, Cramm R, Lu S, Schwartz E, Hecker M, and Friedrich B (2011) Analyses of Soluble and Membrane Proteomes of *Ralstonia eutropha* H16 Reveal Major Changes in the Protein Complement in Adaptation to Lithoautotrophy. *J Proteome Res* 10: 2767–2776
- Koutinas AA, Xu Y, Wang R, and Webb C (2007) Polyhydroxybutyrate production from a novel feedstock derived from a wheat-based biorefinery. *Enzyme Microb Technol* 40: 1035–1044
- Kusian B, Sültemeyer D, and Bowien B (2002) Carbonic anhydrase is essential for growth of *Ralstonia eutropha* at ambient CO₂ concentrations. *J Bacteriol* 184: 5018–5026
- Lan EI, and Liao JC (2013) Microbial synthesis of n-butanol, isobutanol, and other higher alcohols from diverse resources. *Bioresour Technol* 135: 339–349
- Lee SY, and Lee Y (2003) Metabolic Engineering of *Escherichia coli* for Production of Enantiomerically Pure (R)-Hydroxycarboxylic Acids. *Appl Environ Microbiol* 69: 3421–3426

- Lee SE, Li QX, and Yu J (2006) Proteomic examination of *Ralstonia eutropha* in cellular responses to formic acid. *PROTEOMICS* 6: 4259–4268
- Lenz O, Ludwig M, Schubert T, Bürstel I, Ganskow S, Goris T, Schwarze A, and Friedrich B (2010) H₂ conversion in the presence of O₂ as performed by the membrane-bound [NiFe]-hydrogenase of *Ralstonia eutropha*. *Chemphyschem Eur J Chem Phys Phys Chem* 11: 1107–1119
- Li H, Opgenorth PH, Wernick DG, Rogers S, Wu TY, Higashide W, Malati P, Huo YX, Cho KM, and Liao JC (2012) Integrated Electromicrobial Conversion of CO₂ to Higher Alcohols. *Science* 335: 1596–1596
- Linden EV, der Burgdorf T, Bernhard M, Bleijlevens B, Friedrich B, and Albracht SPJ (2004) The soluble [NiFe]-hydrogenase from *Ralstonia eutropha* contains four cyanides in its active site, one of which is responsible for the insensitivity towards oxygen. *JBIC J Biol Inorg Chem* 9: 616–626
- Lu J, Brigham CJ, Gai CS, and Sinskey AJ (2012) Studies on the production of branched-chain alcohols in engineered *Ralstonia eutropha*. *Appl Microbiol Biotechnol* 96: 283–297
- Lu J, Brigham CJ, Rha C, and Sinskey AJ (2013) Characterization of an extracellular lipase and its chaperone from *Ralstonia eutropha* H16. *Appl. Microbiol Biotechnol* 97: 2443–2454
- Lütke-Eversloh T, Steinbüchel A (2003) Novel precursor substrates for polythioesters (PTE) and limits of PTE biosynthesis in *Ralstonia eutropha*. *FEMS Microbiol Lett* 221: 191–196
- Matsumoto K, and Taguchi S (2013) Biosynthetic polyesters consisting of 2-hydroxyalkanoic acids: current challenges and unresolved questions. *Appl Microbiol Biotechnol* 97: 8011–8021
- Mohd Zahari MAK, Ariffin H, Mokhtar MN, Salihon J, Shirai Y, and Hassan MA (2012) Factors affecting poly(3-hydroxybutyrate) production from oil palm frond juice by *Cupriavidus necator* (CCUG52238(T)). *J Biomed Biotechnol* 2012: 125865
- Müller J, MacEachran D, Burd H, Sathitsuksanoh N, Bi C, Yeh YC, Lee TS, Hillson NJ, Chhabra SR, Singer SW (2013) Engineering of *Ralstonia eutropha* H16 for autotrophic and heterotrophic production of methyl ketones. *Appl Environ Microbiol* 79: 4433–4439
- Oda T, Oda K, Yamamoto H, Matsuyama A, Ishii M, Igarashi Y, and Nishihara H (2013) Hydrogen-driven asymmetric reduction of hydroxyacetone to (R)-1,2-propanediol by *Ralstonia eutropha* transformant expressing alcohol dehydrogenase from *Kluyveromyces lactis*. *Microb Cell Factories* 12: 2
- Oh JI, and Bowien B (1999) Dual control by regulatory gene *fdsR* of the *fds* operon encoding the NAD⁺-linked formate dehydrogenase of *Ralstonia eutropha*. *Mol Microbiol* 34: 365–376
- Oliveira FC, Dias ML, Castilho LR, and Freire DMG (2007) Characterization of poly(3-hydroxybutyrate) produced by *Cupriavidus necator* in solid-state fermentation. *Bioresour Technol* 98: 633–638
- Pandey G, and Jain RK (2002) Bacterial Chemotaxis toward Environmental Pollutants: Role in Bioremediation. *Appl Environ Microbiol* 68: 5789–5795
- Park JM, Kim TY, and Lee SY (2011) Genome-scale reconstruction and in silico analysis of the *Ralstonia eutropha* H16 for polyhydroxyalkanoate synthesis, lithoautotrophic growth, and 2-methyl citric acid production. *BMC Syst Biol* 5: 101

- Park SJ, Jang YA, Lee H, Park AR, Yang JE, Shin J, Oh YH, Song BK, Jegal J, Lee SH (2013) Metabolic engineering of *Ralstonia eutropha* for the biosynthesis of 2-hydroxyacid-containing polyhydroxyalkanoates. *Metab Eng* 20: 20–28
- Patnaik PR (2008) Response coefficient analysis of a fed-batch bioreactor to dissolved oxygen perturbation in complementary cultures during PHB production. *J Biol Eng* 2: 4
- Philip S, Keshavarz T, and Roy I (2007) Polyhydroxyalkanoates: biodegradable polymers with a range of applications. *J Chem Technol Biotechnol* 82: 233–247
- Pohlmann A, Fricke WF, Reinecke F, Kusian B, Liesegang H, Cramm R, Eitinger T, Ewering C, Pötter M, Schwartz E (2006) Genome sequence of the bioplastic-producing “Knallgas” bacterium *Ralstonia eutropha* H16. *Nat Biotechnol* 24: 1257–1262
- Price GD, and Badger MR (1991) Evidence for the role of carboxysomes in the cyanobacterial CO₂-concentrating mechanism. *Can J Bot* 69: 963–973
- Raberg M, Kaddor C, Kusian B, Stahlhut G, Budinova R, Kolev N, Bowien B, and Steinbüchel A (2012). Impact of each individual component of the mutated PTS(Nag) on glucose uptake and phosphorylation in *Ralstonia eutropha* G⁺1. *Appl Microbiol Biotechnol* 95: 735–744
- Rae BD, Long BM, Whitehead LF, Förster B, Badger MR, and Price GD (2013) Cyanobacterial carboxysomes: microcompartments that facilitate CO₂ fixation. *J Mol Microbiol Biotechnol* 23: 300–307
- Riedel SL, Lu J, Stahl U, and Brigham CJ (2014) Lipid and fatty acid metabolism in *Ralstonia eutropha*: relevance for the biotechnological production of value-added products. *Appl Microbiol Biotechnol* 98: 1469–1483
- Saggu M, Zebger I, Ludwig M, Lenz O, Friedrich B, Hildebrandt P, and Lenz F (2009) Spectroscopic Insights into the Oxygen-tolerant Membrane-associated [NiFe] Hydrogenase of *Ralstonia eutropha* H16. *J Biol Chem* 284: 16264–16276
- Schäferjohann J, Yoo JG, Kusian B, and Bowien B (1993) The cbb operons of the facultative chemoautotroph *Alcaligenes eutrophus* encode phosphoglycolate phosphatase. *J Bacteriol* 175: 7329–7340
- Schenzle A, Lenke H, Fischer P, Williams PA, and Knackmuss H (1997) Catabolism of 3-Nitrophenol by *Ralstonia eutropha* JMP 134. *Appl Environ Microbiol* 63: 1421–1427
- Schlegel HG, and Lafferty RM (1971) Novel energy and carbon sources A. The production of biomass from hydrogen and carbon dioxide. In *Advances in Biochemical Engineering, Volume 1*, (Springer Berlin Heidelberg) pp. 143–168
- Schmidt FR (2004) Recombinant expression systems in the pharmaceutical industry. *Appl Microbiol Biotechnol* 65, 363–372
- Schwartz E, Henne A, Cramm R, Eitinger T, Friedrich B, and Gottschalk G (2003) Complete Nucleotide Sequence of pHG1: A *Ralstonia eutropha* H16 Megaplasmid Encoding Key Enzymes of H₂-based Lithoautotrophy and Anaerobiosis. *J Mol Biol* 332: 369–383

Schwartz E, Voigt B, Zühlke D, Pohlmann A, Lenz O, Albrecht D, Schwarze A, Kohlmann Y, Krause C, Hecker M (2009) A proteomic view of the facultatively chemolithoautotrophic lifestyle of *Ralstonia eutropha* H16. *Proteomics* 9: 5132–5142

Shiraki M, Endo T, and Saito T (2006) Fermentative production of (R)-3-hydroxybutyrate using 3-hydroxybutyrate dehydrogenase null mutant of *Ralstonia eutropha* and recombinant *Escherichia coli*. *J Biosci Bioeng* 102: 529–534

Solaiman DKY, Ashby RD, Foglia TA, and Marmer WN (2006) Conversion of agricultural feedstock and coproducts into poly(hydroxyalkanoates). *Appl Microbiol Biotechnol* 71: 783–789

Spain JC (1995) Biodegradation of nitroaromatic compounds. *Annu Rev Microbiol* 49: 523–555

Srinivasan S, Barnard GC, and Gerngross TU (2002) A Novel High-Cell-Density Protein Expression System Based on *Ralstonia eutropha*. *Appl Environ Microbiol* 68: 5925–5932

Sudesh K, Bhubalan K, Chuah JA, Kek YK, Kamilah H, Sridewi N, and Lee YF (2011) Synthesis of polyhydroxyalkanoate from palm oil and some new applications. *Appl Microbiol Biotechnol* 89: 1373–1386

Syamsu KM, Fauzi A, Hartoto L, Ani Suryani AS, and Nur Atifah NA (2006) Production of Pha (poly hydroxy alkanoates) by *Ralstonia eutropha* on hydrolysed sago starch as main substrate using fed-batch cultivation method. (Putrajaya, Malaysia), pp. 153–157

Tcherkez GGB, Farquhar GD, and Andrews TJ (2006) Despite slow catalysis and confused substrate specificity, all ribulose biphosphate carboxylases may be nearly perfectly optimized. *Proc Natl Acad Sci USA* 103: 7246–7251

Torella JP, Ford TJ, Kim SN, Chen AM, Way JC, and Silver PA (2013) Tailored fatty acid synthesis via dynamic control of fatty acid elongation. *Proc Natl Acad Sci USA* 110: 11290–11295

Trefault N, De la Iglesia R, Molina AM, Manzano M, Ledger T, Pérez-Pantoja D, Sánchez MA, Stuardo M, and González B (2004) Genetic organization of the catabolic plasmid pJP4 from *Ralstonia eutropha* JMP134 (pJP4) reveals mechanisms of adaptation to chloroaromatic pollutants and evolution of specialized chloroaromatic degradation pathways. *Environ Microbiol* 6: 655–668

Tsuge T, Tanaka K, and Ishizaki A (2001) Development of a novel method for feeding a mixture of L-lactic acid and acetic acid in fed-batch culture of *Ralstonia eutropha* for poly-D-3-hydroxybutyrate production. *J Biosci Bioeng* 91: 545–550

Vandamme P, and Coenye T (2004) Taxonomy of the genus *Cupriavidus*: a tale of lost and found. *Int J Syst Evol Microbiol* 54: 2285–2289

Voinova ON, Kalacheva GS, Grodnitskaya ID, and Volova TG (2009) Microbial polymers as a degradable carrier for pesticide delivery. *Appl Biochem Microbiol* 45: 384–388

Volodina E, Schürmann M, Lindenkamp N, and Steinbüchel A (2014) Characterization of propionate CoA-transferase from *Ralstonia eutropha* H16. *Appl Microbiol Biotechnol* 98: 3579–3589

Wang Y, Chen R, Cai J, Liu Z, Zheng Y, Wang H, Li Q, He N (2013) Biosynthesis and thermal properties of PHBV produced from levulinic acid by *Ralstonia eutropha*. *PLoS ONE* 8

- Wang ZX, Brämer CO, and Steinbüchel A (2003) The glyoxylate bypass of *Ralstonia eutropha*. FEMS Microbiol Lett 228: 63–71
- Waslien CI, and Calloway DH (1969) Nutritional value of lipids in *Hydrogenomonas eutropha* as measured in the rat. Appl Microbiol 18: 152–155
- Watanabe K (2001) Microorganisms relevant to bioremediation. Curr Opin Biotechnol 12: 237–241
- Winkler M, Kawelke S, and Happe T (2011) Light driven hydrogen production in protein based semi-artificial systems. Bioresour Technol 102: 8493–8500
- Yan Q, Du G, and Chen J (2003) Biosynthesis of polyhydroxyalkanoates (PHAs) with continuous feeding of mixed organic acids as carbon sources by *Ralstonia eutropha*. Process Biochem 39: 387–391
- Yang YH, Brigham CJ, Budde CF, Boccazzi P, Willis LB, Hassan MA, Yusof ZAM, Rha C, and Sinskey AJ (2010) Optimization of growth media components for polyhydroxyalkanoate (PHA) production from organic acids by *Ralstonia eutropha*. Appl Microbiol Biotechnol 87: 2037–2045
- Ye RW, and Thomas SM (2001) Microbial nitrogen cycles: physiology, genomics and applications. Curr Opin Microbiol 4: 307–312
- Yeates TO, Kerfeld CA, Heinhorst S, Cannon GC, and Shively JM (2008) Protein-based organelles in bacteria: carboxysomes and related microcompartments. Nat Rev Microbiol 6: 681–691
- Yu J, Chen LXL, Sato S (2009) Biopolyester synthesis and protein regulations in *Ralstonia eutropha* on levulinic acid and its derivatives from biomass refining. J Biobased Mater Bioenergy 3: 113–122
- Yu J, and Si Y (2004) Metabolic Carbon Fluxes and Biosynthesis of Polyhydroxyalkanoates in *Ralstonia eutropha* on Short Chain Fatty Acids. Biotechnol Prog 20: 1015–1024
- Yu J, Stahl H (2008) Microbial utilization and biopolyester synthesis of bagasse hydrolysates. Bioresour Technol 99: 8042–8048
- Zarzycki J, Brecht V, Müller M, and Fuchs G (2009) Identifying the missing steps of the autotrophic 3-hydroxypropionate CO₂ fixation cycle in *Chloroflexus aurantiacus*. Proc Natl Acad Sci USA 106: 21317–21322

CHAPTER 2

Branched-chain alcohols production in engineered *Ralstonia eutropha*

(This chapter was modified from a previously published article in Applied Microbiology and Biotechnology, 2012. 96: 283-297 'Studies on the production of branched-chain alcohols in engineered *Ralstonia eutropha*' Jingnan Lu, Christopher Brigham, Claudia Gai, and Anthony Sisney © Springer-Verlag)

INTRODUCTION

Catabolism of branched-chain amino acids (leucine, valine, and isoleucine) to fusel acids and alcohols was first described in 1904 (Hazelwood et al. 2008). The transfer of an amino group from a branched-chain amino acid via transamination to an α -keto acid results in a branched-chain α -keto acid. Unlike α -ketoglutarate and oxaloacetate, the deamination products of glutamate and aspartate respectively, branched-chain α -keto acid cannot be redirected into central carbon metabolism. Before the branched-chain α -keto acid is secreted into the surrounding medium, microorganisms such as *Saccharomyces* and *Lactococcus* are able to decarboxylate it into the corresponding aldehyde and subsequently reduce it into a fusel alcohol via the Ehrlich pathway (Hazelwood et al. 2008; Larroy et al. 2003). For more than a century, the Ehrlich pathway was mainly studied in the food industry for off-flavor formations in cheese and beer (de Palencia et al. 2006). Current scientific interest in the Ehrlich pathway was initiated by Atsumi et al. who demonstrated the production of branched-chain alcohols from glucose in engineered *Escherchia coli* strains (Atsumi et al. 2008). As depicted in Figure 2.1, 2-ketoisovalerate and 2-ketoisocaproate, the intermediates of valine and leucine biosynthesis pathway are decarboxylated to form isobutyraldehyde and 3-methyl-1-butyraldehyde and subsequently reduced to branched-chain alcohols isobutanol and 3-methyl-1-butanol, respectively. Previous studies showed that these branched-chain alcohols could be produced by a synthetic pathway using heterologous branched-chain amino acid biosynthesis and Ehrlich pathway enzymes from *Bacillus subtilis*, *Saccharomyces cerevisiae*, and *Lactococcus lactis* (Atsumi et al. 2008; Atsumi et al. 2009; Blombach et al. 2011; Savrasova et al. 2011; Smith et al. 2010).

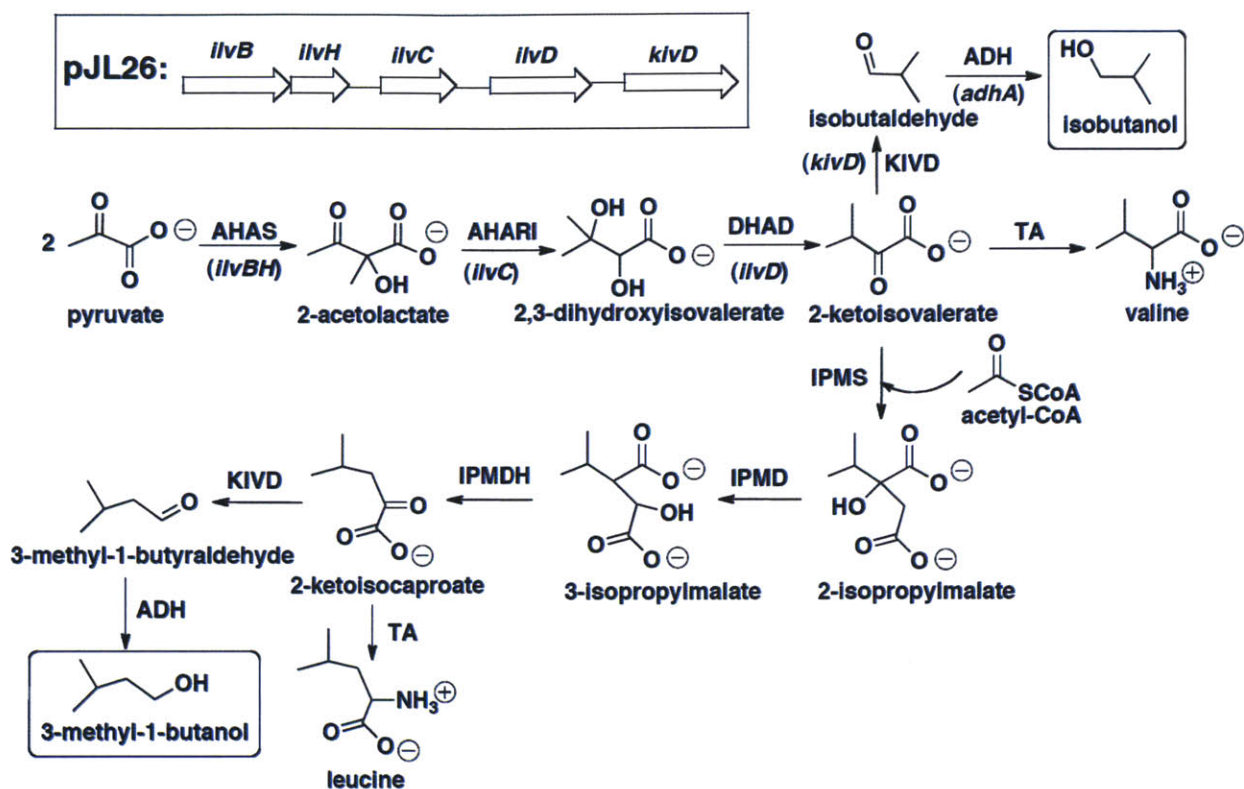


Figure 2.1: Schematic of isobutanol and 3-methyl-1-butanol production pathways. The production of isobutanol (top right, boxed) uses precursors diverted from the valine biosynthesis pathway via enzymes acetohydroxyacid synthase (AHAS), acetohydroxyacid isomeroreductase (AHARI), dihydroxyacid dehydratase (DHAD), ketoisovalerate decarboxylase (KIVD), and alcohol dehydrogenase (ADH). Redirection of 2-ketoisocaproate from leucine biosynthesis pathway via isopropylmalate synthase (IPMS), isopropylmalate dehydratase (IPMD), isopropylmalate dehydrogenase (IPMDH), KIVD, and ADH leads to the production of 3-methyl-1-butanol (lower left, boxed). In wild type cells, transaminase (TA) converts 2-ketoisovalerate and 2-ketoisocaproate to valine and leucine respectively. The isobutanol production operon (pJL26) consists of the following genes *ilvBH*, *ilvC*, *ilvD*, and *kivD* encodes for the following enzymes respectively AHAS, AHARI, DHAD, and KIVD.

Branched-chain alcohols, such as isobutanol and 3-methyl-1-butanol, have attracted both research and industrial attentions as an alternative biofuel to ethanol and biodiesel. These alcohols have approximately 98 % of the energy content of gasoline, 17 % higher than ethanol, the current gasoline-additive (Sheehan 2009). Unlike ethanol, these branched-chain alcohols have low vapor pressure, hygroscopicity, and water solubility, which make them compatible with the existing pipelines, gasoline pumps, and engines (Atsumi et al. 2008; Atsumi et al. 2009; Blombach et al. 2011; Smith et al. 2010; Yan and Liao 2009). Due to the current concerns of fossil fuel shortage and rising oil prices, use of alternative energies from solar, wind, geothermal and hydroelectric has spread. These energy sources, although effective in stationary power applications, cannot be easily or efficiently employed in current or future transportation systems (Connor and Liao 2009; Connor and Atsumi 2010). Thus alternative biofuels like branched-chain higher alcohols hold promise as a more suitable 'mobile' energy in the future. Additionally, isobutanol can be utilized as a precursor for the production of isobutylene, which is

used in large quantity by the oil refinery, rubber, and specialty chemical industries (Gogerty and Bobik 2010; Macho et al. 2001).

Ralstonia eutropha (also known as *Cuprivaoidus necator*) is a Gram-negative, facultatively chemolithoautotrophic organism (Pohlmann et al. 2006). It has long been the model organism for the study of polyhydroxybutyrate (PHB) biosynthesis. Under nutrient stress in the presence of excess carbon source, wild type *R. eutropha* can accumulate approximately 80 % of its cell dry weight (CDW) as PHB, an intracellular carbon storage material (Budde et al. 2011; Yang et al. 2010). This intracellular polymer can be isolated from the cell and processed into biodegradable and biocompatible plastic for various applications (Rehm 2003; Brigham and Sinskey 2012). Uniquely, *R. eutropha* also contains two carbon-fixation Calvin-Benson-Bassham cycle operons, two oxygen-tolerant hydrogenases, and several formate dehydrogenases and has been studied extensively for its ability to fix carbon dioxide into complex cellular molecules while obtaining energy from hydrogen or formate oxidation under ambient oxygen concentration conditions (Bowien and Kusian 2002; Ishizaki et al. 2001; Lenz et al.; Pohlmann et al. 2006; Schwartz et al. 2009). Recently, Li et al. constructed a system that couples electrochemical generation of formate with CO₂ fixation and the addition of heterologous genes for the conversion of formate to isobutanol and 3-methyl-1-butanol by *R. eutropha*. Via this electromicrobial conversion, over 140 mg/L branched-chain alcohols were synthesized in engineered *R. eutropha* strains (Li et al. 2012).

Steinbüchel et al. examined *R. eutropha* mutant strains that were defective in PHB formation and found that these mutants secreted large amounts of pyruvate into the growth medium when cultivated under nitrogen starvation (Steinbüchel and Schlegel 1989). Such findings suggest that, under stress conditions, the pyruvate dehydrogenase complex becomes less active in these *R. eutropha* strains, leading to the buildup of excess pyruvate. Additionally, it suggested that the excess carbon might be effectively redirected from PHB storage to the production of other molecules such as branched-chain alcohols. In this study, we examined the conditions for the production of branched-chain alcohols in *R. eutropha* using native branched-chain amino acid biosynthesis genes. We also surveyed numerous *R. eutropha* mutant strains constitutively expressing alcohol dehydrogenase gene isolated previously (Jendrossek et al. 1990; Steinbüchel and Schlegel 1984; Steinbüchel et al. 1987) for their ability to reduce isobutyraldehyde into isobutanol. In addition, we tested tolerance to isobutanol by wild type and mutant *R. eutropha* strains. Lastly, we demonstrated a prolonged semi-continuous flask cultivation of engineered *R. eutropha* for the production of branched-chain alcohols.

MATERIALS AND METHODS

Chemicals, bacterial strains and plasmids

Chemicals were purchased from Sigma-Aldrich unless indicated otherwise. Experiments were performed with strains and plasmids listed in Table 2.1 and Table 2.2. Primers used in the construction of these strains and plasmids are listed in Appendix 2.1. Mutant and engineered strains were all derived from wild type *R. eutropha* H16 (ATCC 17699).

Table 2.1: Strains used in this work.

Strains	Genotype	Reference
<i>R. eutropha</i>		
H16	Wild-type, gentamicin resistant (Gen ^r)	ATCC17699
Re2061	H16 Δ <i>phaCAB</i> Gen ^r	This work
CF17	H16 <i>adh</i> (Con) ethanol ⁺ 2,3-butanediol ⁺ Gen ^r	(Steinbüchel <i>et al.</i> 1987)
CF101	H16 <i>adh</i> (Con) ethanol ⁺ 2,3-butanediol ⁺ Gen ^r	(Steinbüchel <i>et al.</i> 1987)
CF106	H16 <i>adh</i> (Con) ethanol ⁺ 2,3-butanediol ⁺ Gen ^r	(Jendrossek <i>et al.</i> 1990)
CF108	H16 <i>adh</i> (Con) ethanol ⁺ 2,3-butanediol ⁺ Gen ^r	(Jendrossek <i>et al.</i> 1990)
CF303	H16 <i>adh</i> (Con) ethanol ⁺ 2,3-butanediol ⁺ Gen ^r	(Steinbüchel <i>et al.</i> 1987)
DJ21	H16 <i>adh</i> (Con) ethanol ⁺ 2,3-butanediol ⁺ Gen ^r	(Jendrossek <i>et al.</i> 1990)
Re2403	CF17 Δ <i>phaCAB</i> Gen ^r	This work
Re2404	CF101 Δ <i>phaCAB</i> Gen ^r	This work
Re2405	CF106 Δ <i>phaCAB</i> Gen ^r	This work
Re2406	CF108 Δ <i>phaCAB</i> Gen ^r	This work
Re2407	CF303 Δ <i>phaCAB</i> Gen ^r	This work
Re2401	DJ21 Δ <i>phaCAB</i> Gen ^r	This work
Re2402	DJ21 Δ <i>phaCAB, ilvE</i> Gen ^r	This work
Re2410	DJ21 Δ <i>phaCAB, ilvE, bkdAB</i> Gen ^r	This work
Re2425	DJ21 Δ <i>phaCAB, ilvE, bkdAB, aceE</i> Gen ^r	This work
<i>E. coli</i>		
S17-1	Conjugation strain for transfer of plasmids into <i>R. eutropha</i>	(Simon <i>et al.</i> , 1983)

Table 2.2: Plasmids used in this work.

Plasmids	Genotype	Reference
pJV7	pJQ200Kan with Δ <i>phaC1</i> allele inserted into BamHI restriction site, confers kanamycin resistance (Kan ^r)	(Budde <i>et al.</i> , 2011a)
pJL33	pJV7 with Δ <i>phaC1</i> allele removed by XbaI and SacI digestion and replace with <i>phaCAB</i> allele (Kan ^r)	This work
pCJB6	pJV7 with Δ <i>phaC1</i> allele removed by XbaI and SacI digestion and replace with Δ <i>ilvE</i> allele (Kan ^r)	This work
pCJB7	pJV7 with Δ <i>phaC1</i> allele removed by XbaI and SacI digestion and replace with Δ <i>bkdAB</i> allele (Kan ^r)	This work
pJL32	pJV7 with Δ <i>phaC1</i> allele removed by XbaI and SacI digestion and replace with Δ <i>aceE</i> allele (Kan ^r)	This work
pBBR1MCS-2	Broad-host-range cloning vector (Kan ^r)	(Kovach <i>et al.</i> , 1996)
pJL23	pBBR1MCS-2 with <i>L. lactis kivD</i> gene and <i>R. eutropha adh</i> (H16_A0757) alcohol dehydrogenase	This work

pJL21	gene inserted into the multiple cloning site (Kan ^r) pBBR1MCS-2 with <i>R. eutropha</i> H16_A0861 alcohol dehydrogenase gene inserted into the multiple cloning site (Kan ^r)	This work
pJL20	pBBR1MCS-2 with <i>R. eutropha</i> H16_A0757 alcohol dehydrogenase gene inserted into the multiple cloning site (Kan ^r)	This work
pJL22	pBBR1MCS-2 with <i>E. coli yqhD</i> alcohol dehydrogenase gene inserted into the multiple cloning site (Kan ^r)	This work
pJL26	pBBR1MCS-2 with branched-chain alcohol production operon (<i>ilvBHCDkivd</i>) inserted into the multiple cloning site (Kan ^r)	This work

Growth media and cultivation conditions

All *R. eutropha* strains were cultivated aerobically in rich and minimal media at 30°C. Rich medium consisted of 2.75 % (w/v) dextrose-free tryptic soy broth (TSB) (Becton Dickinson, Sparks, MD). Minimal medium used to cultivate *R. eutropha* was formulated as described previously (Lu et al. 2012). Carbon sources used in minimal medium cultivations were 2 % (final w/v) fructose or sodium gluconate. For all *R. eutropha* cultures, 10 µg/mL final concentration of gentamicin was added. In cultivations of *R. eutropha* containing plasmid, kanamycin at 200 µg/mL final concentration was also supplemented.

A single colony of *R. eutropha* from a TSB agar plate was used to inoculate 5 mL of TSB medium. The culture was then incubated on a roller drum for 24 h at 30°C before being used to inoculate a flask culture of 100 mL minimal medium, containing carbon sources mentioned above, to an initial OD₆₀₀ of 0.1. The minimal medium culture was continuously shaken in a 30°C incubator at 200 rpm. At intermittent time points, aliquots were removed from the flask culture for analysis, as described below.

Plasmid and strain construction

Standard molecular biology techniques were performed for all DNA manipulations (Chong, 2001). DNA sequence amplification was achieved using Phusion DNA polymerase (New England Biolabs, Ipswich, MA). QIAquick gel extraction kit (Qiagen, Valencia, CA) was used for gel purifications of all DNA products. Plasmid extractions were carried out using QIAprep spin miniprep kit (Qiagen, Valencia, CA). Restriction enzymes used in this study were from New England Biolabs (Ipswich, MA).

The plasmids for markerless deletion were constructed by first amplifying approximately 500 base pairs of DNA sequences upstream and downstream of the gene targeted for deletion using primers with identical sequence overlap at the end (Appendix 2.1). Overlap PCR using these primers resulted in a DNA fragment of approximately 1,000 bp in length that contained both the upstream and downstream region of the target deletion gene. Both the resulting DNA fragment and the parent plasmid, pJV7 (Budde et al. 2010) (Table 2.2), were digested with the restriction enzymes XbaI and SacI or BamHI. The digested plasmid and DNA fragment were then ligated together and transformed into high efficiency *Escherichia coli* DH10-beta competent cells (New England Biolabs, Ipswich, MA) to create the gene deletion plasmid. The gene

deletion plasmid was then isolated from *E. coli* DH10-beta cells and transformed into *E. coli* S17-1 (Simon et al. 1983), which was used as a donor for the conjugative transfer of mobilizable plasmids. A standard mating-procedure was performed to introduce the gene deletion plasmid into *R. eutropha* via conjugation (Slater et al. 1998). Gene deletions from *R. eutropha* H16 genome were carried out by a standard procedure described previously (Quandt and Hynes 1993; York et al. 2001). Deletion strains were screened by diagnostic PCR with pairs of internal and external primer sets (Appendix 2.1).

A synthetic isobutanol production operon was constructed by overlap PCR using primers with identical sequence overlap. Each gene was first amplified, purified, and sequenced. Then an artificial ribosome-binding site (5'-AAAGGAGG-3') and a nucleotide linker sequence (5'-ACAACC-3') were incorporated in the beginning of each gene. Finally, all the genes were ligated together in an artificial operon via multiple rounds of overlap PCR. The isobutanol production operon and broad-host-range cloning vector pBBR1MCS-2 (Kovach et al. 1995) were digested with BamHI and SacII. The digested vector and operon DNA insert were ligated, transformed, and transferred into *R. eutropha* as described above.

Polymer quantification

The cell dry weight (CDW) and PHB content were measured as described previously (Karr et al. 1983; York et al. 2003).

Branched-chain alcohols extraction and detection

Culture aliquots, taken at various time points, were centrifuged at $4,000 \times g$ to separate the pellet from the supernatant. Isobutanol and 3-methyl-1-butanol were extracted from the supernatant using chloroform in a 1:1 ratio. The concentrations of isobutanol and 3-methyl-1-butanol were determined using gas chromatograph (GC; Agilent Technologies, Santa Clara, CA) with a DB-Wax column (Agilent Technologies, 30 m x 0.32 mm x 0.5 μ m) and a flame ionization detector. The split ratio is 20:1 and a 2 μ L sample was injected at each run. Hydrogen was used as the carrier gas at a flow rate of 1.1 mL/min. The oven was held at 35°C for 5 min, then heated to 230°C at a rate of 12°C/min, and lastly held at 220°C for 5 min. Commercial isobutanol and 3-methyl-1-butanol were analyzed on the GC as described above for standards.

Carbon, nitrogen, reducing-cofactor analysis

Culture supernatants were filtered and injected into HPLC to determine concentrations of fructose or gluconate, and pyruvate. The HPLC was equipped with an ion exchange column, and the detection methods used were previously described (Kurosawa et al. 2010). Ammonium concentrations in the supernatant were measured using an ammonium assay kit (Sigma-Aldrich) following the manufacturer's instructions. The intracellular concentrations of NADH and NADPH were measured using modified assays from previously described works (Leyval et al. 2003; Zhang et al. 2000). The concentrations of NADH and NADPH were normalized per colony forming unit (CFU).

Product tolerance assay

Cultures of *R. eutropha* were grown in minimal medium with 2 % fructose and 0.05 % NH₄Cl. Various concentrations of isobutanol (0%, 0.2%, 0.5%, 0.8%, and 1% v/v) were added to the growth media at 0 h. Growth was monitored by measuring OD₆₀₀ and colony counting units (CFU) per mL culture intermittently throughout the 96 h cultivation time. Relative viability was calculated by a modified tolerance assay described by Smith et al. (Smith et al. 2010). Briefly, CFU measurements of remaining viable cells cultured in the presence of isobutanol were normalized with the values obtained from cells cultured in the absence of isobutanol, 24 h after inoculation.

Enzymatic activity assays

R. eutropha cultures harvested at different time points were pelleted and stored at -80°C for activity assays of acetohydroxyacid synthase (AHAS), acetohydroxyacid isomeroreductase (AHAIR), dihydroxyacid dehydratase (DHAH), ketoisovalerate decarboxylase (KIVD), and alcohol dehydrogenase (ADH). Cell lysates were prepared by thawing the frozen pellets on ice and resuspending them in phosphate buffered saline. Zirconia/silica beads (0.1 mm; BioSpec Products, Bartlesville, OK) were added to the resuspended cells. These samples were shaken vigorously three times at 5.0 m/s for 30 s, with a 5 min rest between each treatment at 4°C by FastPrep-24 (MP Biomedicals, Solon, OH). Cellular debris and beads were removed by centrifugation for 10 min at 4°C and 6,500 × g. The soluble cell lysates were filtered through 0.2 µm low-protein-binding Supor syringe filters (Pall, NY) and stored on ice for enzymatic assays. Protein concentrations were determined by a modified Bradford assay (Zor and Selinger, 1996) using bovine serum albumin as the protein concentration standard.

The AHAS, AHAIR, and DHAD activity assays were based and modified from Leyval, et al. (Leyval et al. 2003). The AHAS activity assay is a discontinuous assay that converts pyruvate first to α-acetolactate and finally to acetoin. The 1 mL assay mixture contained 100 mM potassium phosphate buffer at pH 7.0, 50 mM sodium pyruvate, 100 mM MgCl₂, 100 µM thiamine pyrophosphate (TPP), and cell lysate. The reaction was initiated by the addition of sodium pyruvate at 30°C and terminated by acidifying 100 µL aliquots of assay mixture with 10 µL 50% H₂SO₄ every 3 min for 30 min total. The acidified assay mixture was then incubated at 37°C for 30 min to allow the formation of acetoin from α-acetolactate. The acetoin formed was quantified by the Voges-Proskauer method (Westerfield, 1945) with a slight adjustment of mixing 35 µL instead of 25 µL of 1-naphthol (5 % w/v in 2.5 M NaOH). The mixture of acetoin, 1-naphthol, and creatine created a pink color and was measured at 535 nm with Varioskan Flash Plate Reader (Thermo Scientific, Asheville, NC). Pure acetoin was used as a standard.

The AHAIR activity assay mixture (1 mL total volume) contains 100 mM potassium phosphate buffer (pH 7.0), 10 mM α-acetolactate, 3 mM MgCl₂, 0.1 mM NADPH, and cell lysate. The reaction was initiated by the addition of α-acetolactate at 30°C. A spectrophotometer (Agilent 8453 UV-visible Kinetic Mode) was used to monitor the reaction at 340 nm for the consumption of NADPH. The α-acetolactate was chemically synthesized based on the previously developed method (Leyval et al. 2003). Enzyme activity was calculated in µmol of NADPH oxidized using its molar extinction coefficient of 6220 M⁻¹cm⁻¹.

The DHAD activity assay is also a discontinuous assay. The 1 mL reaction mixture contained 100 mM potassium phosphate buffer (pH 7.0), 5 mM MgCl₂, 10 mM DL-α,β-dihydroxyisovalerate, and cell lysate. Substrate DL-α,β-dihydroxyisovalerate was added to initiate the reaction. Every 2 min, for a total of 20 min, 100 µL of the reaction was removed and

terminated by mixing with 12.5 μL trichloroacetic acid (10 % v/v). Terminated reaction mixtures were mixed with 25 μL saturated 2,4-dinitrophenylhydrazine in 2 M HCl and incubated at room temperature for 20 min and afterwards neutralized with 85 μL of 2 M NaOH for 30 min. The product derivative (α -ketoisovalerate-dinitrophenylhydrazone) was detected at 540 nm using the plate reader. Commercial α -ketoisovaleric acid sodium salt served as standard.

The KIVD activity assay was adapted and modified from de la Plaza et al. and de Palencia et al. (de la Plaza et al. 2004; de Palencia et al. 2006). The assay couples the formation of isobutyraldehyde, using aldehyde dehydrogenase from *Saccharomyces cerevisiae*, to the formation of isobutyrate. In the 1 mL assay mixture were 100 mM potassium phosphate buffer (pH 7.0), 15 mM pyrazole, 30 mM TPP, 1 mM NAD^+ , 3 μM MgCl_2 , 20 mM α -ketoisovaleric acid, 1 mM DTT, 0.5 mg aldehyde dehydrogenase, and cell lysate. The reaction was initiated by the addition of α -ketoisovaleric acid and monitored at 340 nm for the reduction of NAD^+ . Enzyme activity was calculated in μmol of NAD^+ reduced, using the molar extinction coefficient of $6220 \text{ M}^{-1}\text{cm}^{-1}$.

The ADH activity assay was based on Steinbüchel, et al. (Steinbüchel and Schlegel 1984). The activity was monitored at 340 nm and the 1 mL enzyme assay mixture consists of 95 mM citrate buffer (pH 5.8), 0.1 mM NADPH, 200 mM isobutyraldehyde, and cell lysate. Enzyme activity was calculated in μmol of NADPH oxidized, using the molar extinction coefficient mentioned above.

All enzyme activities discussed in this work are a result of triplicate assays reported \pm standard deviation. As controls, assays were conducted in the absence of cell lysates and also separately in the absence of substrates. Enzyme unit (U) was defined as 1 μmol product formed per min.

Semi-continuous flask cultures

Triplicate cultures of Re2425/pJL26 (Table 2.1) were performed in 100 mL minimal medium containing 1 % fructose and 0.05 % NH_4Cl . Every 24 h, the growth media containing branched-chain alcohols were separated from the cells via centrifugation at $4,000 \times g$. Isobutanol and 3-methyl-1-butanol were extracted from the growth media and analyzed as described above. Fresh media (without branched-chain alcohols) were then added to the cells in each culture. The cultures continued for another 24 h, until the process was repeated. This cycle was continued for 50 days. At each 24 h cycle, OD_{600} and concentrations of branched-chain alcohols were measured.

RESULTS

Redirecting excess carbon and reducing-equivalents

Wild type *R. eutropha* produces PHB as an intracellular carbon and energy storage polymer during nutrient stress in the presence of excess carbon (Potter et al. 2004). In order to redirect the excess carbon from PHB, the *phaCAB* operon, which encodes the polymer biosynthesis enzymes β -ketothiolase (PhaA), acetoacetyl-CoA reductase (PhaB), and PHB synthase (PhaC) (Pohlmann et al. 2006), was eliminated from the *R. eutropha* genome. As shown in Table 2.3, the wild type (H16) was able to produce more than 80 % of CDW as PHB, but strain Re2061 (H16 Δ *phaCAB*), produced no detectable PHB after 96 h of growth. Deletion

of the *phaCAB* operon did not affect cell growth significantly, since the residual CDW were similar in both strains. Compared to H16, Re2061 utilized 0.5 % (w/v) less gluconate during growth. Re2061 also secreted pyruvate into the growth medium, but H16 did not secrete any pyruvate throughout the entire growth period. This finding was similar to those reported by Steinbüchel et al. (Steinbüchel and Schlegel 1989). In addition, Re2061 cells contained greater concentrations of the reducing-cofactor NADH than H16 (Table 2.3). Since PHB acts as a carbon and energy storage mechanism in *R. eutropha* (Schwartz et al. 2009), Re2061 cells used less carbon source, secreted pyruvate into the extracellular milieu, and retained more energy in the form of NADH, likely directly resulting from their inability to produce polymer.

Table 2.3: Physiologic differences between wild type *R. eutropha* (H16) and Re2061 (H16 Δ *phaCAB*)^a.

Strains	Residua I CDW	[Gluc] (% w/v)	[Pyr] (% w/v)	[PHB] (% CDW)	[NADH] (pmol/CFU)	[NADPH] (pmol/CFU)
H16	1.1±0.1	1.2±0.03	0	83±2.9	0.01±0	7.5E-5±1E-5
Re2061	1.3±0.2	0.7±0.04	0.6±0.01	0	0.04±0.002	8.2E-5±0.7E-5
<i>p</i> -value	NA	6.5E-5	NA	NA	1.3E-5	0.36

^aThe values presented were measured at the end of 96 h growth period. Concentrations of gluconate (Gluc) consumed, pyruvate (Pyr) and PHB produced were detected by HPLC as discussed in Materials and Methods. Intracellular reducing equivalents NADH and NADPH were measured using a cofactor cycling assay (Ref) and normalized per each colony forming unit (CFU). Each value represents the mean ± standard error on n = 3. Student's *t*-test was performed to evaluate the significance of differences in the concentrations of gluconate, NADH, and NADPH.

Assembly of a branched-chain alcohols biosynthesis operon

In order for *R. eutropha* to appropriate its branched-chain amino acid pathway, specifically the intermediates α -ketoisovalerate and α -ketoisocaproate, for the production of isobutyraldehyde and 3-methyl-1-butyraldehyde respectively, a heterologous ketoisovalerate decarboxylase (KivD) is needed. The *kivD* gene from *L. lactis* (de la Plaza et al. 2004), which encodes a ketoisovalerate decarboxylase enzyme was expressed and found active towards α -ketoisovalerate when expressed on a plasmid in *R. eutropha* (Data not shown). Subsequently, isobutyraldehyde and 3-methyl-1-butyraldehyde are reduced to their corresponding alcohols by alcohol dehydrogenase with short-chain substrate specificity. In an environment with ambient oxygen concentrations, *R. eutropha* does not exhibit any alcohol dehydrogenase (ADH) activity (Figure 2.4A), despite the presence of various putative alcohol dehydrogenase genes on both chromosomes. A search in the *R. eutropha* H16 genome database (NCBI: <http://www.ncbi.nlm.nih.gov/>) revealed putative short-chain substrate *adh* genes, locus tags H16_A0757 (*adh*) and H16_A0861 (*adhA*). The sequence of *adh* is similar to the well-studied *E. coli* Zn-dependent NADPH alcohol dehydrogenase (Jarboe 2011), YqhD (data not shown). Genes encoding *adh*, *adhA*, and *yqhD* were separately inserted into a plasmid under the control of a constitutive promoter (pBBR1MCS-2 (Fukui et al. 2011)) to create pJL20, pJL21, and pJL22 respectively. The plasmid-borne *adh* genes were introduced into Re2061, and assayed for ADH activity towards isobutyraldehyde. ADH, AdhA, and YqhD were active toward isobutyraldehyde (Figure 2.4A) and prefer NADPH as cofactor (data not shown). ADH and

YqhD had similar activities of 180 mU/mg and 200 mU/mg, respectively, whereas AdhA at 20 mU/mg was less active towards isobutyraldehyde.

Expressing *kivD* and *adh* in Re2061 (Re2061/pJL23) allowed the strain to produce 10 mg/L isobutanol from fructose (Figure 2.2). Such low production suggests that there was insufficient α -ketoisovalerate synthesized from the native branched-chain amino acid biosynthesis pathway to be diverted to isobutanol. To test this hypothesis, 1 % (w/v) pyruvate and 1 % (w/v) α -ketoisovaleric acid were separately supplemented to the growth media. Addition of pyruvate increased isobutanol production to 350 mg/L and production reached 4.5 g/L after supplying the growth media with α -ketoisovaleric acid (Figure 2.2). Thus, we concluded that indeed insufficient carbon was being shunted through the branched-chain amino acid pathway in Re2061/pJL23 for the production of isobutanol. To address this, the *ilvBHCD* genes from the valine biosynthesis pathway in *R. eutropha* H16 were overexpressed, along with *kivD*, on plasmid pJL26 (Table 2.2, Figure 2.1). Appendix 2.2 compares the activities of valine biosynthesis pathway enzymes from wild type *R. eutropha* with engineered strains containing plasmid pJL26 at 24 h. Overexpression of *ilvBHCD* and *kivD* genes from the plasmid pJL26 increased the overall activities of valine biosynthesis pathway enzymes.

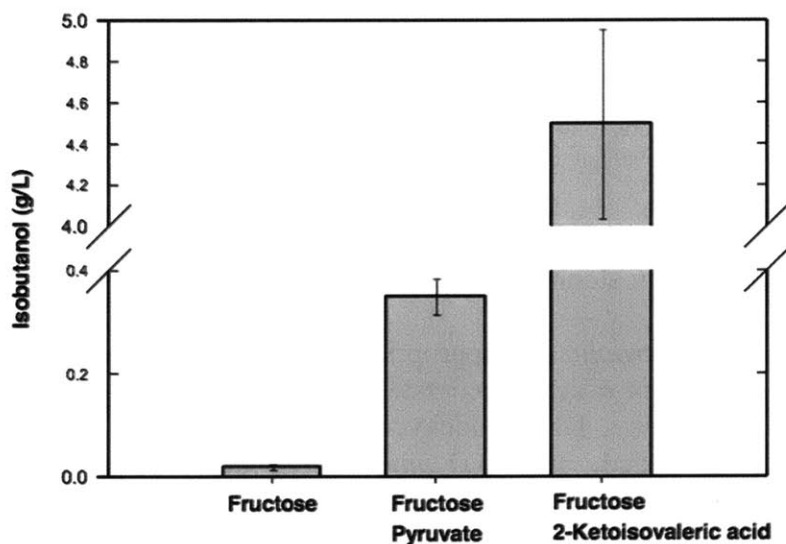


Figure 2.2: Production of isobutanol in strain Re2061/pJL23. *R. eutropha* Re2061/pJL23 (see Table 2.1) was cultivated in minimal media with 0.05 % NH_4Cl with the following carbon sources: 2 % w/v Fructose, 2 % w/v Fructose with 1 % w/v Pyruvate, or 2 % w/v Fructose with 1 % w/v 2-ketoisovaleric acid. Each value represents the mean \pm standard error (error bars) of $n = 3$.

R. eutropha adh mutant has isobutyraldehyde dehydrogenase activity

Steinbüchel et al. demonstrated that the *adh* gene in wild type *R. eutropha* was only expressed and active when cells were cultivated under anaerobic conditions. It was hypothesized that such gene activation increases the usage of reducing power in the absence of the terminal electron acceptor, oxygen (Steinbüchel and Schlegel 1984; Steinbüchel et al. 1987). In previous studies, a number of *R. eutropha* mutant strains constitutively expressing *adh* under aerobic conditions were isolated after continuous growth of H16 on ethanol and/or 2,3-butanediol and characterized for their alcohol dehydrogenase activities (Jendrossek et al. 1990; Steinbüchel et al.

1987). We demonstrate, as shown in Figure 2.4A, that these strains also reduce isobutyraldehyde. In all cases, the cofactor NADPH is preferred over NADH for the reduction of isobutyraldehyde (data not shown). Strain Re2403 (CF17 Δ *phaCAB*) showed similar activity compared to strains that overexpress ADH and YqhD. The strain with the most active isobutyraldehyde dehydrogenase activity (300 mU/mg) was Re2401 (DJ21 Δ *phaCAB*) (Figure 2.3A). DJ21 was also found to have the highest activity towards the reduction of 2,3-butanediol and ethanol compared to all other *adh* mutant strains (Jendrossek et al. 1990).

It is hypothesized that the differences in activity of ADH in the mutant strains compared to plasmid-borne ADH could be due to mutation in the open reading frame (ORF) of the gene and/or in the promoter region. Therefore, the *adh* gene, including 100 bases up and downstream of the gene, of strains H16, CF17, CF303, and DJ21 were cloned and inserted into a TOPO plasmid separately. The clones were sequenced using two pairs of internal and external primers to cover the entire length of the *adh* gene. Compared to wild type H16, using ClustalW (EMBL-EBI: <http://www.ebi.ac.uk/Tools/msa/clustalw2/>), *adh* of strains CF17, CF303, and DJ21 did not have any mutations in the *adh* ORF (sequence not shown); however, mutations were detected in the promoter regions of *adh* (Figure 2.3). The results were similar to those of Jendrossek, et al. All three mutants have mutations at the guanine on position -77 from the start codon. In DJ21, this guanine was deleted, whereas it was substituted by a thymine in CF17 and CF303. Additionally the thymine at position -86 was substituted by a cytosine in CF17 (Figure 2.3). Without having sequenced the entire genome of the mutant strains, it is possible that mutations could have occurred on other regulatory genes in these mutant strains, that contribute to the constitutive expression of *adh*. From multiple sequence alignment, conclusion can be drawn that the presence of guanine at position -77 of *adh* promoter region is required for the repression of the gene under aerobic conditions, since all three mutants with derepressed *adh* had mutations at this position. One can insert such mutation in the wild type H16 genome and analyze the specific promoter mutation that derepresses the *adh* expression.

```

H16          NNTACNNNNCCGTGCCTATCAGTGGAGTAAGCGGGCCGGCAACGTCCCGCACCCTCCACC 59
DJ21         ----NNNNCCGTGCCTATCA  TGAGCGGGCCGGCAACGTCCCGCACCCTCCACCACC 40
              *****
H16          CACCGCGCATCCCTCTGCGCCTTCCCTGGGAGCAACGCATGACCGCAATGATGAAAGCCG 119
DJ21         CACCGCGCATCCCTCTGCGCCTTCCCTGGGAGCAACGCATGACCGCAATGATGAAAGCCG 100
              *****

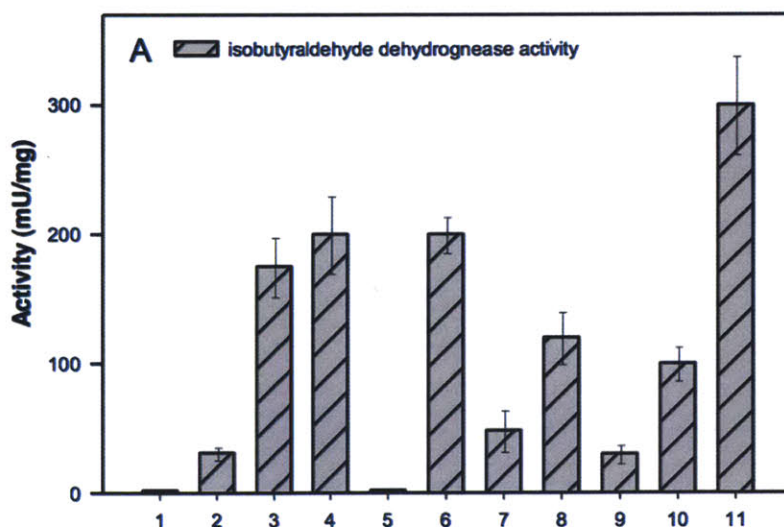
H16          NNTACNNNNCCGTGCCTATCAGTGGAGTAAGCGGGCCGGCAACGTCCCGCACCCTCCACC 59
CF17         ----NNNNNNGGCCTATCATTTGAGTAAGCGGGCCGGCAACGTCCCGCACCCTCCACC 39
              ****  *
H16          CACCGCGCATCCCTCTGCGCCTTCCCTGGGAGCAACGCATGACCGCAATGATGAAAGCCG 119
CF17         CACCGCGCATCCCTCTGCGCCTTCCCTGGGAGCAACGCATGACCGCAATGATGAAAGCCG 99
              *****

H16          NNTACNNNNCCGTGCCTATCAGTGGAGTAAGCGGGCCGGCAACGTCCCGCACCCTCCACC 59
CF303        ----NNNNTCCGTGCCTATCATTTGAGTAAGCGGGCCGGCAACGTCCCGCACCCTCCACC 54
              ***  *  *
H16          CACCGCGCATCCCTCTGCGCCTTCCCTGGGAGCAACGCATGACCGCAATGATGAAAGCCG 119
CF303        CACCGCGCATCCCTCTGCGCCTTCCCTGGGAGCAACGCATGACCGCAATGATGAAAGCCG 114
              *****

```

Figure 2.3: Upstream nucleotide sequences in the *adh* gene of *R. etropha* H16 compared to mutants CF17, CF303, and DJ21 using ClustalW. The starting-codon ATG is highlighted in yellow. Mutation(s) are boxed in green.

The engineered isobutanol production plasmid, pJL26, was incorporated into each of the constitutive ADH mutant strains (CF17, CF 101, CF 106, CF 108 CF 303 and DJ21) from which the *phaCAB* operon was previously deleted (Table 2.2). Growth rates were similar among all these strains (Appendix 2.3). With valine biosynthesis pathway genes overexpressed on pJL26, the production of isobutanol and 3-methyl-1-butanol was increased by at least 10 fold (Figure 2.4B). Since wild type *R. etropha* is not able to reduce isobutyraldehyde under ambient culture conditions, no isobutanol or 3-methyl-1-butanol were produced by Re2061/pJL26. Strains Re2403, Re2404, Re2405, Re2406, and Re2407, all containing pJL26, each produced over 100 mg/L isobutanol. Re2401/pJL26, with the highest isobutyraldehyde dehydrogenase activity, also produced the highest amount of isobutanol (200 mg/L). All strains produced similar amount (30 mg/L) of 3-methyl-1-butanol, likely due to low activity of the IPMS enzyme, responsible for the conversion of α -ketovalerate to α -isopropylmalate (Figure 2.4B). The amounts of isobutanol produced increased concomitant with higher measured activities of ADH towards isobutyraldehyde and vice versa (Figure 2.4).



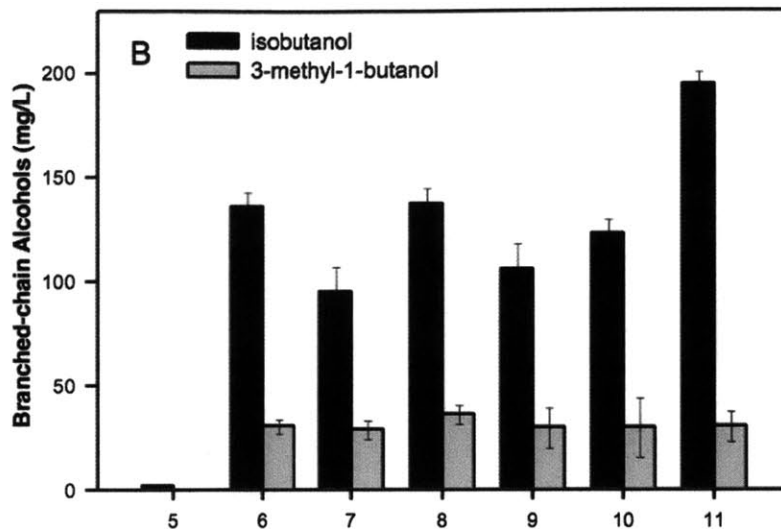


Figure 2.4: Isobutyraldehyde dehydrogenase activity (A) and production of branched-chain alcohols (B) by *R. eutropha* wild type and ADH mutant strains harboring isobutanol production plasmids (see Table 2.2).

1: Re2061 (H16 Δ *phaCAB*); 2: Re2061/pJL21 (H16 Δ *phaCAB/padhA*); 3: Re2061/pJL20 (H16 Δ *phaCAB/padh*); 4: Re2061/pJL22 (H16 Δ *phaCAB/pyqhD*); 5: Re2061/pBBR1MCS-2; 6: Re2403/pJL26 (CF17 Δ *phaCAB/pilvBHCDkivD*); 7: Re2404/pJL26 (CF101 Δ *phaCAB/pilvBHCDkivD*); 8: Re2405/pJL26 (CF106 Δ *phaCAB/pilvBHCDkivD*); 9: Re2406/pJL26 (CF108 Δ *phaCAB/pilvBHCDkivD*); 10: Re2407/pJL26 (CF303 Δ *phaCAB/pilvBHCDkivD*); 11: Re2401/pJL26 (DJ21 Δ *phaCAB/pilvBHCDkivD*). Data points represent the mean values of $n = 3 \pm$ standard deviation (error bars).

Figure 2.5 summarizes the enzymatic activities of isobutanol production pathway enzymes in Re2401/pJL26 over a 96 h cultivation period. All enzymes were active throughout the entire cultivation time. AHAS, AHAI, DHAD, and KIVD exhibited the same trend of decrease in activity over time, since these genes were engineered into an operon (*ilvBHCDkivD*), overexpressed from a single promoter on plasmid pJL26. Alcohol dehydrogenase, on the other hand, was constitutively expressed in our engineered strain, thus its activity was correlated with cell growth. AHAS, being a potentially rate limiting node in the branched-chain biosynthesis pathway, exhibited the lowest activity of all enzymes tested (9 mU/mg at 24 h). KivD also exhibited relatively low activity in *R. eutropha*, as it is a heterologously expressed enzyme from gene originating in the AT-rich bacterium, *L. lactis* (Figure 2.5).

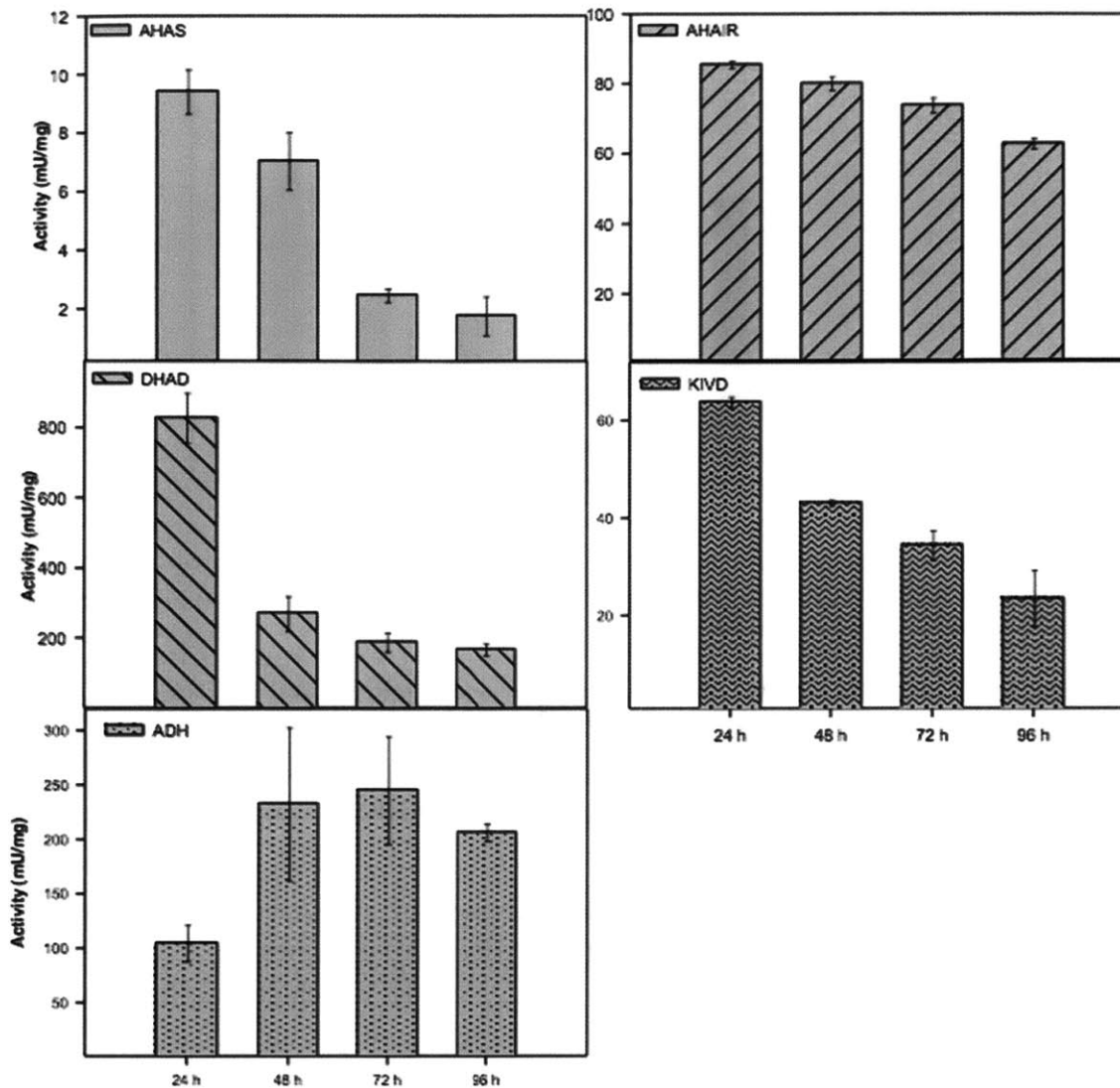


Figure 2.5: Activities of isobutanol production pathway enzymes: AHAS-acetohydroxyacid synthase, AHAIR-acetohydroxyacid isomeroeductase, DHAD-dihydroxyacid dehydratase, KIVD-ketoisovalerate decarboxylase, and ADH-alcohol dehydrogenase over the course of a 96 h culture of Re2401/pJL26. Each enzymatic unit (U) is defined as 1 μmol product formed per min. Average values from three experiments were plotted with error bars representing the standard deviation.

Engineered *R. eutropha* strains exhibit greater isobutanol tolerance than wild type

Short chain alcohols like isobutanol are known to cause toxicity to organisms by inserting themselves in the phospholipid membrane, thus causing membrane fluidity and cell death (Atsumi et al. 2010b; Baer et al. 1987; Minty et al. 2011; Vollherbst-Schneck et al. 1984). Isobutanol tolerance by *R. eutropha* wild type and engineered strains was evaluated and summarized in Table 2.4. After 24 h, all strains had grown to the same levels ($\text{OD}_{600} \approx 2.3$, $\text{CFU/mL} \approx 10^8$) in the absence of isobutanol. In the presence of 0.2 % (v/v) isobutanol, only strains Re2403 and Re2405 experienced any toxicity. Re2403 was unable to grow, and relative viability of Re2405 was decreased by $\sim 70\%$ in the presence of 0.2 % (v/v) isobutanol. In the presence of 0.5 % (v/v) isobutanol concentrations, relative viability of wild type cells was

decreased by half, while Re2406, Re2407 and Re2401 experienced no toxicity effects from this concentration of isobutanol. Concentrations of isobutanol at 0.8 % to 1.0 % (v/v) were extremely toxic to all strains tested, with nearly no cell growth observed (Table 2.4). Since *R. eutropha* mutant strains contained an active ADH enzyme under the conditions studied here, they were likely able to convert the isobutanol to other less toxic molecules, thus experiencing less isobutanol toxicity than wild type at concentrations lower than 0.8 % (v/v).

Table 2.4: Isobutanol tolerance of *R. eutropha* strains: Re2061 (H16 Δ *phaCAB*), Re2401 (DJ21 Δ *phaCAB*), Re2403 (CF17 Δ *phaCAB*), Re2404 (CF101 Δ *phaCAB*), Re2405 (CF106 Δ *phaCAB*), Re2406 (CF108 Δ *phaCAB*), and Re207 (CF303 Δ *phaCAB*)^a.

Strains	CFU at 24 h (0% IBT)	Relative Viability (0.2% IBT)	Relative Viability (0.5% IBT)	Relative Viability (0.8% IBT)	Relative Viability (1% IBT)
Re2061	1.4E9	102	50	8	2
Re2403	3.4E9	2	2	2	1
Re2404	8.2E8	103	13	1	1
Re2405	6.0E8	24	7	1	1
Re2406	9.0E8	100	101	11	2
Re2407	7.2E8	108	111	12	2
Re2401	4.0E8	105	107	16	3

^aIsobutanol (IBT) at 0, 0.2, 0.5, 0.8, and 1 (v/v) % were added to minimal media. Growth of *R. eutropha* wild type Re2061 and Δ *phaCAB* of ADH mutant strains were monitored. Calculation of relative viability was based on the ratio between CFU of cells grown in isobutanol to CFU of cells grown without isobutanol at 24 h. Each value represents n = 3.

Production of branched-chain alcohols in response to nutrient stress

As mentioned previously, intracellular PHB is produced when the cells undergo nutrient stress, such as nitrogen or phosphorus limitation (Khanna and Srivastava 2005). In our initial isobutanol production experiments, the growth medium contained 2 % fructose and 0.05 % NH₄Cl. Under these conditions, *R. eutropha* cells became nitrogen limited by 24 h, and the production of isobutanol was detected after this time (Appendix 2.4). To test if the production of isobutanol was also associated with nitrogen starvation, different concentrations of NH₄Cl (0.07 %, 0.12 %, 0.27 %, and 0.4 % w/v) were used in cultivations of Re2401/pJL26. Results in Figure 2.6A demonstrate the amounts of NH₄Cl present in the growth media measured enzymatically (see Materials and Methods) at various time points, while Figure 2.6B revealed the amount of isobutanol produced in these cultures. At high NH₄Cl concentrations (0.27 and 0.4 %), Re2401/pJL26 cells were unable to utilize the entire amount of nitrogen source, and the production of isobutanol was extremely low (30 mg/L and 20 mg/L respectively). On the other hand, when the NH₄Cl concentrations were lower, at 0.07 and 0.12 %, the cells entered nitrogen limitation at approximately 24 h, and isobutanol production initiated after nitrogen depletion and reached ~170 mg/L (Figure 2.6). Similar results were seen with phosphorus limitation (data not shown). These results suggest that, under nutrient-limited conditions, engineered *R. eutropha* could convert carbon that would otherwise be used for the secreted pyruvate to other molecules like branched-chain alcohols.

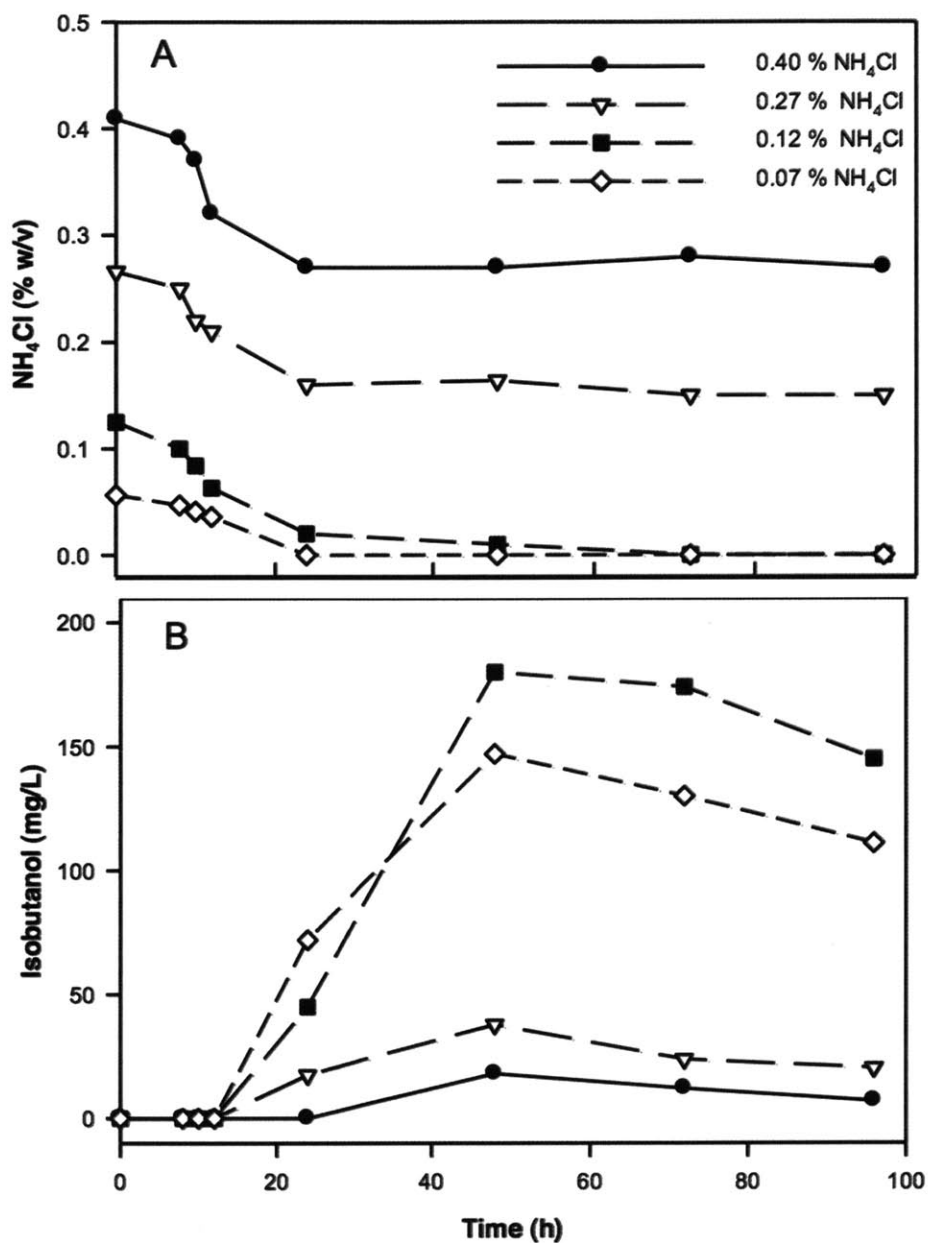


Figure 2.6: Effect of nitrogen concentrations, in the form of NH₄Cl, on the production of isobutanol by Re2401/pJL26 (DJ21 Δ *phaCAB*/*pilvBHCDkivD*). (A) Nitrogen concentrations at various growth time points; (B) Isobutanol produced and collected from the growth media.

Production optimization

R. eutropha strain Re2401/pJL26 was able to produce 150 mg/L isobutanol and 28 mg/L 3-methyl-1-butanol in flask cultures using fructose as the main carbon source. In order to improve this production yield, we identified and deleted various carbon sinks from the genome of Re2401. First, the valine-specific transaminase (*ilvE*) gene, the product of which converts 2-ketoisovalerate to valine, was deleted to create strain Re2402. The resulting strain did not become a valine auxotroph (data not shown), since other *ilvE* homologs specific for leucine or

isoleucine biosynthesis are present in *R. eutropha* and could help catalyze valine biosynthesis in order to ensure the survival of the cells in the absence of an intact *ilvE* gene and valine supplementation. Re2402/pJL26 was improved in isobutanol production by 33 %, compared to Re2401/pJL26 (Figure 2.7). Subsequently, the *bkdAB* operon, which encodes for a branched-chain keto acid dehydrogenase complex for conversion of α -ketoisovalerate to isobutyryl-CoA, was also eliminated from Re2402 to produce strain Re2410. Re2410/pJL26 was boosted in isobutanol production by only an extra 5 % compared to Re2402/pJL26, possibly because isobutyryl-CoA was not the prominent α -ketoisovalerate sink present in *R. eutropha*. Lastly, pyruvate dehydrogenase complex enzyme, encoded by *aceE*, was deleted in Re2410 to produce strain Re2425. These genetic manipulations in Re2425/pJL26 enhanced the production of isobutanol to 270 mg/L, an 80 % increase from the production of Re2401/pJL26 (Figure 2.7). Elimination of these genes did not affect the overall growth of the engineered *R. eutropha* strain (Appendix 2.3).

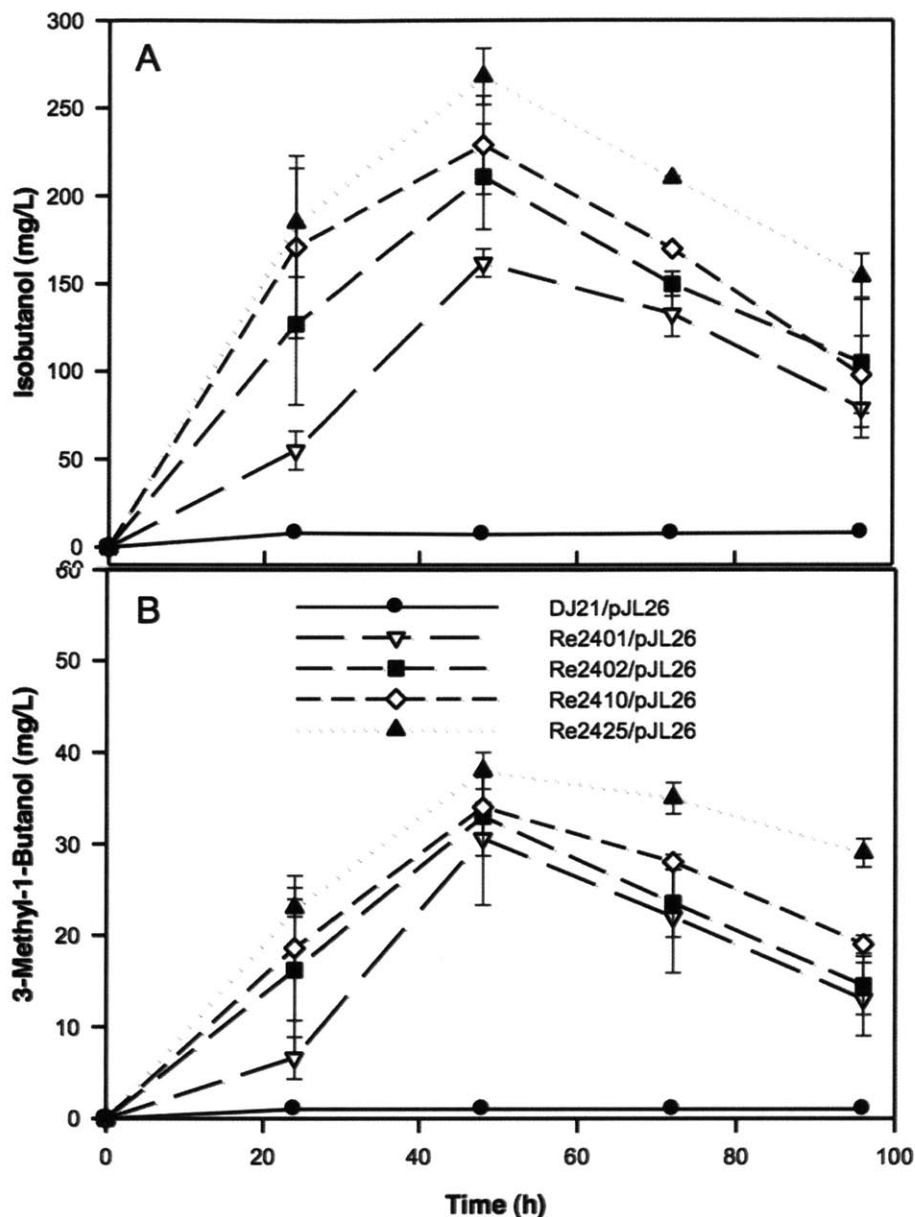


Figure 2.7: Improvement of branched-chain alcohols yield by elimination of carbon sinks. (A) Isobutanol production curve; (B) 3-methyl-1-butanol production curve. DJ 21: Constitutive ADH mutant *R. eutropha* strain; Re2401: (DJ21 Δ *phaCAB*); Re2402: (DJ21 Δ *phaCAB* Δ *ilvE*); Re2410 (DJ21 Δ *phaCAB* Δ *ilvE* Δ *bkdAB*); Re2425 (DJ21 Δ *phaCAB* Δ *ilvE* Δ *bkdAB* Δ *aceE*). Values were average from three replicates with standard deviation values represented as error bars.

Semi-continuous flask cultivations

Since *R. eutropha* experiences isobutanol toxicity at concentrations above 0.5 % (v/v), the production yield might be adversely affected by the product itself. In order to alleviate this inhibition and determine the longevity of engineered *R. eutropha* in both growth and alcohol production, Re2425/pJL26 was cultivated in 100 mL minimal media with 1 % fructose and 0.05 % NH₄Cl. At the end of every 24 h, all isobutanol and 3-methyl-1-butanol produced were

removed with the spent growth media, and fresh minimal media were added to the cultures. Each day, approximately 200 mg/L to 500 mg/L branched-chain alcohols were produced. Re2425/pJL26 was able to continuously utilize fructose as the main carbon source and produce branched-chain alcohols for a duration of greater than 50 days. The total accumulated alcohols produced reached levels of over 14 g/L (Figure 2.8).

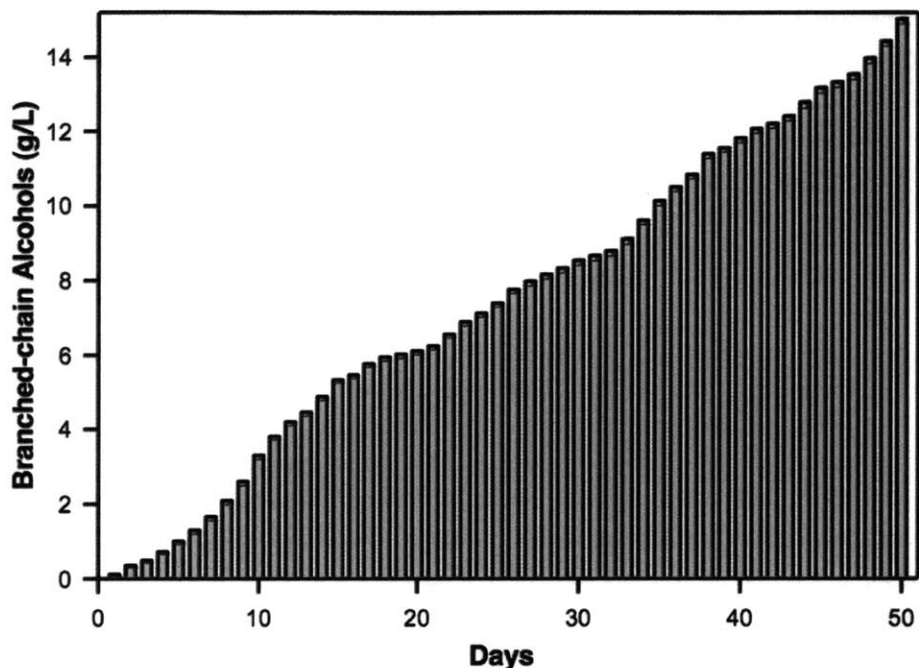


Figure 2.8: Isobutanol and 3-methyl-1-butanol production by Re2425/pJL26 in a semi-continuous flask culture, over the duration of 50 days. Fresh minimal media with 1 % fructose and 0.05 % NH_4Cl was used each day. The concentration values of isobutanol and 3-methyl-1-butanol were added together to get the daily total cumulative branched-chain alcohols concentration. The data shown are the average of three replicated experiments with error bars representing the standard deviation.

Production of isobutanol from CO_2 , O_2 , and H_2

Although *R. eutropha* is traditionally employed for the production of PHB, a growing amount of attention has now centered on engineering this strain for the production of biofuels. Production of biofuels, such as branched-chain alcohols, in *R. eutropha* can act as an alternative to carbon storage when redirected from PHB biosynthesis. Since *R. eutropha* was able to produce ~60 g/L PHB using CO_2 and H_2 as the sole carbon and energy source, respectively (Ishizaki et al. 2001), engineered *R. eutropha*, with branched-chain alcohols production ability, could be utilized to convert CO_2 - and H_2 -rich gas streams to transportational biofuel such as branched-chain alcohols. In a separate study, collaborators at Michigan State University built an autotrophic bioreactor, which is safe to use with flammable gas reactants such as O_2 , and H_2 and achieves cost-effective gas mass transfer. This bioreactor combined efficient gas-mixing system with isobutanol isolation system, thus eliminated product-induced toxicity to the cells. In such fermentation system, production of isobutanol from CO_2 , O_2 , and H_2 reached 1,030 mg/L/day at 0.12 h^{-1} growth rate (unpublished results from the Worden Lab).

DISCUSSION

A biosynthetic pathway for branched-chain alcohols production, while utilizing several native genes and gene products, is a heterologous pathway in *R. eutropha*, and it could decrease the overall fitness of the cell through unbalanced pathway precursors or product inhibition. In order to achieve optimal production of branched-chain alcohols, balanced carbon and energy flow must be achieved and properly analyzed. As mentioned previously, *R. eutropha* is a model organism for carbon storage, due to its ability to redirect carbon flow for the synthesis of large quantities of intracellular polymer (Potter et al. 2004). With PHB biosynthesis enzymes deleted, *R. eutropha* secreted carbon in the form of pyruvate and stored the reducing-energy, originally used by the PhaB enzymes, in the form of NADH (Table 2.3). Branched-chain alcohol production utilizes pyruvate as an initial pathway precursor into the valine-biosynthesis pathway. Additionally, NADPH is the cofactor required by the additional Ehrlich pathway enzyme ADH. Therefore, it is advantageous to use mutant *R. eutropha* incapable of PHB production for biofuel production.

With only the incorporation of the Ehrlich pathway enzymes KivD and ADH, *R. eutropha* synthesized low levels of isobutanol (Figure 2.2). When isobutanol precursors, pyruvate or α -ketoisovalerate, were supplied extracellularly, the isobutanol production levels dramatically improved to ~ 4.5 g/L (Figure 2.2). This result suggested that the production process was limited by low activities of branched-chain amino acid biosynthesis pathway enzymes, specifically the first enzyme of the pathway, AHAS (Appendix 2.2). AHAS contains a catalytic large subunit, encoded by the gene *ilvB*, and a small regulatory subunit, encoded by *ilvH* (Vyazmensky et al. 2009). AHAS not only was tightly regulated by product inhibition, but also through tRNA repression, substrate specificity, and protein degradation (Chipman et al. 1998; Chipman et al. 2005; Gollop et al. 1990; McCourt and Duggleby 2006). In order to shunt more precursors into the production of isobutanol, duplication of selected native branched-chain amino acid biosynthesis genes was employed in this study (Appendix 2.2 and Figure 2.7). Additionally, mutagenic techniques can be employed to decrease regulation of AHAS via feedback inhibition and substrate specificity (Engel et al. 2004; Gollop et al. 1990; Mendel et al. 2001; Slutzker et al. 2011). As described previously, the inhibition of *E. coli* AHAS by valine was alleviated by elimination of the valine-binding residues or C-terminal domain of the regulatory subunit (Mendel et al. 2001; Slutzker et al. 2011). Additionally, Engel et al. were able to construct a mutant AHAS from *E. coli* with increased substrate specificity towards pyruvate instead of α -ketobutyrate by incorporation of a bulky amino acid residue at the AHAS active site (Engel et al. 2004). These techniques can be utilized to engineer *R. eutropha* AHAS with decreased feedback inhibition and substrate specificity, thus increase AHAS activity for the production of isobutanol.

R. eutropha does not have endogenous decarboxylase activity towards branched-chain α -keto acids (Pohlmann et al. 2007; Schwartz et al. 2009). The overexpression of the native valine biosynthesis pathway, the addition of heterologous KivD, in addition to the constitutive expression of native ADH under aerobic conditions, resulted in the production of isobutanol and 3-methyl-1-butanol (Figure 2.4), thus demonstrating that *R. eutropha* can be engineered for the production of branched-chain higher alcohols. Furthermore, the production of branched-chain alcohols in *R. eutropha* was shown to be triggered by nitrogen limitation (Figure 2.6). These observations suggest that such regulation options might be employed for controlled production of isobutanol during fermentation scale ups. Furthermore, controlled production of isobutanol

could be achieved by utilization of inducible promoters like propionate (Plassmeier et al. 2012) and P_{lac} (Fukui et al. 2011).

One of the key points in the production of branched-chain higher alcohols was the utilization of broad substrate range ADH for the conversion of branched-chain aldehydes to alcohols. Although various heterologous ADH enzymes from *L. lactis* (AdhA), *Saccharomyces cerevisiae* (Adh2), and *E. coli* (YqhD) were employed for the production of branched-chain alcohols in *E. coli*, *Corynebacterium glutamicum*, and *R. eutropha* (Atsumi et al. 2008; Atsumi et al. 2010a; Blombach et al. 2011; Jarboe, 2011; Li et al. 2012; Smith et al. 2010), the use of a native ADH enzyme expressed from *R. eutropha* would be more compatible with the host organism. *R. eutropha* mutant strain DJ21 constitutively expressed ADH and exhibited a higher activity towards the reduction of isobutyraldehyde compared to YqhD (Figure 2.4A), which is an enzyme that has been utilized often in heterologous microbial isobutanol production studies (Jarboe, 2011). The DJ21 strain, after deletion of the PHB biosynthesis operon, was also able to produce isobutanol and 3-methyl-1-butanol when native valine-biosynthesis and *kivD* genes were overexpressed (Figure 2.4B). The activity of ADH significantly affected the concentration of isobutanol produced, as shown in Figure 2.4. This could be explained by the fact that the ADH enzyme is bidirectional (Steinbüchel and Schlegel 1984), thus the production of isobutanol relies on the ability of ADH to catalyze isobutyraldehyde reduction instead of isobutanol oxidation.

Production of isobutanol and 3-methyl-1-butanol in engineered *R. eutropha* strains reached a maximum of 270 mg/L and 40 mg/L, respectively, in a $\Delta phaCAB \Delta ilvE \Delta bkdAB \Delta aceE$ (Re2425) background at 48 h. The bottleneck still appears to involve low activities of some of the pathway enzymes (Figure 2.5) potentially due to product inhibition, poor expression, solubility, oxygen sensitivity, and codon usage. Li, et al. used AlsS from *Bacillus subtilis* as an AHAS for branched-chain alcohols production in *R. eutropha*, because AlsS does not experience product inhibition like AHAS from other organisms (Gollop et al. 1990). In this work, it was also shown that the activity of AlsS was five times higher than the native AHAS (Li et al. 2012). However, after substituting *alsS* into our isobutanol production operon, no significant change in isobutanol production was observed (Appendix 2.5). Furthermore, incorporation of valine biosynthesis pathway enzymes from *Corynebacterium glutamicum* for the production of isobutanol in *R. eutropha* also did not improve production (Appendix 2.5). These results could be due to the differences in codon usage between *R. eutropha* and *B. subtilis* or *C. glutamicum*. Synthetic codon-optimized heterologous genes encoding AHAS and KivD could be used to improved protein expression, thus enzyme activity. On the other hand, besides gene duplication, incorporation of promoters at the beginning of each individual pathway genes could also enhance branched-chain alcohol production.

Cultivation of *R. eutropha* beyond 48 h resulted in a loss of more than 50 % of the branched-chain alcohols produced (Figure 2.7). We anticipated that the cells might have converted isobutanol into less toxic compounds, given the toxic effects of isobutanol (Atsumi et al. 2010b; MCGowan 1954; Minty et al. 2011), and the *R. eutropha* mutant strain DJ21 has been shown to utilize isobutanol as its sole carbon source for growth (data not shown). To minimize product consumption, removal of isobutanol from the culture upon formation or deletion of isobutanol utilization pathway genes could be applied.

We investigated the ability of *R. eutropha* to tolerate isobutanol toxicity by growing the cells in the presence of different isobutanol concentrations (0 to 1 %, v/v). Despite observing that some mutants were more tolerant to isobutanol than the wild type strain, the *R. eutropha* strains tested showed that overall isobutanol tolerance was extremely low. At concentrations as

low as 0.8 %, no cell growth was detected (Table 2.4). Such tolerance is much lower than those reported for *E. coli* (1.5 %) and *C. glutamicum* (>2 %) (Smith et al. 2010). Increasing isobutanol tolerance will be crucial for the effective production of isobutanol by *R. eutropha*. Higher tolerance can potentially be achieved by these approaches as demonstrated previously: overexpression of stress related (heat shock) proteins, directed evolution by challenging cells with increasing concentrations of isobutanol, elimination of transporter genes, or rapid product removal from the growth media (Atsumi et al. 2010b; Baez et al. 2011; Minty et al. 2011; Nielsen et al. 2009; Nielsen and Prather 2009). To test the effectiveness of product elimination, we removed all the isobutanol and 3-methyl-1-butanol produced in the media at the end of each 24 h growth period and resupplemented *R. eutropha* with nutrients. The highest rate of branched-chain alcohols produced under such condition was 30 mg/L/h. Overall, more than 14 g/L total branched-chain alcohols were accumulated by *R. eutropha* in the semi-continuous flask culture (Figure 2.8). Such prolonged cultivation and branched-chain alcohols production time make *R. eutropha* a favorable candidate for industrial fermentation scale up processes. In order for the bioproduction of isobutanol to be economically viable, the productivity should reach ~2 g/L/h. Although the current production yield in engineered *R. eutropha* is far from this goal, additional strain engineering to increase carbon flow through the valine biosynthesis pathway, increase isobutanol tolerance, remove potential product re-utilization pathways and fermentation scale up will each facilitate in reaching that goal. This study examined the ability for *R. eutropha* to redirect its carbon and energy storage system from PHB to the production of isobutanol and 3-methyl-1-butanol via the native branched-chain amino acid biosynthesis pathway, with highlights on the production response to nutrient stress, product tolerance, and semi-continuous flask cultivation.

REFERENCES

- Atsumi S, Hanai T, Liao JC (2008) Non-fermentative pathways for synthesis of branched-chain higher alcohols as biofuels. *Nature* 451:86-89
- Atsumi S, Higashide W, Liao JC (2009) Direct photosynthetic recycling of carbon dioxide to isobutyraldehyde. *Nat Biotechnol* 27:1177-1180
- Atsumi S, Wu TY, Eckl EM, Hawkins SD, Buelter T, Liao JC (2010a) Engineering the isobutanol biosynthetic pathway in *Escherichia coli* by comparison of three aldehyde reductase/alcohol dehydrogenase genes. *Appl Microbiol Biotechnol* 85:651-657
- Atsumi S, Wu TY, Machado IMP, Huang WC, Chen PY, Pellegrini M, Liao JC (2010b) Evolution, genomic analysis, and reconstruction of isobutanol tolerance in *Escherichia coli*. *Mol Syst Biol* 6:449-450
- Baer SH, Blaschek HP, Smith TL (1987) Effect of butanol challenge and temperature on lipid composition and membrane fluidity of butanol-tolerant *Clostridium acetobutylicum*. *Appl Environ Microbiol* 53:2854-2861
- Baez A, Cho KM, Liao JC (2011) High-flux isobutanol production using engineered *Escherichia coli*: a bioreactor study with in situ product removal. *Appl Microbiol Biotechnol* 90:1681-1690
- Blombach B, Riestler T, Wieschalka S, Ziert C, Youn JW, Wendisch VF, Eikmanns BJ, (2011) *Corynebacterium glutamicum* tailored for efficient isobutanol production. *Appl Environ Microbiol* 77:3300-3310
- Bowien B, Kusian B (2002) Genetics and control of CO₂ assimilation in the chemoautotroph *Ralstonia eutropha*. *Arch Microbiol* 178:85-93
- Brigham CJ, Sinskey AJ (2012) Applications of polyhydroxyalkanoates in the medical industry. *Int J Biotechnol Wellness Ind.* 1: 53-60.
- Budde CF, Mahan AE, Lu J, Rha C, Sinskey AJ (2010) Roles of multiple acetoacetyl coenzyme A reductases in polyhydroxybutyrate biosynthesis in *Ralstonia eutropha* H16. *J Bacteriol* 192:5319-5328
- Budde CF, Riedel SL, Hubner F, Risch S, Popovic MK, Rha C, Sinskey AJ (2011) Growth and polyhydroxybutyrate production by *Ralstonia eutropha* in emulsified plant oil medium. *Appl Microbiol Biotechnol* 89:1611-1619
- Chipman DM, Barak Z, Schloss JV (1998) Biosynthesis of 2-aceto-2-hydroxy acids: acetolactate synthases and acetohydroxyacid synthases. *Biochim Biophys Acta* 1385:401-419
- Chipman DM, Duggleby RG, Tittmann K (2005) Mechanisms of acetohydroxyacid synthases. *Curr Opin Chem Biol* 9:475-481
- Sambrook J, Russell DW (2001) *Molecular cloning - A laboratory manual*, 3rd edition. Gold Spring Harbor Laboratory Press
- Connor MR, Liao JC (2009) Microbial production of advanced transportation fuels in non-natural hosts. *Curr Opin Biotechnol* 20:307-315.

Connor MR, Atsumi S (2010) Synthetic biology guides biofuel production. *J Biomed Biotechnol* 2010:1-9

de la Plaza M, Fernandez de Palencia P, Pelaez C, Requena T (2004) Biochemical and molecular characterization of alpha-ketoisovalerate decarboxylase, an enzyme involved in the formation of aldehydes from amino acids by *Lactococcus lactis*. *FEMS Microbiol Lett* 238:367-374.

de Palencia PF, de la Plaza A, Amarita F, Requena T, Pelaez C (2006) Diversity of amino acid converting enzymes in wild lactic acid bacteria. *Enzyme Microb Technol* 38:88-93

Engel S, Vyazmensky M, Vinogradov M, Berkovich D, Bar-Ilan A, Qimron U, Rosiansky Y, Barak Z, Chipman DM (2004) Role of a conserved arginine in the mechanism of acetohydroxyacid synthase: catalysis of condensation with a specific ketoacid substrate. *J Biol Chem* 279:24803-24812

Fukui T, Ohsawa K, Mifune J, Orita I, Nakamura S (2011) Evaluation of promoters for gene expression in polyhydroxyalkanoate-producing *Cupriavidus necator* H16. *Appl Microbiol Biotechnol* 89:1527-1536

Gogerty DS, Bobik TA (2010) Formation of isobutene from 3-hydroxy-3-methylbutyrate by diphosphomevalonate decarboxylase. *Appl Environ Microbiol* 76:8004-8010

Gollop N, Damri B, Chipman DM, Barak Z (1990) Physiological implications of the substrate specificities of acetohydroxy acid synthases from varied organisms. *J Bacteriol* 172:3444-3449

Hazelwood LA, Daran JM, van Maris AJ, Pronk JT, Dickinson JR (2008) The Ehrlich pathway for fusel alcohol production: a century of research on *Saccharomyces cerevisiae* metabolism. *Appl Environ Microbiol* 74:2259-2266

Ishizaki A, Tanaka K, Taga N (2001) Microbial production of poly-D-3-hydroxybutyrate from CO₂. *Appl Microbiol Biotechnol* 57:6-12

Jarboe LR (2011) YqhD: a broad-substrate range aldehyde reductase with various applications in production of biorenewable fuels and chemicals. *Appl Microbiol Biotechnol* 89:249-257

Jendrossek D, Kruger N, Steinbüchel A (1990) Characterization of alcohol dehydrogenase genes of derepressible wild-type *Alcaligenes eutrophus* H16 and constitutive mutants. *J Bacteriol* 172:4844-4851

Karr DB, Waters JK, Emerich DW (1983) Analysis of Poly-β-Hydroxybutyrate in *Rhizobium japonicum* Bacteroids by Ion-Exclusion High-Pressure Liquid Chromatography and UV Detection. *Appl Environ Microbiol* 46:1339-1344

Khanna S, Srivastava AK (2005) Statistical media optimization studies for growth and PHB production by *Ralstonia eutropha*. *Process Biochem* 40:2173-2182

Kovach ME, Elzer PH, Hill DS, Robertson GT, Farris MA, Roop RM, Peterson KM (1995) Four new derivatives of the broad-host-range cloning vector pBBR1MCS, carrying different antibiotic-resistance cassettes. *Gene* 166:175-176

Kurosawa K, Boccazzi P, de Almeida NM, Sinskey AJ (2010) High-cell-density batch fermentation of *Rhodococcus opacus* PD630 using a high glucose concentration for triacylglycerol production. *J Biotechnol* 147:212-218

- Larroy C, Rosario Fernandez M, Gonzalez E, Pares X, Biosca JA (2003) Properties and functional significance of *Saccharomyces cerevisiae* ADHVI. *Chem Biol Interact* 143-144:229-238
- Lenz O, Ludwig M, Schubert T, Burstel I, Ganskow S, Goris T, Schwarze A, Friedrich B (2010) H₂ conversion in the presence of O₂ as performed by the membrane-bound [NiFe]-hydrogenase of *Ralstonia eutropha*. *Chemphyschem* 11:1107-1119
- Leyval D, Uy D, Delaunay S, Goergen JL, Engasser JM (2003) Characterisation of the enzyme activities involved in the valine biosynthetic pathway in a valine-producing strain of *Corynebacterium glutamicum*. *J Biotechnol* 104:241-252
- Li H, Opgenorth PH, Wernick DG, Rogers S, Wu RY, Higashide W, Malati P, Huo YX, Cho KM, Liao JC (2012). Integrated electromicrobial conversion of CO₂ to higher alcohols. *Science* 335:1596
- Lu J, Brigham CJ, Rha C, Sinskey AJ (2012) Characterization of an extracellular lipase and its chaperone from *Ralstonia eutropha* H16. *Appl Microbiol Biotechnol*. 97: 2443-2454
- Macho V, Kralik M, Jurecekova E, Hudec J, Jurecek L (2001) Dehydration of C-4 alkanols conjugated with a positional and skeletal isomerisation of the formed C-4 alkenes. *Appl Catal A Gen* 214:251-257
- McCourt JA, Duggleby RG (2006) Acetohydroxyacid synthase and its role in the biosynthetic pathway for branched-chain amino acids. *Amino Acids* 31:173-210
- Mcgowan JC (1954) The physical toxicity of chemicals IV. solubilities, partition coefficients and physical toxicities. *J Appl Chem* 4:41-47
- Mendel S, Elkayam T, Sella C, Vinogradov V, Vyazmensky M, Chipman DM, Barak Z (2001) Acetohydroxyacid synthase: a proposed structure for regulatory subunits supported by evidence from mutagenesis. *J Mol Biol* 307: 465-477
- Minty JJ, Lesnefsky AA, Lin F, Chen Y, Zaroff TA, Veloso AB, Xie B, McConnell CA, Ward RJ, Schwartz DR, Rouillard JM, Gao Y, Gulari E, Lin XN (2011) Evolution combined with genomic study elucidates genetic bases of isobutanol tolerance in *Escherichia coli*. *Microb Cell Fact* 10:18-56
- Nielsen DR, Leonard E, Yoon SH, Tseng HC, Yuan C, Prather KL (2009) Engineering alternative butanol production platforms in heterologous bacteria. *Metab Eng* 11:262-273
- Nielsen DR, Prather KJ (2009) In situ product recovery of n-butanol using polymeric resins. *Biotechnol Bioeng* 102:811-821
- Plassmeier J, Persicke M, Puhler A, Sterthoff C, Ruckert C, Kalinowski J (2012) Molecular characterization of PrpR, the transcriptional activator of propionate catabolism in *Corynebacterium glutamicum*. *J Biotechnol* 159:1-11
- Pohlmann A, Fricke WF, Reinecke F, Kusian B, Liesegang H, Cramm R, Eitinger T, Ewering C, Potter M, Schwartz E, Strittmatter A, Voß I, Gottschalk G, Stinbüchel A, Friedrich B, Bowien B (2006). Genome sequence of the bioplastic-producing "Knallgas" bacterium *Ralstonia eutropha* H16. *Nat Biotechnol* 24:1257-1262

Potter M, Muller H, Reinecke F, Wiczorek R, Fricke F, Bowien B, Friedrich B, Steinbüchel A (2004) The complex structure of polyhydroxybutyrate (PHB) granules: four orthologous and paralogous phasins occur in *Ralstonia eutropha*. *Microbiology* 150:2301-2311

Quandt J, Hynes MF (1993) Versatile suicide vectors which allow direct selection for gene replacement in gram-negative bacteria. *Gene* 127:15-21

Rehm BH (2003) Polyester synthases: natural catalysts for plastics. *Biochem J* 376:15-33

Savrasova EA, Kivero AD, Shakulov RS, Stoyanova NV (2011) Use of the valine biosynthetic pathway to convert glucose into isobutanol. *J Ind Microbiol Biotechnol* 38:1287-1294

Schwartz E, Voigt B, Zuhlke D, Pohlmann A, Lenz O, Albrecht D, Schwarze A, Kohlmann Y, Krause C, Hecker M, Friedrich B (2009) A proteomic view of the facultatively chemolithoautotrophic lifestyle of *Ralstonia eutropha* H16. *Proteomics* 9:5132-5142

Sheehan J (2009) Engineering direct conversion of CO₂ to biofuel. *Nat Biotechnol* 27:1128-1129

Simon R, Priefer U, Puhler A (1983) A broad host range mobilization system for in vivo genetic-engineering - transposon mutagenesis in gram-negative bacteria. *Bio-Technology* 1:784-791

Slater S, Houmiel KL, Tran M, Mitsky TA, Taylor NB, Padgett SR, Gruys KJ (1998) Multiple β -ketothiolases mediate poly(beta-hydroxyalkanoate) copolymer synthesis in *Ralstonia eutropha*. *J Bacteriol* 180:1979-1987

Slutzker A, Vyazmensky M, Chipman DM, Barak Z (2011) Role of the C-terminal domain of the regulatory subunit of AHAS isozyme III: use of random mutagenesis with in vivo reconstitution (REMI-ivs). *Biochim Biophys Acta* 1814:449-455

Smith KM, Cho KM, Liao JC (2010) Engineering *Corynebacterium glutamicum* for isobutanol production. *Appl Microbiol Biotechnol* 87:1045-1055

Steinbüchel A, Schlegel HG (1984) A multifunctional fermentative alcohol dehydrogenase from the strict aerobic *Alcaligenes eutrophus*: purification and properties. *Eur J Biochem* 141:555-564

Steinbüchel A, Frund C, Jendrossek D, Schlegel HG (1987) Isolation of mutants of *Alcaligenes eutrophus* unable to derepress the fermentative alcohol-dehydrogenase. *Arch Microbiol* 148:178-186

Steinbüchel A, Schlegel HG (1989) Excretion of pyruvate by mutants of *Alcaligenes eutrophus*, which are impaired in the accumulation of poly(β -hydroxybutyric acid) (PHB), under conditions permitting synthesis of PHB. *Appl Microbiol Biotechnol* 31:168-175

Vollherbst-Schneck K, Sands JA, Montenecourt BS (1984) Effect of butanol on lipid composition and fluidity of *Clostridium acetobutylicum* ATCC 824. *Appl Environ Microbiol* 47:193-194

Vyazmensky M, Zherdev Y, Slutzker A, Belenky I, Kryukov O, Barak Z, Chipman DM (2009) Interactions between large and small subunits of different acetohydroxyacid synthase isozymes of *Escherichia coli*. *Biochemistry* 48:8731-8737

Westerfield WW (1945) A colorimetric determination of blood acetoin. *J Biol Chem* 161:495-502

Yan Y, Liao JC (2009) Engineering metabolic systems for production of advanced fuels. *J Ind Microbiol Biotechnol* 36:471-479

Yang YH, Brigham CJ, Budde CF, Boccazzi P, Willis LB, Hassan MA, Yusof ZA, Rha C, Sinskey AJ (2010) Optimization of growth media components for polyhydroxyalkanoate (PHA) production from organic acids by *Ralstonia eutropha*. *Appl Microbiol Biotechnol* 87:2037-2045

York GM, Stubbe J, Sinskey AJ (2001) New insight into the role of the PhaP phasin of *Ralstonia eutropha* in promoting synthesis of polyhydroxybutyrate. *J Bacteriol* 183:2394-2397

York GM, Lupberger J, Tian J, Lawrence AG, Stubbe J, Sinskey AJ (2003) *Ralstonia eutropha* H16 encodes two and possibly three intracellular poly[D-3-hydroxybutyrate] depolymerase genes. *J Bacteriol* 185:3788-3794

Zhang ZQ, Yu J, Stanton RC (2000) A method for determination of pyridine nucleotides using a single extract. *Anal Biochem* 285:163-167

Zor T, Selinger Z (1996) Linearization of the Bradford protein assay increases its sensitivity: theoretical and experimental studies. *Anal Biochem* 236: 302-308

APPENDIX

Appendix 2.1: List of primers used in this study. Restriction sites are underlined.

Name	Sequence ^a
<i>ΔphaCAB</i> upstream F	GAAT <u>GGATCC</u> GTGCTCGGTGATCGCCATCAT
<i>ΔphaCAB</i> upstream R	GACTGGTTGAACCAGGCCGGCAGGTCCTCGAGCATATGCATGATTTG ATTGTCTCTCTG
<i>ΔphaCAB</i> downstream F	CAGAGAGACAATCAAATCATGCATATGCTCGAGTGACCTGCCGGCCTG GTTCAACCAGTC
<i>ΔphaCAB</i> downstream R	GAAT <u>GGATCC</u> CAGGGTGATGTAGGTGCTGGT
<i>ΔphaCAB</i> digF	CGACGCCACCAACCTGCCGGG
<i>ΔphaCAB</i> digR	GTCCACTCCTTGATTGGCTTCG
<i>ΔilvE</i> upstream F	ATAA <u>GGATCC</u> TGCTCGAGCGGCTCGATCGT
<i>ΔilvE</i> upstream R	GGCTGGCAGCCGGTGCTCACATGTCTGTTCTCCCTGCG
<i>ΔilvE</i> downstream F	CGCAGGGAGAACAGACATGTGAGCACCGGCTGCCAGCC
<i>ΔilvE</i> downstream R	AACT <u>GGATCC</u> CCTTGAGCAGCGCAAAGAGC
<i>ΔilvE</i> digF	ATGTGGGGTCAAAGGCAC
<i>ΔilvE</i> digR	TAGACGGTGCCGCAGTAC
<i>ΔbkdAB</i> upstream F	TGAAG <u>AGCTC</u> CCTTCGTCAACGGCAACTATG
<i>ΔbkdAB</i> upstream R	CCTGTTGTCTTCGACCGCTACATGGCAGGTCTCTCGATGC
<i>ΔbkdAB</i> downstream F	GCATCGAGAGACCTGCCATGTAGCGGTCGAAGACAACAGG
<i>ΔbkdAB</i> downstream R	CTTG <u>TCTAGA</u> AACTACGTGGATTCGCTGGC
<i>ΔbkdAB</i> digF	TCAAGGACATCCGAGAGGCC
<i>ΔbkdAB</i> digR	CGCTGAGTCACTTCTTCTGC
<i>ΔaceE</i> upstream F	GCCGG <u>GATCC</u> GAAGCCTTGCTGGCTTCATCC
<i>ΔaceE</i> upstream R	TGCCCGATGGCCGATCGTTTACACGGCAAGTCTCCGTTAAGG
<i>ΔaceE</i> downstream F	CCTTAACGGAGACTTGCCGTGTGAACGATGGGCCATCGGGCA
<i>ΔaceE</i> downstream R	GCAT <u>GGATCC</u> GCTGGCAAACGCTGAGCATTGAG
<i>ΔaceE</i> digF	GTGATCCTGGCCAAGACCATC
<i>ΔaceE</i> digR	GGCATCCTGCGGGGTGTAGCG

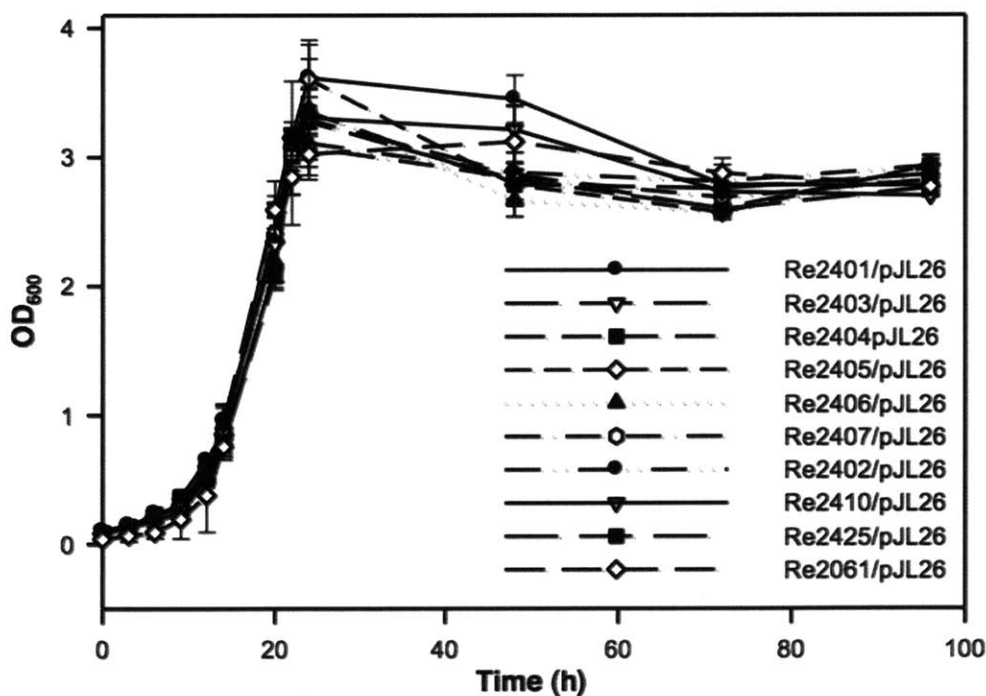
kivD F GCGGTCTAGAAAGGAGAATGCGATGTA
kivD R GCACGAGCTCTGAATTATTTTGTTC
adh F GAATGAGCTCGCGGGCCGGCAACGTC
adh R GCCGTCTAGAACTAGTTCAGTGC GGCTTGATGGCG
adhA F GAATGAATTCGTGCGCGGAGACCGGCA
adhA R GCCGGGATCCTTACATCGCTGCAGCGAA
yqhD F GCCGGAATTCATGAACAAC TTTAATCTGCACACCCC
yqhD R GAATGGATCCTTAGCGGGCGGCTTCGTATATAC
ilvBH F GCATACTAGTATGCCAGCGCGGAATTCTC
ilvBH R CTTGTCGTAAAACACTTTCATGGTTGTCCTCCTTTCTAGAGAGCTTTCGTT
TTCATG
ilvC F GCCGCATATGAAAGTGTTTTACGACAAGGACGCG
ilvC R GCCGACTAGTTTAGTTCTTCGACTGGTTCGACC
ilvD F GTCGACCAGTCGAAGA ACTAAAAGGAGGACGACCATGGCATTCAACA
AACGCTCGCAG
ilvD R GGTCGTCCTCCTTTTCAGTCCGTC ACTGCCCCCTTG
kivD F AAGGGGGCAGTGACGGACTGAAAAGGAGGACGACCATGTATACAGTAG
GAGATTACC
kivD R GCAGTCTAGAGGTCGTCCTCCTTTTTATGATTTATTTTGTTCAGC
ilvBHCDkivD digF1 GCCAACATGAACTATTCGATC
ilvBHCDkivD digR1 GCCCTCGGTGCCCATCGACATG
ilvBHCDkivD digF2 CTGTTGCTGCAGCTGAACGTC
ilvBHCDkivD digR2 GCCAAAGCTAATTATTTTCATG
alsS F (*B. subtilis*) GCATACTAGTGCCGCTCGAGATGACAAAAGCAACAAAAGAA
alsS R GCATGGATCCCTAGAGAGCTTTCGTTTTTCATG
ilvBNc F (*C. glutamicum*) GCCGTCTAGAGTGAATGTGGCAGCTTCTCAAC
ilvBNc R GCCGTCTAGATTAAGCGGTTTCTGCGCGAGC
ilvCc F GCATACTAGTTTAGTCGACCTGACGGACTGC
ilvCc R CTTTTGAACGAAGTGGGATCATGGTTGTCCTCCTTTTTAAGCGGTTTCTGC
GCGAGC
ilvDc F GCTCGCGCAGAAACCGCTTAAAAGGAGGACAACCATGATCCC ACTTC
GTTCAAAAG
ilvDc R GCAGTCTAGATTAGTCGACCTGACGGACTGC

Appendix 2.2: Activities of valine biosynthesis pathway enzymes in *R. eutropha* (Re2061) with empty vector (Re2061/pBBR1MCS-2) and overexpression plasmid (Re2061/pJL26). Cells were grown in minimal media with 2 % fructose and 0.05 % NH₄Cl, and harvested for enzymatic activity at 24 h.

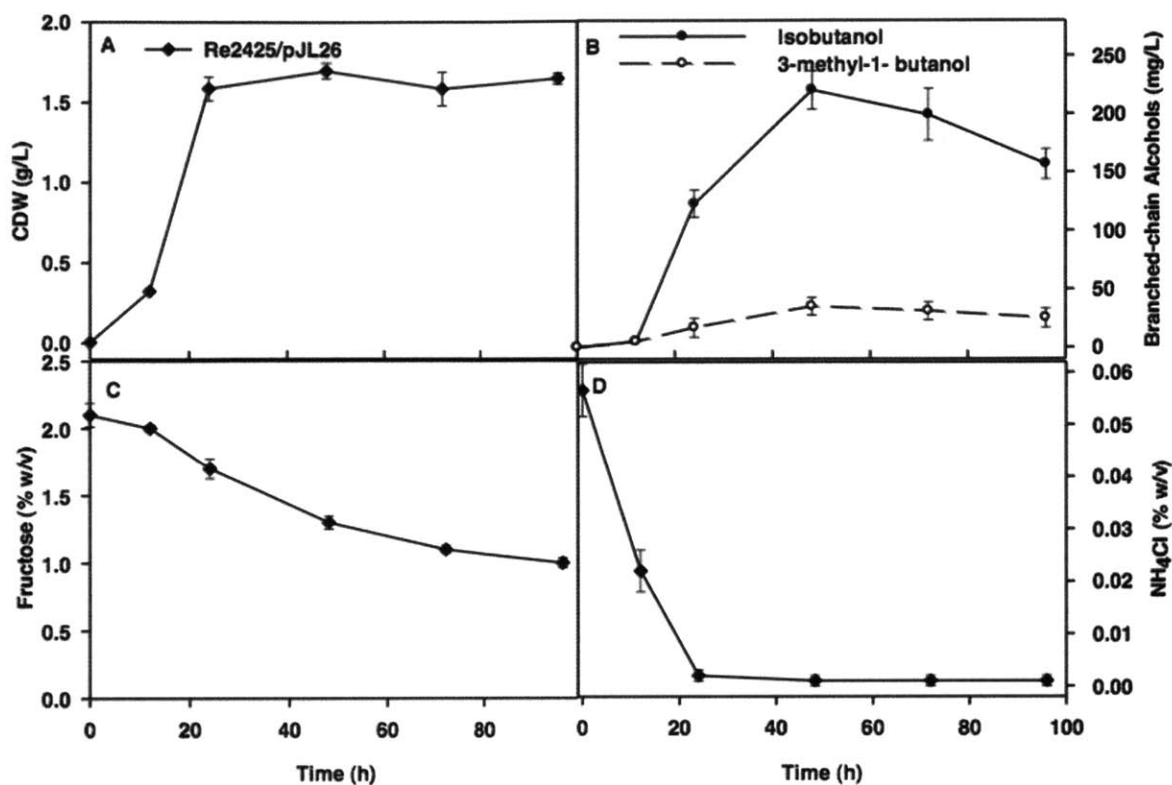
Enzymes	Re2061/pBBR1MCS-2	Re2061/pJL26
AHAS (mU/mg)	5	10
AHAIR (mU/mg)	16	86
DHAD (mU/mg)	32	780

Appendix 2.3: Growth of *R. eutropha* deletion strains and mutant strains constitutively expressing ADH containing the isobutanol production plasmid, pJL26. See Table 2.1 and Table 2.2 for more information regarding strains and plasmids used in this experiment.

Re2061 (H16 Δ *phaCAB*)
 Re2401 (DJ21 Δ *phaCAB*)
 Re2403 (CF17 Δ *phaCAB*)
 Re2404 (CF101 Δ *phaCAB*)
 Re2405 (CF106 Δ *phaCAB*)
 Re2406 (CF108 Δ *phaCAB*)
 Re2407 (CF303 Δ *phaCAB*)
 Re2402 (DJ21 Δ *phaCAB* Δ *ilvE*)
 Re2410 (DJ21 Δ *phaCAB* Δ *ilvE* Δ *bkdAB*)
 Re2425 (DJ21 Δ *phaCAB* Δ *ilvE* Δ *bkdAB* Δ *aceE*)



Appendix 2.4: Growth (A), branched-chain alcohols (isobutanol and 3-methyl-1-butanol) production (B), fructose utilization (C), and ammonia utilization (D) profile of Re2425/pJL26 over 96 h in minimal media with 2 % fructose and 0.05 % NH₄Cl.



Appendix 2.5: Production of isobutyraldehyde and isobutanol by strain Re2425 with plasmid pJL26 (*ilvBHCDkivD*), pJL27 (*alsS^ailvCDkivD*), pJL29 (*ilvBNCD_c^bkivD*) in minimal media with 2 % fructose and 0.05 % NH₄Cl at 48 h.

Strain	Isobutyraldehyde (mg/L)	Isobutanol (mg/L)
Re2425/pJL26	150	20
Re2425/pJL27	30	60
Re2425/pJL29	80	10

^a*alsS*-gene encoding AHAS from *Bacillus subtilis*

^b*ilvBNCD_c*-*Corynebacterium glutamicum* valine biosynthesis pathway genes encoding AHAS, AHAIR, and DHAD

CHAPTER 3

Production of branched-chain alcohols by engineered *Ralstonia eutropha* in fed-batch fermentation

(This chapter was modified from a previously published article in Biomass and Bioenergy, 2013. 56: 334-341 'Production of branched-chain alcohols by recombinant *Ralstonia eutropha* in fed-batch cultivation' Qiang Fei, Christopher Bringham, Jingnan Lu, Rongzhan Fu, and Anthony Sinskey © Elsevier Ltd.)

INTRODUCTION

Much attention has been focused on discovery and production of novel renewable and sustainable fuels due to decreased and unstable supply of fossil fuel, ever-increasing consumption of petroleum, and rising crude oil prices (Cook et al. 2000; An et al. 2011; Jang et al. 2012; Kim and Dale 2005). Among the advanced-biofuels, branched-chain alcohols have gained considerable attention for their potential as the next-generation drop-in transportation fuel. These branched-biofuels have many desirable characteristics that make them better choices than bioethanol, the major biofuel on the market currently (Barala and Bakshi 2010; Dürre 2007). Isobutanol, one of the branched-chain biofuels, can be used in pure form or blended in at any concentration with gasoline or diesel for any automobile engine without modifications. Such qualities suggest that isobutanol could be an ideal supplement or a promising replacement for gasoline (Peralta and Keasling 2010; Pfromm et al. 2010). Several traditional fuels and biofuels were compared here in Table 3.1. Isobutanol has the highest energy density and research octane number among other biofuels, due to its branched-carbon chains (Sheehan 2009; Junginger et al. 2008; Harvey and Meylemans 2011; Evidogan et al 2010). The higher the research octane number, the more compression the fuel can withstand before detonating. In broad terms, fuels with a higher octane rating are used in high-compression engines, which generally have higher performance (Lee et al. 2008). Other advantages of isobutanol, such as lower hygroscopicity, vapor pressure, and water solubility also give it characteristics of a superior fuel to bioethanol (Yan and Liao 2009; Nasib et al. 2008).

Table 3.1. Specification comparison of biofuels and fossil fuels.

Fuel	Energy content, MJ/L	Research octane number
E100 (100% Ethanol)	21	109
E85(85% Ethanol)	25	102-105
E10(10% Ethanol)	33	95.
Gasoline (Regular)	34	91-99
Gasoline (Aviation)	35-37	-
Autogas(LGP)	25-28	100-105
Methanol	16	104
Isopropanol	24	108
n-Butanol	27	96
Isobutanol	32 (95% of gasoline)	110-113

Advancements in genetic engineering have led to the production of advanced drop-in fuels by introducing heterologous genes or entire production pathways in microorganisms. (Atsumi and Liao 2008) *Ralstonia eutropha*, which can accumulate polyhydroxyalkanoate (PHA) at more than 80% of its cell dry weight as a form of carbon and energy storage molecule. It has been investigated for PHA production for over two decades (Kim et al. 1992; Chen et al. 2009; Budde et al. 2011). Recently, *R. eutropha* has been engineered to produce branched-chain alcohols by eliminating various competing pathway genes, in addition to overexpressing native *ilvBHCD* (2-ketoisovalerate biosynthesis pathway) genes, heterologous gene encode for ketoisovalerate decarboxylase, and a constitutively expressed alcohol dehydrogenase gene. In this previous study, a final isobutanol titer of 270 mg/L and cell dry weight of 1.6 g/L were obtained in flask (batch) cultures (Lu et al. 2012). Since production of isobutanol is associated with the amount of cell density, this low titer could have resulted from poor growth in batch flask cultures.

Economically viable, renewable biological production of branched-chain alcohols for liquid transportation fuels is not currently performed at large scale. However, in order to fulfill production of branched-chain alcohols in a large quantity, a fermentation system may provide a cost effective, large-scale alternative method for microorganisms that produce target fuel molecules using a variety of carbon substrates. Batch culture is one of the most often used operation modes for the production of isobutanol by various microorganisms (Lu et al 2012; Smith et al. 2010; Huo et al. 2011). However, a major disadvantage of batch fermentation is that the production of aimed metabolites is restricted due to the significant inhibitions caused by the high concentration of substrates or catabolite repression (Li et al. 2011; Ding and Tan 2006; Knoshaug and Zhang 2009). One of the widely applied fermentation methods to achieve high production titer without inhibition effects, combined with high yield and productivity of the desired products, is a fed-batch culture with controlled nutrient feeding. Fed-batch culture is fed continuously or sequentially with substrate without the removal of fermentation broth. Fed-batch fermentation is generally superior to batch fermentation, and is especially beneficial when changing nutrient concentrations and compositions affects the production of the desired products (Son et al. 2007; Qureshi et al. 2008; Zhang et al .2011).

R. eutropha is able to convert excess carbon sources into PHAs in response to conditions of physiological stress. The basic mechanism of PHAs accumulation initiated by nitrogen or phosphate source limitation in culture medium has been studied previously (Shang et al. 2003; Riedel et al. 2012). A two-stage culture system, which separates the cell growth and production stages, has been shown to improve the product yield and content (Hartlep et al. 2002; Fei et al. 2011). In the first stage, a nitrogen-excess feeding solution was fed into bioreactor to enhance cell density without the branched-chain alcohols production. In the second stage, the nitrogen supply was ceased, preventing cell proliferation and triggering the biosynthesis of branched-chain alcohols with excess amounts of supplied carbon being assimilated into the cells. However, there are no reports on the production of branched-chain alcohols by a two-stage fed-batch culture of *R. eutropha*. Therefore, a simple and comprehensive isobutanol fermentation process is necessary for optimization and increase of product yield. The aim of this study was to develop a higher yield branched-chain alcohol production system using the previously developed *R. eutropha* isobutanol production strain, Re2410/pJL26 (Lu et al. 2012). In this study, the effects of nitrogen source on cell growth and branched-chain alcohol production were first investigated in batch cultures. Three different carbon source concentrations were employed to test the carbon source inhibition effect on cell growth in a pH-stat fed-batch culture with an

intermittent substrate feeding procedure. Subsequently, in order to achieve high production titer of branched-chain alcohols, a two-stage fed-batch cultivation was also performed.

MATERIALS AND METHODS

Chemicals, bacterial strains, and plasmids

The strains used in this study were engineered from *R. eutropha* strain H16 (ATCC 17699). The plasmids and strain construction methods were previously described (Lu et al. 2012). The strain Re2410/pJL26 was employed for advanced biofuel production in batch and two-stage fed-batch cultures. In order to enhance the cell growth without the effect of isobutanol inhibition, Re2410/pBBR1MCS-2, was also used to explore the culture strategies in fed-batch cultures. In the strain of Re2410/pBBR1MCS-2, the PHA synthesis genes, valine-specific transaminase gene, and branched-chain keto acid dehydrogenase complex genes have been deleted, and an empty vector pBBR1MCS-2 was incorporated for control purposes. TSB (dextrose-free tryptic soy broth) and minimal medium were utilized for seed cultures and fermentation experiments respectively. The compositions of TSB and minimal medium have been reported elsewhere (Budde et al. 2011; Lu et al. 2012). Unless otherwise stated, all chemicals were purchased from Sigma-Aldrich Co. LLC (St. Louis, MO, USA)

Seed cultures

A loop of mutant cells from a single colony grown on TSB agar plate was used for the initial seed cultures in glass tubes with 5 ml TSB on a roller drum at 30°C for 18 h. The tube-seed cultures were harvested and centrifuged at 1,370 ×g and then resuspended in sterile 0.85% saline for inoculation into the seed culture flasks. Minimal medium cultures of 50 ml, containing 20 g/L fructose and 5 g/L NH₄Cl, were utilized for the flask-seed cultures in 250 ml flasks. The flask cultures were continuously shaken in a 30°C incubator at 200 rpm. After 26 h, cells from flask cultures were harvested by centrifugation and cell pellets were resuspended in sterile 0.85% saline for inoculation in fermenter cultures.

Fermentation conditions

All batch and fed-batch cultures were performed with 500 ml working volume of 1,500 ml laboratory scale fermenters with a Multifors proportional–integral–derivative (PID) controller system (Infors, Switzerland). All cultures were inoculated at OD₆₀₀ of 0.6 ± 0.1. Fermentation cultures were initially fed with 20 g/L fructose as carbon source and 5 g/L NH₄Cl as nitrogen source at an operating temperature of 30°C. The pH of the medium was maintained at 6.75 with a pH probe and automatic addition of 2 mmol/L NaOH. Dissolved oxygen (pO₂) was measured with an Ingold polarographic probe and maintained at above 40% O₂ saturation by automatically adjusting the flow of a mixture of air and pure oxygen via flow controllers while maintaining an air flow of 500 ml/min and also by automatically adjusting the agitation speed from 200 to 900 rpm. In a two-stage fed-batch culture, the gas flow was increased from 500 to 750 ml/min. The increase in gas flow allows for vaporized-isobutanol to be more rapidly removed from the fermenter headspace, thus allowing for the more rapid and complete capture of alcohols during the cultivation. Alcohols were removed from the fermenter headspace along with the off-gas and

collected in a glass vessel containing chilled water. When necessary, silicone oil (AR 2000, Sigma-Aldrich Co. LLC) was manually added to each vessel to prevent foam formation.

Batch and fed-batch cultures of Re 2410/pJL26

To investigate the effect of nitrogen source on cell growth and branched-chain alcohol production, different media were prepared to contain an initial NH_4Cl concentration of 0.5, 1, 2, and 5 g/L in batch cultures. The initial carbon source of these batch cultures contains 20 g/L fructose. Two different feeding strategies were employed during the fermentations. Feeding solution composed of 500 g/L fructose, which was sterilized by filtration membrane. When fructose concentration was lower than 10 g/L, which was detected by fructose assay kit (FA-20, Sigma-Aldrich Co. LLC), 10 or 20 ml of feeding solution was manually added into two separate fermenters to keep carbon source from exhaustion.

pH-stat fed-batch culture of Re2410/pBBR1MCS-2

The pH-stat fed-batch cultures were carried out as described previously (Suzuki et al. 1990). When glucose became exhausted, pH rose rapidly. In this study, certain volumes of feeding solution composed of 500 g/L fructose and 150 g/L NH_4Cl were supplied automatically, when the detected pH became higher than 6.85. To investigate the effects of carbon source concentration on cell growth, 10 ml, 20 ml, and 40 ml of feeding solution (corresponding to 10 g/L, 20 g/L, and 40 g/L fructose, respectively) was added automatically into three different fermenters. Feeding solutions were transferred into the fermentation vassal by peristaltic pumps (Cole-Palmer Instrument Co., Vernon Hills, IL, USA). Feeding volumes were adjusted via computer control, which connects the pH meter in the fermenter to various adjustable readings.

Two-stage fed-batch culture of Re 2410/pJL26 with pH-stat control

During this two-stage fed-batch cultivation, two different feeding solutions were utilized for the branched-chain alcohol production. The first feeding solution was composed of 500 g/L fructose with 150 g/L NH_4Cl , which could provide higher cell density without triggering branched-chain alcohol production. While 500 g/L fructose with 12.5 g/L NH_4Cl was used as the second stage feeding solution to initiate branched-chain alcohol production conditions in nitrogen-limited culture medium. Feeding solutions at increments of 10 ml were added into the fermenter when the pH increased up to 6.85.

Analyses

The OD_{600} , cell dry weight (CDW), and concentration of branched-chain alcohols were measured according to the procedures reported previously (Lu et al. 2012). Branched-chain alcohols were recovered by a gas stripping process as described previously (Baez et al. 2011). Nitrogen source concentrations were determined using an ammonia assay kit (AA0100, Sigma-Aldrich Co. LLC). Residual fructose concentrations in pH-stat fed-batch cultures were analyzed by Agilent 1100 high performance liquid chromatography fitted with a Bio-Rad Aminex HPX87H column (Bio-Rad Laboratories, Hercules, CA, USA). The column was eluted with 5 mM H_2SO_4 as mobile stage at 40°C and a flow rate of 0.6 ml/min.

RESULTS

Effect of nitrogen source concentrations on cell growth and branched-chain alcohol production

Production of branched-chain alcohol biosynthesis has been demonstrated in an engineered strain of *R. eutropha*, Re2410/pJL26 (Lu et al. 2012). Since this previous study was performed in flask cultures and the cell density was low, optimum culture conditions for cell growth and branched-chain alcohol production in fermentation settings were explored in this study. The effect of nitrogen source concentration in cultures was initially investigated. Four different initial concentrations of NH_4Cl were tested in fermenter cultures over 96 h. Re2410/pJL26 was cultured in defined minimal medium with 20 g/L fructose as the sole carbon source. The CDW and total branched-chain alcohols produced in batch cultures are listed in Table 3.2. A trend can be observed that shows increasing NH_4Cl concentration in the culture medium with increased CDW of Re2410/pJL26. The highest final CDW of 8.5 g/L was observed in experiment #4, when 5 g/L NH_4Cl was used. However, the total branched-chain alcohols produced in this fermentation at any given time point only reached 21 mg/L. A maximum branched-chain alcohol production of 380 mg/L was observed in experiment #3 with 2 g/L NH_4Cl concentration. The highest cell density, achieved in experiment #4, did not correlate with the highest yield of branched-chain alcohols, which was most likely due to the depletion of carbon source during the period of branched-chain alcohol synthesis (data not shown). The higher concentration of nitrogen source in experiment #4 led to a faster carbon source consumption rate in the beginning of the culture, which resulted in higher growth rate and cell density. Unfortunately there was not enough carbon source left for branched-chain alcohol production after such a boost of cell growth.

Table 3.2: Effect of the nitrogen source concentration on cell growth and total alcohols production by Re 2410/pJL26 in batch cultures^a

Fermentation	Culture Time (h)	Initial NH_4Cl concentration(g/L)	Residual NH_4Cl concentration(g/L)	CDW ^b (g/L)	ROH ^c (mg/L)
#1	96	0.5	0	1.34	101
#2	96	1	0	2.04	339
#3	96	2	0	3.56	376
#4	96	5	0.62	8.49	21

^a The concentration of carbon source (Fructose) in all batch cultures was 20 g/L.

^b CDW, cell dry weight;

^c ROH, total branched-chain alcohols.

Fed-batch cultures for branched-chain alcohol production by Re 2410/pJL26

From the results of the batch cultures in the fermenters described above, additional carbon in fed-batch cultures would presumably be helpful in enhancing the production titer of branched-chain alcohols (Qureshi et al. 2008; Boonsawang et al. 2012). Two feeding-strategies were performed by adding either 10 or 20 ml of the feeding solution into two different fermenters to avoid carbon source exhaustion. The feed solution was added into fermenters at 31 h and 55 h during the fed-batch cultivation, respectively. The time-courses of CDW, residual

carbon source, and total branched-chain alcohol production for the 72 h fed-batch culture are shown in Figure 3.1. CDW reached 10.8 g/L in experiment #2 by adding 20 ml carbon source solution, but overall produced less branched-chain alcohol production (Figure 3.1B). Although the highest CDW was more than 10 g/L, branched-chain alcohol production in experiment #2 was only 120 mg/L. In contrast, the total branched-chain alcohol production was nearly 450 mg/L in experiment #1 by feeding only 10 ml carbon source solution (Figure 3.1A).

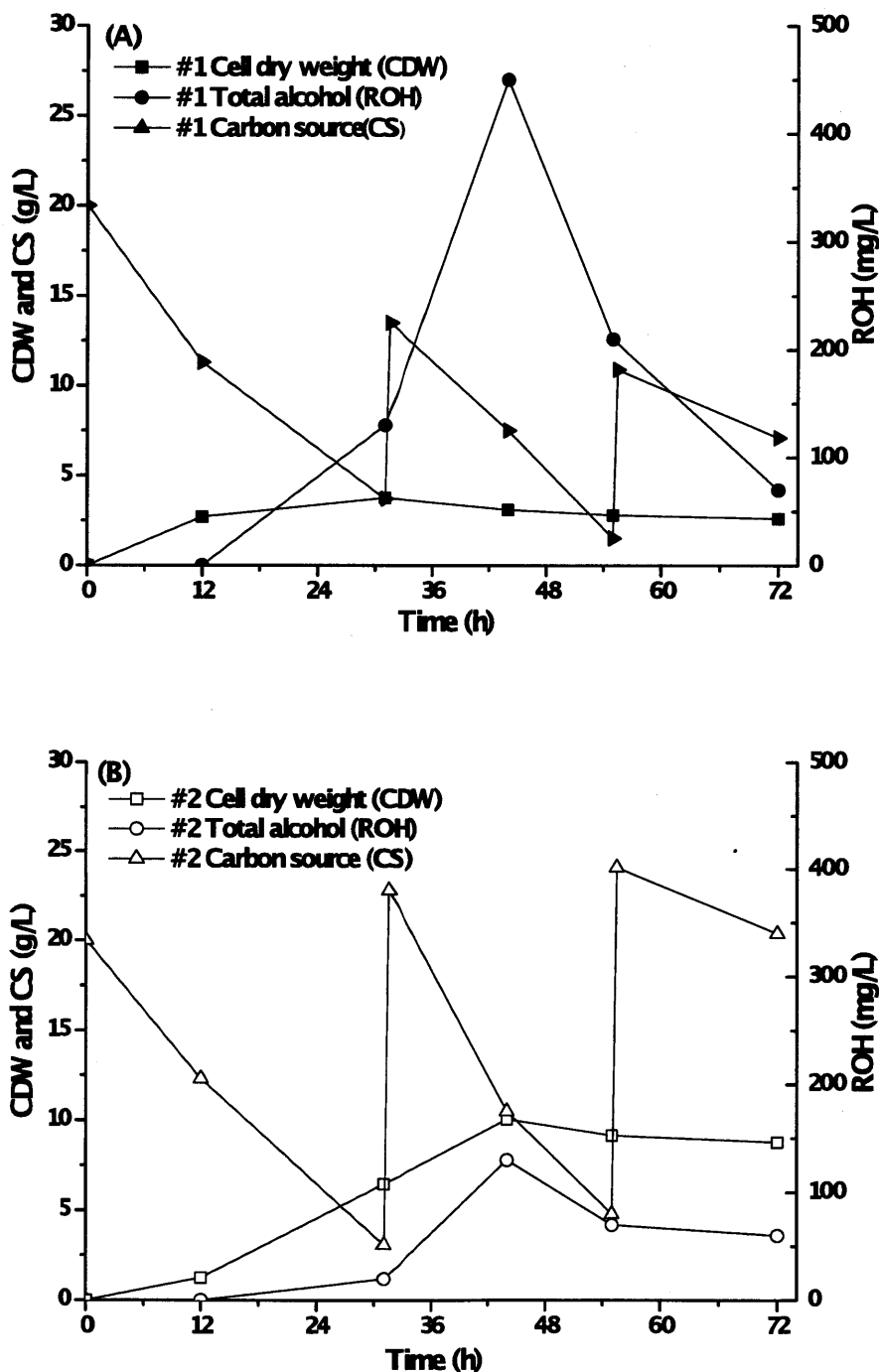


Figure 3.1: Time profile of cell dry weight (CDW), residual carbon source, and total alcohols (ROH) production by Re 2410/pJL26 in fed-batch cultures. The initial concentration of carbon source (fructose) and nitrogen source (NH₄Cl) was 20 g/L and 5 g/L, respectively. Feeding solution composed of 500 g/L fructose. Feeding volume of 10 mL (Experiment #1, A) or 20 mL (Experiment #2, B) was manually carried out into two different fermenters when fructose concentration was lower than 10 g/L.

Fed-batch culture for high cell density of Re2410/ pBBR1MCS-2 with pH-stat control

Although higher branched-chain alcohol production was achieved by using fed-batch culture strategies, cell growth is potentially inhibited in fermentations by the presence of increased concentrations of total branched-chain alcohols. In order to avoid this, a two-stage culture system could be used as a viable alternative solution. In the first stage phase, cell density would be enhanced to high level without branched-chain alcohol production, which could then be accomplished by triggering in the second stage through induction mechanisms. The induction systems for controlling expression of branched-chain alcohol production genes could be achieved by altering culture medium compositions. Therefore, branched-chain alcohol production will be improved due to the high cell density obtained in the first stage, and growth inhibition by branched-chain alcohols present in the culture media should be less of a concern in the second stage. In order to mimic the culture condition of the first stage in a two-stage fed-batch culture, strain Re2410/pBBR1MCS-2 (incapable of producing branched-chain alcohols) was employed to achieve high cell density in the absence of branched-chain alcohol production.

To accomplish a high cell density culture of Re2410/pBBR1MCS-2, a pH-stat modal fed-batch culture under different carbon source concentrations with intermittent feeding strategy was carried out. When the pH value became higher than pH 6.85, feeding volumes of 10 ml, 20 ml, and 40 ml (corresponding to 10 g/L, 20 g/L, and 40 g/L fructose, respectively) was automatically added to different fermenters. The maximum CDW of 36 g/L and biomass yield of 0.45 g g⁻¹ were achieved when 10 g/L fructose was added in the fed-batch cultures (Table 3.3). Biomass productivity of 0.51 g/L/h was also obtained by feeding 10 ml nutrient solution during the fed-batch culture. It is obvious that a higher carbon source concentration in the culture medium exhibits an inhibitory effect on cell growth, which was found in the fed-batch cultures when fed 20 ml or 40 ml nutrient solution. These results indicate that the optimal feeding volume should be controlled at 10 ml during the pH-stat modal fed-batch culture. The time profile of 10 g/L carbon source feeding fed-batch culture can be seen in Figure 3.2. When 10 g/L of carbon source was pumped into the fermenter by using pH-stat control. No carbon source limitation effect was observed during the fed-batch culture; therefore a relatively lower concentration of carbon source fed during fermentation should be favorable for cell growth of *R. eutropha* in a two-stage fed-batch culture system.

Table 3.3: Fed-batch cultures of Re2410/ pBBR1MCS-2 with pH-stat control by feeding different carbon source concentration

Carbon source concentration fed into fermenters	Time	Carbon source consumed (g)	CDW ^a (g/L)	Y _{x/s} ^b (g/g)	Pr ^c (g/L/h)
10 g/L	72h	81.3	36.7	0.45	0.51
20 g/L	72h	71.9	30.2	0.42	0.42
40 g/L	72h	73.4	28.2	0.38	0.39

^aCDW, cell dry weight

^b $Y_{X/S}$, biomass yield, CDW g/ consumed carbon source g
^cPr, biomass productivity

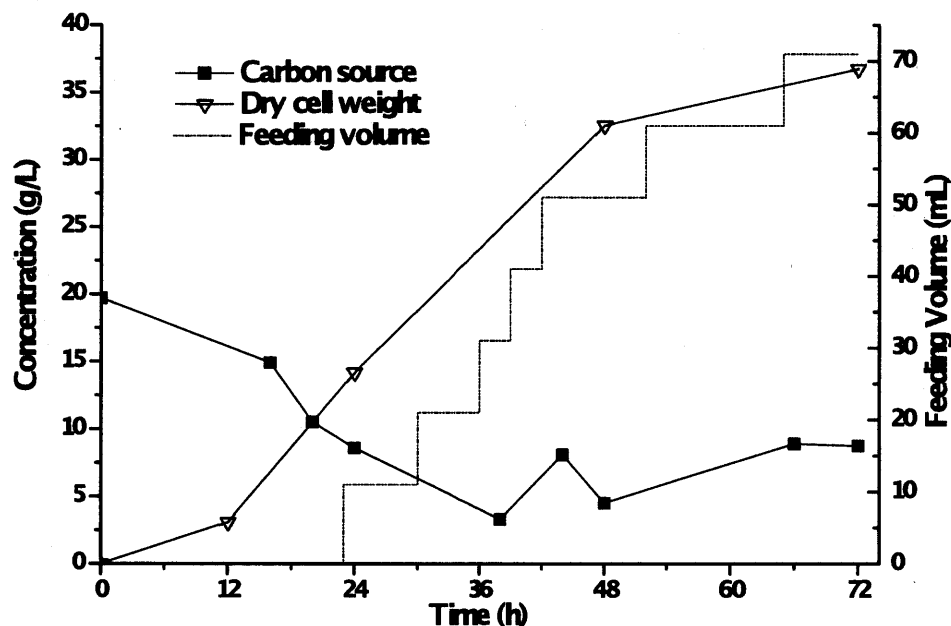


Figure 3.2: Time profile of cell growth of Re2410/pBBR1MCS-2 in the fed-batch cultures with pH-stat control. The initial concentration of carbon source (fructose) and nitrogen source (NH_4Cl) was 20 g/L and 5 g/L, respectively. Feeding solution was composed of 500 g/L fructose and 150 g/L NH_4Cl . Feeding volume of 10 mL was automatically fed into fermenter when pH became above 6.85.

Two-stage fed-batch culture for branched-chain alcohol production by Re 2410/pJL26 with pH-stat control

Since branched-chain alcohol production is controlled by the limitation of nitrogen source, a two-stage fed-batch culture was performed for high branched-chain alcohol productivity by adding two feeds with different carbon/nitrogen (C/N) ratios. Nitrogen-excess culture condition was maintained by feeding lower C/N ratio nutrient solution (500 g/L fructose with 150 g/L NH_4Cl) during the first stage culture to facilitate biomass accumulation. When the culture OD_{600} reached 30 at 72h, the first stage feed was replaced by a nutrient solution with a higher C/N ratio (500 g/L fructose with 12.5 g/L NH_4Cl) intended for the branched-chain alcohol production stage. The maximum CDW of 21 g/L and OD_{600} of 36 were observed in this two-stage fed-batch cultivation (Figure 3.3A). It is clear that branched-chain alcohol production was initiated as long as nitrogen source became exhausted at 92h in the second stage. A total 25.6 g fructose was used to produce branched-chain alcohols in the second stage, which led to a branched-chain alcohol yield and productivity of 0.031 g g^{-1} and 8.23 mg/L/h, respectively. Finally, a maximum total branched-chain alcohol of 790 g/L was achieved toward the end of the second stage of the two-stage fed-batch culture (Figure 3.3B). By using a pH-stat control

strategy, a 20 fold greater production of CDW and a 4 fold greater production of total branched-chain alcohols were achieved, as compared to the results achieved from flask cultures. These results indicate that both higher CDW and branched-chain alcohol production could be accomplished in this two-stage, fed-batch culture.

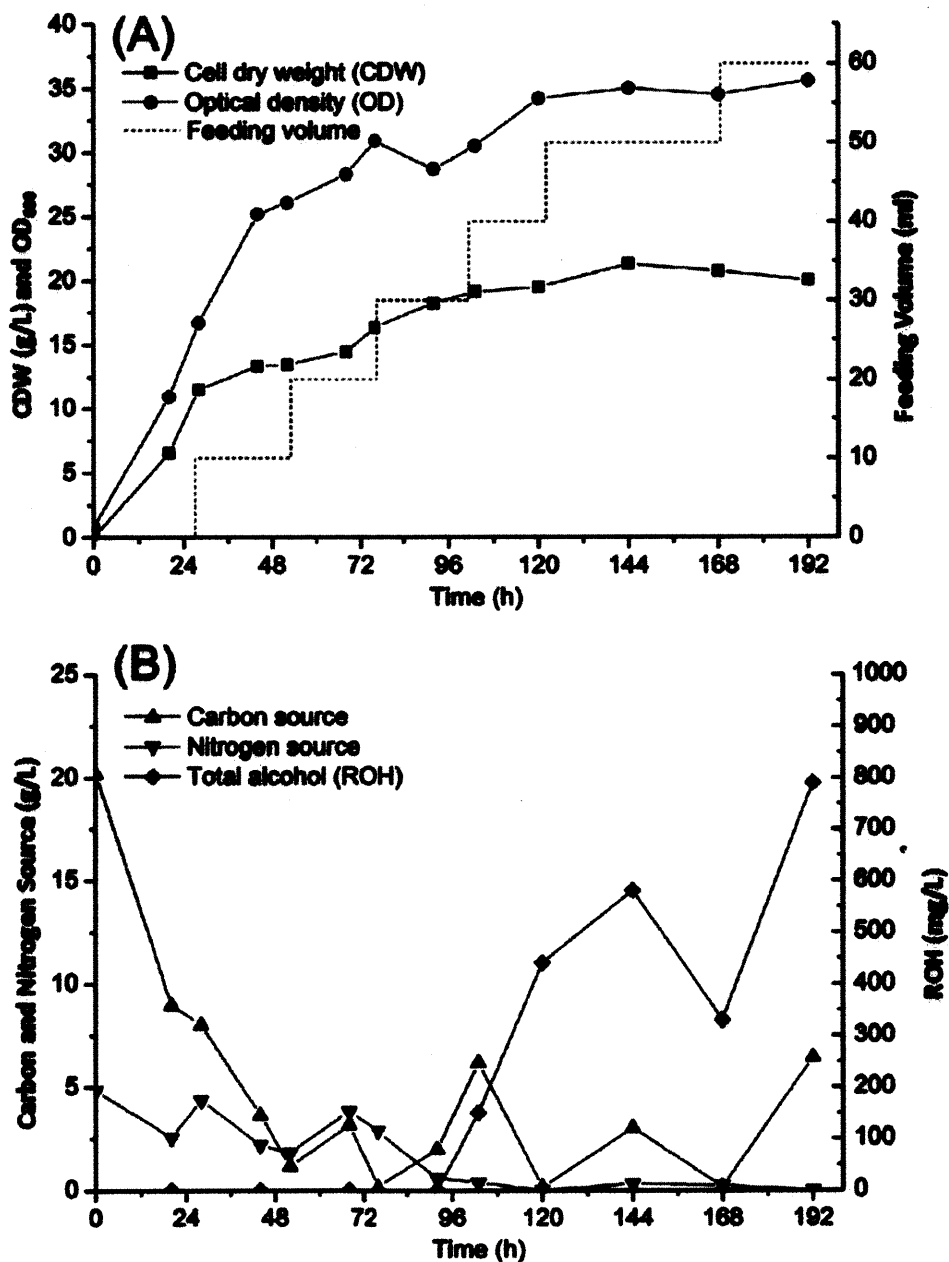


Figure 3.3: Time profile of cell growth (A) and total alcohols (B) production by Re2410/pJL26 in a two-phase fed-batch culture. The initial concentration of carbon source (Fructose) and nitrogen source (NH_4Cl) was 20 g/L and 5 g/L, respectively. The first feeding solution composed of 500 g/L fructose with 150 g/L NH_4Cl was used in the first phase culture (0-72h). The second phase feeding solution composed of 500 g/L fructose with 12.5 g/L NH_4Cl was applied at 72h of this two-phase fed-batch culture. Feeding volume of 10 mL was automatically fed into fermenter when pH was up to 6.85 during the fermentation.

The composition of total branched-chain alcohols obtained in this two-stage fed-batch cultivation was analyzed by gas chromatography (GC), which can be seen in Figure 3.4. The total branched-chain alcohols were composed of isobutanol and 3-methyl-1-butanol, with isobutanol being over 95% of the total branched-chain alcohols produced. It is clear that the amount of total branched-chain alcohols produced decreased significantly at 168 h when the carbon source was exhausted (Figure 3.3). These results may be due to the consumption of isobutanol in high cell density conditions, which is in agreement with data collected from our flask cultures (Lu et al. 2012). Since cells could utilize isobutanol as a carbon source, a feeding delay was also observed (Figure 3.3B). However, isobutanol consumption was terminated when carbon source was supplied into the fermenter.

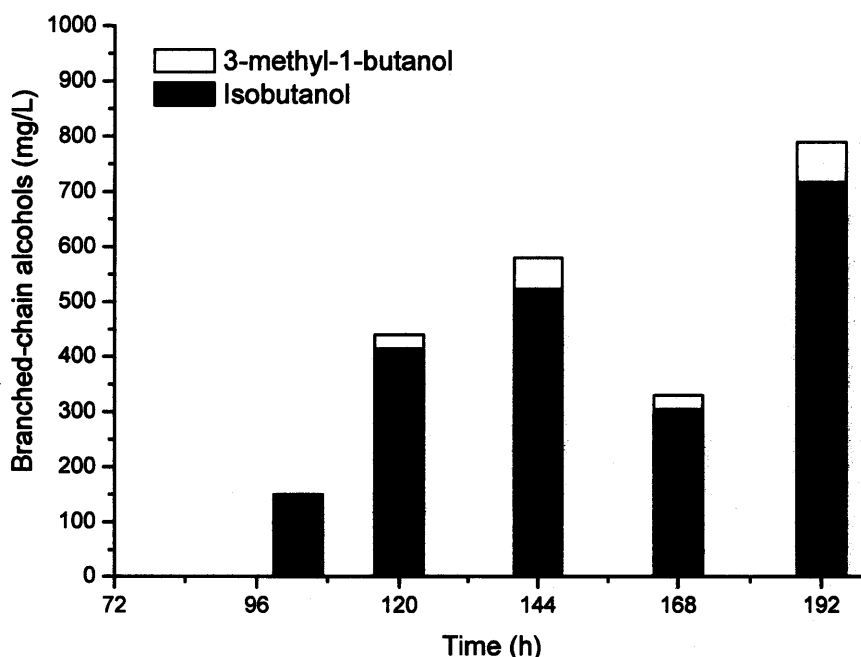


Figure 3.4: The concentration and compositions of branched-chain alcohols produced by Re2410/pJL26 in a two-phase fed-batch culture.

DISCUSSION

Three cultivation modes (batch, fed-batch and two-stage fed-batch culture) were investigated for improving the production of branched-chain alcohols by recombinant *R. eutropha*. Through these analysis, it is concluded that balanced carbon and nitrogen source during cultivation of Re2410/pJL26 for both growth and branched-chain alcohols production is very important. In future experiments, a fed-batch culture mode could be employed for enhancing both the CDW and branched-chain alcohol production by supplying enough carbon sources. The results presented in this study have demonstrated that fed-batch culture was useful for efficient production of total branched-chain alcohols in the cultivation of Re 2410/pJL26.

However, the maximum CDW was only 3.1 g/L. These results lend evidence to the conclusion that higher branched-chain alcohol concentrations will inhibit the cell growth, as suggested from previous flask culture results (Lu et al. 2012; Li et al. 2011; Knoshaug and Zhang 2009). It needs to be pointed out that higher CDW was achieved with 20 ml feeding strategy. On the other hand, 10 ml feeding strategy resulted in higher branched-chain alcohol production. The above result indicates simple fed-batch feeding strategy is not the ideal method to enhance both total CDW and branched-chain alcohol production. Therefore, further research on optimization of the fed-batch fermentation process was carried out to increase cell density without the branched-chain alcohol inhibitory effect. It is often seen that the extremely high or low nutrient concentration in culture medium will inhibit cell growth rate and yield (Shang et al. 2003; Fei et al. 2011). Thus, the fed-batch strategy in which the addition of fructose and NH_4Cl during fermentation should be adopted to avoid the inhibitory nutrient concentration levels in culture medium. An unbalanced consumption rate between the carbon source and nitrogen source often causes the accumulation of ammonium ion, which will result in culture pH increase (Suzuki et al. 1990; Li et al. 2011). By using PID control system, nutrients can be transferred into fermenters automatically without nutrient limitation.

Further development of other advanced culture systems should also be considered for branched-chain alcohol production, such as implementation of a membrane cell recycling continuous culture system. In this system, cells would be recovered by a hollow fiber membrane and the culture medium, containing branched-chain alcohol products, will pass through the membrane and be collected for branched-chain alcohol recovery. By using this culture system, it is believed that inhibition and consumption effect of branched-chain alcohol will be controlled and limited.

For the first time, a pH-stat modal, two-stage fed-batch cultivation was described for the production of branched-chain alcohols. By controlling the C/N ratio of the feeding solution, a branched-chain alcohol titer of 790 mg/L and cell dry weight of 21 g/L was achieved with pH-stat modal feeding. The production of branched-chain alcohols was improved by more than 60% comparing with the results of batch cultures. However, the growth inhibitory effect of isobutanol during the cultivation was also observed which resulted in eventual cell growth limitation. It should be noted that a mixture of two branched-chain alcohols were produced with more than 95% of the total branched-chain alcohols titer as isobutanol. Both alcohols can be used as drop-in blend fuels. High isobutanol content could provide higher energy density than other advanced drop-in biofuels because of its high octane number.

REFERENCES

- Cook J, Beyea J (2000) Bioenergy in the United States: progress and possibilities. *Biomass Bioenerg* 18 (6): 441-455
- An H, Wilhelm WE, Searcy SW (2011) Biofuel and petroleum-based fuel supply chain research: A literature review. *Biomass Bioenerg* 35(9): 3763-3774
- Jang Y, Kim B, Shin JH, Choi YJ, Choi S (2012) Bio-Based Production of C2-C6 Platform Chemicals. *Biotechnol Bioeng* 109(10): 2437-2459
- Kim S, Dale BE (2005) Life cycle assessment of various cropping systems utilized for producing biofuels: Bioethanol and biodiesel. *Biomass Bioenerg* 29(6):426-439
- Barala A, Bakshi BR (2010) Emergy analysis using US economic input–output models with applications to life cycles of gasoline and corn ethanol. *Ecol Modell* 221(15): 1807-1818
- Dürre P (2007) Biobutanol: An attractive biofuel. *J Biotechnol* 2(12): 1525-1534
- Peralta-Yahya PP, Keasling JD (2010) Advanced biofuel production in microbes. *J Biotechnol* 5(2): 147-162
- Pfromm PH, Amanor-Boadub V, Nelson R, Praveen V, Madl R (2010) Bio-butanol vs. bio-ethanol: A technical and economic assessment for corn and switchgrass fermented by yeast or *Clostridium acetobutylicum*. *Biomass Bioenerg*34(4): 515-524
- Sheehan J (2008) Engineering direct conversion of CO₂ to biofuel. *Nat Biotechnol* 27(12):1128-1129
- Junginger M, Torjus Bolkesjø T, Douglas Bradley S (2008) Developments in international bioenergy trade. *Biomass Bioenerg* 32(8): 717-729
- Harvey BG, Meylemans HA (2011) The role of butanol in the development of sustainable fuel technologies. *J Chem Technol Biotechnol* 86(1): 2-9
- Eyidogan M, Ozsezen AN, Canakci M, Turkcan A (2010) Impact of alcohol–gasoline fuel blends on the performance and combustion characteristics of an SI engine. *Fuel* 89(10): 2713-2720
- Lee SY, Park JH, Jang SH, Nielsen LK, Kim J, Jung KS (2008) Fermentative Butanol Production by *Clostridia*. *Biotechnol Bioeng* 101(2): 209-228
- Yan Y, Liao JC (2009) Engineering metabolic systems for production of advanced fuels. *J Ind Microbiol Biotechnol* 36(4):471-479
- Nasib Q, Saha BC, Hector RE, Hughes SR, Cotta MA (2008) Butanol production from wheat straw by simultaneous saccharification and fermentation using *Clostridium beijerinckii*: Part I-Batch fermentation. *Biomass Bioenerg* 32(2): 176-183
- Atsumi S, Liao JC (2008) Metabolic engineering for advanced biofuels production from *Escherichia coli*. *Curr Opin Biotechnol* 19(5): 414-419

- Kim BS, Lee SY, Chang HN (1992) Production of poly- β -hydroxybutyrate by fed-batch culture of recombinant *Escherichia coli*. *Biotechnol Lett* 14(9): 811-816
- Chen H, Huang H, Wu H (2009) Process optimization for PHA production by activated sludge using response surface methodology. *Biomass Bioenerg* 33(4): 721-727
- Budde CF, Riedel SL, Willis LB, Rha C, Sinskey AJ (2011) Production of Poly (3-Hydroxybutyrate-co-3-Hydroxyhexanoate) from Plant Oil by Engineered *Ralstonia eutropha* Strains. *Appl Environ Microbiol* 77(9): 2847-2854
- Lu J, Brigham CJ, Gai CS, Sinskey AJ. Studies on the production of branched-chain alcohols in engineered *Ralstonia eutropha*. *Appl Microbiol Biotechnol* 2012; 96(1): 283-97.
- Smith KM, Cho KM, Liao JC (2010) Engineering *Corynebacterium glutamicum* for isobutanol production. *Appl Microbiol Biotechnol* 87(3): 1045-1055
- Huo YX, Cho KM, Rivera JGL, Monte E, Shen CR (2011) Conversion of proteins into biofuels by engineering nitrogen flux. *Nat Biotechnol* 29(4): 346-351
- Li S, Wen J, Jia X (2011) Engineering *Bacillus subtilis* for isobutanol production by heterologous Ehrlich pathway construction and the biosynthetic 2-ketoisovalerate precursor pathway overexpression. *Appl Microbiol Biotechnol* 91(3): 577-589
- Ding SF, Tan TW (2006) L-Lactic acid production by *Lactobacillus casei* fermentation using different fed-batch feeding strategies. *Process Biochem* 41(6): 1451-1454
- Knoshaug EP, Zhang M (2009) Butanol tolerance in a selection of microorganisms. *Appl Biochem Biotechnol* 153(1): 13-20
- Son YJ, Park KH, Lee SY (2007) Effects of temperature shift strategies on human preproinsulin production in the fed-batch fermentation of recombinant *Escherichia coli*. *Biotechnol Bioprocess Eng* 12(5): 556-561
- Qureshi N, Saha BC, Cotta MA (2008) Butanol production from wheat straw by simultaneous saccharification and fermentation using *Clostridium beijerinckii*: Part II-Fed-batch fermentation. *Biomass Bioenerg* 32(2): 176-183
- Zhang J, Fang X, Zhu X, Li Y (2011) Microbial lipid production by the oleaginous yeast *Cryptococcus curvatus* O3 grown in fed-batch culture. *Biomass Bioenerg* 35(5): 1906-1911
- Shang L, Jiang M, Chang HN (2003) Poly (3-hydroxybutyrate) synthesis in fed-batch culture of *Ralstonia eutropha* with phosphate limitation under different glucose concentrations. *Biotechnol Lett* 25(17): 1415-1419
- Riedel SL, Bader J, Brigham CJ (2012) Production of poly(3-hydroxybutyrate-co-3-hydroxyhexanoate) by *Ralstonia eutropha* in high cell density palm oil fermentations. *Biotechnol Bioeng* 109(1): 74-83
- Hartlep M, Hussmann W, Prayitno N, Meynial-Salles I, Zeng AP (2002) Study of two-stage processes for the microbial production of 1, 3-propanediol from glucose. *Appl Microbiol Biotechnol* 60(1): 60-66

- Fei Q, Chang HN, Shang L, Choi J (2011) Exploring low-cost carbon sources for microbial lipids production by fed-batch cultivation of *Cryptococcus albidus*. *Biotechnol Bioprocess Eng* 16(3): 482-487
- Praveenkumar R, Shameera K, Mahalakshmi G, Akbarsha MA, Thajuddin N (2012) Influence of nutrient deprivations on lipid accumulation in a dominant indigenous microalga *Chlorella sp.*, BUM11008: Evaluation for biodiesel production. *Biomass Bioenerg* 37: 60-66
- Suzuki T, Yamane T, Shimizu S (1990) Phenomenological background and some preliminary trials of automated substrate supply in pH-Stat modal fed-batch culture using a set point of high limit. *J Ferment Bioeng* 69(5): 292-297
- Baez A, Cho KM, Liao JC (2011) High-flux isobutanol production using engineered *Escherichia coli*: a bioreactor study with in situ product removal. *Appl Microbiol Biotechnol* 90(5): 1681-1690
- Boonsawang P, Subkaree Y, Srinorakutara T (2012) Ethanol production from palm pressed fiber by prehydrolysis prior to simultaneous saccharification and fermentation (SSF). *Biomass Bioenerg* 40: 127-132
- Fei Q, Chang HN, Shang L, Choi J, Kim N, Kang J (2011) The effect of volatile fatty acids as a sole carbon source on lipid accumulation by *Cryptococcus albidus* for biodiesel production. *Bioresour Technol* 102(3): 2695-2701
- Li SY, Srivastava R, Steven SL, Li Y, Parnas RS (2011) Performance of batch, fed-batch, and continuous A-B-E fermentation with pH-control. *Bioresour Technol* 102(5): 4241-4250

CHAPTER 4

Characterization and modification of enzymes in the 2-ketoisovalerate biosynthesis pathway of *Ralstonia eutropha* H16

(This chapter was modified from a manuscript that has been accepted for publication in Applied Microbiology and Biotechnology, 2014 'Characterization and Modification of Enzymes in the 2-Ketoisovalerate Biosynthesis Pathway of *Ralstonia eutropha*' Jingnan Lu, Christopher Brigham, Jens Plassmeier, and Anthony Sinskey © Springer-Verlag)

INTRODUCTION

The metabolically versatile proteobacterium *Ralstonia eutropha*, also known as *Cupriavidus necator*, is a tremendously important organism in biotechnological research and development. *R. eutropha* is notably capable of utilizing numerous simple and complex carbon sources derived from common waste streams, including carbon dioxide, oils and fats, and mixed organic acids (Bowien and Kusian 2002; Cramm 2009; Kohlmann et al. 2011; Pohlmann et al. 2006; Schwartz et al. 2009). Wild type *R. eutropha* stores carbon and energy in the form of polyhydroxyalkanoate (PHA), a type of biodegradable plastic, under unbalanced nutrient stress high in carbon (Brigham et al. 2012; Cramm 2009; Ishizaki et al. 2001; Pohlmann et al. 2006). Elimination of the enzymes responsible for the production of PHA in *R. eutropha* resulted in a strain capable of secreting a large amount of pyruvate and stored more NADH reducing equivalent compared to the wild type (Lu et al. 2012; Raberg et al. 2014). Additionally, other reduced metabolites such as 2,3-butanediol, ethanol, lactate, butanol, and 3-hydroxybutyrate are also secreted (Vollbrecht et al. 1978; Vollbrecht and Schlegel 1978; Vollbrecht and Schlegel 1979). There is a growing interest in repurposing these secreted pyruvate and extra energy compounds in these PHA-negative strains into value-added chemicals, such as biofuels, pharmaceutical precursors, and flavoring agents (Brigham et al. 2012). Recent accomplishments among many others in engineering PHA-negative strains of *R. eutropha* include the production of biofuels from branched-chain amino acid (BCAA) and PHA production precursors (Brigham et al. 2013; Brigham et al. 2012; Grousseau et al. 2014; Lan and Liao 2013; Li and Liao 2014; Li et al. 2012; Lu et al. 2012).

The production of isobutanol, a next-generation drop-in biofuel, was achieved through the BCAA biosynthesis pathway. The key precursor 2-ketoisovalerate, an intermediate of the valine biosynthesis pathway synthesized from pyruvate, can be decarboxylated to form isobutyraldehyde and subsequently reduced into isobutanol. Recently, numerous groups were able to redirect pyruvate into isobutanol in engineered *R. eutropha*; however, the production titer remains relatively low as compared to other engineered organisms (Brigham et al. 2013; Li et al. 2012; Lu et al. 2012). The main challenge faced has been the lack of understanding of the interaction and regulation of enzymes that produce the key precursor molecule, 2-ketoisovalerate, in *R. eutropha* (Lu et al. 2012). Utilization of the well-studied biosynthesis enzyme AHAS from *Bacillus subtilis* was reported to be toxic to *R. eutropha* cells, thus precluding their use in production strain engineering (Li and Liao 2014; Li et al. 2012).

Acetoxyacid synthase (AHAS) catalyzes the most important step in the 2-ketoisovalerate biosynthesis pathway, since the reactions it catalyzes are irreversible and are the

first committed steps towards the synthesis of all three BCAAs (Figure 1). AHAS is capable of synthesizing 2-acetolactate, a precursor of valine and leucine from two molecules of pyruvate, in addition to 2-aceto-2-hydroxybutyrate, a precursor of isoleucine from pyruvate and 2-ketobutyrate. A bifunctional AHAS catalyzes both of the above-mentioned reactions in most organisms, whereas in a few organisms, two separate enzymes catalyze these reactions (Chipman et al. 1998; McCourt and Duggleby 2006). *R. eutropha* AHAS enzyme consists of two subunits, IlvB and IlvH, encoded by genes in the operon *ilvBHC* (locus tags H16_A1035 and H16_A1036). To date, there is no definitive structural information on AHAS, although individual subunits have been crystallized separately from *Escherichia coli* (Chipman et al. 1998; Kaplun et al. 2006; McCourt and Duggleby 2006; Park and Lee 2010; Petkowski et al. 2007). Studies of AHAS from *E. coli*, *Corynebacterium glutamicum*, *B. subtilis*, *Lactococcus lactis*, and others have led to the hypothesis that catalysis occurs at the IlvB homodimer interface and IlvH is required for catalysis, but serves a regulatory role. The expression of *ilvBH* is controlled by the amount of charged-tRNA^{BCAAs} available in the cell. High levels of charged-tRNA^{BCAAs} repress the transcription of *ilvBH*. Furthermore, AHAS activity is controlled allosterically at the activity level by its regulatory subunit IlvH, through binding of BCAA at the homodimer interface (Barak and Chipman 2012; Chipman et al. 1998; Eggeling et al. 1987; Eoyang and Silverman 1986; McCourt and Duggleby 2006; Vinogradov et al. 2006).

E. coli has three extensively-studied AHAS isozymes, each with a different substrate specificity and regulation mechanism. The sequence of *E. coli* AHAS isozyme II differs from the other two AHASs, and its regulatory subunit is insensitive to direct feedback inhibition by valine (Eoyang and Silverman 1986; Park and Lee 2010; Steinmetz et al., 2010; Vinogradov et al. 2006; Vyazmensky et al. 2009; Vyazmensky et al. 1996). *R. eutropha* AHAS shares the greatest sequence similarity with *E. coli* AHAS isozyme I (52%); therefore, it could also be subject to allosteric feedback inhibition by the pathway intermediates 2,3-dihydroxy-isovalerate and 2-ketoisovalerate, in addition to the end products valine, leucine, and isoleucine. Thus, understanding and minimizing allosteric inhibition by products and intermediates are essential to optimize the production of 2-ketoisovalerate in *R. eutropha*.

In the case of *R. eutropha*, AHAS catalyzes both the formation of 2-acetolactate and 2-aceto-2-hydroxybutyrate (Figure 4.1). The substrate selectivity ratio (R) towards 2-ketobutyrate as the second substrate over pyruvate can be calculated by the following equation:

$$R = \frac{[AHB]}{[2KB]} \cdot \frac{[AL]}{[P]} \quad (\text{Equation 4.1}),$$

where AHB, 2KB, AL, and P represent 2-aceto-2-hydroxybutyrate, 2-ketobutyrate, 2-acetolactate, and pyruvate respectively (Barak et al. 1987; Gollop et al. 1990). There is a competition between pyruvate and 2-ketobutyrate for an active 2-hydroxyethyl-ThDP carbanion/enamine intermediate formed irreversibly after the addition and decarboxylation of the first pyruvate moiety to the enzyme (Bar-Ilan et al. 2001; Chipman et al. 2005; Engel et al. 2004; Steinmetz et al. 2010; Tittmann et al. 2004; Vyazmensky et al. 2011). R values for *E. coli* AHAS isozymes I, II, and III are respectively 1, 185, and 53. These ratios, besides that of isozyme I, strongly favor the formation of 2-aceto-2-hydroxybutyrate over 2-acetolactate (Barak et al. 1987).

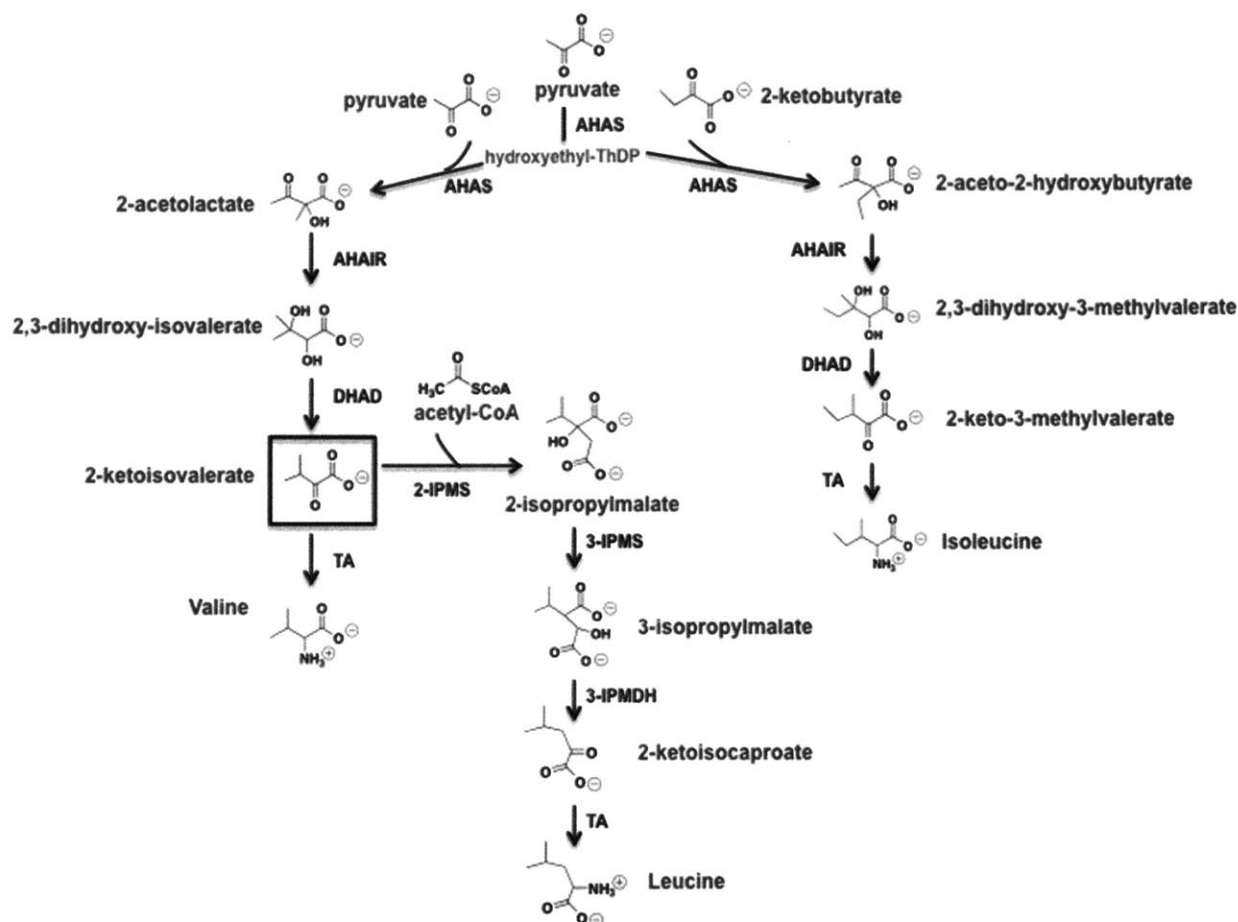


Figure 4.1: Schematic of the branched-chain amino acid (BCAA) biosynthesis pathway in *R. eutropha*. Pyruvate is the precursor for the production of all three branched-chain amino acids. Via acetoxyacid synthase (AHAS), two molecules of pyruvate condense to form 2-acetolactate, a precursor for valine. AHAS can also incorporate 2-ketobutyrate as the second substrate with pyruvate to form 2-aceto-2-hydroxybutyrate for the production of isoleucine. Both 2-acetolactate and 2-aceto-2-hydroxybutyrate are then reduced and isomerized to 2,3-dihydroxyisovalerate and 2,3-dihydroxy-3-methylvalerate respectively by the same enzyme, acetoxyacid isomeroreductase (AHAIR). Dihydroxyacid dehydratase (DHAD) converts 2,3-dihydroxyisovalerate and 2,3-dihydroxy-3-methylvalerate to the key intermediate 2-ketoisovalerate and 2-keto-3-methylvalerate accordingly. Transaminase (TA) catalyzes the production of valine from 2-ketoisovalerate and isoleucine from 2-keto-3-methylvalerate. Three other enzymes: isopropylmalate synthase (IPMS), isopropylmalate synthase (IPMS), and isopropylmalate dehydrogenase (IPMDH) sequentially divert 2-ketoisovalerate to leucine production.

Acetoxyacid isomeroreductase (AHAIR), encoded by *ilvC* (locus tags H16_A1037) within the operon *ilvBHC* in *R. eutropha*, catalyzes the formation of 2,3-dihydroxyisovalerate from 2-acetolactate, in addition to the formation of 2,3-dihydroxy-3-methylvalerate from 2-aceto-2-hydroxybutyrate. Unlike AHAS, AHAIR has similar substrate preference towards both substrates. AHAIR requires NADPH and a divalent metal ion, in most cases Mg^{2+} , for catalysis. The metal cofactor is involved in the alkyl migration isomerization step, whereas NADPH is the electron donor for the reduction step. A unique feature of its reaction mechanism is that it simultaneously catalyzes both an isomerization and a reduction reaction. Mutations in active site

residues that abolished the reductase activity also eliminated the isomerization reaction, suggesting that isomerization and reduction are coupled without any detectable intermediate (Chunduru et al. 1989; Harper et al. 1984; Schomburg and Stephan 1995).

Dihydroxyacid dehydratase (DHAD) catalyzes the formation of ketoacids from the products of AHAIR. In most organisms, DHAD encoded by *ilvD* is found in the BCAA biosynthesis operon *ilvBHCD* (Eggeling et al. 1987; Krause et al. 2010; Leyval et al. 2003). However, the *R. eutropha ilvD* (locus tag H16_A2987) gene is not found in the operon, but elsewhere on chromosome I. The mechanism of action is not yet elucidated, but was hypothesized to involve the dehydration of vicinal diols to ketoacids via an enol intermediate. *E. coli*'s oxygen-sensitive DHAD contains a [4Fe-4S]²⁺ cluster. The reaction mechanism is proposed to be similar to that of aconitase in the TCA cycle, which also involves a FeS cluster (Flint and Emptage 1988; Flint et al. 1993; Leyval et al. 2003). As shown in Figure 4.1, the combined activities of AHAS, AHAIR, and DHAD convert pyruvate into the key intermediate 2-ketoisovalerate.

The specific activity, substrate specificity, and feedback inhibition of *R. eutropha* AHAS, AHAIR, and DHAD have not been previously studied. In order to better understand the catalysis of these enzymes and to minimize allosteric inhibition, AHAS, AHAIR, and DHAD were isolated as pure enzymes and evaluated in this study.

MATERIALS AND METHODS

Chemicals, bacterial strains, and plasmids

Unless indicated otherwise, chemicals used in this study were purchased from Sigma-Aldrich. Strains and plasmids used were listed in Table 4.1 and Table 4.2. Mutant strains were all derived from wild type *R. eutropha* H16 (ATCC 17699). Primers used in the construction of plasmids and strains were listed in Appendix 4.1.

Table 4.1: Strains used in this work.

Strains	Genotype	Reference
<i>R. eutropha</i>		
H16	Wild-type, gentamicin resistant (Gen ^r)	ATCC17699
Re2451	H16Δ <i>ilvH</i> (Gen ^r)	This work
Re2452	H16 evolved on L-valine (Gen ^r)	This work
<i>E. coli</i>		
DH5α	General cloning strain	Invitrogen
S17-1	Conjugation strain for transfer of plasmids into <i>R. eutropha</i>	(Simon <i>et al.</i> , 1983)
Tuner(DE3)	Protein expression strain	Novagen

Table 4.2: Plasmids used in this work.

Plasmids	Genotype	Reference
pJV7	pJQ200Kan with Δ <i>phaC1</i> allele inserted into BamHI restriction site, confers kanamycin resistance (Kan ^r)	(Budde <i>et al.</i> , 2011a)
pJL44	pJV7 with Δ <i>phaC1</i> allele removed by XbaI and SacI digestion and replace with Δ <i>ilvH</i> allele (Kan ^r)	This work
pET-15b	Plasmid for inducible and His-tagged protein expression in <i>E. coli</i> (Amp ^r)	Novagen
pRARE2	Plasmid supplying seven rare <i>E. coli</i> tRNAs (Cm ^r)	Novagen
pJL13	Plasmid for expression of native IlvB with N-terminal His-tag	This work
pJL14	Plasmid for expression of native IlvH with N-terminal His-tag	This work
pJL15	Plasmid for expression of native IlvC with N-terminal His-tag	This work
pJL16	Plasmid for expression of native IlvD with N-terminal His-tag	This work
pJL45	Plasmid for expression of mutated-IlvH from strain Re2452 with N-terminal His-tag	This work
pJL46	Plasmid for expression of native IlvH (N11F) with N-terminal His-tag	This work
pJL47	Plasmid for expression of native IlvH (G14E) with N-terminal His-tag	This work
pJL48	Plasmid for expression of native IlvH (G21R) with N-terminal His-tag	This work
pJL48	Plasmid for expression of native IlvH (L22V) with N-terminal His-tag	This work
pJL50	Plasmid for expression of native IlvH (F23V) with N-terminal His-tag	This work
pJL51	Plasmid for expression of native IlvH (N29H) with N-terminal His-tag	This work
pJL52	Plasmid for expression of native IlvH (E31C) with N-terminal His-tag	This work
pJL53	Plasmid for expression of native IlvH (P38A) with N-terminal His-tag	This work

Growth media and cultivation conditions

As described previously by Lu *et al.* 2012, *R. eutropha* strains were cultivated aerobically in rich and minimal media with 2% (w/v) fructose at 30°C. Gentamicin at 10 µg/mL final concentration was added to all *R. eutropha* cultures (Walde 1962). *E. coli* cultures were grown in lysogeny broth (LB) at 30°C with the addition of 100 µg/mL ampicillin and 34 µg/mL chloramphenicol (Lu *et al.* 2013; Lu *et al.* 2012).

R. eutropha growth experiments with different concentrations of 2-ketoisovalerate or valine were conducted by supplementing minimal media with 0 to 0.5% (w/v) 3-methyl-2-oxobutanoic acid sodium salt or 0 to 1 mM L-valine, respectively. Fructose, antibiotics, 3-methyl-2-oxobutanoic acid sodium salt, and L-valine, were all filter sterilized while the rest of the medium components were sterilized by autoclaving.

Experimental evolution of L-valine

Wild type *R. eutropha* H16 cells were cultivated in minimal media until OD₆₀₀ reached 3.0. Aliquots of the culture were then transferred to fresh minimal media supplemented with L-valine at concentrations of 0.1 mM to reach initial OD₆₀₀ of 0.1. The cultures were sequentially transferred to inoculate fresh minimal media with increasing concentration of L-valine when they reached OD₆₀₀ of 3.0. Over the 60-day time course, L-valine concentration was increased from 0.1 mM to 10 mM in the growth media.

In order to detect mutations evolved that could contribute to valine insensitivity by AHAS, *ilvB* and *ilvH* genes in addition to 100 base pairs (bp) of DNA sequence upstream and downstream of *ilvBH* were amplified by PCR, sequenced, and compared between wild type and mutant (Re2452) strains.

Plasmid and strain construction

Standard molecular biology techniques were utilized for all DNA manipulations (Sambrook et al. 2001). Amplification of DNA sequence was achieved using Phusion DNA polymerase (New England Biolabs, Ipswich, MA). QIAquick gel extraction kit (Qiagen, Valencia, CA) and QIAprep spin miniprep kit (Qiagen, Valencia, CA) were used for gel purifications of all DNA products and plasmid extractions respectively. Restriction enzymes used in this study were from New England Biolabs (Ipswich, MA).

Construction of plasmids for the heterologous overexpression of BCAA enzymes was first carried out by amplifying genes *ilvB*, *ilvH*, *ilvC*, and *ilvD* that encode IlvB, IlvH, IlvC, and IlvD, respectively, from the genome of wild type *R. eutropha* H16. The PCR amplifications with primers listed in Appendix 4.1 added a *NdeI* site to the 5' end of each gene and a *BamHI* site to the 3' end. The PCR fragments were purified on 0.8% agarose gel. Both PCR fragments and expression vector pET15b were digested with *NdeI* and *BamHI*, and then ligated together and transformed into high efficiency *E. coli* DH10-beta competent cells (New England Biolabs, Ipswich, MA) to create the expression plasmid. Each expression plasmid contained a gene encoding N-terminal six-His-tagged version of each enzyme. Lastly, the plasmids were transformed into *E. coli* strain Tuner(DE3) for inducible protein expression. The Tuner(DE3) strain also contained an additional plasmid, pRARE that allows for translation of protein with rare-codons.

Plasmid for markerless deletion of *ilvH* was constructed by first amplifying approximately 500 bp of DNA sequence upstream and downstream of *ilvH* using primers with identical sequence overlap at the end (Appendix 4.1). Overlap PCR using these primers resulted in a DNA fragment of approximately 1,000 bp in length that contained both the upstream and downstream region of *ilvH*. The DNA fragment and plasmid pJV7 (Budde et al. 2010) (Table 4.2) were digested with the restriction enzymes *XbaI* and *BamHI*, and then ligated together with the *ilvH* deletion fragment to form the deletion plasmid. The resulting plasmid was verified in *E. coli* DH10-beta competent cells before being transformed into *E. coli* S17-1 (Simon et al. 1983), which was used as a donor for the conjugative transfer of mobilizable plasmids. A standard mating and gene deletion procedure was performed as described previously (Quandt and Hynes 1993; Slater et al. 1998; York et al. 2001). Deletion strains were screened by diagnostic PCR with pairs of internal and external primer sets (Appendix 4.1).

Site-directed mutagenesis was achieved by overlap extension PCR method using primers listed in Appendix 4.1 using plasmid pJL14 as the template DNA. This method allowed for single nucleotide mutations with site specificity.

Purification of His-tagged proteins and removal of the His-tag

R. eutropha enzymes in the 2-ketoisovalerate production pathway were expressed in *E. coli* (Table 4.1) and purified. *E. coli* Tuner(DE3) with pRARE and BCAA enzyme overexpression plasmid were cultivated in lysogeny broth (LB) containing 100 µg/mL ampicillin and 34 µg/mL chloramphenicol at 30°C. When OD₆₀₀ reached 0.5, the cells were induced with 0.5 mM Isopropyl β-D-1-thiogalactopyranoside. Cells were harvested 4 h post-induction and pelleted by centrifugation. Cell pellets were washed with phosphate buffered saline and resuspended in sodium phosphate buffer (20 mM, pH7.4) with 0.1 M NaCl. Cells were lysed with a French press via three passes at 1,200 psi and 4°C. Cell debris was removed by centrifugation and filtration through 0.2-µm low-protein-binding filters. Lysate was then loaded onto a 5-mL Ni Sepharose fast-flow column (GE Healthcare, Piscataway, NJ) connected to a low pressure BioLogic liquid chromatography system (Bio-Rad, Hercules, CA). The column was first washed with buffer containing 20 mM sodium phosphate (pH 7.4), 0.5 M NaCl, and 40 mM imidazole to eliminate nonspecifically bound protein. Elution of the His-tagged enzymes was achieved by increasing the concentration of imidazole from 40 mM to 500 mM in the buffer at a flow rate of 5 mL/min. Fractions containing purified protein of interest were detected on 15% SDS-PAGE gels. These fractions were collected and dialyzed against 20 mM sodium phosphate buffer (pH 7.4) with 0.1 M NaCl using a Slide-A-Lyzer Dialysis Cassette (Thermo Scientific, Asheville, NC, USA) at 4°C. The proteins were then concentrated using Amicon Ultra-15 Centrifugal Filter Units (EMD Millipore Corporation, Billerica, MA, USA). Lastly, His-tags were removed from the purified proteins using Thrombin Cleavage Kit (Novagen, St. Louis, MO).

Enzymatic activity assays

Purified IlvB, IlvH, IlvC, and IlvD with epitope tags removed were used immediately for enzymatic assays. AHAS was reconstituted by incubating IlvB and IlvH at room temperature for 10 min in solution with 100 mM potassium phosphate buffer (pH 7) and 0.1 mM DTT. IlvB and IlvH mixtures in a molar ratio of 1:0 to 1:100 were tested for reconstitution and enzymatic activity. Protein concentrations were determined by a modified Bradford assay (Zor and Selinger 1996) using bovine serum albumin as the protein concentration standard.

The AHAS, AHAI, and DHAD activity assays were modified from published methods (Leyval et al. 2003; Lu et al. 2012). The AHAS activity assay is a discontinuous colorimetric assay. The reaction mixture contained 100 mM potassium phosphate buffer (pH 7.0), 50 mM sodium pyruvate, 100 mM MgCl₂, 100 µM thiamine pyrophosphate (TPP), and reconstituted AHAS. Addition of sodium pyruvate initiated the reaction at 30°C. Over the course of the reaction (30 min), 100 µL aliquots of assay mixture were removed every 5 min, and the reaction was terminated by acidification with 10 µL 50% H₂SO₄. The acidified reaction was then incubated at 37°C for 30 min to allow spontaneous decarboxylation of 2-acetolactate to acetoin. Acetoin was quantified by the Voges-Proskauer method (Westerfield et al. 1945) and detected at 535 nm with a Varioskan Flash Plate Reader (Thermo Scientific, Asheville, NC). Different

micromolar concentrations of acetoin (3-hydroxy-2-butanone) were used as a standard for determination of the quantity of 2-acetolactate formed.

The AHAIR activity reaction mixture contains 100 mM potassium phosphate buffer (pH 7.0), 10 mM α -acetolactate, 3 mM MgCl₂, 0.1 mM NADPH, and purified IlvC. The substrate, α -acetolactate, was chemically synthesized based on a previously published method (Leyval et al. 2003). The addition of α -acetolactate at 30°C initiated the reaction, which was constantly monitored at 340 nm by a spectrophotometer (Agilent 8453 UV-visible Kinetic Mode). Molar extinction coefficient of NADPH (6220 M⁻¹cm⁻¹) was used to calculate μ mol NADPH oxidized.

The DHAD activity assay indirectly detects the product derivative, α -ketoisovalerate-dinitrophenylhydrazine. The reaction mixture contained 100 mM potassium phosphate buffer (pH 7.0), 5 mM MgCl₂, 10 mM DL- α,β -dihydroxyisovalerate, and purified IlvD. Substrate DL- α,β -dihydroxyisovalerate was added to initiate the reaction at 30°C. A 100 μ L aliquot of the reaction mixture was removed and the reaction terminated by addition of 12.5 μ L trichloroacetic acid (10 % v/v). Aliquots were sampled every 2 min for a total of 20 min. The mixtures were then derivatized with 25 μ L saturated 2,4-dinitrophenylhydrazine in 2 M HCl for the formation of α -ketoisovalerate-dinitrophenylhydrazine, which was then detected at 540 nm using a Varioskan Flash Plate Reader. Commercial 3-methyl-2-oxobutanoic acid sodium salt was derivatized and used as a standard for this assay.

Kinetic parameters of AHAS, AHAIR, and DHAD towards substrates and cofactors were determined by measuring the activity of each enzyme at various substrate and cofactor concentrations in the presence of saturating concentrations of all other factors. Pyruvate (from 0.1 mM to 50 mM), 2-acetolactate (from 0.1 mM to 10 mM), and 2,3-dihydroxy-isovalerate (from 0.1 mM to 10 mM) were used for AHAS, AHAIR, and DHAD respectively. FAD from 0.1 μ M to 1 μ M was used for the AHAS cofactor K_M study and NADPH from 1 μ M to 20 μ M was used for the AHAIR cofactor K_M study. The K_M and V_{max} values were determined from double-reciprocal plots of kinetic data (Lineweaver-Burk plot). Inhibition assays were conducted by supplementing activity assay mixture with different concentrations of L-valine, L-leucine, or L-isoleucine. The substrate specificity for 2-ketobutyrate as the second substrate (R), was determined by measuring the formation of acetohydroxybutyrate and acetolactate in experiments that contained both pyruvate and 2-ketobutyrate. The results were plotted and fit to Equation 4.1.

All results discussed in this work were average of triplicate reactions \pm standard deviation unless indicated otherwise. Assay reactions without the addition of enzyme or substrates were conducted separately as controls. Enzyme unit (U) was defined as 1 μ mol product formed per min.

RESULTS

Purification of AHAS, AHAIR, and DHAD protein from *R. eutropha*

His-tagged versions of IlvB, IlvH, IlvC, and IlvD were expressed in *E. coli* and purified to homogeneity as described in Materials and Methods. Initial solubility tests indicated that both IlvB and IlvH were present mainly in the insoluble fraction (data not shown), even though they are cytosolic proteins. Attempted purification of IlvB and IlvH from the soluble fraction only resulted in both proteins precipitating from the buffer solution after elution with imidazole. In order to increase the solubility of the target proteins, nonionic detergents were utilized to

dissociate any lipid-protein or protein-protein interactions. Nonionic detergents were chosen over ionic and zwitterionic detergent classes, because these detergents do not denature proteins. Tween 20 or Triton X-100 at final concentrations of 1% (v/v) was added separately before cell disruption by French press. The purification process was carried out as described in Materials and Methods, except that both the binding and elution buffers contained 1% (v/v) detergent. The addition of either Tween 20 or Triton X-100 greatly improved solubility of IlvB and IlvH, and also prevented precipitation after purification (data not shown). The purified IlvB protein solution was bright yellow, which indicated the presence of FAD cofactor bound to the protein. Both IlvC and IlvD are soluble proteins, which were able to be purified without the addition of any detergents. Figure 4.2 shows an SDS-PAGE analysis of each of the purified proteins, all of which appear homogeneous.

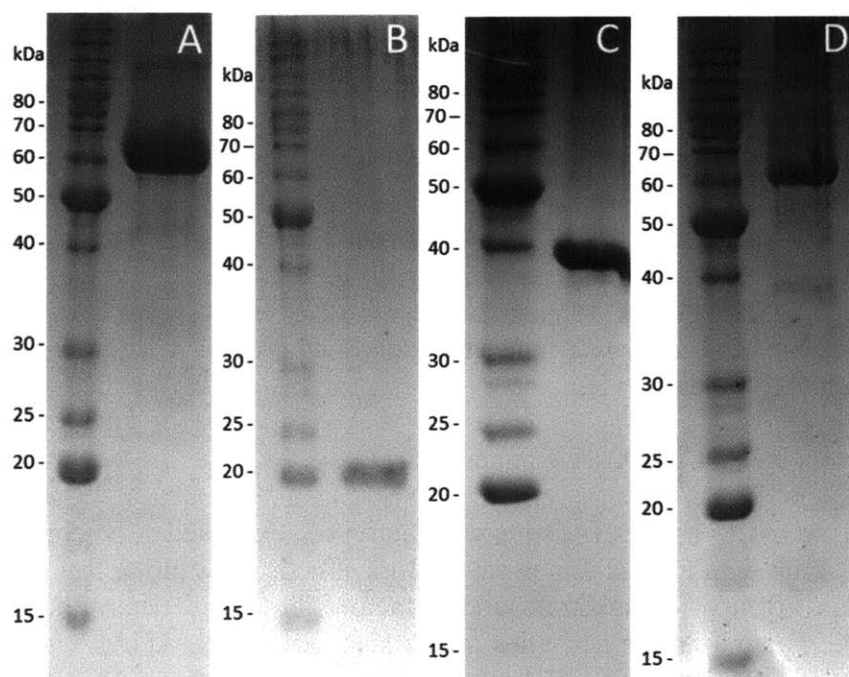


Figure 4.2: SDS-PAGE gel images of His-tag purified IlvB (A), IlvH (B), IlvC (C), and IlvD (D) after thrombin cleavage. The molecular weight of each protein is 64 kDa, 18 kDa, 36 kDa, and 59 kDa respectively for IlvB, IlvH, IlvC, and IlvD.

Reconstitution of AHAS holoenzyme from isolated subunits IlvB and IlvH

The purified and His-tag removed catalytic subunit (IlvB) alone was able to catalyze the formation of 2-acetolactate, although its activity was only ~12% of AHAS maximum activity (Table 4.3). The addition of the regulatory subunit (IlvH) was able to enhance the catalytic activity of AHAS. Table 4.3 shows the increase in specific activity of AHAS upon addition of increasing molar concentration of regulatory subunit. Saturation point was reached at a 1:5 molar ratio of IlvB and IlvH; therefore, for further studies, AHAS was reconstituted in a 1:5 molar ratio of IlvB and IlvH. The specific activity increase with the addition of IlvH indicated that both subunits have been successfully purified in active and fully reconstitutable forms.

Table 4.3: Reconstitution of AHAS holoenzyme from isolated subunits IlvB and IlvH^a.

Ratio of IlvB to IlvH	Specific activity (mU/mg)
1:0	36 ± 5
1:1	130 ± 13
1:5	179 ± 8
1:10	203 ± 41
1:25	194 ± 12
1:50	130 ± 7
1:100	94 ± 11

^aPurified IlvB and IlvH proteins were mixed in the molar ratio indicated here and incubated at room temperature for 10 min. AHAS activity assay was performed with each of the ratio mixture to determine the rate of acetolactate formation. Specific activity represents nmol acetolactate formed per mg of reconstituted-holoenzyme from its subunits (mU/mg).

Since the catalytic subunit (IlvB) alone has some enzymatic activity, it was unknown if *R. eutropha* cells could survive in the absence of a functional IlvH. To test this, the *ilvH* gene was deleted from the *R. eutropha* genome. The resulting deletion strain (Re2451) was cultivated in minimal media without any supplementation of branched-chain amino acids, and separately in TSB (tryptic soy broth) rich media. Although the wild type *R. eutropha* strain was able to grow in both media and reach OD₆₀₀ of 3.0 in less than 24 h, Re2451 only grew in TSB media, and the growth rate was slightly reduced (data not shown). This result indicated that there is only one active AHAS present in *R. eutropha* under the examined growth conditions and the holoenzyme requires its regulatory subunit IlvH.

Kinetic parameters for AHAS, AHAIR, and DHAD

AHAS, AHAIR, and DHAD enzyme activities exhibited a Michaelis-Menten kinetic profile. Using double-reciprocal Lineweaver-Burk kinetic data plots, the maximal rate (V_{max}) and the apparent affinity for substrate and cofactor (K_M) were determined for each enzyme (Appendix 4.2). The maximum activities of the purified AHAS, AHAIR, and DHAD enzymes are 203 mU/mg, 191 mU/mg, and 6,064 mU/mg respectively (Table 4.4). Compared to activities measured in crude extracts of wild type *R. eutropha*, the purified proteins had greater than 20-fold improvement in activities (Lu et al, 2012).

AHAS has a very weak apparent affinity towards pyruvate (10.5 mM), while AHAIR and DHAD have a slight higher affinity for their corresponding substrates at 6.2 mM and 2.7 mM, respectively (Table 4.4). In order to determine the apparent affinity of AHAS for its cofactors, FAD, which was tightly bonded to the purified IlvB, was removed. The FAD stripping process involved incubation of purified IlvB in 2% (w/v) activated charcoal in a 1.5 M KCl solution containing potassium phosphate buffer (pH 7.0) for 30 min at 4°C. The charcoal was then removed by centrifugation and filtration. The reconstituted AHAS was colorless in the absence of FAD and had a very high affinity towards FAD (0.42 μM), which was surprising since mechanistically this enzyme should not involve redox cofactors. TPP is required in the catalysis for the decarboxylation of pyruvate and ligation with the second substrate, whether it be pyruvate or 2-ketobutyrate (Duggleby 2006). The amount of TPP required to reach half-maximum activity cannot be determined, since TPP was co-purified with IlvB and could not be removed *in vitro*. AHAIR requires NADPH to catalyze the substrate isomerization and reduction. The

apparent affinity of AHAIR towards NADPH, determined from the cofactor concentration required to support half-saturation of enzymatic activity, was 12.5 μ M (Table 4.4).

Table 4.4: Specific activity, K_M , and V_{max} values for substrates and cofactors of AHAS, AHAIR, and DHAD^a.

	Specific activity (mU/mg)	K_M (substrate)	K_M (cofactor)	V_{max} (mU/mg)
AHAS	179 \pm 8	10.5 mM (pyruvate)	0.42 μ M (FAD)	203 \pm 41
AHAIR	288 \pm 63	6.2 mM (α -acetolactate)	12.5 μ M (NADPH)	191 \pm 3
DHAD	3,380 \pm 306	2.7 mM (2,3-dihydroxy- isovalerate)	NA ^b	6,064 \pm 610

^a K_M , and V_{max} values were determined from the double-reciprocal plot of kinetic data on Lineweaver-Burk plots. Value represents the mean \pm standard error on n = 3.

^bDHAD does not require any cofactor for catalysis.

R. eutropha AHAS catalyzes the formation of both 2-acetolactate and 2-aceto-2-hydroxybutyrate (Figure 4.1). The flow of substrates depends on the affinity of AHAS for its substrate, therefore substrate specificity of AHAS was determined over a wide range of substrate concentrations. The specificity constant (R) is related to the ratio of product formation rate in relation to substrate concentration. R for the *R. eutropha* AHAS enzyme was determined to be 140, which indicated that the enzyme is highly biased towards 2-ketobutyrate as the second substrate (Table 4.5). This is also consistent with the low apparent affinity of this enzyme towards pyruvate.

Table 4.5: Rate of formation of 2-acetolactate and 2-acetohydroxybutyrate by AHAS with increasing concentration of 2-ketobutyrate.

Pyruvate (mM)	2-ketobutyrate (mM)	2-acetolactate (μ mol/mg)	2-aceto-2-hydroxybutyrate (μ mol/mg)	R
50	0	201	0	NA
50	0.1	191	52	136
50	0.5	125	167	134
50	1	98	263	135
50	5	17	229	113
50	25	4	238	136
50	50	2	259	131

Influence of branched-chain amino acids and keto acids on enzyme activity

Wild type *R. eutropha* experiences a lag in growth when cultivated in increasing concentrations of 2-ketoisovalerate or L-valine (Appendix 4.3 and 4.4). At a 2-ketoisovalerate concentration of 0.5% (w/v), the lag phase lasted for more than 24 h (Appendix 4.3). Valine inhibited the growth even further at a concentration of 1 mM (Appendix 4.4). Such observations indicated that branched-chain amino acids and their intermediate keto acids could influence the activities of AHAS, AHAIR, or DHAD enzymes via allosteric feedback inhibition. Such

inhibition led to growth inhibition because the cells are unable to produce isoleucine, which is essential for cell growth in minimal media.

Table 4.6 shows the amount of L-valine, L-leucine, and L-isoleucine required for reduction of the specific activities of AHAS, AHAI, and DHAD by 50%. AHAS, being the first committed step in the BCAA biosynthesis pathway, is very sensitive to valine and isoleucine, but moderately sensitive to leucine. Specific activity of AHAS was reduced to 50% by valine, isoleucine, and leucine, in decreasing order of effectiveness (Table 4.6). Although AHAS is very sensitive to valine, the inhibition is not complete and the inhibition by all three BCAAs is not accumulative (Figure 4.3). AHAS activity reduction reached a saturation point at approximately 70% with 10 mM valine. Addition of 5 mM of each valine, leucine, and isoleucine reduced the specific activity by only 56% (Figure 4.3). Intermediates in the valine biosynthesis pathway, 2,3-dihydroxyisovalerate and 2-ketoisovalerate also showed significant inhibition effects towards AHAS. Specific activity was reduced to 14% and 39% by 10 mM 2,3-dihydroxyisovalerate and 2-ketoisovalerate respectively (Figure 4.3).

Table 4.6: Influence of L-valine, L-leucine, and L-isoleucine on the specific activities of AHAS, AHAI, and DHAD^a.

IC ₅₀	Val (mM)	Leu (mM)	Ile (mM)
AHAS	1.3	5.4	2.3
AHAI	6.9	9.4	39.2
DHAD	131	128	NA ^b

^aActivity assays were carried out with supplementation of each branched-chain amino acid. L-valine, L-leucine, and L-isoleucine concentration ranges of 0.1 to 10 mM, 1 to 10 mM, and 10 to 200 mM were added for the 50% activity reduction determination of AHAS, AHAI, and DHAD respectively.

^b200 mM of L-isoleucine reduced DHAD activity by less than 5%.

The activities of AHAI and DHAD were also reduced by valine, leucine, and isoleucine. Valine, leucine, and isoleucine at concentrations of 6.9 mM, 9.4 mM, and 39.2 mM, respectively, were required to reduce AHAI activity by 50%. DHAD was moderately tolerant to high concentrations of valine and leucine, and only slightly inhibited by isoleucine at 200 mM (Table 4.6). These inhibitions are very specific to BCAAs, since other amino acids such as threonine and methionine had no effect on the specific activities of these enzymes (Figure 4.3).

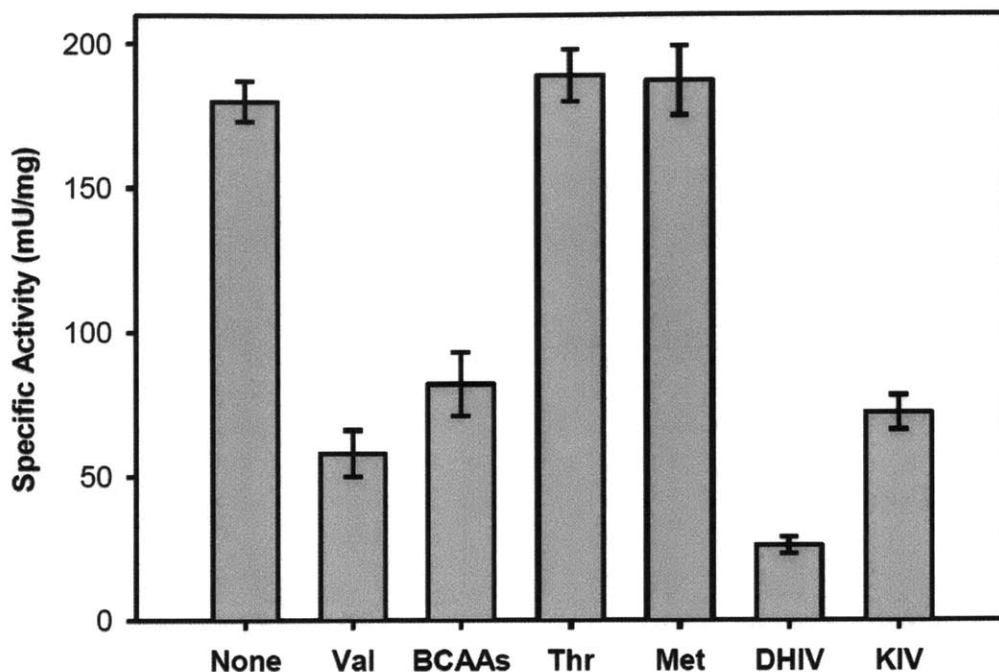


Figure 4.3: Specific activities of AHAS in the presence of no inhibitors (None), 10 mM L-valine (Val), 5 mM each of valine, leucine, and isoleucine (BCAAs), 10 mM L-threonine (Thr), 10 mM L-methionine (Met), 10 mM 2,3-dihydroxy-isovalerate (DHIV), and 10 mM 2-ketoisovalerate (KIV). Data present average of three experiments and error bars represent the standard deviation.

Experimental evolution and site-directed mutations

Experimental evolution, followed by isolation and sequencing of the mutated *ilvBH* genes, was employed to generate mutant strain that is resistant to valine regulation. After 60 days of continuous cultivation on increasing concentrations of valine, mutant strain Re2452 was isolated and its growth rate in the presence of various valine concentrations was determined. The growth rate of *R. eutropha* H16 was reduced by more than 50% when the valine concentration in minimal media reached 5 mM. At the same concentration of extracellular valine, Re2452 grew normally and had the same growth rate as in the absence of valine. Only an approximate 17-20% reduction of Re2452 growth rate was observed when the valine concentration reached 10-18 mM (Figure 4.4). This indicates that this evolved mutant strain is capable of tolerating high concentrations of valine, and its AHAS could be catalytically active with concentrations as high as 18 mM (Figure 4.4). Four mutations (N11S, T34M, T104S, and a frameshift at 133) were detected on the IlvH of Re2452 mutant strain (Appendix 4.5). Reconstitution of the wild type catalytic subunit and the regulatory subunit of Re2452 yielded an enzyme that has characteristics of the wild type holoenzyme, but is less sensitive to valine. This also implies that the frameshift at position 133 did not affect catalytic activity (Figure 4.5). The mutant strain has a slight higher tolerance towards valine, in addition to increased tolerance towards leucine and isoleucine (Figure 4.5).

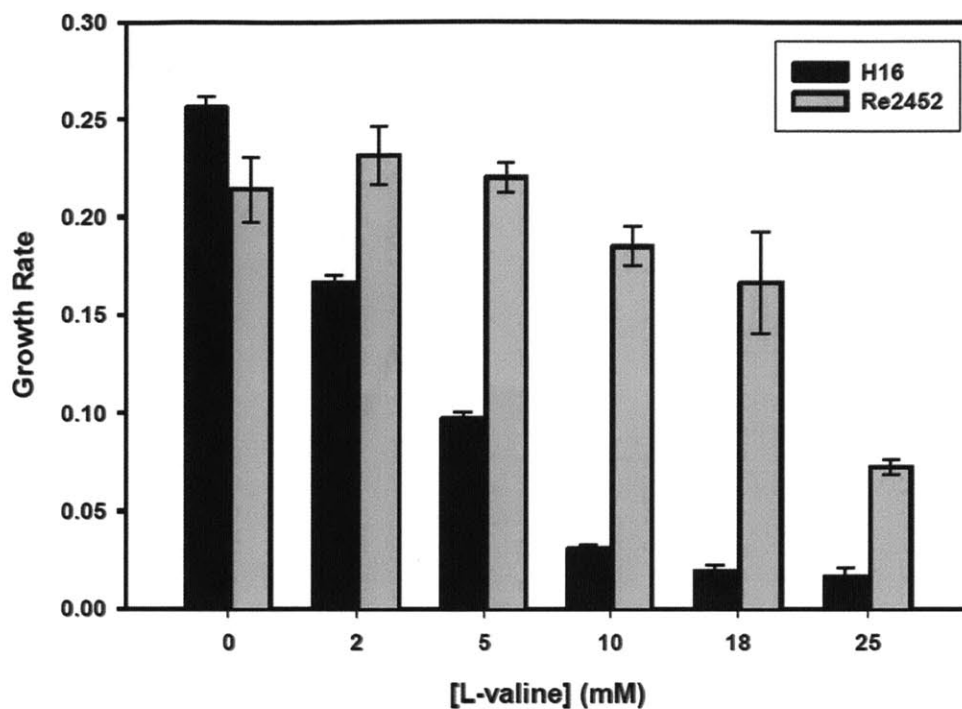


Figure 4.4: Growth rate of wild type *R. eutropha* H16 compared to mutant strain Re2452 on L-valine concentrations of 0 mM, 2 mM, 5 mM, 10 mM, 18 mM, and 25 mM. All data points are averages from triplicate cultures and error bars represent the standard deviation.

Asparagine at position 11 is conserved in various valine-sensitive AHAS enzymes, but not in valine-insensitive AHAS. Perhaps other conserved residues could also contribute to valine-sensitivity. An alignment of the amino acid sequences of the small subunits of three valine-sensitive AHASs of *E. coli* and *R. eutropha*, and valine-insensitive AHAS II from *E. coli* was conducted and revealed ten amino acid residues (N11, G14, G21, L22, F23, N29, E31, P38, E58, and Q59) that were found to be present only in valine-sensitive AHASs (Appendix 4.6). It was hypothesized that the N-terminus of IlvH could be responsible for binding valine (Eoyang and Silverman 1986; Kyselková et al, 2010; Leyval et al, 2003), and therefore these conserved residues were replaced individually with residues found in valine-insensitive AHAS II (N11F, G14E, G21R, L22V, F23V, N29H, E31C, and P38A). The resulting IlvH expression plasmids are listed in Table 4.2. Each mutated IlvH was purified and reconstituted with wild type IlvB. The reconstituted IlvBH(G21R), IlvBH(L22V), IlvBH(F23V), and IlvBH(E31C) enzymes exhibited no catalytic activity. The other mutations had similar specific activities as the wild type AHAS, except for IlvBH(P38A), which had approximately 25% reduction in enzymatic activity (Figure 4.5). The ability to tolerate valine was enhanced in enzymes with N11F, G14E, and N29H mutations (Figure 4.5). The amount of leucine required to reduce AHAS specific activity by 50% was nearly doubled with these point mutations, although these mutations did not dramatically increase tolerance to isoleucine (Figure 4.5). These mutations also did not improve AHAS tolerance on valine biosynthesis intermediates 2,3-dihydroxyisovalerate and 2-ketoisovalerate (data not shown), which suggested that the binding site for BCAA is distinctive

from the binding site of intermediates and their inhibition mechanisms could differ, or the point mutations did not exclude the binding of intermediates.

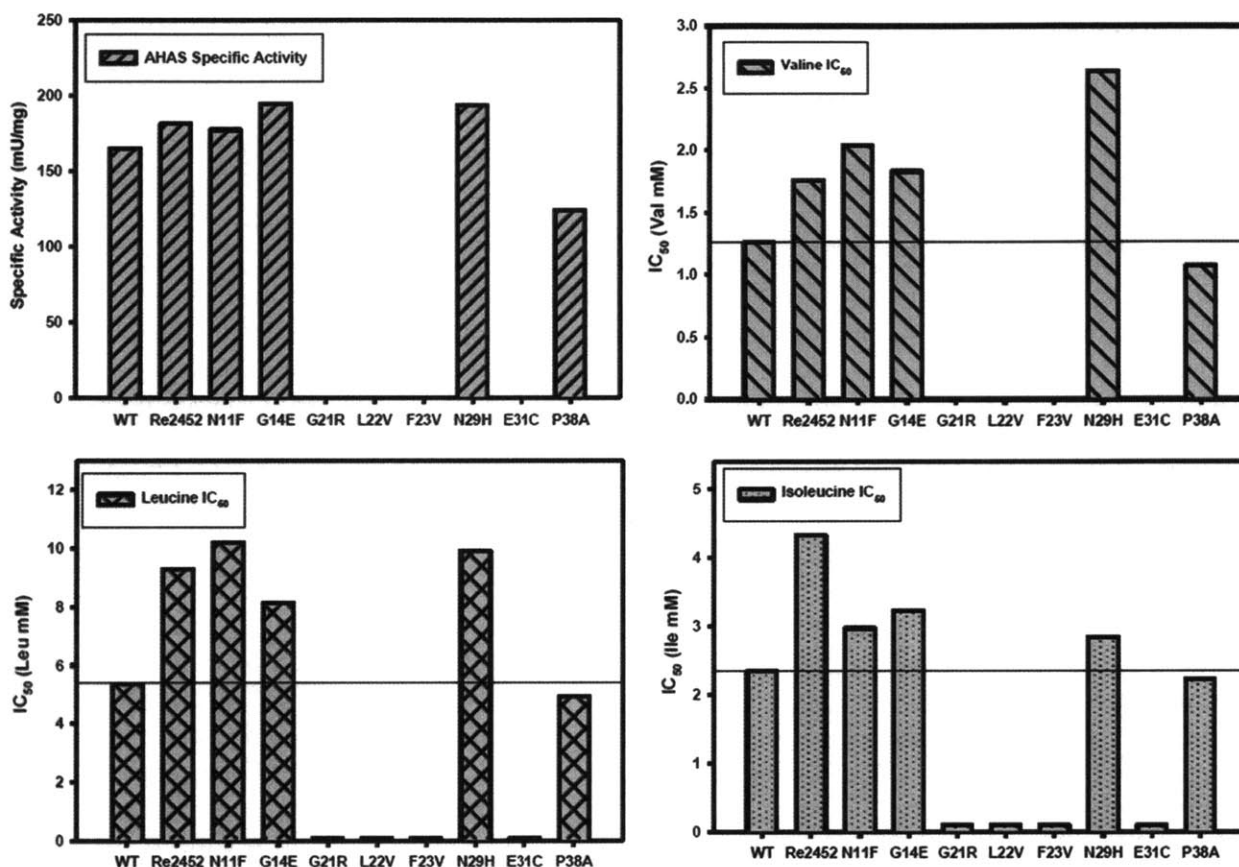


Figure 4.5: Influence of L-valine, L-leucine, and L-isoleucine on the specific activities of native IlvB reconstituted with mutated IlvH. Purified wild type IlvB and mutated IlvH proteins were mixed in 1:5 molar ratio. AHAS activity assays were carried out with supplementation of L-valine, L-leucine, and L-isoleucine at concentration range of 0.2 to 10 mM separately. IlvB and IlvH with single mutation of G21R, L22V, F23V, and E31C did not have any AHAS enzymatic activity.

DISCUSSION

Many technology platforms are being developed to capture and convert common waste carbon-containing compounds into value-added materials. The Gram-negative, facultatively chemolithoautotrophic *R. eutropha* has been demonstrated as a bioproduction platform for biodegradable plastics, biofuels, and pharmaceutical precursors (Brigham et al. 2013; Brigham et al. 2012; Ishizaki et al. 2001; Lan and Liao 2013). A bottleneck in the production of isobutanol in engineered *R. eutropha* has been shown to be the synthesis of 2-ketoisovalerate, a precursor for the synthesis of branched-chain amino acids and various other valuable products. In this study, enzymes involved in the 2-ketoisovalerate biosynthetic pathway were isolated and characterized from *R. eutropha*.

Although DHAD is the most active enzyme of the pathway (~3,000 mU/mg), the flow of carbon into the 2-ketoisovalerate biosynthesis pathway is controlled by AHAS, which is the first

enzyme in the pathway and has the lowest specific activity (~180 mU/mg). Compared to other AHAS enzymes (Chipman et al. 1998; Leyval et al. 2003; McCourt and Duggleby 2006), *R. eutropha* AHAS has a very low apparent affinity towards pyruvate. This observation could be explained by the presence of an excess amount of pyruvate inside the cells, since pyruvate is a precursor for PHA, the native carbon storage molecule. The low affinity could help balance and control the flow of pyruvate into BCAA biosynthesis pathways. Both AHAS and DHAD have moderate affinities towards their corresponding substrates, since these substrates are intermediates and are present in non-detectable low concentrations (Table 4.4).

Intracellular concentrations of valine, leucine, and isoleucine were fairly low (<0.5 mM each) in wild type *R. eutropha*. These concentrations reached 1.5 mM, 1.8 mM, and 1.7 mM, respectively, in engineered *R. eutropha* with *ilvBHC* and *ilvD* overexpressed (Lu et al. 2012). At such intracellular BCAA concentrations, the activities of AHAS and DHAS in the 2-ketoisovalerate biosynthesis pathway are impacted, which causes the cells to have a low growth rate and 2-ketoisovalerate production (Appendix 4.4, Table 4.6). AHAS experiences the most dramatic impact, since the enzyme's IC_{50} for valine is below the intracellular valine concentration. On the other hand, DHAS activity is most likely not affected since the amount of valine, leucine, or isoleucine required to reduce its activity by 50% is well above 100 mM (Table 4.6).

R. eutropha AHAS is regulated in a sophisticated, complex manner. As depicted in Appendix 4.7, AHAS holoenzyme is hypothesized to be a heterotetramer composed of homodimers of large (IlvB) and small (IlvH) subunits. IlvH is required to reach maximal activity of the enzyme (Table 4.3) and for feedback inhibition by valine, leucine, isoleucine and pathway intermediates (Table 4.6, Figure 4.3). The specific activity of *R. eutropha* AHAS (180 mU/mg) is very low compared to that of *C. glutamicum* (157 mU/mg unpurified AHAS) and *E. coli* (300 mU/mg) (Chipman et al. 1998; Krause et al. 2010; Leyval et al. 2003; McCourt and Duggleby 2006). Since no structure is available for any bacterial AHAS, the relevant structural information was inferred from mutagenesis studies and experimental observations. Cofactor FAD, although not hypothesized to be involved in the enzymatic mechanism (Chipman et al, 2005), was co-purified with IlvB, since the purified IlvB was bright yellow in color. Additionally, the reconstituted apo-AHAS (IlvB and IlvH) has a high apparent affinity towards FAD (Table 4.4), which indicates that FAD could play a structural role in the assembly of AHAS holoenzyme.

The binding site of valine, leucine, and isoleucine could be located at the homodimer interface of the IlvH N-terminal domain. The relatively valine-insensitive Re2452 differs from wild type at N11S, T34M, T104S, and a frameshift at 133 of its IlvH subunit. Asparagine (N) hypothesized to be located at the interface of the IlvH dimers, was mutated to serine (S), which is smaller in size. This change in size could be responsible for the binding of valine at the IlvH homodimer interface. Mutation at residue 34 from threonine (T) to methionine (M) could also change the size of the binding pocket, thus further inhibited binding of valine. The frameshift mutation at position 133 could have resulted in a mis-translated C-terminus, or truncated protein. This mutated IlvH, when combined with IlvB, had full catalytic activity and was slightly valine insensitive (Online Resource 6, Figure 5). Therefore, the C-terminal portion of IlvH may not be of importance in AHAS catalytic activity, but could take part in BCAA regulation. Such findings were also supported by previously published results on truncated *E. coli* AHAS. *E. coli* IlvH lacking 35, 48, or 80 amino acid residues from the C terminus is capable of activating AHAS for catalysis (Duggleby 2006; Slutzker et al, 2011). Furthermore, these constructs do not

bind valine or respond to BCAA-inhibition (Kaplun et al. 2006; Mendel et al. 2003; Mendel et al. 2001). It is unclear how both the N and C terminus of IlvH interact with BCAAs, although studies hypothesized that the mutant forms of AHAS has a weakened IlvH subunit interaction (Kyselková et al. 2010). Additional potential mutations that might contribute to lack of valine sensitivity may exist, although not generated in this study.

Various single mutations (N11F, G14E, and N29H) on the IlvH N-terminus were also able to decrease BCAA inhibition (Figure 4.5). Mendel et al. (2001) proposed that the IlvH subunit has an α - β sandwich topology, which is structurally homologous to the regulatory domain of 3-phosphoglycerate dehydrogenase (Chipman and Shaanan 2001; Mendel et al. 2001). An *E. coli* IlvH structural model based on the regulatory domain of 3-phosphoglycerate dehydrogenase revealed that N11 and G14 at opposite ends of the putative domain are involved in valine-binding (Kaplun et al. 2006; Mendel et al. 2001; Petkowski et al. 2007). Studies also showed that N11A, G14D, N29H, and A36V mutations in regulatory subunit of *E. coli* IlvH lead to AHAS with drastically reduced valine sensitivity (Mendel et al. 2003, Mendel et al. 2001), which supports the findings in this study regarding *R. eutropha* IlvH. In the reported studies, *E. coli* IlvH subunit with mutation G14D or N29H do not even bind valine. Interestingly, mutations on IlvH that resulted in tolerance to BCAA did not improve tolerance towards 2,3-dihydroxyisovalerate and 2-ketoisovalerate. This could imply that the binding-site for valine-pathway intermediates is different from BCAA binding-site and/or the binding site mutation excludes BCAAs, but not the intermediates. Such finding was also reported for *C. glutamicum* AHAS (Krause et al. 2010). The binding of BCAA and pathway intermediates at IlvH was hypothesized to cause a conformational change in the heterotetramer interaction, thus resulting in a less stable complex and reducing the catalytic activity of AHAS (Appendix 4.7) (Chipman et al. 1998; Eggeling et al. 1987; Eggeling et al. 1997; McCourt and Duggleby 2006; Vinogradov et al. 2006).

Specificity ratio, R, determined for *R. eutropha* AHAS is 140 and is constant over a wide range of substrate concentrations (Appendix 4.2). An R-value higher than 60 indicates remarkably high specificity in favor of 2-ketobutyrate (Chipman et al. 1998). Such a bias towards 2-ketobutyrate is likely due to the relative concentrations of pyruvate and 2-ketobutyrate in *R. eutropha* cells, which implies that the concentration of 2-ketobutyrate is much lower than the pyruvate concentration. In PHA-negative *R. eutropha* strains, intracellular pyruvate concentrations can reach approximately 5.7 mM, since pyruvate is a major intermediate in metabolism and the precursor for PHA biosynthesis (Lu et al. 2012). Ketobutyrate, on the other hand, was non-detectable and kept at low intracellular concentrations to avoid metabolic side-reactions and toxicity. Physical limitations exist for any enzyme to select one substrate in the presence of a competing substrate that is smaller by a single methyl group. It is unknown what contributes to this unique and highly specific selection in *R. eutropha*. Understanding of the molecular basis behind the *R. eutropha* AHAS R-value could allow prediction of product formation rates in an engineered system.

In order to reduce BCAA-induced AHAS inhibition for improved production of 2-ketoisovalerate, N-terminal single amino acid mutation or C-terminal truncation on IlvH (Figure 4.5, Appendix 4.5 and 4.6) could be utilized in engineered *R. eutropha*. Reducing the AHAS R-value would also help direct carbon flow towards 2-ketoisovalerate, and consequently valuable products. Previous mutagenesis studies on the *E. coli* AHAS II catalytic subunit revealed a ten-fold reduction in R-value when a tryptophan residue at position 464 was mutated to lysine, glutamine, or tyrosine. It was suggested that the indole ring of tryptophan interacts with the

extra methyl group on 2-ketobutyrate and stabilizes it in the active site (Steinmetz et al. 2010). Such site-specific mutations on *R. eutropha* AHAS could also improve selectivity towards biosynthesis of 2-ketoisovalerate.

In the present study, enzymes for the production of 2-ketoisovalerate, an intermediate in BCAA biosynthesis pathway of *R. eutropha*, were overexpressed in *E. coli*, isolated and characterized. The synthesis of BCAA is strongly regulated, especially at the AHAS node, by valine, leucine, isoleucine, and pathway intermediates. In order to engineer *R. eutropha* with increased production of 2-ketoisovalerate, AHAS should be engineered to decrease feedback inhibition by intermediates and product of interest, in addition to present a higher affinity towards pyruvate as the second substrate.

REFERENCES

- Bar-Ilan A, Balan V, Tittmann K, Golbik R, Vyazmensky M, Hübner G, Barak Z, Chipman DM (2001) Binding and activation of thiamin diphosphate in acetohydroxyacid synthase. *Biochemistry* 40(39): 11946–11954
- Barak Z, Chipman DM (2012) Allosteric regulation in acetohydroxyacid synthases (AHASs) – different structures and kinetic behavior in isozymes in the same organisms. *Arch Biochem Biophys* 519(2): 167–174
- Barak Z, Chipman DM, Gollop N (1987) Physiological implications of the specificity of acetohydroxy acid synthase isozymes of enteric bacteria. *J Bacteriol* 169(8): 3750–3756
- Bowien B, Kusian B (2002) Genetics and control of CO₂ assimilation in the chemoautotroph *Ralstonia eutropha*. *Arch Microbiol* 178(2): 85–93
- Brigham CJ, Gai CS, Lu J, Speth DR, Worden RM, Sinskey AJ (2013) Engineering *Ralstonia eutropha* for production of isobutanol from CO₂, H₂, and O₂ in Advanced Biofuels and Bioproducts. Springer New York 1065–1090
- Brigham CJ, Speth DR, Rha C, Sinskey AJ (2012) Whole-genome microarray and gene deletion studies reveal regulation of the polyhydroxyalkanoate production cycle by the stringent response in *Ralstonia eutropha* H16. *Appl Environ Microbiol* 78(22): 8033–8044
- Brigham CJ, Zhila N, Shishatskaya E, Volova TG, Sinskey AJ (2012) Manipulation of *Ralstonia eutropha* carbon storage pathways to produce useful bio-based products: reprogramming microbial metabolic pathways in *Subcellular Biochemistry* Springer Netherlands 64: 343–366
- Budde CF, Mahan AE, Lu J, Rha C, Sinskey AJ (2010) Roles of Multiple Acetoacetyl Coenzyme A Reductases in Polyhydroxybutyrate Biosynthesis in *Ralstonia eutropha* H16. *J Bacteriol* 192(20): 5319–5328
- Chipman D, Barak Z, Schloss JV (1998) Biosynthesis of 2-aceto-2-hydroxy acids: acetolactate synthases and acetohydroxyacid synthases. *Biochim Biophys Acta BBA - Protein Struct Mol Enzymol* 1385(2): 401–419
- Chipman DM, Duggleby RG, Tittmann K (2005) Mechanisms of acetohydroxyacid synthases. *Curr Opin Chem Biol* 9(5): 475–481
- Chipman DM, Shaanan B (2001) The ACT domain family. *Curr Opin Struct Biol* 11(6): 694–700
- Chunduru SK, Mrachko GT, Calvo KC (1989) Mechanism of ketol acid reductoisomerase steady-state analysis and metal ion requirement. *Biochemistry* 28(2): 486–493
- Cramm R (2009) Genomic view of energy metabolism in *Ralstonia eutropha* H16. *J Mol Microbiol Biotechnol* 16(1-2): 38–52
- Duggleby RG (2006) Domain Relationships in Thiamine Diphosphate-Dependent Enzymes. *Acc Chem Res* 39(8): 550–557

- Eggeling I, Cordes C, Eggeling L, Sahm H (1987) Regulation of acetohydroxy acid synthase in *Corynebacterium glutamicum* during fermentation of α -ketobutyrate to l-isoleucine. *Appl Microbiol Biotechnol* 25(4): 346–351
- Eggeling L, Morbach S, Sahm H (1997) The fruits of molecular physiology: engineering the l-isoleucine biosynthesis pathway in *Corynebacterium glutamicum*. *J Biotechnol* 56(3): 167–182
- Engel S, Vyazmensky M, Vinogradov M, Berkovich D, Bar-Ilan A, Qimron U, Rosiansky Y, Barak Z, Chipman DM (2004) Role of a conserved arginine in the mechanism of acetohydroxyacid synthase: catalysis of condensation with a specific ketoacid substrate. *J Biol Chem* 279(23): 24803–24812
- Eoyang L, Silverman PM (1986) Role of small subunit (IlvN polypeptide) of acetohydroxyacid synthase I from *Escherichia coli* K-12 in sensitivity of the enzyme to valine inhibition. *J Bacteriol* 166(3): 901–904
- Flint DH, Emptage MH (1988) Dihydroxy acid dehydratase from spinach contains a [2Fe-2S] cluster. *J Biol Chem* 263(8): 3558–3564
- Flint DH, Smyk-Randall E, Tuminello JF, Draczynska-Lusiak B, Brown OR (1993) The inactivation of dihydroxy-acid dehydratase in *Escherichia coli* treated with hyperbaric oxygen occurs because of the destruction of its Fe-S cluster, but the enzyme remains in the cell in a form that can be reactivated. *J Biol Chem* 268(8): 25547–25552
- Gollop N, Damri B, Chipman DM, Barak Z (1990) Physiological implications of the substrate specificities of acetohydroxy acid synthases from varied organisms. *J Bacteriol* 172(6): 3444–3449
- Grousseau E, Lu J, Gorret N, Guillouet SE, Sinskey AJ (2014) Isopropanol production with engineered *Cupriavidus necator* as bioproduction platform. *Appl Microbiol Biotechnol* 98(9): 4277–4290
- Harper AE, Miller RH, Block KP (1984) Branched-Chain Amino Acid Metabolism. *Annu Rev Nutr* 4(1): 409–454
- Ishizaki A, Tanaka K, Taga N (2001) Microbial production of poly-D-3-hydroxybutyrate from CO₂. *Appl Microbiol Biotechnol* 57(1-2): 6–12
- Kaplun A, Vyazmensky M, Zherdev Y, Belenky I, Slutzker A, Mendel S, Barak Z, Chipman DM, Shaanan B (2006) Structure of the regulatory subunit of acetohydroxyacid synthase isozyme III from *Escherichia coli*. *J Mol Biol* 357(3): 951–963
- Kohlmann Y, Pohlmann A, Otto A, Becher D, Cramm R, Lütte S, Schwartz E, Hecker M, Friedrich B (2011) Analyses of soluble and membrane proteomes of *Ralstonia eutropha* H16 reveal major changes in the protein complement in adaptation to lithoautotrophy. *J Proteome Res* 10(6): 2767–2776
- Krause FS, Blombach B, Eikmanns BJ (2010) Metabolic engineering of *Corynebacterium glutamicum* for 2-ketoisovalerate production. *Appl Environ Microbiol* 76(24): 8053–8061
- Kyselková M, Janata J, Ságová-Marečková M, Kopecký J (2010) Subunit–subunit interactions are weakened in mutant forms of acetohydroxy acid synthase insensitive to valine inhibition. *Arch Microbiol* 192(3): 195–200
- Lan EI, Liao JC (2013) Microbial synthesis of n-butanol, isobutanol, and other higher alcohols from diverse resources. *Bioresour Technol Biorefineries* 135(1): 339–349

- Leyval D, Uy D, Delaunay S, Goergen JL, Engasser JM (2003) Characterisation of the enzyme activities involved in the valine biosynthetic pathway in a valine-producing strain of *Corynebacterium glutamicum*. *J Biotechnol* 104(1-3): 241–252
- Li H, Liao JC (2014) A Synthetic Anhydrotetracycline-controllable gene expression system in *Ralstonia eutropha* H16. *ACS Synth Biol* ASAP
- Li H, Opgenorth PH, Wernick DG, Rogers S, Wu TY, Higashide W, Malati P, Huo YX, Cho KM, Liao JC (2012) Integrated electromicrobial conversion of CO₂ to higher alcohols. *science* 335(7067): 1596–1596
- Lu J, Brigham CJ, Gai CS, Sinskey AJ (2012) Studies on the production of branched-chain alcohols in engineered *Ralstonia eutropha*. *Appl Microbiol Biotechnol* 96(1): 283–297
- Lu J, Brigham CJ, Rha C, Sinskey AJ (2013) Characterization of an extracellular lipase and its chaperone from *Ralstonia eutropha* H16. *Appl Microbiol Biotechnol* 97(6): 2443–2454
- McCourt JA, Duggleby RG (2006) Acetohydroxyacid synthase and its role in the biosynthetic pathway for branched-chain amino acids. *Amino Acids* 31(2): 173–210
- Mendel S, Elkayam T, Sella C, Vinogradov V, Vyazmensky M, Chipman DM, Barak Z (2001) Acetohydroxyacid synthase: a proposed structure for regulatory subunits supported by evidence from mutagenesis. *J Mol Biol* 307(1): 465–477
- Mendel S, Vinogradov M, Vyazmensky M, Chipman DM, Barak Z (2003) The N-terminal domain of the regulatory subunit is sufficient for complete activation of acetohydroxyacid synthase III from *Escherichia coli*. *J Mol Biol* 325(2): 275–284
- Park JH, Lee SY (2010) Fermentative production of branched chain amino acids: a focus on metabolic engineering. *Appl Microbiol Biotechnol* 85(3): 491–506
- Petkowski JJ, Chruszcz M, Zimmerman MD, Zheng H, Skarina T, Onopriyenko O, Cymborowski MT, Koclega KD, Savchenko A, Edwards A, Minor W (2007) Crystal structures of TM0549 and NE1324—two orthologs of *E. coli* AHAS isozyme III small regulatory subunit. *Protein Sci Publ Protein Soc* 16(7): 1360–1367
- Pohlmann A, Fricke WF, Reinecke F, Kusian B, Liesegang H, Cramm R, Eitinger T, Ewering C, Pötter M, Schwartz E, Strittmatter A, Voss I, Gottschalk G, Steinbüchel A, Friedrich B, Bowien B (2006) Genome sequence of the bioplastic-producing “Knallgas” bacterium *Ralstonia eutropha* H16. *Nat Biotechnol* 24(10): 1257–1262
- Quandt J, Hynes MF (1993) Versatile suicide vectors which allow direct selection for gene replacement in Gram-negative bacteria. *Gene* 127(1): 15–21
- Raberg M, Voigt B, Hecker M, Steinbüchel A (2014) A closer look on the polyhydroxybutyrate-(PHB-) negative phenotype of *Ralstonia eutropha* PHB-4. *PloS One* 9(5):
- Slater KLH (1998) Multiple beta-ketothiolases mediate poly(beta-hydroxyalkanoate) copolymer synthesis in *Ralstonia eutropha*. *J Bacteriol* 180(8): 1979–87

Sambrook J, Russell DW (2001) Molecular cloning: a laboratory manual. Cold Spring Harbor Laboratory, Cold Spring Harbor, N.Y.

Schomburg D, Stephan D (1995) Ketol-acid reductoisomerase in Springer Berlin Heidelberg. 433–437

Schwartz E, Voigt B, Zühlke D, Pohlmann A, Lenz O, Albrecht D, Schwarze A, Kohlmann Y, Krause C, Hecker M, Friedrich B (2009) A proteomic view of the facultatively chemolithoautotrophic lifestyle of *Ralstonia eutropha* H16. *Proteomics* 9(22): 5132–5142

Simon R, Priefer U, Pühler A (1983) A broad host range mobilization system for *in vivo* genetic engineering: transposon mutagenesis in gram negative bacteria. *Nat Biotechnol* 1(9): 784–791

Slutzker A, Vyazmensky M, Chipman DM, Barak Z (2011) Role of the C-terminal domain of the regulatory subunit of AHAS isozyme III: use of random mutagenesis with *in vivo* reconstitution (REMI-ivs). *Biochim Biophys Acta* 1814(3): 449–455 doi:10.1016/j.bbapap.2011.01.002

Steinmetz A, Vyazmensky M, Meyer D, Barak ZE, Golbik R, Chipman DM, Tittmann K (2010) Valine 375 and phenylalanine 109 confer affinity and specificity for pyruvate as donor substrate in acetohydroxy acid synthase isozyme II from *Escherichia coli*. *Biochemistry* 49(25): 5188–5199

Tittmann K, Schröder K, Golbik R, McCourt J, Kaplun A, Duggleby RG, Barak Z, Chipman DM, Hübner G (2004) Electron transfer in acetohydroxy acid synthase as a side reaction of catalysis: implications for the reactivity and partitioning of the carbanion/enamine form of (α -Hydroxyethyl)thiamin diphosphate in a “nonredox” flavoenzyme. *Biochemistry* 43(27): 8652–8661

Vinogradov V, Vyazmensky M, Engel S, Belenky I, Kaplun A, Kryukov O, Barak Z, Chipman DM (2006) Acetohydroxyacid synthase isozyme I from *Escherichia coli* has unique catalytic and regulatory properties. *Biochim Biophys Acta* 1760(3): 356–363

Vollbrecht D, El Nawawy MA, Schlegel HG (1978) Excretion of metabolites by hydrogen bacteria. I. Autotrophic and heterotrophic fermentations. *Eur J Appl Microbiol Biotechnol* 6: 145–155

Vollbrecht D, Schlegel HG (1978) Excretion of metabolites by hydrogen bacteria. II. Influences of aeration, pH, temperature, and age of cells. *Eur J Appl Microbiol Biotechnol* 6: 157–166

Vollbrecht D, Schlegel HG (1979) Excretion of metabolites by hydrogen bacteria. III. D(-)-3-hydroxybutanoate. *Eur J Appl Microbiol Biotechnol* 7: 259–266

Vyazmensky M, Sella C, Barak Z, Chipman DM (1996) Isolation and characterization of subunits of acetohydroxy acid synthase isozyme III and reconstitution of the holoenzyme. *Biochemistry* 35(32): 10339–10346

Vyazmensky M, Steinmetz A, Meyer D, Golbik R, Barak Z, Tittmann K, Chipman DM (2011) Significant catalytic roles for Glu47 and Gln 110 in all four of the C-C bond-making and -breaking steps of the reactions of acetohydroxyacid synthase II. *Biochemistry* 50(15): 3250–3260

Vyazmensky M, Zherdev Y, Slutzker A, Belenky I, Kryukov O, Barak Z, Chipman DM (2009) Interactions between large and small subunits of different acetohydroxyacid synthase isozymes of *Escherichia coli*. *Biochemistry* 48(36): 8731–8737

Westerfield WW (1945) A colorimetric determination of blood acetoin. *J Biol Chem* 161(1): 495–502

Wilde E (1962) Untersuchungen über wachstum und speicherstoffsynthese von hydroenomonas. Archiv Für Mikrobiologie 43(2): 109-137

York, G.M., Stubbe, J., Sinskey, A.J., 2001. New insight into the role of the PhaP phasin of *Ralstonia eutropha* in promoting synthesis of polyhydroxybutyrate. J Bacteriol 183(7), 2394–2397

Zor T, Selinger Z (1996) Linearization of the Bradford protein assay increases its sensitivity: theoretical and experimental studies. Anal Biochem 236(2): 302–308

APPENDIX

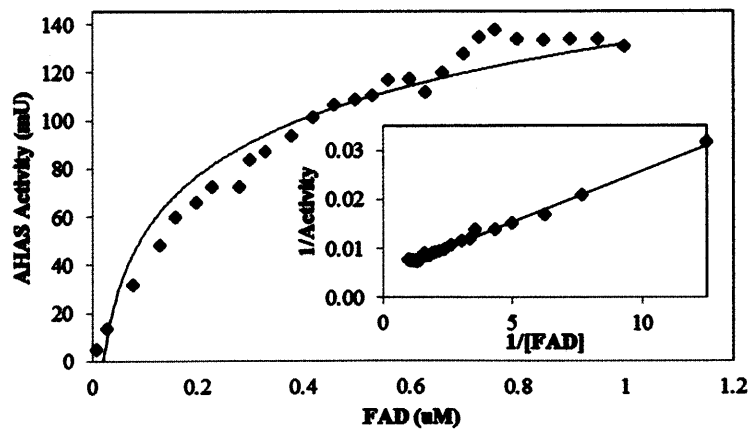
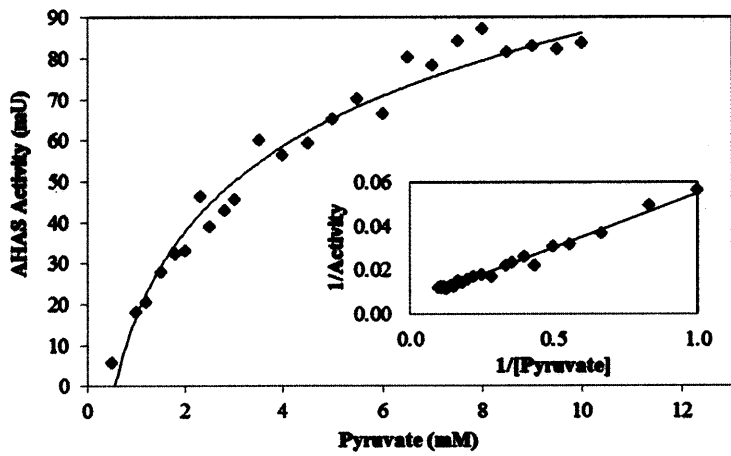
Appendix 4.1: List of primers used in this study.

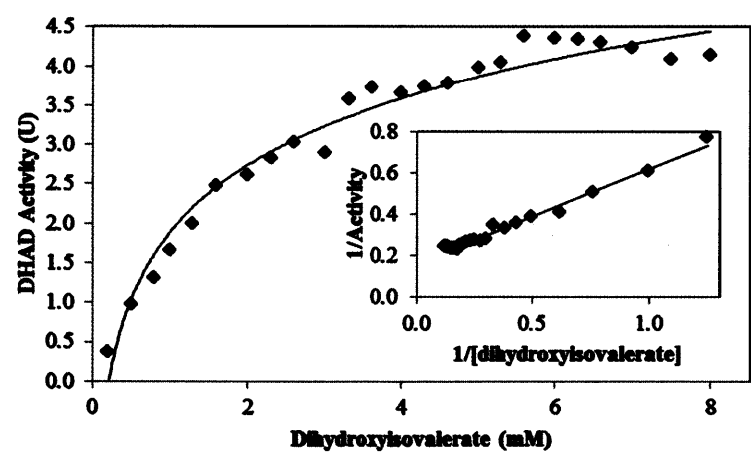
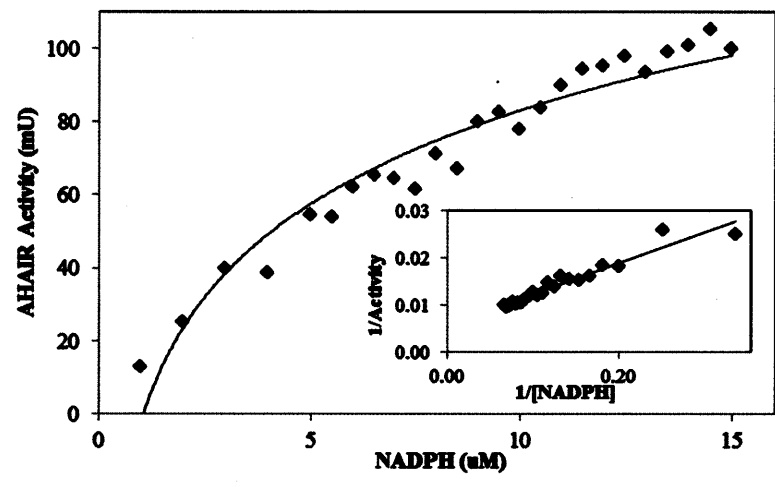
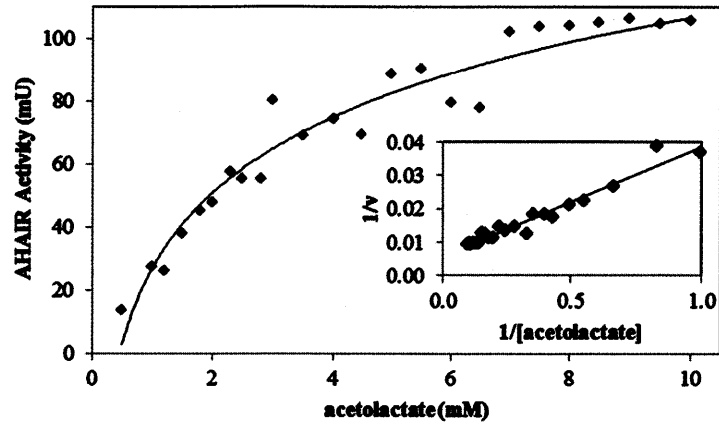
Name	Sequence ^a
<i>ilvB</i> F	GCATCATATGCCAGCGCGGAATTCTCCACGC
<i>ilvB</i> R	GAATGGATCCTTACAGGTCCTCCGCGCC
<i>ilvH</i> F	GCCGCATATGCGTCACATCATTTCGGTCCTG
<i>ilvH</i> R	GAATGGATCCTCAGACCTTCAGGATGCGCTC
<i>ilvC</i> F	GCCGCATATGAAAGTGTTTTACGACAAGGACGCC
<i>ilvC</i> R	GCATGGATCCTTAGTTCTTCGACTGGTC
<i>ilvD</i> F	GCCGCATATGGCATTCAACAAACGCTCGCAG
<i>ilvD</i> R	GAATGGATCCTCAGTCCGTCCTGCCCCCTTG
$\Delta ilvH$ upstream F	GAATGGATCCCAAGTTCGACGAGCCGCGCCG
$\Delta ilvH$ upstream R	GGGTGAGCCGGGGCCCGGTCACATTACAGGTCCTCCGCGCCG
$\Delta ilvH$ downstream F	CGGCGCGGAGGACCTGTAATGTGACCGGGCCCCGGCTCACCC
$\Delta ilvH$ downstream R	GCCGTCTAGAGGCGCGATCATGATCACGTCC
$\Delta ilvH$ dig. internal F	CGGTCCTGCTGGAAAACGAA
$\Delta ilvH$ dig. internal R	GTCAGCTCGATGGTGTAGGT
$\Delta ilvH$ dig. external F	GCAATGCCTGCAAGTACGAG
$\Delta ilvH$ dig. external R	GCGCCTTCCTTGATGTTGTC
<i>ilvB</i> sequence F	GTCTTCCATGCAGACGCGCAC
<i>ilvB</i> sequence R	GTCAGCGTCTCGATGTTATAG
<i>ilvH</i> sequence F	TACGACACCCCGGTGAAGATC
<i>ilvH</i> sequence R	CGATGATGGTGACGTTCTTGC
N11F F	TCGGTCCTGCTGGAATTCGAACCGGGCGCG
N11F R	CGCGCCCGGTTTCGAATTCCAGCAGGACCG
G14E F	GAAAACGAACCGGAGGCGCTGTCGCGCGTG
G14E R	CACGCGGACAGCGCCTCCGGTTCGTTTTTC
G21R F	TCGCGCGTGGTGCGCCTGTTCTCGGGC
G21R R	GGCCGAGAACAGGCCACCACGCGCGA
L22V F	CGCGTGGTGGGCGTGTTCGCGCCCGCGGC
L22V R	GCCGCGGGCCGAGAACACGCCACCACGCG
F23V F	GTGGTGGGCTGGTCTCGGCCCGCGGCTAT
F23V R	GCCGCGGGCCGAGACCAGGCCACCAC
N29H F	GCCCGCGGCTATCACATCGAGACGCTG

N29H R	CAGCGTCTCGATGTGATAGCCGCGGGC
E31C F-1	GGCTATAACATCTAGACGCTGACCGTG
E31C R-1	CACGGTCAGCGTCTAGATGTTATAGCC
E31C F-2	GGCTATAACATGTGCACGCTGACCGTG
E31C R-2	CACGGTCAGCGTGCAGATGTTATAGCC
P38A F	CTGACCTGTGCAGCCACCGAGGATGCC
P38A R	GGCATCCTCGGTGGGGCCACGGTCAG

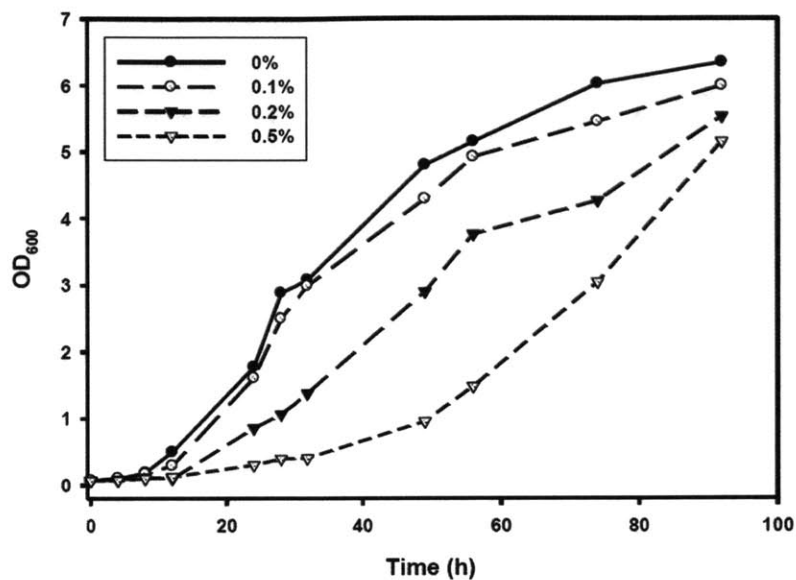
^a Restriction sites are underlined

Appendix 4.3: Activities of AHAS, AHAI, and DHAD with varying concentrations of substrate or cofactor. Insert: Lineweaver-Burk plot used to determine kinetic parameters.

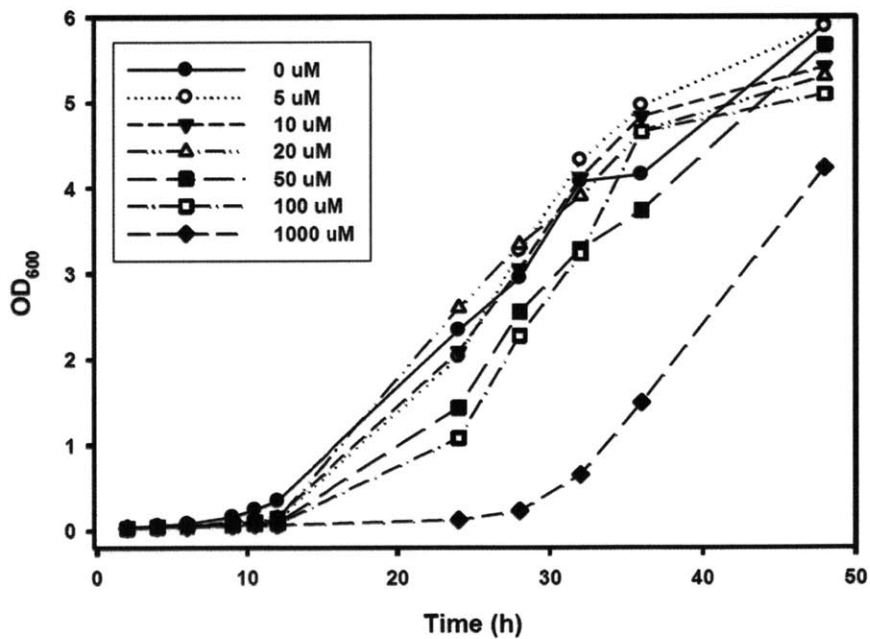




Appendix 4.3: Growth profile of wild type *R. eutropha* H16 over 96 h in minimal media with 2 % fructose, 0.05 % NH₄Cl, and 0% to 0.5% (w/v) of 2-ketoisovalerate.



Appendix 4.3: Growth profile of wild type *R. eutropha* H16 over 96 h in minimal media with 2 % fructose, 0.05 % NH₄Cl, and 0 to 1000 μ M of L-valine.



Appendix 4.4: Alignment of the AHAS regulatory subunit (IlvH) sequence of wild type *R. eutropha* H16 and mutant strain (Re2452) from experimental evolution. Amino acid mutations (N11S, T34M, and T104S) and a frameshift at 133 were highlighted in red.

```

H16-IlvH      MRHIISVLLLENEPGALSRVVGLFSARGYNIETLTVAPTEDASLSRMTIVTSGSDDVIEQI 60
Re2452-IlvH  MRHIISVLLLESEPGALSRVVGLFSARGYNIETLMVAPTEDASLSRMTIVTSGSDDVIEQI 60
              *                               *

H16-IlvH      TKHLNRLVEVVKVVDLTEGAHIERELMLVKVRAVGKEREEMKRTADIFRGRIIDVTEKTY 120
Re2452-IlvH  TKHLNRLVEVVKVVDLTEGAHIERELMLVKVRAVGKEREEMKRSADIFRGRIIDVTEKTY 120
              *

H16-IlvH      TIELTGNGVKLDAFLDAIDRTAILETVRTGGSGIGRGERILKV 163
Re2452-IlvH  TIELTGNGVKLD-FLDAIDRTAILETVRTGGTGIGRGERILKV 163
              *

```

Appendix 4.5: Alignment of the AHAS regulatory subunit (IlvH) sequence of wild type *R. eutropha* H16 and three *E. coli* isozymes (IlvN, IlvM, IlvH). Amino acid residues highlighted in blue represents the ones that's conserved in valine-sensitive subunit, but not present in valine-insensitive subunit. The mutations studied here were (N11F, G14E, G21R, L22V, F23V, N29H, E31C, and P38A).

```

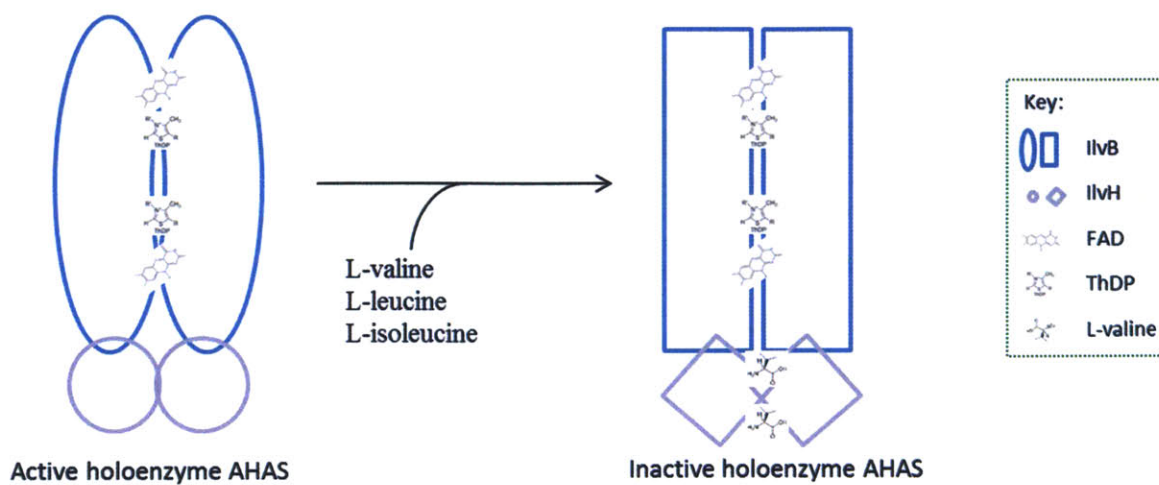
H16-IlvH      -MRH-----IISVLLLENEPGALSRVVGLFSARGYNIETLTVAPTEDASLSRMT-IVTSG 52
Ecoli-IlvN    -MQNTTHDNVILELTVRNHPGVMTHVCGLFARRAFNVEGILCLPIQDSDKSHIW--LLVN 57
Ecoli-IlvM  MMQH-----QVNV SARFNPETLERVLRVVRHRGFHVC SMNMAAASDAQNINIE--LTVA 52
Ecoli-IlvH    -MRR-----ILSVLLENESGALSRVIGLFSQRGYNIESLTVAPTDDPTLSRMT-IQTVG 52
              * *      ***      * *      *

H16-IlvH      SDDVIEQITKHLNRLVEVVKVVDLTEGAHIERELMLVKVRAVGKEREEMKRTADIFRGRI 112
Ecoli-IlvN    DDQRLEQMISQIDKLEDVVKVQRNQSDPTMFNKIAVFFQ----- 96
Ecoli-IlvM  SPRSVDLLFSQLNKLVDVAHVA-ICQSTTTSQQIRA----- 87
Ecoli-IlvH    DEKVLEQIEKQLHKLVDVLRVSELGQGAHVEREIMLVKIQASGYGRDEVKRNTEIFRGQI 112
              **

H16-IlvH      IDVTEKTYTIELTGNGVKLDAFLDAI-DRTAILETVRTGGSGIGRGERILKV----- 163
Ecoli-IlvN    ----- 163
Ecoli-IlvM  ----- 163
Ecoli-IlvH    IDVTPSLYTVQLAGTSGKLDASIRDAKIVEVARSGVVGLSRGDKIMR----- 163

```

Appendix 4.6: Cartoon illustration of the AHAS heterotetramer with potential catalytic and valine-binding sites.



CHAPTER 5

Experimental evolution and gene knockout studies revealed an ArcA-mediated isobutanol tolerance in *Ralstonia eutropha*

INTRODUCTION

The demand for alternative fuel sources has increased in recent years due to the dwindling fossil fuel supplies. Previous studies have described the production of branched-chain alcohols by a synthetic Ehrlich pathway (de Palencia et al. 2006; Hwang et al. 2009) using genes from the branched-chain amino acid biosynthesis pathways of *Bacillus subtilis*, *Saccharomyces cerevisiae*, *Ralstonia eutropha*, and *Lactococcus lactis* (Atsumi et al. 2008; Smith et al. 2010; Blombach et al. 2011; Savrasova et al. 2011). These branched-chain alcohols have high potential as an alternative to fossil fuels, because their energy contents are close to gasoline and they can be directly distributed and used in the current infrastructure and engine (Atsumi et al. 2008; Yan and Liao 2009; Smith et al. 2010; Savrasova et al. 2011; Brigham et al. 2012).

A major challenge facing bioproduction of branched-chain alcohol is product toxicity to the cells, which limits the organism's production potential. Recently, a few studies have focused on understanding isobutanol toxicity, in order to develop tolerance mechanism that can be transferred to a desired strain (Tomas et al. 2003; Alper et al. 2006). Branched-chain alcohol toxicity is complex, often related to general stress responses and can vary greatly depending on the microbial species and strains being used. Toxicity is usually correlated with partitioning in the cell membrane and increases with solvent hydrophobicity (Dunlop 2011). The presence of isobutanol, one of the branched-chain alcohols, was shown to be toxic to *E. coli* and caused growth arrest at concentrations higher than 1% (v/v). This growth arrest is believed to be a consequence of changes in the respiratory machinery, as well as in iron and phosphate homeostasis. Isobutanol is hypothesized to insert itself in the membrane and thus dissociate and disrupt the interaction between quinone and cell membrane. Quinone is anchored to the membrane via its isoprenoid chain and facilitates electron transfer. Such a change in interaction causes quinone depletion and affects the response to redox state in the cell.

The major regulator of these respiratory changes is the ArcAB-TolC system. ArcA is activated by ArcB autophosphorylation through a release in quinone inhibition. This is a consequence of isobutanol-related quinone malfunction, specifically by dissociation or disruption of quinones interaction with the cell membrane (Brynildsen and Liao 2009). The system protects the cell against various stresses including antibiotics and organic solvents by exporting these substances outside of the cell (Atsumi et al. 2010b; Minty et al. 2011).

Much effort has been undertaken in seeking tools to increase branched-chain alcohol tolerance in microbes, and different strategies are being implemented, such as membrane modification (Junker and Ramos 1999), employment of heat shock proteins (Piter 1995), and increase in efflux pump activity (Kieboom et al. 1998; Rojas et al. 2001; Takatsuka et al. 2010). Previous isobutanol tolerance studies in *E. coli* (Atsumi et al. 2010b; Minty et al. 2011) used an experimental evolution approach, which obtained strains that are able to survive in high concentrations of isobutanol due to a series of mutations in the genome. Among the detected-mutations, five identified genes that are common to both works are either components of a

multidrug efflux pump (*acrA6* and *acrA*) or part of its regulator, and the *marCRAB* operon (*marA*, *marc*, and *yhbJ*), having their role on alcohol tolerance widely describe in the literature (Demple et al. 1997; Kieboom et al. 1998; Rojas et al. 2001; Brown et al. 2007; Atsumi S. et al. 2010b; Minty et al. 2011; Doukyu et al. 2012).

Isobutanol can be produced by metabolically engineered *R. eutropha*, a Gram-negative bacterium known to produce polyhydroxybutyrate (PHB), an intracellular carbon storage polymer, during nutrient starvation. Previous work by Lu et al. (2012b) described that isobutanol production by *R. eutropha* is possible through the incorporation of an engineered biosynthetic pathway, which redirects the carbon flow from PHB to isobutanol production. Wild type *R. eutropha* however, is unable to grow on isobutanol concentrations higher than 0.5% (v/v) (Lu et al. 2012b), which limits its potential as an industrial isobutanol production strain.

The main objective of this work is to identify genes involved in isobutanol tolerance in *R. eutropha* and to develop a strain capable of withstanding increased extracellular isobutanol concentrations. Using similar approaches by Atsumi et al. (2010b) and Minty et al. (2011), *R. eutropha* were evolved in the presence of increasing concentrations of isobutanol via sequential transfer. Five homologous genes previously described in *E. coli* for contributing to isobutanol tolerance were identified, sequenced, and analyzed in these evolved mutant strains for potential mutations. Isobutanol tolerance phenotype was then reconstructed in both the wild type and engineered isobutanol-producing *R. eutropha* strains by deletion of genes responsible for isobutanol efflux.

MATERIALS AND METHODS

Bacterial strains and plasmids

Chemicals were purchased from Sigma-Aldrich. Strains and plasmids used in the experiments are listed in Table 5.1 and Table 5.2 respectively.

Table 5.1: Strains used in this work.

Strain	Genotype	Reference
<i>R. eutropha</i>		
H16	Wild type, Gentamicin resistant (Gen ^r)	ATCC17699
Re2061	H16 Δ <i>phaCAB</i> (Gen ^r)	Lu et al. (2012)
Re2410	DJ21 Δ <i>phaCAB</i> , Δ <i>ilvE</i> , Δ <i>bkdAB</i> (Gen ^r)	Lu et al. (2012)
CF106	H16 <i>adh</i> (Con) ethanol+ 2,3-butanediol+ (Gen ^r)	Jendrossek et al. (1990)
DJ21	H16 <i>adh</i> (Con) ethanol+ 2,3-butanediol+ (Gen ^r)	Jendrossek et al. (1990)
Re2432	isobutanol-tolerant strain evolved from H16 (Gen ^r)	This work
Re2433	isobutanol-tolerant strain evolved from Re2061 (Gen ^r)	This work
Re2405	CF106 Δ <i>phaCAB</i> Gen ^r	Lu et al. (2012)
Re2425	DJ21 Δ <i>phaCAB</i> , <i>ilvE</i> , <i>bkdAB</i> , <i>aceE</i> (Gen ^r)	Lu et al. (2012)
Re2438	H16 Δ <i>acrA6</i> (Gen ^r)	This work
Re2439	Re2425 Δ <i>acrA6</i> (Gen ^r)	This work
Re2442	H16 Δ <i>acrA</i> (Gen ^r)	This work
Re2443	H16 Δ <i>acrA6</i> Δ <i>acrA</i> (Gen ^r)	This work

Re2444	Re2425 Δ <i>acrA6</i> Δ <i>acrA</i> (Gen ^r)	This work
Re2445	Re2425 Δ <i>acrA</i> (Gen ^r)	This work
<i>E. coli</i>		
S17-1	Conjugation strain	Simon et al. (1983)

Table 5.2: Plasmids used in this study.

Plasmid	Genotype	Reference
pJV7	pJQ200Kan with Δ <i>phaC1</i> allele inserted into <i>Bam</i> HI restriction site, confers kanamycin resistance (Kan ^r)	Budde et al. (2011)
pJL26	pJL26 pBBR1MCS-2 with branched-chain alcohol production operon (<i>ilvBHCDkivd</i>) inserted into the multiple cloning site (Kan ^r)	Lu et al. (2012)
p Δ 3357	pJV7 used for in-frame deletion of <i>acrA6</i> gene (Kan ^r)	This work
p Δ 3729	pJV7 used for in-frame deletion of <i>acrA</i> gene (Kan ^r)	This work

Cultivation Media and Conditions

R. eutropha strains were cultivated at 30°C in rich and minimal media. Rich media used in this study was 2.75 % (w/v) dextrose-free tryptic soy broth (TSB) (Becton Dickinson, Sparks, MD, USA). Minimal medium was formulated as described previously (Lu et al. 2012b), using 2% (w/v) fructose or 0.2% isobutanol (v/v) as carbon source. Gentamicin was added in a 10 μ g/ml final concentration, and for *R. eutropha* harboring plasmid, kanamycin was added to a final concentration of 200 μ g ml⁻¹. *E. coli* strains used for deletions were cultivated at 37°C in Luria-Bertani medium (LB) (Bertani 1951) with kanamycin added to a final concentration of 50 μ g/ml.

Experimental Evolution

In order to develop and isolate an isobutanol-tolerant *R. eutropha* strain, we performed experimental evolution experiments using the sequential transfer method previously described for alcohol tolerance (Yomano et al. 1998; Atsumi et al. 2010b; Minty et al. 2011). A single colony of *R. eutropha* was transferred from a TSB agar plate into culture tube containing 5 mL of TSB media. Tubes were incubated on a roller drum for 24 h at 30°C. Two mL aliquot cultures were transferred to fresh rich media containing isobutanol. Over the course of the cultivation experiment, the isobutanol concentration was increased from 0.5% (v/v) to 2.5% (v/v) at a rate of 0.5% (v/v) every 15 days. Evolved strains (Re2432 and Re2433) were isolated from a final bacterial population after 75 days of sequential cultivation.

Identification of gene mutations in evolved strains

Genome sequencing followed by gene expression studies revealed various genes contributing to alcohol tolerant in *E. coli* strains (Atsumi et al. 2010b and Minty et al. 2011).

Several genetic lesions in the genome were described as being primarily responsible for increased isobutanol tolerance. An analysis of the evolved strains obtained in the currently study was also performed in order to screen for gene mutations that are related to isobutanol tolerance. Five mutated genes reported in both prior studies were identified in *R. eutropha* (Table 5.3). To detect mutations potentially related to isobutanol tolerance in *R. eutropha*, these genes along with 100 upstream and downstream base pairs were sequenced from the evolved strains using primers listed in Table 5.4. The resulting sequences were compared to those from the parental strains using Mega5 software (Tamura et al. 2011).

Table 5.3: Potential genes related to isobutanol tolerance and their respective location and description.

<i>E. coli</i> gene (Atsumi et al. 2010b; Minty et al. 2011)	<i>R. eutropha</i> (Homologous gene locus tag)	Description
<i>marC</i>	H16_A3413	Putative transporter
<i>marA</i>	H16_A3378	AraC family transcriptional regulator
<i>acrA6</i>	H16_A3357	Cation/multidrug efflux system, membrane-fusion component
<i>acrA</i>	H16_A3729	Acriflavin resistance protein A
<i>yhbJ</i>	H16_A0381	Hypothetical protein

Plasmid and Strains Construction

All plasmids used for gene deletion were constructed using Gibson Assembly (Gibson et al. 2009). For the deletion of target genes in *R. eutropha*, standard mating and deletion procedures were implemented as described previously (Quandt and Hynes 1993, Slater et al. 1998). Diagnostic PCR was used to confirm each in-frame gene deletion and the gene-specific primers are listed in Table 5.4.

Table 5.4: Primers used in this work.

Name	Primer
A0381Fw	5' GGCGACGAATACAAGGCCTACAT 3'
A0381Rv	5' TCGGTCGAGGACATGCAGTG 3'
A3378Fw	5' CATGGCCGACGCATGCCTT 3'
A3378Rv	5' ACCGGCTTCCATGGGGAATGT 3'
A3357Fw	5' GCGGGCAAAGCAAGTCGAAAGC 3'
A3357Rv	5' ACGTCCGGGAAGTGGGCAA 3'
A3413Fw	5' CAGTGCGAAACCGTGTTCAAGGCC 3'
A3413Rv	5' GATGCCTTCGGGGGCATCCAC 3'
A3729Fw	5' CCAGCCGGTCATGAATCCAGT 3'
A3729Rv	5' TGCAGGATCGACAATATGCCGC 3'
delA3357gib1	5' TACGAATTCGAGCTCGGTACCCGGGGATCC AGAACAATGCGGTGGTGTGGAAC 3'
delA3357gib2	5' CATGAAGAAGTGGGCAAGCTGGATCCCTC TCCCGCCATGG 3'
delA3357gib3	5' CCATGGCGGGAGAGGGATCCAGCTTGCCC ACTTCTTCATC 3'

delA3357gib4	5' AAGCTTGCATGCCTGCAGGTCGACTCTAGA GAGCGCATCCAGCACATAGA 3'
delA3729gib1	5' TACGAATTCGAGCTCGGTACCCGGGGATCC CGTTGTCGTCACATGCCAAT 3'
delA3729gib2	5' GTATTGGTGGTACGGCAGGGTTCGATAACCC CATGATGGCAA 3'
delA3729gib3	5' TTGCCATCATGGGGTTATCGACCCTGCCGT ACCACCAATAC 3'
delA3729gib4	5' AAGCTTGCATGCCTGCAGGTCGACTCTAGAGACTTGA CGACACGGTCAG 3'
A3357delcheckFw	5' TCAAGACCGCCAATGCCGAC 3'
A3357delcheckRv	5' TGCCGTCAGGGTTGGCAA 3'
A3729delcheckFw	5' CAACGCCGACGTGGCCTC 3'
A3729delcheckRv	5' CGACATTGCCGTCCGTGCC 3'
pJV7Fw	5' GACCATGATTACGAATTCGAGCTCGGTACC CGG 3'
pJV7Rv	5' GCTTGCATGCCTGCAGTCGACTCTAGA 3'

Isobutanol Tolerance Evaluation

Evolved and wild type *R. eutropha* were subjected to two different assays in order to assess their tolerance on isobutanol. The first assay determines the effect of extracellular isobutanol on the growth *R. eutropha*. Strains were cultivated in minimal medium with 2% fructose (w/v), 0.05% NH₄Cl (w/v), and different concentrations of isobutanol (0%, 0.5%, and 1.0% v/v). Growth was monitored by optical density of the culture at 600 nm (OD_{600nm}).

The second assay, which is hereby referred to as the survival assay, determines *R. eutropha*'s viability with exogenous isobutanol exposure. It was performed by exposing overnight TSB media cultures at OD_{600nm} of 1.0 to different isobutanol concentrations (0%, 1.0%, 1.25%, 1.5%, 1.75% and 2.0% v/v). After 12h of isobutanol exposure at 30°C, the cultures were serial-diluted and plated on TSB plates to determine viable cells present in the culture as colony forming units per mL (CFU ml⁻¹) (Smith et al. 2010).

Isobutanol Consumption and Production

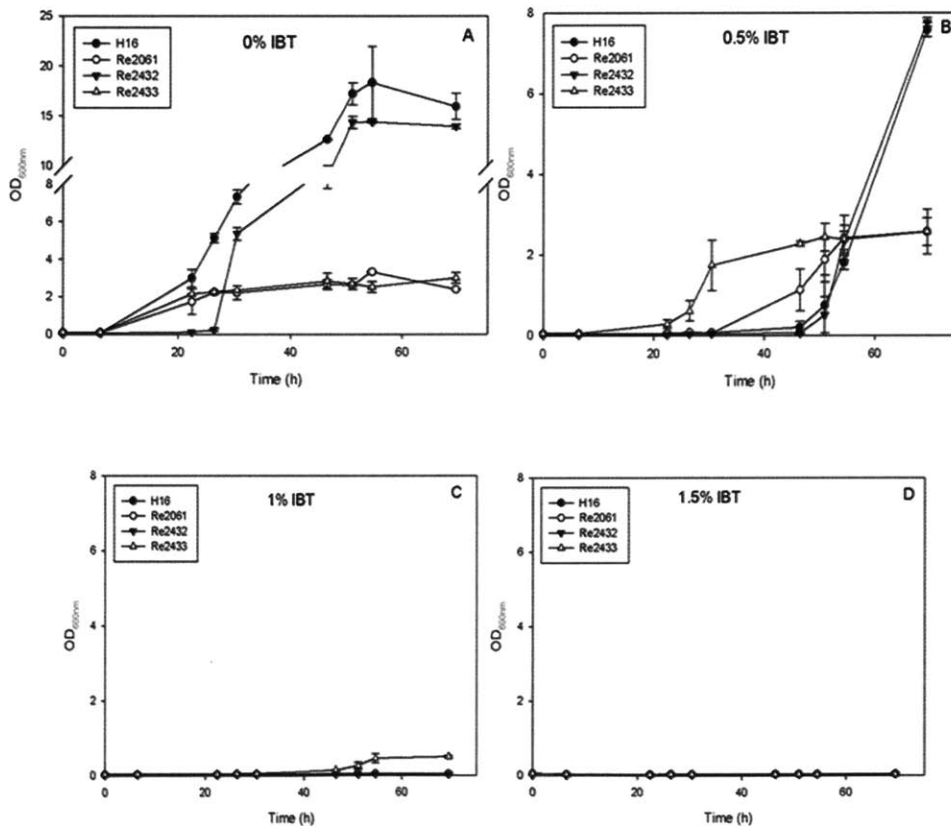
Consumption of isobutanol by the mutant and engineered strains was evaluated by cultivating each strain in minimal media with isobutanol as the only carbon source. To avoid isobutanol toxicity, initially isobutanol concentration was kept low at 0.2% (v/v). After 48 hours, additional isobutanol was supplemented to the medium until a final concentration of 1% to ensure enough carbon for growth.

To access whether if isobutanol tolerance also contribute to enhanced isobutanol production. Isobutanol production plasmid pJL26 (Table 5.1) was introduced in both control and isobutanol-tolerant strains. The resulting strains (Re2405/pJL26, Re 2410/pJL26, Re2425/pJL26, Re2439/pJL26, Re2444/pJL26 and Re2445/pJL26) were cultured in minimal media containing 2% fructose (w/v) and 0.05% NH₄Cl (w/v) at 30°C. Culture supernatants were harvested at various time points and evaluated for isobutanol concentration as described previously (Lu et al. 2012b).

RESULTS

Isobutanol tolerance in evolved strains

Experimental evolution on increasing concentrations of isobutanol resulted in two strains, Re2432 and Re2433, which are capable of growing in media with up to 2.5% (v/v) isobutanol. Their perspective parental strains, wild type H16 and Re2061, cannot survive in more than 0.5% (v/v) isobutanol. Isobutanol tolerance was measured and compared using the growth and survival tolerance assays. Growth assays indicated that both strains had reduced final OD and lengthened lag phase as extracellular isobutanol concentration increases. Strain Re2433, however, exhibits more robust growth in 0.5% and 1.0% isobutanol (v/v) compared to its parental strain Re2061. Both Re2432 and Re2433, along with their parental strains did not grow in isobutanol concentration above 0.5% (Figure 5.1), which was surprising considering both evolved strains grew in 2.5% isobutanol during experimental evolution experiment. This difference in growth and isobutanol tolerance can only be explained by the difference in growth media used in the evolution experiment (TSB) and tolerance assay (minimal media). On the other hand, cell survival was greatly improved in both evolved strains, especially at higher concentrations of isobutanol (1.75% and 2.0% v/v) (Figure 5.1).



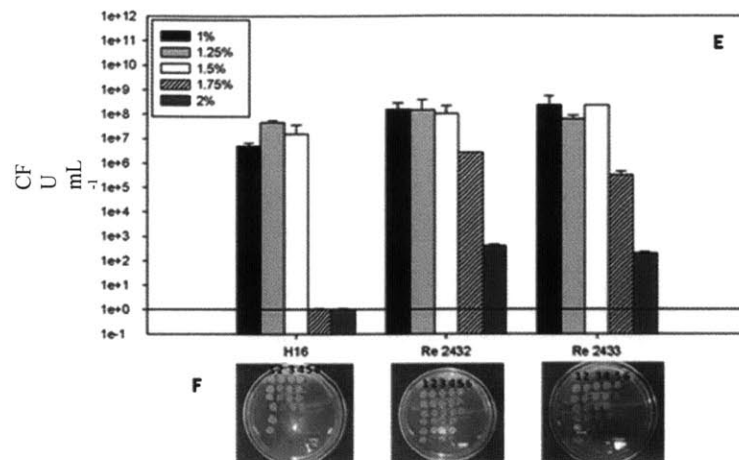


Figure 5.1. Result of isobutanol tolerance growth and survival assays. Growth of evolved strains Re2432 and Re2433 and their respective parental strains H16 and Re2061 in minimal media with 2% (w/v) fructose in the presence of increasing external isobutanol concentration. A) 0%, B) 0.5%, C) 1% and D) 1.5% (v/v) isobutanol. Clear difference between the final OD of H16 and Re2432 vs. Re2061 and Re2433 is due to the absence of intracellular PHB in the later two strains. The ability for *R. eutropha* (H16) and evolved strains (Re2432 and Re2433) strains to survive in the presence of different isobutanol concentrations were shown in E and F. E) Strains were exposed to different concentrations of isobutanol (1%, 1.25%, 1.5%, 1.75% and 2% v/v) in TSB media for 12h. Tolerance was determined in terms of CFU/ml of culture (see Materials and Methods). F) Pictures of TSB plates containing serial dilutions of H16, Re2432, and Re2433. Average values from three experiments were plotted with error bars representing the standard deviation.

Identification of mutations in evolved strains

Sequencing of the five genes stated in Table 5.3, revealed several mutations on *acrA* and *acrA6* genes from Re2432 and Re2433. DNA amplification showed a gene duplication insertion in Re2433 *acrA* compared to its parental strain and wild type (Figure 5.2). Such insertion was also confirmed by sequencing. Gene *acrA6* of the evolved strains revealed a point mutation, which generated a stop codon resulting in a truncated protein. The two genes incurred lesions during the experimental evolution process, *acrA* (H16_A3729) and *acrA6* (H16_A3357), are putatively part of a multidrug efflux transport system. It is described as being responsible for the protection of cells against environmental stresses, such as antibiotics and organic solvents. An inactivation of the components of these efflux systems has previously been shown to increase isobutanol tolerance in *E. coli* (Atsumi et al. 2010b; Minty et al. 2011). In frame single and double deletions of *acrA6* and *acrA* were created in wild type (H16) and isobutanol production strain (Re2425) in order to create new tolerant host devoid of negative mutation commonly accumulated during evolution. The resulting strains were further evaluated in terms of their ability to grow in the presence of isobutanol, ability to survive in elevated isobutanol concentrations, isobutanol consumption, and isobutanol production.

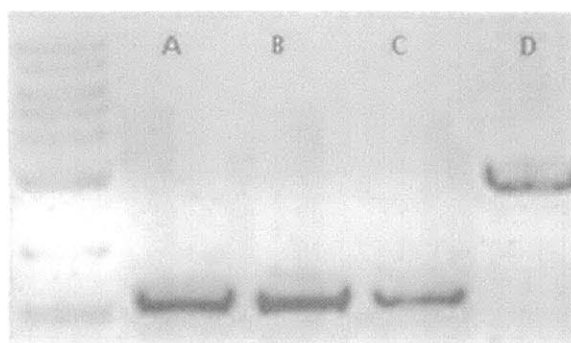


Figure 5.2: Agarose gel showing amplified *acrA* from wild type *R. eutropha* H16 (A); Re2425 (B); Re2432 (C); and Re2433 (D). Gene *acrA* from Re2433 had a lengthy insertion that can be seen on the gel.

Isobutanol tolerance in engineered strains

Strains with single or double deletion of *acrA* and *arcA6* were tested for isobutanol tolerance. Growth assay results indicate no significant difference in growth between the parental and deletion strains (Table 5.5). Nevertheless, survival assays show that all strains with *arcA* and/or *acrA6* deletion exhibited greater capacity to maintain viability in the presence of isobutanol. These deletions caused an increase in the number of cells able to survive when exposed to high concentrations of isobutanol (> 0.5%) for 12 h compared to both wild type (H16) and Re2425 parental strains (Figure 5.3). Similar results were observed in the evolved strain Re2432, which showed the highest number of viable cells in the presence of 1.75% and 2.0% (v/v) isobutanol (Figure 5.3). Re2432 also exhibited no growth improvement in the presence of isobutanol when compared to its parental strain (H16) (Figure 5.3), even though Re2432 came from a selected population capable of growth in the presence of high concentrations of isobutanol. This difference could be a result of growth media between TSB used in the experimental evolution and minimal media used in the isobutanol tolerant growth assays.

Table 5.5. Growth rate (μ_{\max} /h) of mutant strains Re2438, Re2442, Re2443, Re2439, Re2444 and Re2445 with their parental strain H16 and Re2425 in different isobutanol concentrations of minimal media with 2% (w v) fructose. Values indicate no significant difference between the growth rate of mutated and parental strains.

Strain	0% isobutanol	0.5% isobutanol	1% isobutanol
H16	0.458	0.107	<0.0005
Re2438	0.485	0.161	<0.0005
Re2442	0.458	0.136	<0.0005
Re2443	0.49	0.145	<0.0005
Re2425	0.084	0.013	<0.0005
Re2439	0.093	0.007	0.002
Re4444	0.142	0.003	0.001
Re4445	0.044	0.008	0.002

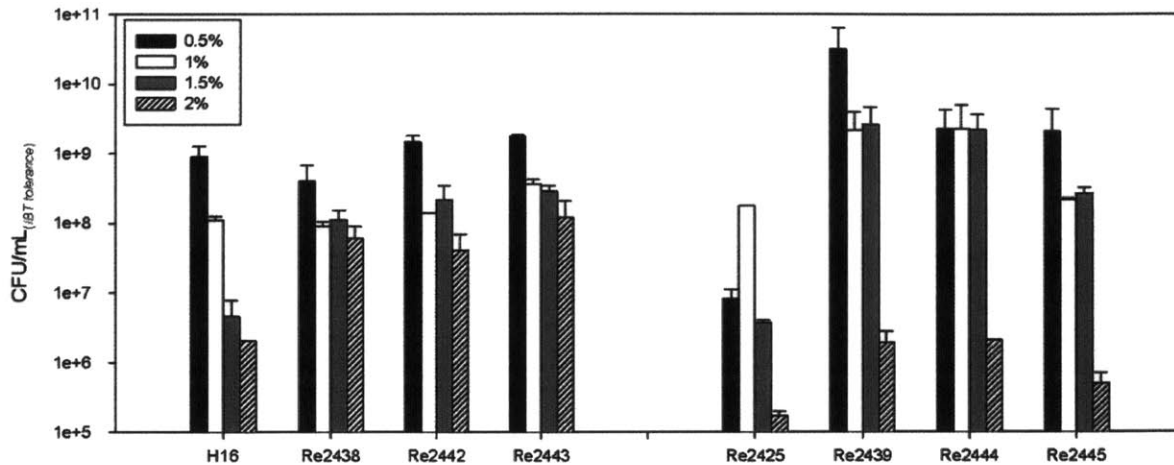


Figure 5.3. Viable cell counts of H16, Re2438, Re2442, Re2443, Re2425, Re2439, Re2444, Re2445 showing survival after exposure to 0.5%, 1.0%, 1.5%, and 2.0% isobutanol ($v v^{-1}$) in TSB media for a duration of 12h. Average values from three experiments were plotted with error bars representing the standard deviation.

Isobutanol consumption by engineered strains

One aspect to be considered when choosing a suitable strain for isobutanol production is its ability to consume isobutanol, the product of interest. Product consumption could compromise large-scale production and complicate the carbon feeding strategy. To evaluate *R. eutropha* and mutant strains' ability to consume isobutanol, strains (Re2425, Re2439, Re2444 and Re2445) were cultivated in minimal media containing only isobutanol. Results showed that all tested strains were able to utilize and grow on isobutanol as the sole carbon source, which indicates that deletion of *acrA* and/or *acrA6* did not affect the strain's ability to consume isobutanol (Figure 5.4).

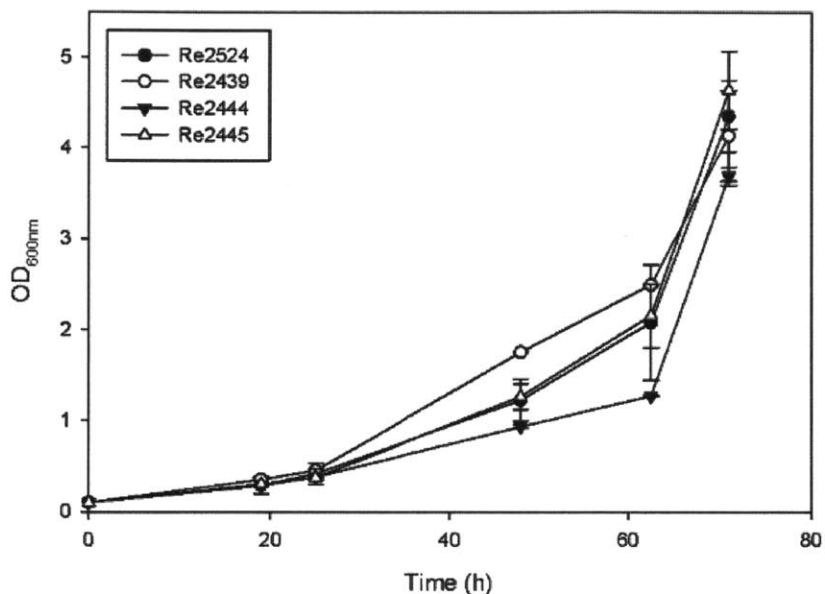


Figure 5.4: Isobutanol consumption characterized in strains Re2405, Re2425, Re2439, Re2444 and Re2445. Minimal medial supplemented with isobutanol as the only carbon source were used. Error bar represents standard deviation of triplicate experiments.

Isobutanol production by engineered strains

Isobutanol production operon (pJL26), which contains *kivD* gene from *L. lactis* and *ilvBHCD* genes from the *R. eutropha* valine biosynthesis pathway were inserted in Re2439, Re2444, and Re2445 (Table 5.1) in order to evaluate isobutanol production under enhanced isobutanol tolerance phenotype. The strains containing pJL26 were cultivated in minimal media with 2% fructose ($w v^{-1}$) and 0.05% NH_4Cl ($w v^{-1}$) along with controls Re2405/pJL26 and Re2425/pJL26 previously published by Lu et al. (2012). Overall, production titer did not improve with increased isobutanol tolerance, except for strain Re2445, which had ~25% improvement in isobutanol production (Figure 5.5). Re2445 has a single *arcA* deletion, which was reported to cause quinone depletion due to isobutanol stress. Similar to studies found in *E. coli*, deletion of *acrA* could have eliminated this efflux system and maintained the interaction between quinone and cellular membrane for electron transfer. Interestingly, Re2444 with both *arcA* and *arcA6* deleted, did not produce any isobutanol, while the single deletion of *arcA6* (Re2439) did not show impaired isobutanol production.

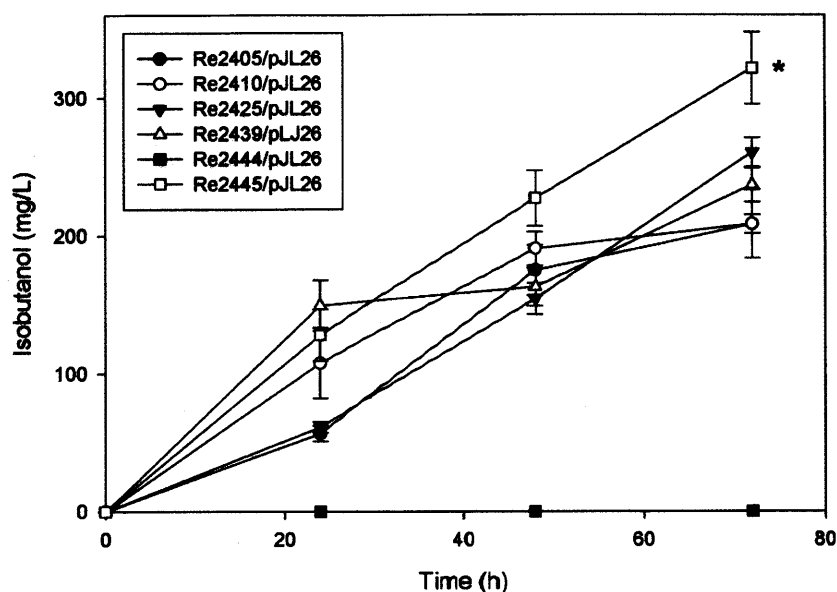


Figure 5.5. A) Isobutanol productions in mg/L by parental and engineered production strains Re2405, Re 2410, Re2425, Re2439, Re2444 and Re2445 containing plasmid pJL26 during 72h. Strain Re2445 show elevated isobutanol production when compared with either parental as other engineered strains. (*) represents significant difference in isobutanol concentration $p < 0.01$.

DISCUSSION

Isobutanol has unique chemical properties that make this molecule a very attractive target as the next generation biofuel. One major challenge facing the usage of isobutanol as a fuel additive or direct substitute for gasoline is its availability. In other words, production of isobutanol is far from meeting the economic scale. Volumetric production at large scales and final production titer were hindered because isobutanol is toxic to its cellular producer. Recently, two studies focused on characterizing the genotype-phenotype relationships in response to isobutanol in *E. coli*. Although these studies did not improve the final isobutanol production titer, the isobutanol tolerance mechanism was elucidated (Demple et al. 1997; Atsumi et al. 2010b). *R. eutropha* has high industrial potential for the production of isobutanol, because it does not require carbon derived from food sources and instead can utilize carbon dioxide for the production of isobutanol. A major downside with the utilization of *R. eutropha* is its low tolerance towards isobutanol. Strains showed no growth in media with more than 0.5% (v/v) isobutanol, which reduces its scale up potential (Lu et al. 2012).

In this study, *R. eutropha* strains were evolved on increasing concentrations of isobutanol by the sequential transfer method. The resulting strains were able to grow in 2.5% (v/v) isobutanol. Analysis and sequencing revealed mutations in both *acrA* and *acrA6* of evolved *R. eutropha* strains, which could contribute to the enhanced isobutanol tolerance. The tolerance phenotype was reconstructed in wild type and engineered isobutanol production strains by deletion of single or both *acrA* and *acrA6* gene. Strains with deletions resulted in the most significant enhancement in isobutanol tolerance with the ability to maintain cell viability in the presence of high isobutanol concentrations. The Re2443, which had both *acrA* and *acrA6*

deleted from its genome, had six times enhanced survival rate than wild type in an environment of 2% (v/v) isobutanol.

Both *acrA* and *acrA6* are involved in efflux systems in nearly all microorganisms. The AcrAB-TolC multidrug efflux system is an important mechanism for tolerance. It protects cells against stress caused by antibiotics and organic solvents by exporting these substances outside of the cell (Dempfle et al. 1997; Atsumi S. et al. 2010b). It is composed of a transporter (AcrB), a periplasmic accessory protein (AcrA), and an outer membrane protein (TolC) (Nikaido and Zgurskaya 2001). Various studies showed that the deletion of *acrA* increased cell susceptibility to different solvents in *E. coli* (Ma et al. 1995). Other studies illustrated a different response for isobutanol stress, which states that the presence of extracellular isobutanol causes quinone depletion, which significantly induces *acrAB-tolC* transcription, leading to an increase in quinone flux. Which in turn causes a decrease in electron transfer and ATP synthesis, which is the energy used for cellular metabolism and growth (Brynildsen and Liao 2009). Therefore, deletion of AcrAB-TolC units could increase isobutanol tolerance by reducing quinone depletion as was seen previously in *E. coli* (Atsumi et al. 2010b). Such a mechanism of tolerance is similar in *R. eutropha* as concluded in this study.

This study also shows that an improvement in tolerance can lead to an improve in isobutanol production. Strain Re2445 had its *arcA* efflux component eliminated and was able to produce 260 mg/L isobutanol, an ~25% increase from the 208.2 mg/L parental strain production titer. Although single deletion of *arcA6*, which improved isobutanol tolerance, but did not improve the production of isobutanol. Oddly, double deletion of both *arcA* and *acrA6* produced no detectable isobutanol. One hypothesis could be that ArcA and ArcA6 are efflux proteins responsible for the elimination of isobutanol from the cell, although such system has not been reported to date. When both genes were eliminated, the cells are unable to pump out any isobutanol produced inside the cell, thus no isobutanol was detected in the supernatant of the double deletion strain.

Further studies must be performed to understand the physiological role of AcrA and AcrA6 in *R. eutropha* in order to optimize tolerance in production strains. It is important to look into other regulatory systems, such as the *marCRAB* operon, *yhbJ*, and *tnaA*, which have been reported to regulate membrane permeability, outer membrane repair, and another multidrug efflux protein respectively. In similar studies with *E. coli*, the best results in growth improvement in the presence of isobutanol were achieved when an *acrA* deletion was combined with deletion of *marCRAB*. In *R. eutropha*, *marC* is not located within an operon, and there are >13 potential homologues, thus providing a significant challenge in determining its role in *R. eutropha*. The potential role of ArcA and ArcA6 in isobutanol transport could also shed insights for rational design of *R. eturopha* with enhanced isobutanol tolerance and production.

REFERENCES

- Brynildsen, M. P., & Liao, J. C. (2009). An integrated network approach identifies the isobutanol response network of *Escherichia coli*. *Molecular Systems Biology*.
- Alper, H., Moxley, J., Nevoigt, E., Fink, G. R., & Stephanopoulos, G. (2006). Engineering yeast transcription machinery for improved ethanol tolerance and production. *Science*, 1565-1568.
- Atsumi, S., Hanai, T., & Liao, J. C. (2008). Non-fermentative pathways for synthesis of branched-chain higher alcohols as biofuels. *Nature*, 86-89.
- Atsumi, S., Higashide, W., & Liao, J. (2009). Direct photosynthetic recycling of carbon dioxide to isobutyraldehyde. *Nature Biotechnology*, 1177-1180.
- Atsumi, S., Wu, T.-Y., Eckl, E.-M., Hawkins, D. S., Buelter, T., & Liao, C. J. (2010). Engineering the isobutanol biosynthetic pathway in *Escherichia coli* by comparison of three aldehyde reductase/alcohol dehydrogenase genes. *Applied Microbiology and Biotechnology*, 651-657.
- Atsumi, S., Wu, T.-Y., Machado, I. M., Huang, W. C., Chen, P. Y., Pellegrini, M., et al. (2010b). Evolution, genomic analysis, and reconstruction of isobutanol tolerance in *Escherichia coli*. *Molecular Systems Biology*.
- Bertani, G. (1951). Studies on lysogenesis. I. The mode of phage liberation by lysogenic *Escherichia coli*. *Journal of Bacteriology*, 293-300.
- Blombach, B., Riester, T., Wieschalka, S., Ziert, C., Youn, J.-W., Wendisch, V. F., et al. (2011). *Corynebacterium glutamicum* tailored for efficient isobutanol production. *Applied and Environmental Microbiology*, 3300-3310.
- Brigham, C. J., Gai, C. S., Lu, J., Speth, D. R., Sinskey, A. J., & Worden, R. M. (2012). Engineering *Ralstonia eutropha* for Production of Isobutanol from CO₂, H₂, and O₂. In J. W. Lee, *Advanced Biofuels and Bioproducts*. New York: Springer.
- Brigham, C. J., Zhila, N., Shishatskaya, E., Volova, T. G., & Sinskey, A. J. (2012b). Manipulation of *Ralstonia eutropha* Carbon Storage Pathways to Produce Useful Bio-Based Products. In X. Wang, J. Chen, & P. Quinn, *Reprogramming Microbial Metabolic Pathways* (pp. 343-366). Springer Science+Business Media Dordrecht 2012.
- Brown, D. G., Swanson, J. K., & Allen, C. (2007). Two Host-Induced *Ralstonia solanacearum* Genes, *acrA* and *dinF*, Encode Multidrug Efflux Pumps and Contribute to Bacterial Wilt Virulence. *Applied and Environmental Microbiology*, 2777-2786.
- Brynildsen, M. P., & Liao, J. C. (2009). An integrated network approach identifies the isobutanol response network of *Escherichia coli*. *Molecular Systems Biology*.
- de Palencia, P. F., de la Plaza, M., Amárta, F., Requena, T., & Peláez, C. (2006). Diversity of amino acid converting enzymes in wild lactic acid bacteria. *Enzyme and Microbial Technology*, 88-93.
- Dempse, B., Goldman, J. D., White, D. G., & Levy, S. B. (1997). Role of the *acrAB* locus in organic solvent tolerance mediated by expression of *marA*, *soxS*, or *robA* in *Escherichia coli*. *Journal of Bacteriology*, 6122-6126.

- Doukyu, N., Ishikawa, K., Watanabe, R., & Ogino, H. (2012). Improvement in organic solvent tolerance by double disruptions of proV and marR genes in Escherichia coli. *Journal of Applied Microbiology*, 464-474.
- Dunlop, M. J. (2011). Engineering microbes for tolerance to next-generation biofuels. *Biotechnology for Biofuels*, 4 (32), 9.
- Gibson, D. G., Young, L., Chuang, R.-Y., Venter, J. C., Hutchison III, C. A., & Smith, H. O. (2009). Enzymatic assembly of DNA molecules up to several hundred kilobases. *Nature Methods*, 343-345.
- Hwang, J.-Y., Park, J., Seo, J.-H., Cha, M., Cho, B.-K., Kim, J., et al. (2009). Simultaneous synthesis of 2-phenylethanol and L-homophenylalanine using aromatic transaminase with yeast Ehrlich pathway. *Biotechnology and Bioengineering*, 1323-1329.
- Jendrossek, D., Kruger, N., & Steinbuchel, A. (1990). Characterization of Alcohol Dehydrogenase Genes of Derepressible Wild-Type Alcaligenes eutrophus H16 and Constitutive Mutants. *Journal of Bacteriology*, 172 (9), 4844-4851.
- Junker, F., & Ramos, J. (1999). Involvement of the cis/trans isomerase Cti in solvent resistance of Pseudomonas putida DOT-T1E.
- Kieboom, J., Dennis, J. J., de Bont, J. A., & Zylstra, G. J. (1998). Identification and Molecular Characterization of an Efflux Pump Involved in Pseudomonas putida S12 Solvent Tolerance. *The Journal of Biological Chemistry*, 85-91.
- Li, H., Opgenorth, P. H., Wernick, D. G., Rogers, S., Wu, T.-Y., Higashide, W., et al. (2012). Integrated Electromicrobial Conversion of CO₂ to Higher Alcohols. *Science*, 335 (March 2012), 1596.
- Liao, M. P. (2009). An integrated network approach identifies the isobutanol response network of Escherichia coli. *Molecular System Biology*.
- Lu, J., Brigham, C. J., Gai, C. S., & Sinskey, A. J. (2012b). Studies on the production of branched-chain alcohols. *Appl Microbiol Biotechnol*.
- Lu, J., Brigham, C. J., Rha, C., & Sinskey, A. J. (2012a). Characterization of an extracellular lipase and its chaperone from Ralstonia eutropha H16. *Appl Microbiol Biotechnol*.
- Ma, D., Cook, D. N., Alberti, M., PO, N. G., Nikaido, H., & Hearst, J. E. (1995). Genes acrA and acrB encode a stress-induced efflux system of Escherichia coli. *Molecular Microbiology*, 45-55.
- Minty, J. J., Lesnefsky, A. A., Lin, F., Chen, Y., Zaroff, T. A., Veloso, A. B., et al. (2011). Evolution combined with genomic study elucidates genetic bases of isobutanol tolerance in Escherichia coli. *Microbial Cell Factories*, 18-56.
- Nikaido, H. (1996). Multidrug Efflux Pumps of Gram-Negative Bacteria. *American Society for Microbiology*, 5853-5859.
- Nikaido, H. (2009). Multidrug Resistance in Bacteria. *Annual review of biochemistry*, 119-146.
- Nikaido, H., & Zgurskaya, H. I. (2001). AcrAB and Related Multidrug Efflux Pumps of Escherichia coli. *Journal of Molecular Microbiology and Biotechnology*, 215-218.

- Oh, H. Y., Lee, J. O., & Kim, O. B. (2012). Increase of organic solvent tolerance of *Escherichia coli*. *Applied Microbiology and Biotechnology*, 1619–1627.
- Piter, P. W. (1995). The heat-shock and ethanol stress responses of yeast exhibit extensive similarity and functional overlap. *FEMS Microbiology Letters*, 121-127.
- Quandt, J., & Hynes, M. F. (1993). Versatile suicide vectors which allow direct selection for gene replacement in gram-negative bacteria. *Gene*, 15-21.
- Reyes, L. H., Almario, M. P., Winkler, J., Orozco, M. M., & Kao, K. C. (2012). Visualizing evolution in real time to determine the molecular mechanisms of n-butanol tolerance in *Escherichia coli*. *Metabolic Engineering*.
- Rojas, A., Duque, E., Mosqueda, G., Golden, G., Hurtado, A., Ramos, J. L., et al. (2001). Three Efflux Pumps Are Required To Provide Efficient Tolerance to Toluene in *Pseudomonas putida* DOT-T1E. *Journal of Bacteriology*, 3967–3973.
- Savrasova, E. A., Kivero, A. D., Shakulov, R. S., & Stoyanova, N. V. (2011). Use of the valine biosynthetic pathway to convert glucose into isobutanol. *Industrial Microbiology and Biotechnology*, 1287-1294.
- Slater, S., Houmiel, K. L., Tran, M., Mitsky, T. A., Taylor, N. B., Padgett, S. R., et al. (1998). Multiple b-Ketothiolases Mediate Poly(b-Hydroxyalkanoate) Copolymer Synthesis in *Ralstonia eutropha*. *Journal of Bacteriology*, 180, 1979-1987.
- Smith, K. M., Cho, K.-M., & Liao, J. C. (2010). Engineering *Corynebacterium glutamicum* for isobutanol production. *Applied Microbiology and Biotechnology*, 1045-1055.
- Takatsuka, Y., Chen, C., & Nikaido, H. (2010). Mechanism of recognition of compounds of diverse structures by the multidrug efflux pump AcrB of *Escherichia coli*. *PNAS*, 107 (15).
- Tamura, K., Peterson, D., Peterson, N., Stecher, G., Nei, M., & Kumar, S. (2011). MEGA5: Molecular Evolutionary Genetics Analysis Using Maximum Likelihood, Evolutionary Distance, and Maximum Parsimony Methods. *Molecular Biology and Evolution*, 28, 2731-2739.
- Tomas, C. A., Welker, N. E., & Papoutsakis, E. T. (2003). Overexpression of groESL in *Clostridium acetobutylicum* results in increased solvent production and tolerance, prolonged metabolism, and changes in the cell's transcriptional program. *Applied and Environmental Microbiology*, 4951–4965.
- Watanabe, R., & Doukyu, N. (2012). Contributions of mutations in *acrR* and *marR* genes to organic solvent tolerance in *Escherichia coli*. *AMB Express*.
- Yan, Y., & Liao, J. C. (2009). Engineering metabolic systems for production of advanced fuels. *Journal of Industrial Microbiology & Biotechnology*, 471–479.
- Yomano, L. P., York, S. W., & Ingram, L. O. (1998). Isolation and characterization of ethanol-tolerant mutants of *Escherichia coli* KO11 for fuel ethanol production. *J Ind Microbiol Biotechnol*, 132-138.

CHAPTER 6

Insights into bacterial fitness revealed by the characterization of carbonic anhydrases in *Ralstonia eutropha* H16

(This chapter was modified from a previously published article in Applied Microbiology and Biotechnology Express, 2014. 4:1-12 'Insights into bacterial CO₂ metabolism revealed by the characterization of four carbonic anhydrases in *Ralstonia eutropha* H16' Claudia Gai, Jingnan Lu, Christopher Brigham, Amanda Bernardi, and Anthony Sinskey © Springer-Verlag)

INTRODUCTION

Carbon dioxide, bicarbonate, carbonic acid, and carbonate are key metabolites in all living systems, and the equilibrium of these different species in living cells is important for proper physiological functioning. Carbonic anhydrase (CA) catalyzes the interconversion between carbon dioxide and bicarbonate ($\text{CO}_2 + \text{H}_2\text{O} \rightarrow \text{HCO}_3^- + \text{H}^+$). The CA-catalyzed metabolic hydration/dehydration of CO₂ and HCO₃⁻ supports physiological functions in the cell, even though the uncatalyzed (enzyme-free) reaction proceeds at significant rates (Kusian et al. 2002).

There are five main classes of CA enzyme found in nature (α , β , γ , δ and ζ). Although no significant sequence similarities were observed between representatives of the different classes, implying that CA enzymes evolved convergently in diverse biological systems (Smith and Ferry 2000; Lionetto et al. 2012). The α -CA enzymes are the most studied to date and are found in many different genera. They are monomeric, zinc-containing enzymes with multiple isozymes, which have different expression patterns and localizations (Smith and Ferry 2000; Tripp et al. 2001; Marcus et al. 2005; Fasseas et al. 2011). In α -CA enzymes, Zn²⁺ is coordinated by three amino acids (usually histidines) and a water molecule. The role of Zn²⁺ is to facilitate the deprotonation of water for the formation of a nucleophilic hydroxide ion. This hydroxide ion can then initiate a nucleophilic attack on the carbonyl group of CO₂ and convert it into bicarbonate. Specifically, the +2 charge of the zinc ion associates with the oxygen atom of water, supplying positive charge to the hydroxide ion, which is then able to attack the CO₂ (Lionetto et al. 2012) (Figure 6.1). All CA classes present differences in their secondary, tertiary, and quaternary structures. Enzymes of the α class are monomeric, β -CA enzymes are usually oligomeric and contain 2 to 6 monomers, and γ -CA enzymes associate as homotrimers. Also, the active site ligands are potentially different among the CA classes, although β -CA and γ -CA enzymes are believed to function in a similar manner, in which both use the same zinc hydroxide mechanism (Supuran 2004).

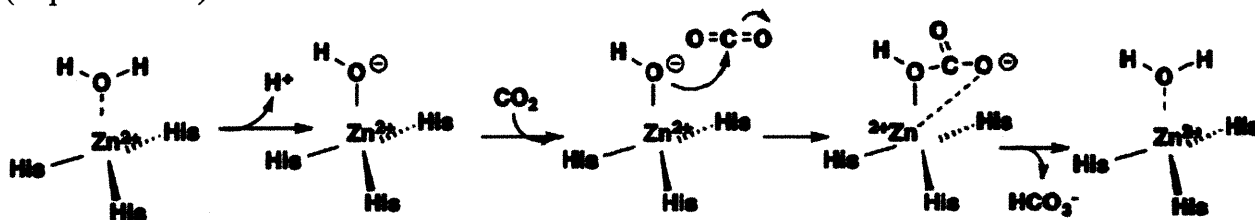


Figure 6.1: Reaction mechanism of carbonic anhydrase.

Ralstonia eutropha (also *Cupriavidus necator*) is a Gram-negative facultative chemoautotrophic betaproteobacterium. It is well known for its ability to produce polyhydroxyalkanoate under high carbon but limited nitrogen or phosphorus conditions (Budde et al. 2010; Brigham et al. 2012b). The capacity of *R. eutropha* to grow autotrophically using CO₂ as the sole carbon source has been recently explored and studied for the production of alternative biofuels (Li et al. 2012; Lu et al. 2012). Assimilation of CO₂ during autotrophic growth of *R. eutropha* proceeds by the Calvin-Benson-Bassham (CBB) cycle (Kusian and Bowien 1997) and requires large amounts of energy to fuel the synthesis of cellular building blocks. Organisms must have a reliable and efficient system of controlling intracellular pH and CO₂ concentrations in order to carry out carbon fixation (Codd and Kuenen 1987). Cyanobacteria evolved carboxysomes as an efficient mechanism to increase CO₂ concentration and consequently its fixation efficiency (Badger and Price 2003, Bonacci et al. 2012), but *R. eutropha* lacks this system although it contains its two main enzymes, CA and RuBisCO (Pohlmann et al. 2006). Besides the key CBB cycle enzyme, RuBisCO, CA is of great importance for fine-tuning the concentration of CO₂ in autotrophic metabolism.

In this study, four putative CA genes were identified in the genome sequence of *R. eutropha* strain H16. Two CA genes are located on chromosome 1, and the others are on chromosome 2. The *can* (locus tag H16_A0169) and *can2* (locus tag H16_B2270) genes encode β -CA enzymes, the *caa* (locus tag H16_B2403) gene encodes a putative periplasmic α -CA, and the gene with locus tag H16_A1192 (hereafter known as *cag*) encodes a γ -like-CA/acetyltransferase (Pohlmann et al. 2006). The presence of CA genes of multiple classes in *R. eutropha* suggests that the gene products play major roles in CO₂ transport and metabolism. Additionally, the diversity of CA gene products expressed in *R. eutropha* implies that the functions of these different enzymes could all be unique. Dobrisnki et al. (2010) examined four CA enzymes (α , β , γ and CsoSCA) from the deep sea proteobacterium *Thiomicrospira crunogena* and suggested different roles for each of the enzymes in relation to carbon fixation capabilities and survival mechanisms of the microorganism. Currently, the exact roles of all four *R. eutropha* CA enzymes are still largely unknown and the only CA studied in depth to date is Can, which was identified as being essential for growth under atmospheric concentrations of CO₂ (Kusian et al. 2002).

In the present study, the activities of all four CA enzymes from *R. eutropha* were studied, following heterologous expression and purification from *Escherichia coli*. The effects of single and combinatorial CA gene deletions on cell physiology and fitness were also assessed. The importance of Caa localization in the cell was further examined by overexpressing the enzyme with and without a periplasmic localization signal peptide in a Δ *caa* strain. Periplasmic localization was confirmed by detection of a Red Fluorescent Protein (RFP) and Caa fusion protein using fluorescent microscopy.

MATERIALS AND METHODS

Chemicals, bacterial strains and plasmids

Chemicals were purchased from Sigma-Aldrich unless indicated otherwise. Experiments were performed with strains and plasmids listed in Table 6.1 and Table 6.2 respectively.

Table 6.1: Bacterial strains used in this study.

Strains	Relevant characteristics	References
<i>R. eutropha</i>		
H16	Wild-type gentamycin resistant (Gen ^r)	ATCC 17699
Re2061	H16 Δ <i>phaCAB</i> (Gen ^r)	Lu et al. (2012)
Re2427	H16 Δ <i>can</i>	This study
Re2428	H16 Δ <i>caa</i>	This study
Re2430	H16 Δ <i>cag</i>	This study
Re2437	H16 Δ <i>can2</i>	This study
Re2436	H16 Δ <i>can</i> Δ <i>can2</i> Δ <i>caa</i> Δ <i>cag</i>	This study
<i>E. coli</i>		
DH10-beta competent cells	strain suitable for high efficiency transformation	New England Biolabs
BL21(DE3)	strain suitable for transformation and protein expression.	New England Biolabs
S17-1	Conjugation strain for transfer of plasmids into <i>R. eutropha</i>	Simon et al. (1983)

Table 6.2: Plasmids used in this study.

Plasmids	Relevant characteristics	References
pBBR1MCS-2	Broad-host-range cloning vector confers kanamycin resistance (Kan ^r)	Kovach et al. (1995)
pCan	pBBR1MCS-2 containing <i>can</i> gene (H16 A0169) (Kan ^r)	This work
pCan2	pBBR1MCS-2 containing <i>can2</i> gene (H16 B2270) (Kan ^r)	This work
pCaa	pBBR1MCS-2 containing <i>caa</i> gene (H16 B2403) (Kan ^r)	This work
pCaaB	pBBR1MCS-2 containing <i>caa</i> gene without the <i>N</i> terminal signaling peptide sequence (H16 B2403) (Kan ^r)	This work
pCag	pBBR1MCS-2 containing <i>cag</i> gene (H16 A1192) (Kan ^r)	This work
pETCan	pET14b containing <i>can</i> gene (H16 A0169) (Amp ^r)	This work
pETCan2	pET14b containing <i>can2</i> gene (H16 B2270) (Amp ^r)	This work
pETCaa	pET14b containing <i>caa</i> gene (H16 B2403) (Amp ^r)	This work
pETCag	pET14b containing <i>cag</i> gene (H16 A1192) (Amp ^r)	This work
pStrepCan	pET51b containing <i>can</i> gene (H16 A0169) (Amp ^r)	This work
pStrepCaa	pET51b containing <i>caa</i> gene (H16_B2403) (Amp ^r)	This work
pStrepCaaB	pET51b containing <i>caa</i> gene without the <i>N</i> terminal signaling peptide sequence (H16_B2403) (Amp ^r)	This work
pRARE	Overcoming the codon bias of <i>E. coli</i> for enhanced protein expression (Cam ^r)	Novagen INC
pJV7	pJQ200Kan with Δ <i>phaC1</i> inserted into <i>Bam</i> HI restriction site, confers kanamycin resistance (Kan ^r)	Budde et al. (2011)
pJV7 Δ <i>can</i>	pJV7 with Δ <i>phaC1</i> allele removed by <i>Bam</i> HI digestion and replaced with Δ <i>can</i> allele (Kan ^r)	This work
pJV7 Δ <i>can2</i>	pJV7 with Δ <i>phaC1</i> allele removed by <i>Bam</i> HI digestion and replaced with Δ <i>can2</i> allele (Kan ^r)	This work
pJV7 Δ <i>caa</i>	pJV7 with Δ <i>phaC1</i> allele removed by <i>Bam</i> HI digestion and replaced with Δ <i>caa</i> allele (Kan ^r)	This work
pJV7 Δ <i>cag</i>	pJV7 with Δ <i>phaC1</i> allele removed by <i>Bam</i> HI digestion and	This work

pRFP	replaced with Δ cag allele (Kan ^r) pBBR1MCS-2 containing <i>rfp</i> gene amplified from JBp000066 kindly offered by J. Mueller (JBEI) (Kan ^r)	This work
pCAA_RFP	pBBR1MCS-2 containing <i>caa</i> gene fused by a 6aa linker to the <i>rfp</i> gene (Kan ^r).	This work

Growth media and cultivation conditions

R. eutropha strains were propagated in tryptic soy broth (TSB) (Becton Dickinson, Sparks, MD) or minimal medium (Lu et al. 2012) with fructose at a final concentration of 1% or 2% (w vol⁻¹), or pyruvate, lactate, succinate, or formate, each at a final concentration of 0.2% (w vol⁻¹). All cultures were inoculated to an initial OD_{600nm} of 0.05. *E. coli* strains were grown in LB medium (Bertani, 1951) at 37°C. For growth experiments in a CO₂-rich environment, cultures were performed inside a CO₂ incubator (Napco 6100 - Thermo Electron Corporation, Winchester, VA USA) with an atmosphere of 10% CO₂ at 30°C, under 200 rpm agitation. Appropriate antibiotics were added to the growth media at the following concentrations: gentamicin, 10 µg mL⁻¹; kanamycin, 200 µg mL⁻¹ (for *R. eutropha*); kanamycin, 50 µg mL⁻¹ (for *E. coli*); ampicillin, 100 µg mL⁻¹; chloramphenicol, 34 µg mL⁻¹.

Autotrophic cultures were prepared using minimal media without carbon source. For these cultures, a 250-mL Erlenmeyer flask containing 30 mL of culture is placed into a 15,000 Vacu-Quik Jar System (Almore International, Inc., Portland, OR, USA). Agitation inside the flask was assured by stirring with a stir bar. Vacuum and nitrogen were applied alternatively and repeatedly three times to flush the chamber and remove all air. An approximate molecular ratio of 8:1:1 (H₂: O₂: CO₂) (Leadbeater and Bowien 1984) gas mixture was then supplied to the jar. Any additional space in the jar was filled with 100% nitrogen.

Plasmid and strain construction

Standard protocols were employed for DNA manipulation (Sambrook and Rusell 2001). PCR amplification of DNA was performed using Phusion DNA Polymerase (New England Biolabs, Ipswich, MA, USA). Restriction enzymes and T4 DNA ligase used in this study were from New England Biolabs (Ipswich, MA, USA). The QIAquick Gel Extraction Kit (Qiagen, Valencia, CA, USA) was used for all gel purifications of DNA products and plasmid extractions were carried out using QIAprep Spin Miniprep Kit.

For the construction of overexpression and complementation plasmids, each of the four CA genes was cloned into pBBR1MCS-2 between restriction sites *KpnI* and *HindIII* (*can*, *can2* and *caa*) or *Sall* and *HindIII* (*cag*) to create the plasmids pCan, pCan2, pCaa and pCag respectively (Table 6.2). Each plasmid was transformed by electroporation into *E. coli* S17-1, which was then used as a donor strain for the conjugative transfer of plasmid into *R. eutropha* by a standard mating procedure (Slater et al. 1998). For control experiments, *R. eutropha* was also transformed with the empty vector pBBR1MCS-2.

For the construction of CA heterologous overexpression plasmids in *E. coli*, followed by protein purification, CA genes were amplified and cloned as described above using the restriction sites with *NdeI* and *XhoI* (*can*, *can2* and *caa*) or *NdeI* and *BamHI* (*cag*) on both plasmids pET14b (*N*-terminal His-tag) and pET51b (*C*-terminal Strep2-tag) (Table 6.2). Each plasmid was then transformed into *E. coli* BL21 (DE3) harboring pRARE (Table 6.2).

For the assessment of the role of the predicted Caa signaling peptide and the effect of the correct localization of the enzyme on *R. eutropha* physiology, the entire annotated gene (*caa* - H16_B2403), with (*caa*) and without (*caaB*) the nucleotide sequence encoding the 23-aa *N*-

terminal predicted signal-peptide were amplified and separately cloned into expression vectors (Table 6.2). The 22-aa *N*-terminal periplasmic signal peptide of Caa was predicted using SignalP 4.0 software (Petersen et al. 2011) and shown in Appendix 6.1.

RFP fusion plasmids were prepared by amplifying and inserting the *rfp* gene from the plasmid JBp000066 (kindly provided by J. Mueller and S. Singer – JBEI, Emeryville, CA, USA) at the 3' end of the *caa* gene, with DNA sequence encoding a 6-glycine linker between the genes, into pBBR1MCS-2 using the Gibson assembly method (Gibson et al. 2009) to produce pCaa_RFP. The *rfp* gene alone was expressed separately as a control (pRFP). Plasmids were introduced separately, as described above, into *R. eutropha* strain Re2061 (Table 6.1), which does not produce intracellular polyhydroxyalkanoate.

Plasmids for markerless deletion of CA genes were constructed according to Lu et al. (2012). Once the deletion strains Re2427 (H16 Δcan), Re2428 (H16 Δcaa), Re2430 (H16 Δcag), and Re 2437(H16 $\Delta can2$) were constructed, overexpression plasmids containing *can*, *can2*, *caa* or *cag* genes were introduced *in trans* to create Re2427/pCan, Re2428/pCaa, Re2430/pCag, Re2437/pCan2 and Re2428/pCaaB for complementation studies. A strain with quadruple CA gene deletions, Re2436 (H16 $\Delta can\Delta can2\Delta caa\Delta cag$), was also constructed, and each CA enzyme, expressed *in trans*, was complemented back into the strain to create Re2436/pCan, Re2436/pCaa, Re2436/pCag and Re2436/pCan2. All oligonucleotide primers used for plasmid and strain constructions are listed in the Appendix 6.2.

Cell preparation and protein purification

R. eutropha CA genes were expressed in *E. coli* BL21(DE3)/pRARE using plasmids listed in Table 6.2. Cells were induced with IPTG (Isopropyl β -D-1-thiogalactopyranoside, 0.6 mM) at a culture OD₆₀₀ of 0.4-0.6. Cells were harvested 8 h post-induction by centrifugation and stored at -80°C prior to CA purification and activity assay. Purification of Strep2-tagged proteins was performed using a gravity flow Strep-Tactin® Superflow® high capacity column (IBA, Göttingen, Germany) following the manufacturer's instructions. His-tagged proteins were purified using a 5-mL HisTrap® FF column (Amersham Bioscience, Uppsala, Sweden) operated by a low pressure liquid chromatography system (BioRad, Hercules, California, USA). Fractions containing purified CA were detected on a 12% SDS-PAGE gel (Sambrook and Rusell 2001), concentrated using Amicon Ultra-15 Centrifugal Filter Units (EMD Millipore Corporation, Billerica, MA, USA), and dialyzed overnight using a Slide-A-Lyzer Dialysis Cassette (Thermo Scientific, Asheville, NC, USA) in Tris-HCl (100 mM pH 7) at 4°C.

Determination of CA activity

The CA activity assays were based on methods from Sundaram et al. (1986) and Fasseas et al. (2011) with some modifications. CA activity was measured by comparing the rapid change of pH in the presence of CA to the slower pH change in the absence of CA. The assays were performed using a stopped-flow device (Applied Photophysics Ltd, Leatherhead, United Kingdom) connected to a spectrophotometer (Agilent 8453 UV-Visible Kinetic Mode). Purified CA enzymes were diluted in assay buffer (50 mM Na₂SO₄, 50 mM HEPES, 50mM MgSO₄, 0.004% (w v⁻¹) Phenol red, pH 8 for assays using CO₂ as a substrate or pH 6 for assays using KHCO₃ as a substrate. All reagents were kept on ice while the spectrophotometer and stopped-flow apparatus were kept at 1°C \pm 1°C using a recirculating water bath. The substrates used for

the activity assays were KHCO_3 (50mM) and saturated CO_2 (dry ice in assay buffer for 30 min). The final volume of the assay reaction was 400 μL and the absorbance $A_{557\text{nm}}$ was measured for 60 seconds total. Control assays were carried out in the absence of enzymes. Enzyme Units (EU) were calculated as illustrated below by comparing the time of pH change in the presence of enzyme to reaction without enzyme (Sundaram et al. 1986). Each additional EU speeds the catalytic activity of the enzyme by two fold. The assay was validated using commercially available purified CA from bovine erythrocytes (Sigma-Aldrich C9207). Protein concentration (purified or cell extract) was determined by standard Bradford assay (Bradford, 1976).

$$\text{EU} = \frac{|\text{Time of uncatalized} - \text{Time of catalized reaction (s)}|}{\text{Time of catalized reaction (s)}} \times \frac{1}{\text{Total protein in assay (mg)}}$$

Microscopy

Slides of Re2061/pCaa_RFP or Re2061/pRFP were prepared using 10 μL of overnight TSB cultures placed onto Poly-*L*-Lysine-coated slides. Cells were observed using a Nikon Labophot-2 microscope with phase-contrast and fluorescence attachments. Images were acquired with a SPOT-cooled color digital camera (Diagnostic Instruments, Inc.).

Polymer quantification

Polyhydroxybutyrate (PHB) content was determined as described previously (Karr et al. 1983; York, et al. 2003).

RESULTS

Characterization of CA enzymes

All four carbonic anhydrase enzymes were heterologously overexpressed in recombinant *E. coli*, purified, and examined. Each CA was able to catalyze the interconversion reaction between CO_2 and bicarbonate. Additionally, each CA exhibited different specific activity and substrate preference towards CO_2 and bicarbonate. Caa presented a higher activity using CO_2 as the substrate, compared to the activity of Can, Can2 or Cag, which all preferred bicarbonate (Figure 6.2). The specific activity of Caa towards CO_2 as a substrate ($422.2 \pm 97.1 \text{ EU mg}^{-1}$) was higher than the activity measured for the other CAs (Can $59.5 \pm 15.3 \text{ EU mg}^{-1}$; Can2 $157.9 \pm 4 \text{ EU mg}^{-1}$ and Cag $138.2 \pm 61.3 \text{ EU mg}^{-1}$). On the other hand, the specific activities of both Can and Can2 were similar with bicarbonate as a substrate ($277.9 \pm 12.6 \text{ EU mg}^{-1}$ and $309.4 \pm 103.1 \text{ EU mg}^{-1}$ respectively). Cag presented the highest activity using bicarbonate as a carbon source ($488.5 \pm 122.1 \text{ EU mg}^{-1}$). All CAs were active towards CO_2 and bicarbonate, however only Caa had a distinct preference for CO_2 as a substrate while the other three CAs all preferred bicarbonate. Validation assay were carried out using a commercially available CA and the values obtained were $130.7 \pm 20.1 \text{ EU mg}^{-1}$ using bicarbonate as a substrate and $168.8 \pm 5.9 \text{ EU mg}^{-1}$ using CO_2 as a substrate. Comparative CO_2 hydration values reported for CAs of different microorganisms can be found in Appendix 6.3.

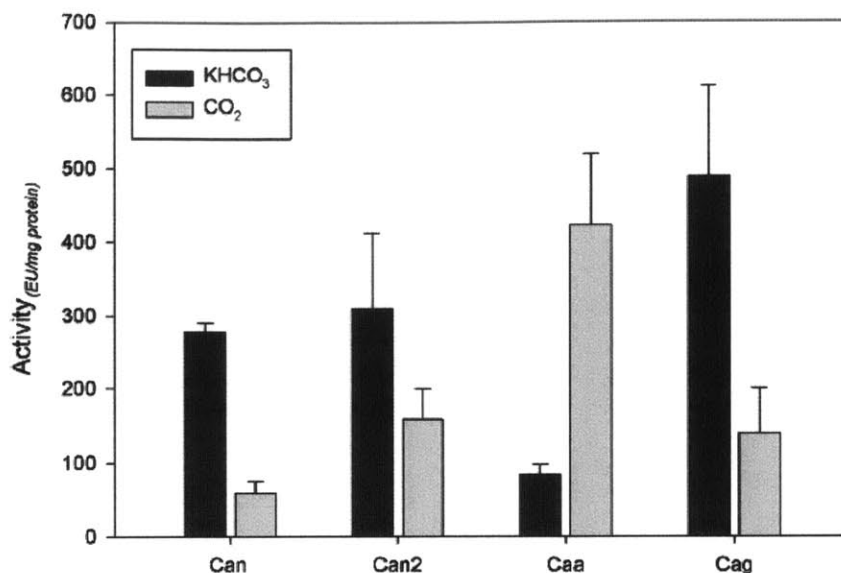


Figure 6.2: Specific activity of purified, His-tagged carbonic anhydrase enzymes. Substrates used for this assay were bicarbonate (50 mM, dark bars) and CO₂ (saturated solution, grey bars). Average values from three experiments were plotted with error bars representing the standard deviation.

Growth characterization of overexpression strains

The growth of CA overexpression strains H16/pCan, H16/pCan2, H16/pCaa and H16/pCag were tested in minimal medium with 2% (v v⁻¹) fructose in the presence of ambient CO₂ concentrations (air) and under autotrophic condition (H₂:CO₂:O₂). Under these conditions, all strains exhibited similar growth behavior (Figure 6.3A).

CA activity of cell extracts of *R. eutropha* strains grown on fructose was determined. As shown in Figure 6.3B, the CA-overexpression strains exhibited higher activity than the control using both substrates. Notably high CA activity was observed in H16/pCaa using CO₂ as a substrate. Using bicarbonate as a substrate, all the strains presented significantly higher activity than the control (P<0.01). However, each CA overexpression strain exhibited no significant difference in activity using bicarbonate as the substrate. These results indicate the preference for CO₂ as a substrate by Caa, which is in accordance with activity results using purified Caa (Figure 6.2). The PHB content of the CA overexpression and control strains was also assessed, and it was observed that all strains grown using fructose as the main carbon source produced similar intracellular amounts of PHB (data not shown).

Under autotrophic conditions, significant differences in growth were observed between the different strains. Growth of H16/pCaa was significantly lower than all the other strains (P<0.01). H16/pCag grew to a greater extent compared to the others (P<0.05), while H16/pCan and H16/pCan2 presented no significant growth difference compared to H16/pBBR1MCS-2. These strains were tested for PHB production after 48 h of autotrophic growth (Figure 6.3D). H16/pCaa produced the lowest amount of PHB per CDW compared to the other CA overexpression and control strains.

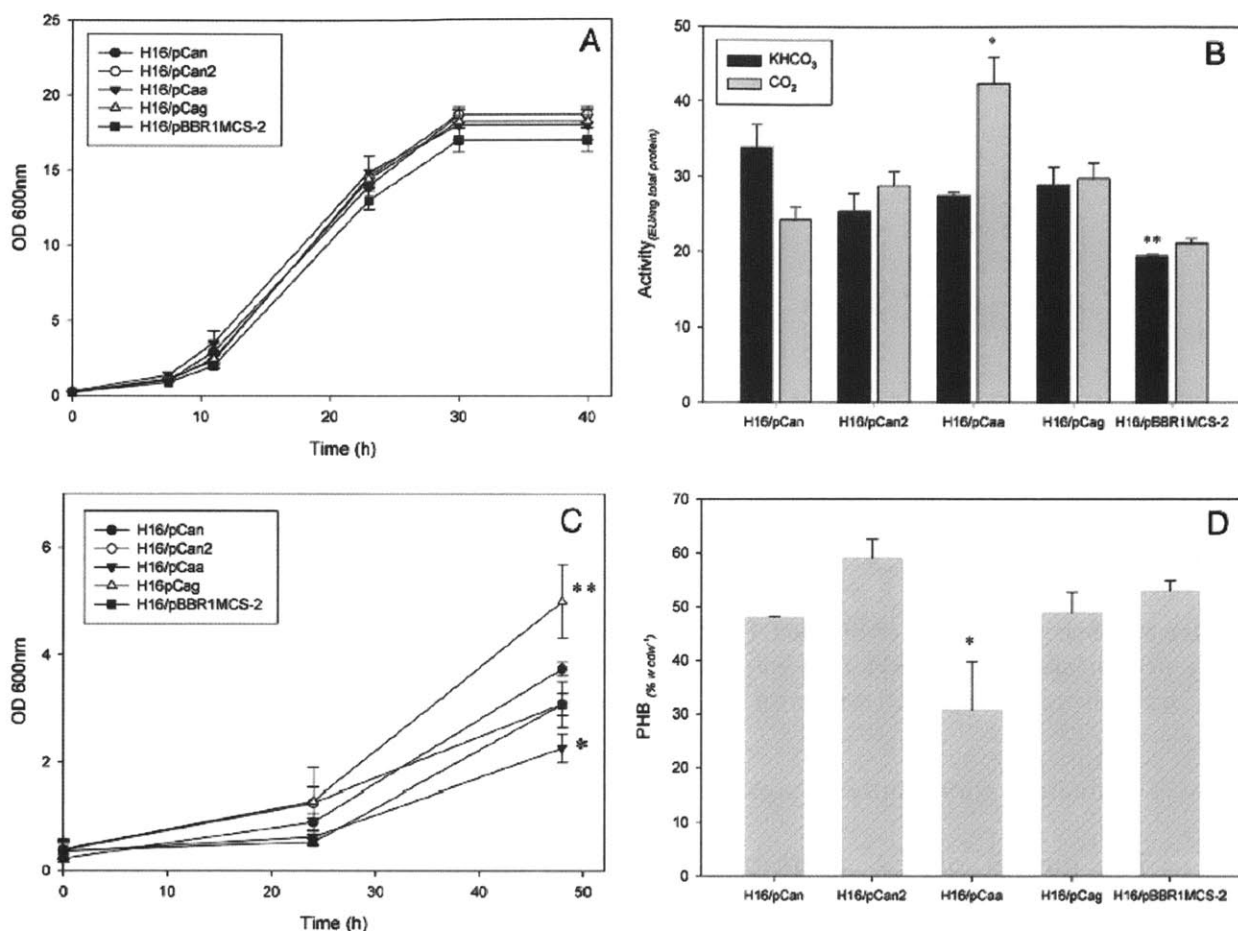


Figure 6.3: A) Growth of CA overexpression strains H16/pCan, H16/pCan2, H16/pCaa and H16/pCag, compared to the control strain (H16/pBBR1MCS-2) with 2% (w^{-1}) fructose as the main carbon source. B) Carbonic anhydrase activity of overexpression strains after 24 h of growth in minimal medium with 2% fructose. H16/pBBR1MCS-2 was used as a control. The Tukey's test was used as statistic test to compare all the strains (*) represents significant difference in activity using CO₂ as a substrate. (**) represents significant difference in activity using bicarbonate, $P < 0.01$. C) Growth of *R. eutropha* strains H16/pCan, H16/pCan2, H16/pCaa and H16/pCag and control strain H16/pBBR1MCS-2 under autotrophic conditions. (*) represents significant difference in final OD_{600nm} $P < 0.01$. (**) represents significant difference in final OD_{600nm}, $P < 0.05$. D) PHB production in 48 h by the overexpression and control strains and under autotrophic conditions. (*) represents significant difference in PHB production per % cell dry weight (CDW) ($w w^{-1}$), $P < 0.01$. Values represented were averages from three replicates with standard deviation represented by error bars.

Growth characteristics of the CA deletion strains

The deletion strains (Re2427, Re2428, Re2430 and Re2437) were cultivated in minimal medium supplemented with various carbon sources (fructose, formate, pyruvate, succinate, or lactate) in the presence of air or air supplemented with 10% CO₂. Strain Re2428 (H16 Δ caa) was unable to grow under all conditions tested, except in fructose with excess CO₂, where it grew slightly to a final OD_{600nm} of 0.2 (Figure 6.4F). The growth of strain Re2427 (H16 Δ can) was completely recovered with the addition of CO₂ to the fructose culture (Figure 6.4F), although this strain grew poorly under other nutrient-supplemented conditions (Figures 6.4A-E). Strain

Re2437 (H16 Δ can2) grew no differently than the wild type, except in the presence of fructose supplemented with CO₂, in which the growth output dropped by nearly 60%. Re2437 cells presented a different morphology under light microscopy without CO₂ supplement. These cells were longer than the wild type cells under such conditions (Appendix 6.4), which can be a sign of stress that was not detected during absorbance measurements and could be caused by a pH imbalance during growth. In the presence of increased CO₂ concentrations, increasing stress could be detected by an observed decrease in absorbance (Figure 6.4F). This suggests the importance of Can2 in maintaining the cellular pH, because the addition of CO₂ to the media decreases the pH in the media, affecting consequently the cytoplasmic pH. To test this theory, strain Re2437 was cultivated in media under different pH values (5.5, 7.0 and 8.5). The growth of Re2437 was less affected by this pH change as compared to wild type (Appendix 6.5). The growth of Re2430 (H16 Δ cag) was similar to wild type under all conditions tested.

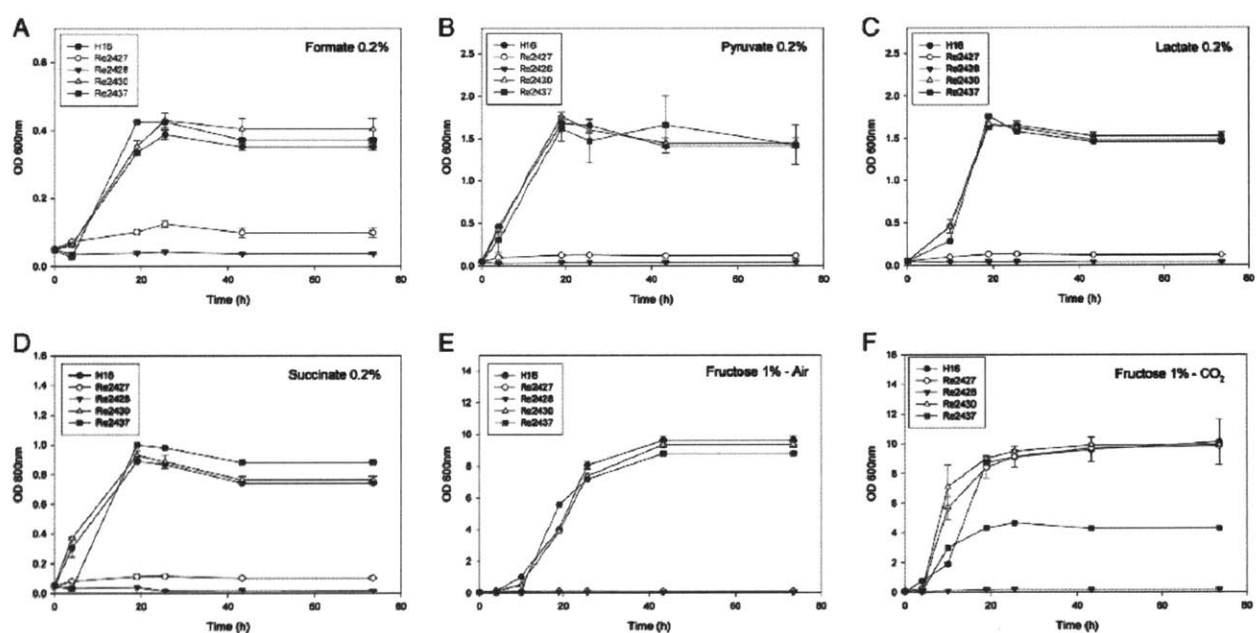


Figure 6.4: A) Growth of *R. eutropha* H16 (wild type - ●) and CA deletion strains Re2427 (H16 Δ can - ○), Re2428 (H16 Δ caa - ▼), Re2430 (H16 Δ cag - Δ) and Re2437 (H16 Δ can2 - ■) on different carbon sources: 0.2% (w vol⁻¹) formate (A), 0.2% (w vol⁻¹) pyruvate (B), 0.2% (w vol⁻¹) lactate (C) and 0.2% (w vol⁻¹) succinate (D), 1.0% (w vol⁻¹) fructose (E), and 1.0% (w vol⁻¹) fructose supplemented with 10% CO₂ (F). Values represented averages from three replicates with standard deviation as error bars.

Investigation of the phenotypic effects of individual CA enzymes

The quadruple mutant, Re2436 (H16 Δ can Δ can2 Δ caa Δ cag), had each of the four CA-encoding genes inserted in trans to create Re2436/pCan, Re2436/pCaa, Re2436/pCag, and Re2436/pCan2 (see Materials and Methods), in order to demonstrate the isolated effect of each CA on *R. eutropha* metabolism. As expected, none of the strains completely recovered the phenotype when growing on minimal media with fructose as a carbon source in air or CO₂-enriched environment (data not shown). In ambient air conditions, no significant difference was observed with growth of all four strains compared to wild type (data not shown). On the other

hand, with the addition of 10% CO₂, Re2436/pCan exhibited a higher growth rate when compared to Re2436 and the other strains (Figure 6.5).

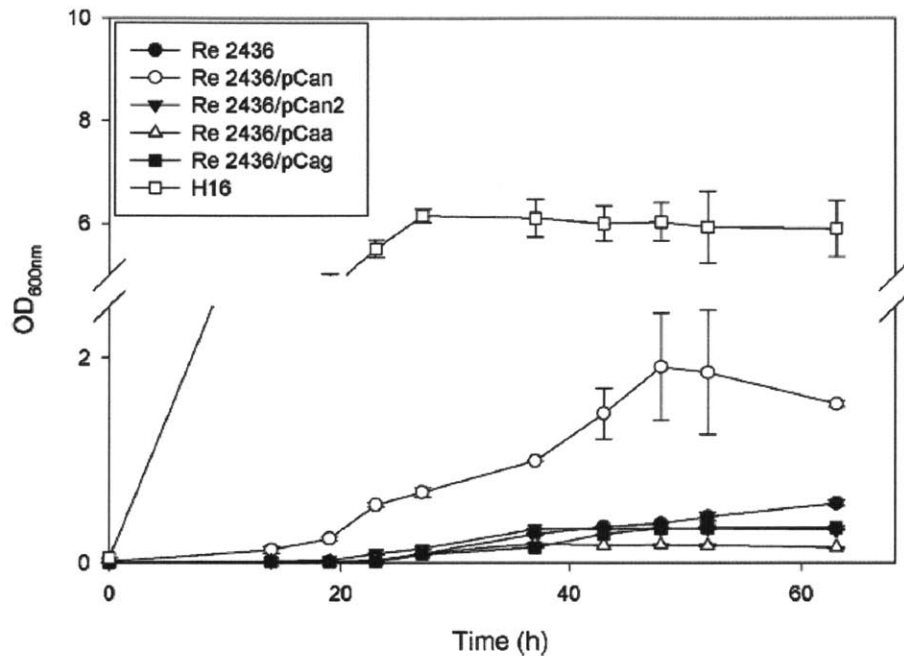


Figure 6.5: Cultures of *R. eutropha* H16 (□), *R. eutropha* CA quadruple deletion mutant Re2436 (H16 $\Delta can \Delta can2 \Delta caa \Delta cag$ - ●) and the complemented strains, Re2436/pCan (○), Re2436/pCan2 (▼), Re2436/Caa (△) and Re2436/pCag (■) in TSB media in the presence of 10% CO₂. Values represent average from three replicates with standard deviation as error bars.

The CA single deletion strains were transformed with the respective plasmid to complement the CA deletion to obtain Re2427/pCan, Re2428/pCaa, Re2430/pCag and Re2437/pCan2. When tested on minimal media with fructose 2% (v/v) the strains Re2427/pCan, Re2430/pCag and Re2437/pCan2 exhibited growth comparable to wild type (Appendix 6.6). The only exception was Re2428/pCaa, which was unable to grow to an extent comparable with the wild type under any condition tested and was therefore the subject of closer examination in this study.

A closer look at Caa

Examination of the α -periplasmic enzyme, Caa, yielded very interesting results during this study. Besides being the only α -carbonic anhydrase identified in the genome sequence of *R. eutropha* strain H16, it is described as a “putative periplasmic enzyme.” In this study, the purified Caa is the only *R. eutropha* CA capable of performing the interconversion of CO₂ and HCO₃⁻ with equilibrium lying towards the formation of HCO₃⁻ (Figure 6.2). The results of Caa overexpression in *R. eutropha* H16 grown in autotrophic culture indicated that the overexpression of Caa in the wild type strain had a negative influence on growth (Figure 6.3C) and PHB production (Figure 6.3D). Moreover, in any medium tested, the *caa* deletion strain, Re2428, was unable to recover growth to the wild type level (Figure 6.4).

In order to study the importance of Caa cellular localization on the phenotype recovery of Re2428, *caa* was cloned both as annotated and without the N-terminal signaling peptide, which hypothetically would prevent it from being targeted to the periplasm of *R. eutropha*. Purified, Strep2-tagged Caa enzyme without the signaling peptide (CaaB) exhibited similar activity values when compared to the purified, Strep-tagged Caa enzyme containing the signaling peptide. Purified Can was used as a control for CA activity assay (Figure 6.6A).

The *caa* and *caaB* genes were reintroduced in trans into Re2428 using plasmids pCaa and pCaaB (Table 6.2), in an attempt to recover *R. eutropha* growth in air and to determine the effect of Caa localization on cell growth. Wild type *R. eutropha*, Re2428, and complemented strains (Re2428/pCaa and Re2428/pCaaB) were cultivated in TSB and minimal media. The results presented in Figure 6.6B and 6.6C show that Re2428/pCaa and Re2428/CaaB grew poorly under the conditions tested when compared to the wild type strain. In TSB media, after 72 h of culture, the presence of Caa or CaaB in Re2428 resulted in OD_{600nm} of 2.96 ± 0.039 and 1.18 ± 0.009 respectively, both of which were much lower than growth of the wild type ($OD_{600nm} = 4.95 \pm 0.35$). In complementation strains, the localization of Caa in the cell during growth on TSB media did not present a significant difference (Figure 6.6B). In minimal media, however, a partial recovery of growth was observed only for Re2428/Caa (Figure 6.6C). These results indicate that overexpression of *caa* in Re2428 was incapable of recovering growth to wild type rates in either rich or minimal medium, even though CA activity was detected in cell extracts of Re2428/pCaa and Re2424/pCaaB (data not shown). The periplasmic localization of Caa, under the conditions tested, was only observed to affect growth of the cells to a significant extent when cultivated in minimal media.

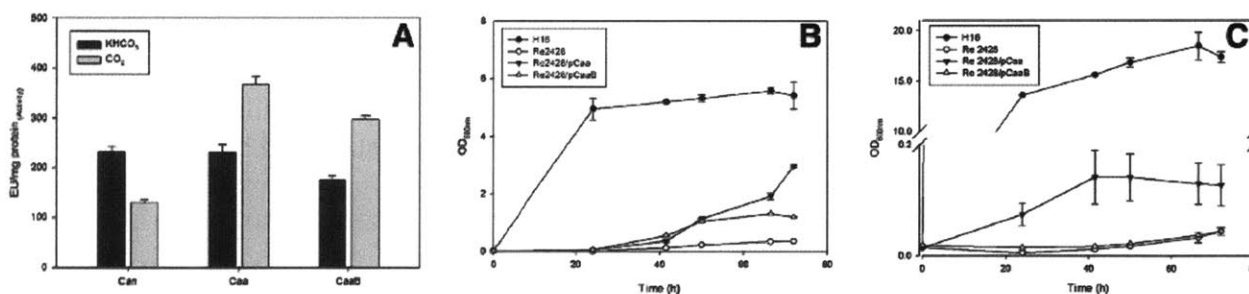


Figure 6.6: A) Specific activity of purified Strep2-tagged CA enzymes. Substrates used for this assay were bicarbonate (50 mM, dark bars) and CO₂ (saturated solution, grey bars). Average values from three experiments were plotted with error bars representing the standard deviation. B) Cultures of *R. eutropha* wild type (H16 - ●), Re2428 (○), Re2428/pCaa (▼), and Re2428pCaaB (△) in TSB media. C) Growth in minimal media with 2% fructose (w v⁻¹). Values represent average from three replicates with standard deviation as error bars.

In order to provide evidence for the periplasmic localization of Caa in *R. eutropha*, RFP was fused to the C-terminus of Caa to allow visualization of the localization in the cell. RFP-tagged Caa and RFP alone (control) were expressed separately in the *R. eutropha* strain Re2061, which is unable to produce intracellular polyhydroxyalkanoate that may disturb the imaging. As shown in Appendix 6.7, the fluorescence was concentrated near the outer perimeter of the cells with RFP-tagged Caa, as opposed to the RFP-only control, where fluorescence was diffused throughout the cytosol. This suggests that Caa enzymes are located near the outer perimeter of the cell, likely the periplasm.

DISCUSSION

In this study, four putative CAs were evaluated from *R. eutropha*. The *can* and *can2* genes encode β -CA enzymes, the *caa* gene encodes a putative periplasmic α -CA, and the *cag* gene encodes a γ -like-CA/acetyltransferase. The ability for all four CA enzymes to catalyze the interconversion of CO₂ and bicarbonate, as purified enzymes and also when overexpressed in *R. eutropha* were demonstrated. CO₂ metabolism in *R. eutropha* is very complex. It has evolutionary importance for the bacteria to retain four separate CA genes, which apparently present similar activities in the cell, but have unique roles within the machinery for controlling its CO₂ metabolism. In short, the presence of one enzyme does not exclude the importance of the others.

Previous microarray data produced in our laboratory demonstrated different expression behavior of the four CA genes when *R. eutropha* was growing on fructose or trioleate in the presence of high or low concentrations of nitrogen (Brigham et al. 2012a). The *can* gene exhibited an expression decrease of 1.7 fold ($p = 0.0048$) when cells entered into nitrogen depletion, *i.e.* the PHB production stage. On the other hand, *cag* exhibited an increase in expression of 3.5 fold ($p = 0.011$) during the same growth condition. When changing the carbon sources from trioleate to fructose, *caa* exhibited an expression decrease of 3.0 fold ($p = 0.001$). All of these previous observations support the idea that the four enzymes are not responsible for the same reactions in the cell. Kusian et al. (2002); however proposed that, out of the four CA enzymes described in *R. eutropha*, only *can* plays an important role on CO₂ metabolism. Supporting our findings of independent roles of CAs in *R. eutropha*, Smith et al. (1999), Merlin et al. (2003), and Kupriyanova et al. (2007) also reported and discussed the separate roles of different CAs expressed in the same organism. Dobrinski et al. (2010) described four different CAs expressed at different levels depending on the physiological state of the microorganism in *T. crunogena*. Among other results, the observed differences in expression levels indicate a specific role of each CA enzyme in carbon fixation, pH homeostasis or other physiological activities not yet elucidated (Dobrinsky et al. 2010).

Overexpression of the CA enzymes separately in the wild type strain resulted in no observable difference in growth (Figure 6.3A) or PHB production (data not shown), but higher CA activities were detected in the cell extracts when compared to the wild type harboring the empty vector (Figure 6.3B). Examination of the purified CA enzymes (Figure 6.2), and CA overexpression strains (Figure 6.3), showed that Caa exhibited greater activity using CO₂ as a carbon source. Under autotrophic growth conditions, when CO₂ is used as the sole carbon source, the growth and PHB accumulation of the CA overexpression strains presented significant differences when compared to each other and to the wild type strain (Figures 6.3C and 6.3D). One reason for the low growth and PHB production of the overexpression strains could be due to the altered regulation of gene expression.

The phenotype recovery effect of the overexpression of Caa in Re2428 (H16 Δ *caa*) is more distinct when cells are grown in minimal media (Figure 6.6C), because in this environment, bicarbonate is required to synthesize essential amino acids and nucleotides, which are not supplied in the media (Merlin et al. 2003).

Several essential metabolic pathways require either CO₂ or bicarbonate as a substrate. Bicarbonate is the substrate of several important enzymes of central metabolism, such as phosphoenolpyruvate carboxylase, pyruvate carboxylase, acetyl-CoA carboxylase and methylcrotonyl CA, among others (Smith and Ferry 2000). Calculated by Merlin et al. (2003),

the spontaneous diffusion of CO₂ in air and conversion to bicarbonate inside the cell are not sufficient for the metabolic needs of a bacterial cell. In *R. eutropha* metabolism, bicarbonate is required for the elimination of a long lag phase during autotrophic growth (Repaske et al. 1971), which is considered to be a negative feature for the use of this microorganism at industrial scale. CAII, a human α -CA, is known to play an important role in the transportation of CO₂ and supplying bicarbonate to mammalian cells (Sterling et al. 2001) and in *T. crunogena*. Dobrinsky et al. (2010) also propose that an α -CA would be converting CO₂ to bicarbonate in the cells. In *R. eutropha*, Caa could be responsible for this same mechanism, since the equilibrium of Caa-catalyzed reaction lies towards the hydration of CO₂ to bicarbonate (Figure 6.2). Can, alternatively, could be responsible for the supplementation of CO₂. These hypotheses were supported by the deletion of *caa* or *can* from the genome of *R. eutropha*. The lack of *can* resulted in a phenotype in which cells were dependent on external CO₂ supplementation in order to grow (Kusian et al. 2002). Without *caa* (i.e., strain Re2428), *R. eutropha* presented a similar phenotype as the *can* deletion strain, but the activities and substrate specificities of these two CA enzymes are remarkably different. Moreover, the growth phenotype of a *caa* deletion could not be compensated by the addition of CO₂ to the culture. These differences imply disparate physiological roles of both of these CA enzymes in the growth and maintenance of *R. eutropha*.

Additionally, both Caa and Can could not replace the roles of one another in *R. eutropha*, because a single deletion of either *can* or *caa* resulted in no growth under ambient CO₂ conditions (Kusian et al. 2002 and this study). Although *in vitro* activity suggested that the enzymes could have complementary activities (Figure 6.2). Overall, Caa is unable to act as a replacement for Can, and vice versa. This conclusion is supported by the physical separation of both CAs in the cell, in which Caa is located in the periplasm and Can is believed to be in the cytosol. The attempt to recover fully the phenotype of Re2428 by overexpressing a plasmid-borne *caa* gene was unsuccessful, as the overall growth yields of the complementary strains Re2428/pCaa and Re2428/pCaaB were much lower than that of the wild type, even when both versions of the enzyme, after purification, exhibited high activity (Figure 6.6A). This could be the result of an expression level imbalance of the plasmid-borne *caa* compared to that of wild type. Interestingly, the strain Re2428/pCaaB was unable to grow at the same rate as Re2428/pCaa in minimal media (Figure 6.6C), although both complemented strains grew similarly in TSB medium (Figure 6.6B). The growth difference could be a result of the differential localization of the two versions of Caa in the cell. The lack of a signaling peptide may have prevented the periplasmic positioning of Caa in the cell, and thus resulted in a lower bacterial growth. This effect can be more clearly observed in minimal media (Figure 6.6C). The results suggest that Caa is a periplasmic CA and its correct location in the cell is essential for the growth of *R. eutropha*. Overall, reintroduction of *caa* or *caaB* in Re2428 was able to recover only partial growth.

The isolated effect of the CAs in the genome could be observed after complementing the quadruple mutant, Re2436 (H16 Δ *can* Δ *caa* Δ *can2* Δ *cag*), with each separate enzyme expressed from a plasmid (Figure 6.5). In a background with no CA enzymes expressed, none of the individual CAs expressed *in trans* could fully recover the growth phenotype under all conditions tested. However, strain Re2436/pCan, expressing the Can enzyme, when grown in minimal media with fructose as the main carbon source could partially recover the growth phenotype (Figure 6.5B). This reinforces the importance of having all four CAs in a complex system in order for carbon metabolism and growth of the cells to function properly.

The localization of Caa in the periplasm of the cell is crucial for the conversion of CO₂, which is passively diffused through the membrane, to dissolved inorganic carbon (bicarbonate). The conversion of CO₂ to bicarbonate is important for the transportation of CO₂ into the cell, as CO₂ is extremely insoluble in aqueous solution and frequently diffuses in and out of the cell. Bicarbonate, on the other hand is negatively charged and highly soluble in aqueous solution, but poorly soluble in lipids. Transport of bicarbonate across the cell membrane must be assisted by CA (Smith and Ferry 2000; Marcus et al. 2005). Figure 6.7 depicts a diagram representing the role of CAs in *R. eutropha* cells. Can is likely the enzyme responsible for supporting CO₂ fixation reaction by providing CO₂ to RuBisCO in the cytosol. Cag can potentially carry out the same reaction, but its role is elusive and thus merits further investigation. Caa is responsible for sequestering the CO₂ diffused into the cell and converting it to bicarbonate for cellular metabolism, while Can2 has a possible role in pH homeostasis. The current study provides a springboard for understanding the differential roles of each CA enzyme in the physiology and CO₂ homeostasis of *R. eutropha*. The exact interplay of each of these enzymes in the cell still continues to be an active area of study.

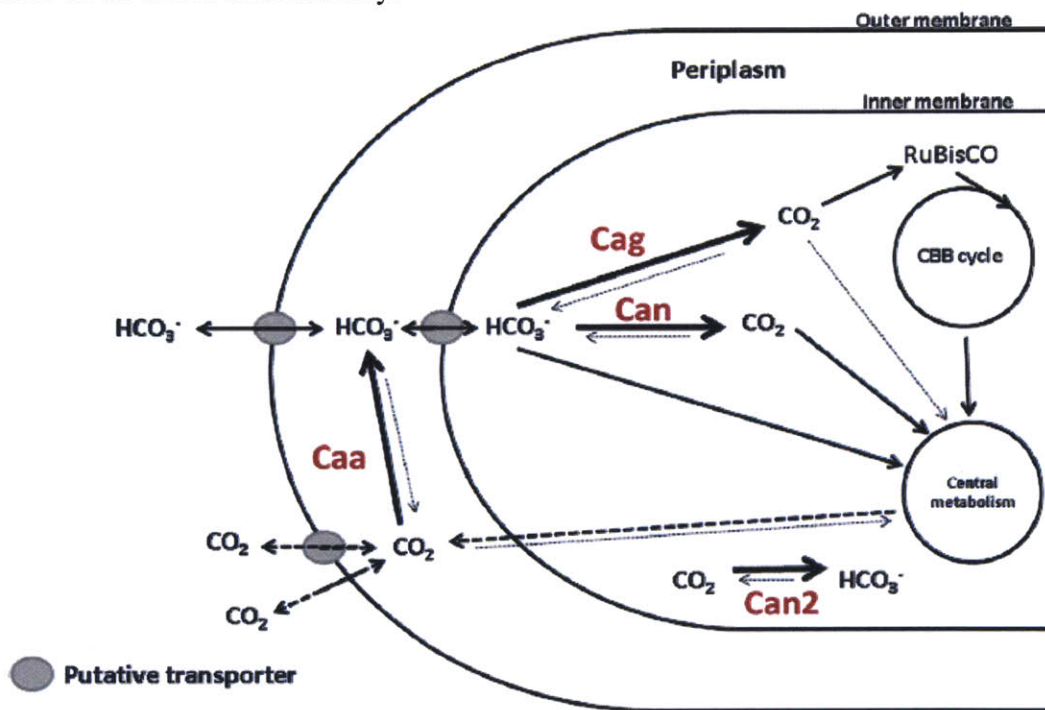


Figure 6.7: Schematic depiction of the role of CAs in *R. eutropha* metabolism. Based on experiments performed in this study, the role of Caa in *R. eutropha* is to convert the diffused CO₂ inside the periplasm into bicarbonate to supply cellular metabolism. Can, and the less well understood Cag, would also be responsible for the supplementation of CO₂ to RuBisCO. Can2, could play a role on the pH maintenance in the cell (see Supplementary Figure 3). CBB cycle = Calvin-Benson-Bassham Cycle; RuBisCO = Ribulose-1,5-bisphosphate carboxylase oxygenase.

REFERENCES

- Amoroso G, Morell-Avrahov L, Müller D, Klug K, Sültemeyer D (2005) The gene NCE103 (YNL036w) from *Saccharomyces cerevisiae* encodes a functional carbonic anhydrase and its transcription is regulated by the concentration of inorganic carbon in the medium. *Molec Microbiol* 56: 549–558
- Badger and Price (2003) CO₂ concentrating mechanisms in cyanobacteria: molecular components, their diversity and evolution. *J Exp Botany* 54:609–622
- Bertani G (1951) Studies on lysogenesis. I. The mode of phage liberation by lysogenic *Escherichia coli*. *J Bacteriol* 62: 293–300
- Bonacci W, Teng PK, Afonso B, Niederholtmeyer H, Grob P, Silver PA, Savage DF (2012) Modularity of a carbon-fixing protein organelle. *PNAS* 109: 478–483
- Bradford MM (1976) Rapid and sensitive method for the quantitation of microgram quantities of protein utilizing the principle of protein-dye binding. *Anal Biochem* 72: 248–254
- Brigham CJ, Speth DR, Rha C, Sinskey, AJ (2012a) Whole-genome microarray and gene deletion studies reveal regulation of the polyhydroxyalkanoate production cycle by the stringent response in *Ralstonia eutropha* H16. *Appl Environ Microb* 78: 8033–8044
- Brigham CJ, Zhila N, Shishatskay E, Volova TG, Sinskey, AJ (2012b). Manipulation of *Ralstonia eutropha* carbon storage pathways to produce useful bio-based products. *In: Reprogramming microbial metabolic pathways* X. Wang et al. (eds.) Springer Science+Business Media Dordrecht. *Subcellular Biochemistry* 64, DOI 10.1007/978-94-007-5055-5_17
- Budde CF, Riedel SL, Hübner F, Risch S, Popović MK, Rha C, Sinskey AJ (2011) Growth and polyhydroxybutyrate production by *Ralstonia eutropha* in emulsified plant oil medium. *Appl Microbiol Biot* 89: 1611–1619
- Chirica LC, Elleby B, Jonsson BH, Lindskog S (1997) The complete sequence, expression in *Escherichia coli*, purification and some properties of carbonic anhydrase from *Neisseria gonorrhoeae*. *Eur J Biochem* 244: 755–760
- Codd GA and Kuenen JG (1987) Physiology and biochemistry of autotrophic bacteria. *Antonie Van Leeuwenhoek* 53: 3–14
- Dobrinski KP, Boller AJ, Scott KM (2010) Expression and function of four carbonic anhydrase homologous in the deep-sea chemolithoautotroph *Thiomicrospira crunogena*. *Appl Environ Microb* 76: 3561–3567
- Fasseas MK, Tsikou D, Flemetakis E, Katinakis P (2011) Molecular and biochemical analysis of the a class carbonic anhydrases in *Caenorhabditis elegans*. *Mol Biol Rep* 38: 1777–1785
- Gibson DG, Young L, Chuang RY, Venter JC, Hutchison CA 3rd, Smith HO (2009) Enzymatic assembly of DNA molecules up to several hundred kilobases. *Nat Methods* 6: 343–345
- Kovach ME, Elzer PH, Hill DS, Robertson GT, Farris MA, Roop RM 2nd, Peterson KM (1995) Four new derivatives of the broad-host-range cloning vector pBBR1MCS, carrying different antibiotic-resistance cassettes. *Gene* 166: 175–176

Kupriyanova E, Villarejo A, Markelova A, Gerasimenko L, Zavarzin G, Samuelsson G, Los DA, Pronina N (2007) Extracellular carbonic anhydrases of the stromatolite-forming cyanobacterium *Microcoleus chthonoplastes*. *Microbiol* 153: 1149–1156

Kupriyanova EV, Sinetova MA, Markelova AG, Allakhverdiev SI, Los DA, Pronina NA (2011) Extracellular β -class carbonic anhydrase of the alkaliphilic cyanobacterium *Microcoleus chthonoplastes*. *J Photochem Photobiol B* 103: 78–86

Kusian B and Bowien B (1997) Organization and regulation of *cbb* CO₂ assimilation genes in autotrophic bacteria. *FEMS Microbiol Rev* 21: 135–155

Kusian B, Sültemeyer D, Bowien B (2002) Carbonic anhydrase is essential for growth of *Ralstonia eutropha* at ambient CO₂ concentrations. *J Bacteriol* 184: 5018–26

Li H, Opgenorth PH, Wernick DG, Rogers S, Wu TY, Higashide W, Malati P, Huo YX, Cho KM, Liao JC (2012) Integrated electromicrobial conversion of CO₂ to higher alcohols. *Science* 335: 1596

Lionetto MG, Caricato R, Giordano ME, Erroi E, Schettino T (2012) Carbonic Anhydrase and Heavy Metals, *Biochemistry*, Prof. Deniz Ekinci (Ed.), ISBN: 978-953-51-0076-8, InTech.<http://www.intechopen.com/books/biochemistry/carbonic-anhydrase-and-heavy-metals>

Lu J, Brigham CJ, Gai CS, Sinskey AJ (2012) Studies on the production of branched-chain alcohols in engineered *Ralstonia eutropha*. *Appl Microbiol Biotechnol* 96: 283–297

Luca VD, Vullo D, Scozzafava A, Carginale V, Rossi M, Supuran CT, Capasso C. (2013) An α -carbonic anhydrase from the thermophilic bacterium *Sulphurihydrogenibium azorense* is the fastest enzyme known for the CO₂ hydration reaction. *Bioorg Med Chem*. 21: 1465–1469

Marcus EA, Moshfegh AP, Sachs G, Scott DR (2005) The periplasmic α -carbonic anhydrase activity of *Helicobacter pylori* is essential for acid acclimation. *J Bacteriol* 187: 729–738

Merlin C, Masters M, McAteer S, Coulson A (2003) Why is carbonic anhydrase essential to *Escherichia coli*? *J Bacteriol* 185: 6415–6424

Mogensen EG, Janbon G, Chaloupka J, Steegborn C, Fu MS, Moyrand F, Klengel T, Pearson DS, Geeves MA, Buck J, Levin LR, Mühlischlegel FA (2006) *Cryptococcus neoformans* senses CO₂ through the carbonic anhydrase Can2 and the adenylyl cyclase Cac1. *Eukariotic Cell* 5: 103–111. Novy R, Drott D, Yaeger K, Mierendorf R (2001) Overcoming the codon bias of *E. coli* for enhanced protein expression. *iNovations* 12: 1–3

Petersen TN, Brunak S, von Heijne G, Nielsen H (2011) SignalP 4.0: discriminating signal peptides from transmembrane regions. *Nat Methods*, 8: 785–786

Pohlmann A, Fricke WF, Reinecke F, Kusian B, Liesegang H, Cramm R, Eitinger T, Ewering C, Pötter M, Schwartz E, Strittmatter A, Voß I, Gottschalk G, Steinbüchel A, Friedrich B, Bowien B (2006) Genome sequence of the bioplastic-producing "Knallgas" bacterium *Ralstonia eutropha* H16. *Nat Biotechnol* 24: 1257–1262

Repaske R, Ambrose CA, Repaske AC, De Lacy ML (1971) Bicarbonate requirement for elimination of the lag period of *Hydrogenomonas eutropha*. *J Bacteriol*. 107: 712–717

Sambrook J and Russell DW (2001) *Molecular cloning: a laboratory manual*, 3rd edn. Cold Spring Harbor Laboratory Press, Cold Spring

Simon R, Priefer U, Pühler A (1983) A broad host range mobilization system for *in vivo* genetic engineering: transposon mutagenesis in gram-negative bacteria. *Nat Biotechnol* 1: 784–791

Slater S, Houmiel KL, Tran M, Mitsky TA, Taylor NB, Padgett SR, Gruys KJ (1998) Multiple β -ketothiolases mediate poly(β -hydroxyalkanoate) copolymer synthesis in *Ralstonia eutropha*. *J Bacteriol* 180: 1979–1987

Smith KS and Ferry JG (2000) Prokaryotic carbonic anhydrases. *FEMS Microbiol Rev* 24: 335–266

Smith KS, Jakubzick C, Whittam TS, Ferry JG (1999) Carbonic anhydrase is an ancient enzyme widespread in prokaryotes. *PNAS* 96: 15184–15189

Sterling D, Reithmeier RA, Casey JR (2001) Carbonic anhydrase: in the driver's seat for bicarbonate transport. *JOP* 4: 165–170

Sültemeyer D (1998) Carbonic anhydrase in eukaryotic algae: characterization, regulation, and possible function during photosynthesis. *Can J Bot* 76: 962–972

Sültemeyer DF, Fock HP, Calvin DT (1990) Mass spectrometric measurement of intracellular carbonic anhydrase activity in high and low C_i cells of *Chlamydomonas*. *Plant Physiol* 89: 1313–1219

Sundaram V, Rumbolo P, Grubb J, Strisciuglio P, Sly WS (1986) Carbonic anhydrase II deficiency: diagnosis and carrier detection using differential enzyme inhibition and inactivation. *Am J Hum Genet* 38: 125–136

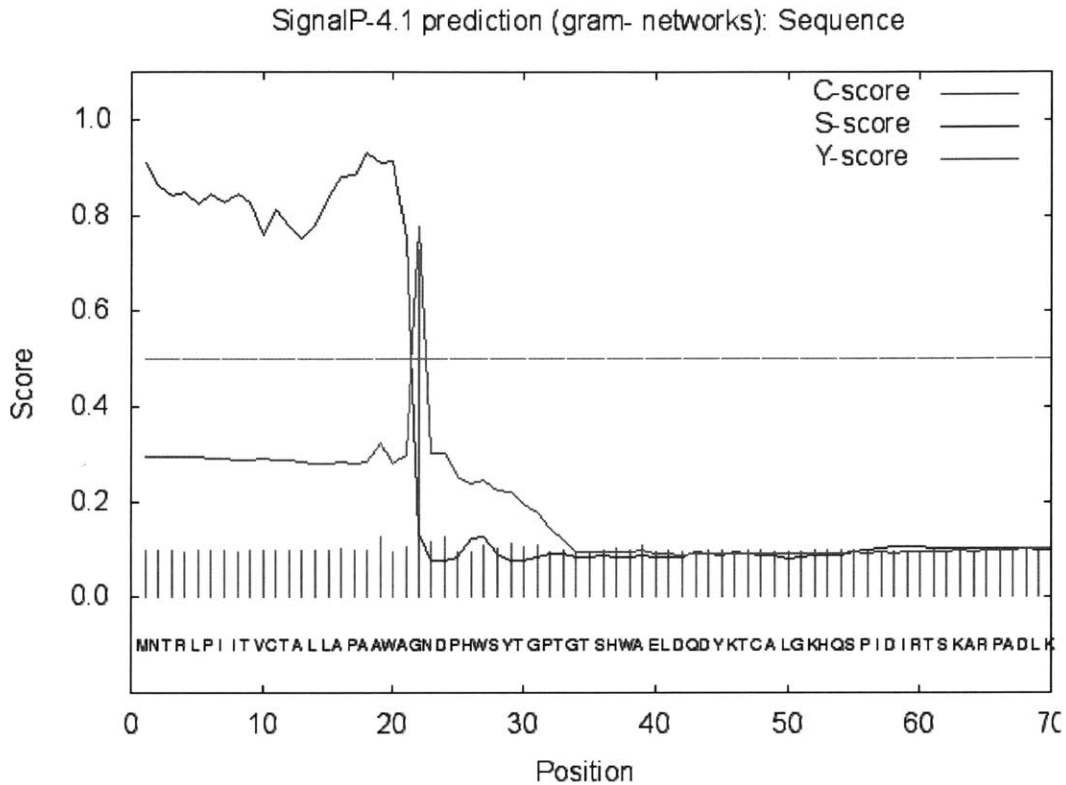
Supuran CT (2004) Carbonic Anhydrases: catalytic and inhibition mechanisms, distribution and physiological roles. In: *carbonic anhydrase: its inhibitors and activators*. Ed: Supuran CT, Scozzafava A, Conway J. CRC press

Tripp BC, Smith K, Ferry JG (2001) Carbonic anhydrase: new insights for an ancient enzyme. *J Biol Chem* 28: 48615–48618

Wilbur KM, Anderson, NG (1948) Electrometric and colorimetric determination of carbonic anhydrase. *J Biol Chem* 176: 147–154

APPENDIX

Appendix 6.1: Signal peptide prediction on Caa.



# Measure	Position	Value	Cutoff	signal peptide?
max. C	22	0.727		
max. Y	22	0.778		
max. S	18	0.932		
mean S	1-21	0.839		
D	1-21	0.807	0.570	YES

Appendix 6.2: List of primers used in this study.

Primer	Sequence
Can_Del 1	ATTGGATCCC <u>ACTGACGAGCAGGTCGAGCAC</u>
Can_Del 2	TGGGCGATGGCGTCAGTCATGCGACCCTCCTTGCAGGACC
Can_Del 3	ATGACTGACGCCATCGCCCACCGGACGCACACACCGCTTCTTC
Can_Del 4	ATTGGATCCC <u>CGTCTTCCAGGCCGTCCAGCATC</u>
Caa_Del 1	GATGGATCCC <u>GCTTGAAGTGCAGTACTGGTGC</u>
Caa_Del 2	ATCGGCAGCCTGGTGTTCATTGTTCGATGCGTCCTAGTGTT
Caa_Del 3	ATGAACACCAGGCTGCCGATAGGACGGCGCCCGATAGAAGTAC C
Caa_Del 4	GGATCCCTGGCAGCGGTGAAGCTGGTGG
Can2_Gibs Del 1	TACGAATTCGAGCTCGGTACCCGGGGATCCGCTTTCGCGACGGC GAATGGGTC
Can2_Del 2	AGTTGTTCGATGTGATGCATGGCGGCATCCAGGCGCTAC

Can2_Del 3	ATGCATCACATCGAACAACTCCCCATGCATCCCTTCATCCTTGG
Can2_Gibs Del 4	AAGCTTGCATGCCTGCAGGTCGACTCTAGACCTCGTCCTTCATG GCGAGGATG
Cag_Del 1	ATTGAGCTCCAGTGCCAGGTTGATGGCATTGAAC
Cag_Del 2	CCGAGCTGGTAAAGCGCCATGGGGTCTCCTGCACGAAAGG
Cag_Del 3	ATGGCGCTTTACCAGCTCGGCGACCGCGGGCGCACTTACC
Cag_Del 4	ATTTCTAGAATCGAGCCCAGCGGGCCATG
Fw can	GATAGGTACCCATATGATGACTGACGCCATCGCCCAGC
Rv can	CGATAAGCTTGGATCCTCAGCGGATCGACGC
Fw can2	GATAGTCGACCATATGATGCATCACATCGAACAACTGC
Rv can2	CGATAAGCTTGGATCCTCAGGGTTCGCAG
Fw caa	GATAGGTACCCATATGATGAACACCAGGCTGCCG
Rv caa	CGATAAGCTTGGATCCCTAGTGGCTGACCTGC
Fw cag	GATAGGTACCCATATGATGGCGCTTTACCAGCTCGGGC
Rv cag	CGATAAGCTTCTCGAGTCAGCCGATCCGCTTGAG
Fw caaB	GATAGGTACCCATATGATGGACCCGCACTGGAGCTACA
Linker Fw	GTGCAGGTCAGCCACTATCCCGCCACCTCCACCTCCATGGCGAG TAGCGAAG
Linker Rv	CTTCGCTACTCGCCATGGAGGTGGAGGTGGCGGGATAGTGGCT GACCTGCAC
Rv RFP	CTGCGTCGACTTAAGCACCGGTGGAGTG

^a Restriction sites are underlined

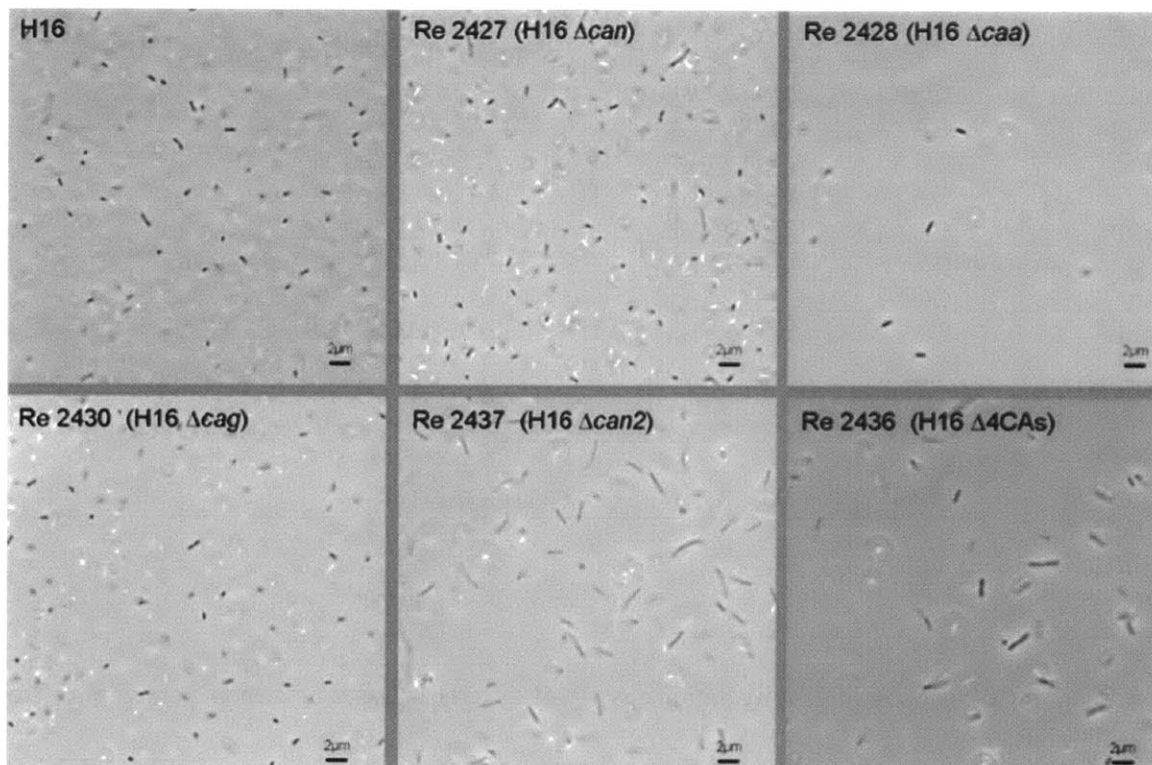
Appendix 6.3: Comparison of CO₂ hydration activity of different classes of carbonic anhydrases from bacteria and fungi.

Class	Organism	Max SA (CO ₂ hydration)	Method used	Reference
β-CA	<i>R. eutropha</i>	~20 UCA/mg protein*	Mass spectrometric method ¹	Kusian et al. 2002
α-CA	<i>Thiomicrospira crunogena</i>	890 ± 17 WAU/mg protein	pH monitored electrometrically ²	Dobrinski et al. 2010
β-CA	<i>T. crunogena</i>	3.41 ± 0.08 WAU/mg protein	pH monitored electrometrically ²	Dobrinski et al. 2010
β like CA	<i>T. crunogena</i>	1.24 ± 0.02 WAU/mg protein	pH monitored electrometrically ²	Dobrinski et al. 2010
α-CA	<i>Microcoleus chthonoplastes</i>	0.238 ± 0.01 WAU/mg protein	pH monitored electrometrically ²	Kupriyanova et al. 2007
β-CA	<i>M. chthonoplastes</i>	~100 WAU/mg protein*	pH monitored electrometrically ²	Kupriyanova et al. 2011
α-CA	<i>Sulphurhydrogenibium azorense</i>	~20000 U/mg protein (80°C)* ~2500 U/mg protein (20°C)*	pH monitored using pH-indicator metacresol purple ³	Luca et al. 2013
γ-CA	<i>Vibrio fischeri</i>	1.5 ± 0.3 U/mg protein	pH monitored ⁴	Smith et al. 1999
β-CA	<i>Staphylococcus aureus</i>	1.2 ± 0.1 U/mg protein	pH monitored ⁴	Smith et al. 1999
CA	<i>Bacillus subtilis</i>	<0.01 U/mg protein	pH monitored ⁴	Smith et al. 1999
γ-CA	<i>Methanoseta concilii</i>	3.0 ± 0.4 U/mg protein	pH monitored ⁴	Smith et al. 1999
β like -CA	<i>Saccharomyces cerevisiae</i>	~6900 U/mg protein	Mass spectrometric method ¹	Amoroso et al. 2005
α-CA	<i>Cryptococcus neoformans</i>	~20 WAU*	pH monitored electrometrically ²	Mogensen et al. 2006
α-CA	<i>R. eutropha</i>	422.32 ± 97.05 EU/mg protein (0°C)	pH monitored using pH standard phenol red ⁵	This study
β-CA	<i>R. eutropha</i>	59.5 ± 15.35 EU/mg protein (0°C)	pH monitored using pH standard phenol red ⁵	This study
β-CA	<i>R. eutropha</i>	157.94 ± 41.16 EU/mg protein (0°C)	pH monitored using pH standard phenol red ⁵	This study
γ-CA	<i>R. eutropha</i>	138.19 ± 61.27 EU/mg protein (0°C)	pH monitored using pH standard phenol red ⁵	This study

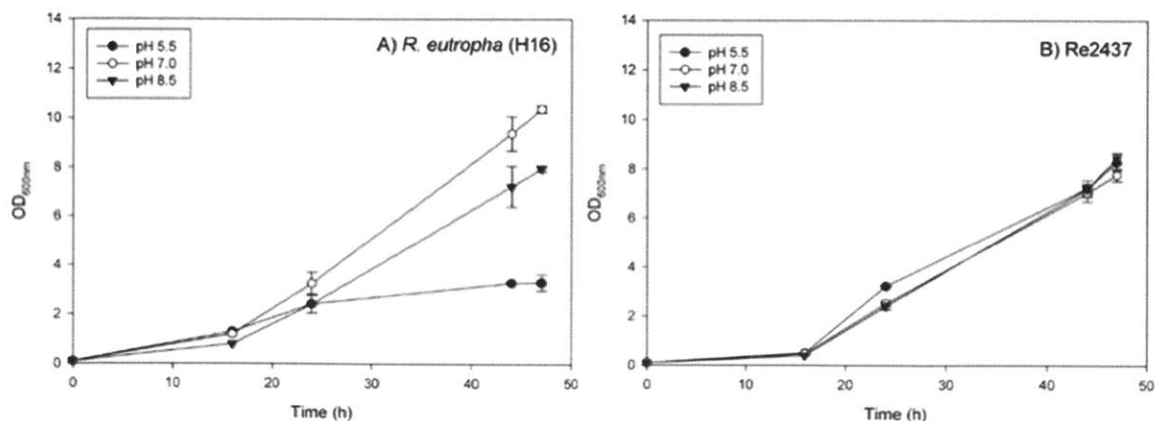
*- Data extracted from a graph.

1. Mass spectrometric method based on loss of ¹⁸O from doubly labeled ¹³C¹⁸O to water. 2. pH monitored from 8.0 to 7.0 electrometrically. Reaction kept at 4°C. 3. pH monitored using pH-indicator Taps/NaOH/metacresol purple monitored at 578 nm. Reaction kept at 25°C. 4. pH monitored from 7.8 to 7.0. Reaction kept at 23°C or 55°C. 5. pH monitored using pH standard phenol red. Reaction kept at 0°C.

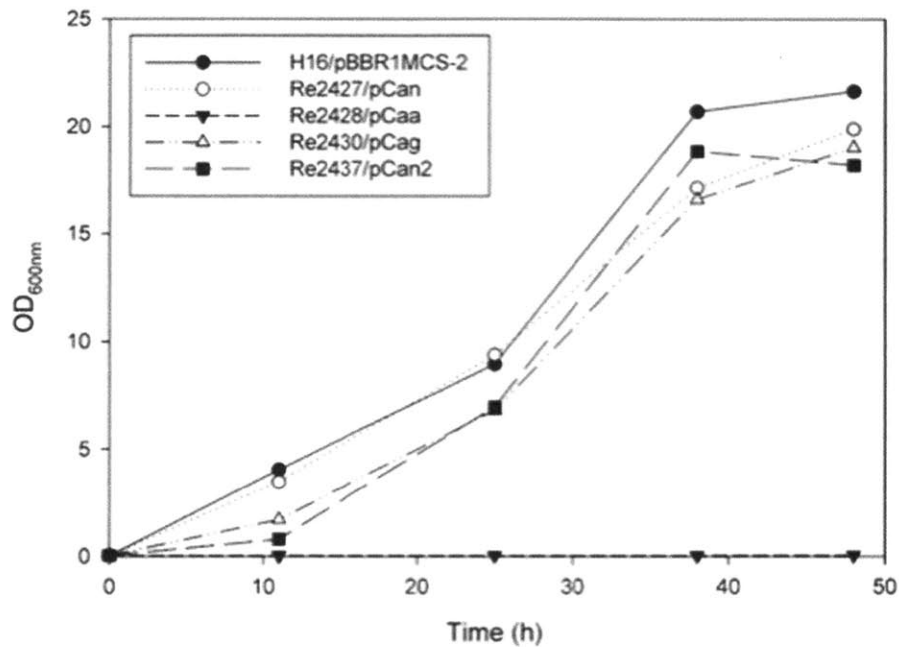
Appendix 6.4: Light microscopy images of all CA gene deletion strains and the wild type strain, *R. eutropha* H16 (100X magnification). Scale bar = 2 μ m. Strains were grown in TSB media and observed after 24 h of cultivation. Re2427 and Re2436 were cultivated under 10% CO₂ supplemented environment. Re2437 cells exhibit a longer cell morphology, which could be a sign of stress that can be seen in the microscope but unnoticed in the absorbance measurements of the cultures.



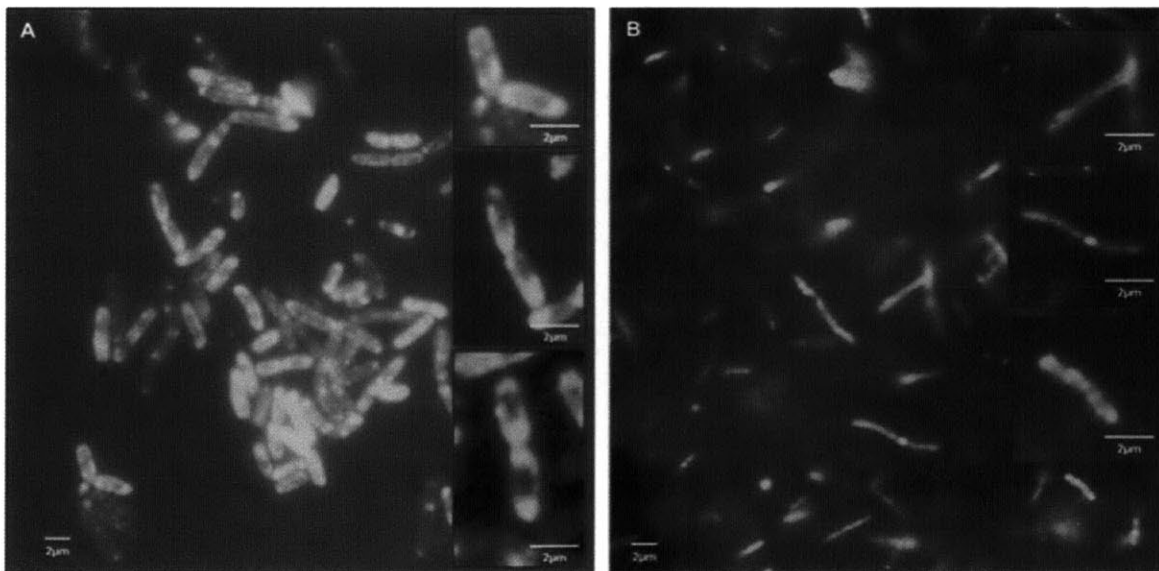
Appendix 6.5: Growth in minimal media containing 1% fructose ($w v^{-1}$) of A) *R. eutropha* (H16) and B) Re2437 (H16 $\Delta can2$) at different initial medium pH values (5.5, 7.0 and 8.5). The effect of the different pH values can be observed on the wild type but not on the deletion strain, which appears not to sense the effect of the pH change. Values represent average from two replicates with maxima and minima values as error bars.



Appendix 6.6: Growth of the CA gene deletion strains, complemented with their respective plasmid-borne genes, in minimal media containing 2% (w v⁻¹) fructose. The growth of all the mutants except Re2428/pCaa was completely recovered by the overexpression of each corresponding CA.



Appendix 6.7: A) Fluorescent microscopy image showing *R. etropha* with constitutively expressed Caa-fused-RFP (Re2061/pCaa_RFP). Details (inset images) show individual cells isolated from the main image where the concentration and localization of the fluorescence near the outer perimeter of the cells were more clearly observed. B) Re2061 control expressing RFP alone (Re2061/pRFP). Details show individual cells isolated from the main image where the detected fluorescence is equally spread in the cytosol of the bacterial cells. Scale bar = 2 μ m.



CHAPTER 7

Isopropanol production in engineered *Ralstonia eutropha*

(This chapter was modified from a previously published article in Applied Microbiology and Biotechnology, 2014 'Isopropanol production with engineered *Cupriavidus necator* as production platform' Estelle Grousseau, Jingnan Lu, Nathalie Gorret, Stephane Guillouet, and Anthony Sinskey 98: 4277-4290 © Springer-Verlag)

INTRODUCTION

With the need to reduce consumption of petroleum-based products, diversified alternative fuels and bulk chemicals from renewable carbon sources have to be developed. Current research on fuel substitutes has focused largely on ethanol, even though numerous technical problems associate with this biofuel. Ethanol is corrosive towards ferrous metals, has lower energy content than gasoline, and degrades elastomers and flexible transfer lines in fuel distribution systems, which makes it challenging to ship via traditional pipelines (Bruno et al. 2009). To overcome some of the challenges associated with the use of ethanol as a fuel, various higher alcohols were evaluated. Higher alcohol molecules such as isobutanol, n-butanol, isopropanol, 1-propanol, 3-methyl-1-butanol, 2-methyl-1-butanol, and isopentenol, can be blended with gasoline at various ratios and act as drop-in fuels, thus having high potential to be implemented as gasoline replacements (Lee et al. 2008a; Connor and Liao 2009; Bruno et al. 2009). Among these higher alcohols, isopropanol has a very high research octane number (129) and is already used as a gasoline and diesel additive (Peralta-Yahya and Keasling 2010). Currently, isopropanol is mainly used as a solvent in the chemical industry and is blended with many everyday household products such as paints and inks (Pharkya et al. 2011). Isopropanol can also be utilized as a chemical intermediate and be converted to propylene by dehydration and subsequently to “green” polypropylene (Kibby and Hall 1973; Araki et al. 1993). Currently isopropanol is chemically produced from propylene or acetone (Pharkya et al. 2011), which are petroleum-based products. Bioproduced-isopropanol from renewable carbon sources, is a promising alternative as a green and renewable chemical target molecule in the chemical, solvent, and alternative energy industries.

Isopropanol can be naturally produced by *Clostridium* species (Krouwel et al. 1980, Chen and Hiu 1986, Survase et al. 2011, Matsumura et al. 1992), with reported maximum production level at 5 g/L (Matsumura et al. 1992; Survase et al. 2011). Nevertheless, production in *Clostridium* species faces several challenges (Connor and Liao 2009), such as complex physiology and narrow genetic engineering capabilities, although some engineered *Clostridium* strains have reached production titer up to 8.8 g/L (Collas et al. 2012). Additionally, isopropanol production in *Clostridium* species is associated with several by-products including lactic acid, acetic acid, butyric acid, butanol, acetone, and ethanol (Dürre 1998, Collas et al. 2012), which impact the carbon yield and complicates the recovery processes. In order to overcome the complexity of using *Clostridium* species, heterologous expression of *Clostridium* isopropanol pathway in other microorganisms has been attempted. For instance, heterologous expression of *Clostridium* isopropanol pathway in *Escherichia coli* led to an isopropanol production of up to 4.9 g/L in batch culture (Hanai et al. 2007) and up to 40 g/L using a fed-batch strategy (Jojima et al. 2008, Inokuma et al. 2010). An engineered yeast, *Candida utilis*, was capable of isopropanol

production at a titer of 9.5 g/L and up to 27.2 g/L in batch and fed-batch strategies respectively (Tamakawa *et al.* 2013). Lately isopropanol production by a cyanobacterium at a titer of 27 mg/L in batch culture was achieved, although not directly from CO₂, but hypothesized to be from stored glycogen (Kusakabe *et al.* 2013).

The facultative chemolithoautotrophic bacterium *Ralstonia eutropha* (also known as *Cupriavidus necator*) is a metabolically versatile bioproduction platform organism. It is metabolically capable of utilizing many simple and complex carbon sources, especially oils (Lee *et al.* 2008b; Budde *et al.* 2011), fatty acids (Wilde 1962; Johnson and Stanier 1971; Friedrich *et al.* 1979; Doi *et al.* 1989) and CO₂ (Wilde 1962; Repaske and Mayer 1976; Tanaka *et al.* 1995), which can be derived from agro-industrial waste streams. *R. eutropha* is a model bacterium for the study of polyhydroxyalkanoate (PHA) biopolymers, in addition to H₂- and CO₂-based lithoautotrophic metabolism for the past few decades (Schlegel 1990; Reinecke and Steinbüchel 2009). *R. eutropha* is able to divert a significant amount of carbon into polyhydroxybutyrate (PHB), a type of PHA, under unfavorable growth conditions of nutrient limitation (oxygen, nitrogen, phosphorus *et al.*), with adequate availability of carbon (Koller *et al.* 2010). This natural ability to store excess carbon is very appealing since isopropanol and PHB share the same production pathway precursors (Figure 7.1), which indicates that few genetic modifications are required to divert PHB precursors to the production of isopropanol. As depicted in Figure 7.1, expression of two genes encoding for an acetoacetate decarboxylase (ADC) and an alcohol dehydrogenase (ADH) is necessary to redirect carbon flow to isopropanol. Moreover *R. eutropha* can be easily engineered, because its genome has been fully sequenced (Schwartz *et al.* 2003; Pohlmann *et al.* 2006) and basic genetic tools are available to manipulate the microorganism since the 1980s (Jendrossek *et al.* 1988; Peoples and Sinskey 1989; Park *et al.* 1995).

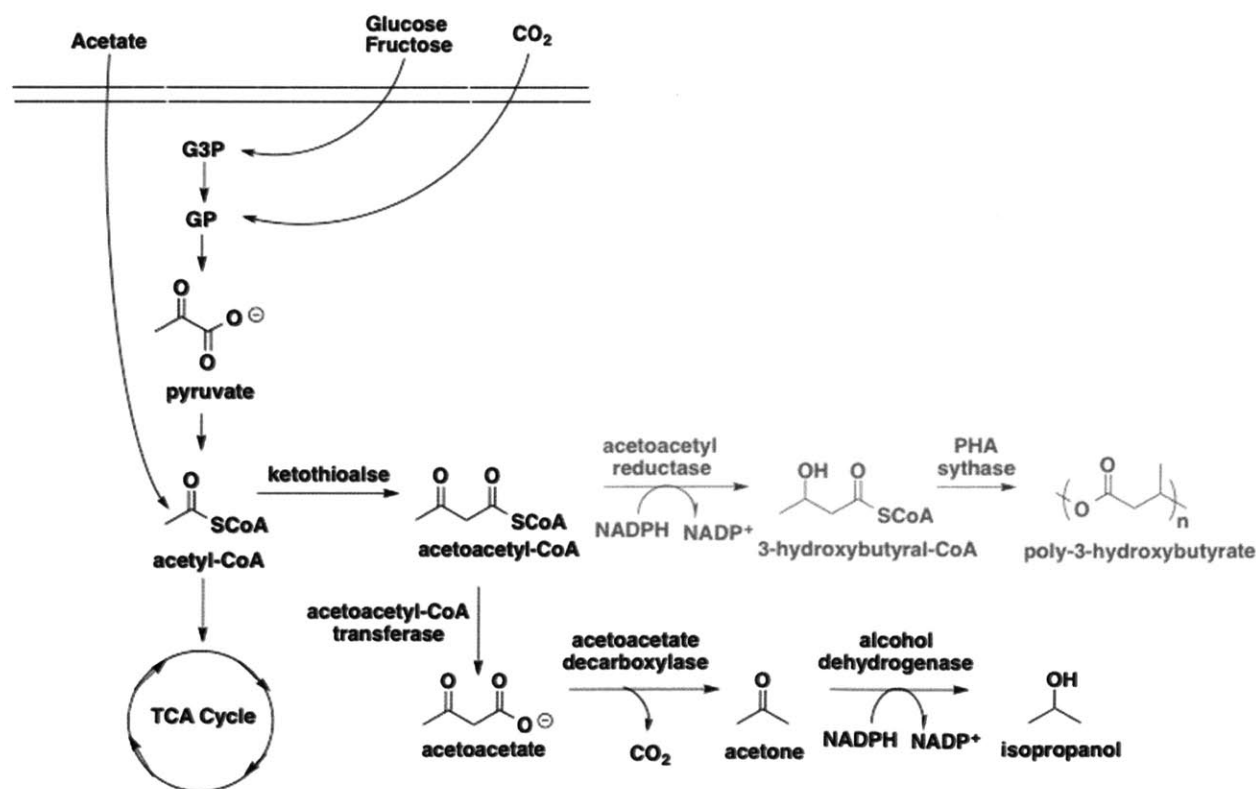


Figure 7.1: Engineered isopropanol production pathway in *R. eutropha*. Enzymes, which are missing in *R. eutropha* for the production of isopropanol are acetoacetate decarboxylase and alcohol dehydrogenase. Carbohydrates are catabolized through Entner-Doudoroff pathway and lead to glyceraldehyde-3-phosphate (G3P) and pyruvate. CO₂ is assimilated through the Calvin-Benson-Bassham Cycle and lead to glycerate-3-phosphate (GP). G3P, pyruvate, GP and acetic acid can all lead to the production of acetyl-CoA. Acetyl-CoA can be directed toward the tricarboxylic acid (TCA) cycle or toward isopropanol or polyhydroxybutyrate synthesis. Isopropanol is synthesized by condensation of two acetyl-CoA molecules into acetoacetyl-CoA via the β -ketothiolase enzyme. Next, acetoacetyl-CoA transferase (CTF) removes the CoA moiety from acetoacetyl-CoA for the formation of acetoacetate. Acetoacetate is then decarboxylated with the aid of acetoacetate decarboxylase (ADC) to form acetone, before an alcohol dehydrogenase (ADH) finally reduces acetone to isopropanol. The last two steps of PHB synthesis pathway must be removed, by the deletion of *phaB* and *phaC* genes respectively encoding for the NADPH-dependent acetoacetyl-reductase and the PHA synthase.

The key features for engineering a microorganism for industrial metabolite production are the following: the selected microorganism must be (i) robust towards industrial process conditions (ii) able to grow with minimal nutrient supplement for cost effective issues (iii) able to grow on cheap substrates (iv) accept heterologous genes (v) the expression of multiple genes must be coordinated to channel the carbon flow (vi) growth and product formation must be uncoupled especially for toxic molecules such as isopropanol. *R. eutropha* meets all of these requirements and was selected for isopropanol production in this study.

Although *R. eutropha* seems to be a good host for isopropanol production, it has never been engineered and tested for the production of isopropanol. In this study, a rational design of production pathways was employed and the production of isopropanol by each engineered pathway was evaluated. The pathway gene-coding sequences, codon usages, gene copy numbers, distance of specific gene from the promoter, and various promoter systems were investigated to optimize the production of isopropanol in terms of titer, yield and specific rate.

MATERIALS AND METHODS

Chemicals, bacterial strains, and plasmids

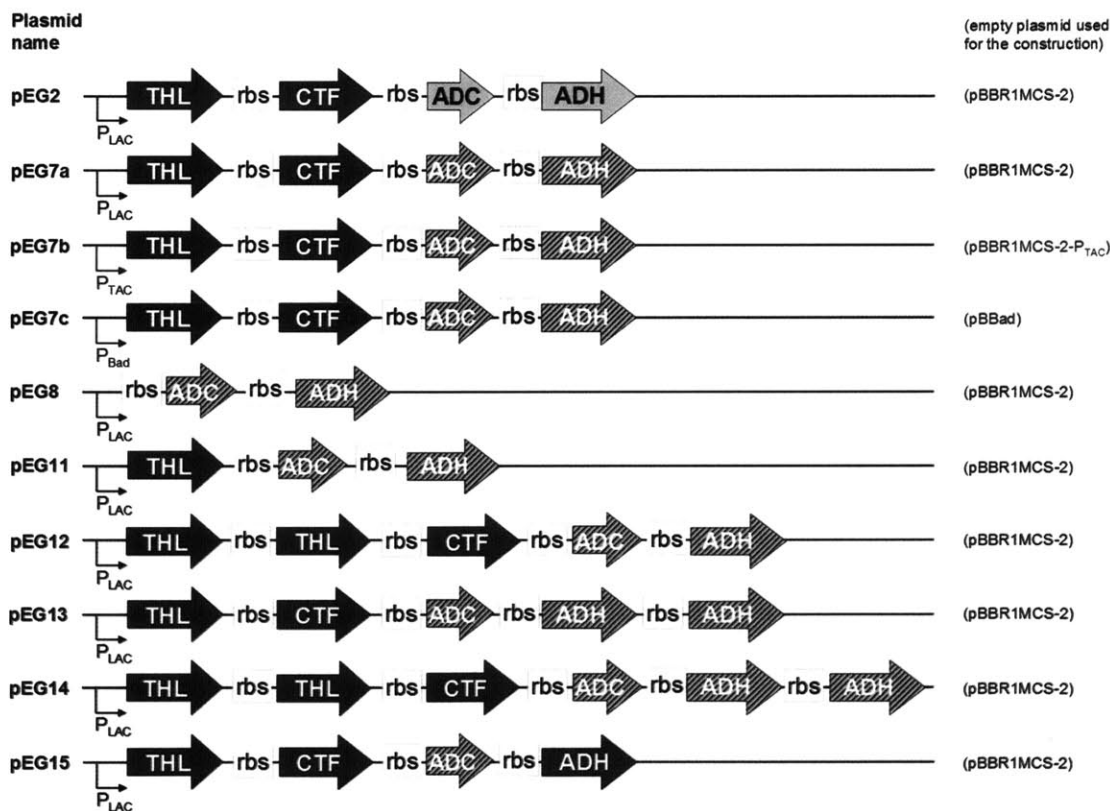
Unless indicated otherwise, chemicals used in this study were purchased from Sigma-Aldrich. *R. eutropha* strain Re2133 was used as the parent strain for isopropanol production. It was derived from wild type *R. eutropha* H16 (ATCC 17699) published previously (Budde et al. 2011). Plasmids used in this study are depicted in Figure 7.2. Primers used in the construction of plasmids and strains were listed in Appendix 7.1.

Growth media and cultivation conditions

Rich medium used for the precultures consisted of 27.5 g/L dextrose-free tryptic soy broth (TSB, Becton Dickinson, Sparks, MD, USA) with addition of 10 mg/L gentamycin, 200 mg/L kanamycin. Minimal medium used for the cultures was previously described by Lu et al. 2012b with addition of gentamycin (10 mg/L) and kanamycin (100 mg/L). The amount of kanamycin was reduced compared to the precultures to decrease the toxic effect of kanamycin on growth. In the literature, the amount of kanamycin used for *R. eutropha* is between 50 mg/L and

450 mg/L (Kusian et al. 2002; Pötter et al. 2002; Aneja et al. 2009; Park et al. 2010; Wahl et al. 2012).

One glycerol stock was streaked on a rich medium Petri dish (rich medium with addition of 20 g/L agar A). The plate was incubated for 48 h at 30°C. One colony was used to inoculate the seed culture, which was grown for 24 h in culture tube at 30°C on a roller-drum with 10 mL of rich medium. Then the volume of broth needed to inoculate a flask with an initial OD_{600nm} of 0.4 was centrifuged in a 15 mL falcon tube (1,900 x g, 10 min, Centrifuge 5804R Eppendorf AG, Hamburg, Germany). The cell pellet was then resuspended in the mineral media used for the flask culture (100 mL in 1 Liter flask). 20 g/L of fructose and 0.38 g/L of NH₄Cl were used as carbon and nitrogen sources respectively. The nitrogen amount corresponded to the amount necessary to produce about 0.7 g/L of biomass cell dry weight (CDW) considering the following biomass formula: C₁H_{1.77}O_{0.44}N_{0.25}, 4% ashes, MW=25.35 g.Cmole⁻¹ (Aragao 1996). The baffled flasks were continuously shaken in a 30°C incubator at 200 rpm to ensure proper oxygen transfer. Culture samples were taken regularly for analysis.



Abbr.	Name	Locus tag	Microorganism	Enzyme
THL:	<i>phaA</i>	(H16_A1438)	from <i>C. necator</i> ,	coding for a β-ketothiolase
CTF:	<i>ctfAB</i>	(H16_A1331 and H16_A1332)	from <i>C. necator</i> ,	coding for a succinyl-CoA transferase
ADC:	<i>adc</i>	(CA_P0165)	from <i>C. acetobutylicum</i> ,	coding for an acetoacetate decarboxylase
ADH:	<i>adh</i>	(AF157307 nt 2351 to 3406)	from <i>C. beijerinckii</i> ,	coding for an alcohol dehydrogenase
ADH:	<i>adh</i>	(H16_A0757)	from <i>C. necator</i> ,	coding for an alcohol dehydrogenase

Figure 7.2: Schematic of isopropanol production pathways constructed and plasmid utilized. Each plasmid was incorporated into strain Re2133 (H16 *ΔphaB1B2B3C1* (Gen^l), Budde et al. 2011).

Plasmid and strain constructions

DNA sequence amplification was achieved using Phusion High-Fidelity PCR Master Mix with GC Buffer (New England Biolabs, Ipswich, MA, USA). QIAQuick Gel Extraction Kit (QIAGEN, Valencia, CA, USA) was used for gel purification of all DNA products. Plasmid extractions were carried out using the QIAprep Spin Miniprep Kit (QIAGEN, Valencia, CA, USA). Restriction enzymes used were purchased from New England Biolabs (Ipswich, MA, USA).

Synthetic ribosome-binding site (rbs) and a nucleotide linker sequence were incorporated between each gene as shown in Figure 7.2. The rbs and linker sequences used were tested and described by Lu et al. 2012a. The synthesized codon-optimized genes (GenScript USA Inc., Piscataway, NJ, USA) were received in pUC57-Kan. The sequence of codon-optimized genes can be found in the Appendix 7.2. The plasmid assemblies were achieved by one-step isothermal DNA assembly protocol (Gibson et al. 2009), except when stated otherwise. Vector pBBR1MCS-2-P_{TAC} was constructed by replacing the P_{LAC} promoter region (TTTACACTTTATGCTTCCGGCTCGTATGTTG) of the broad-host vector pBBR1MCS-2 (Kovach et al. 1995) with the P_{TAC} promoter (TTGACAATTAATCATCGGCTCGTATAATG) using primers listed in Appendix 7.1. Empty vectors digested by ClaI and XhoI were used as backbone DNA for the assembly of all isopropanol production plasmids except for pEG7c. For pEG7c, pBBad (Fukui et al. 2009) was digested with KpnI and XbaI, and the fragments containing the isopropanol production pathway genes were purified from pEG7a via KpnI and XbaI digestion. The pathway genes were then inserted into pBBad to create pEG7c. For pEG7b, the fragment with pathway genes from the digestion of pEG7a with XhoI and ClaI was isolated and purified. The fragment was then ligated with the corresponding digested vector. All ligation and one-step isothermal assembly products were transformed into high efficiency *E. coli* Top10 chemical competent cells (InvitrogenTM, Life technologies). Colonies were screened by diagnostic digestion after plasmid extraction. Correct gene insertions on plasmids were confirmed by sequencing. All constructed plasmids are described in Figure 7.2. Each confirmed plasmid was transformed into *E. coli* S17-1 (ATCC 47055) by electroporation (Simon et al. 1983). *E. coli* S17-1 harboring the plasmid was then used to introduce the plasmid into *R. eutropha* Re2133 by conjugative transfer (Slater et al. 1998).

Analytical procedures

Culture supernatants were obtained by filtration (0.2 mm PTFE or PES syringe filters, VWR, Radnor, PA, USA) of the flask broth samples and used for substrate and products determination. The residual substrate and product concentrations were quantified by High Performance Liquid Chromatography (HPLC). The HPLC Instrument (Series 1100, Agilent, Santa Clara, CA, USA) was equipped with an ion-exchange column (Aminex HPX-87H, 300x7.8 mm, Bio-Rad, Hercules, CA, USA) protected with a guard column (Cation H+ cartridge, 30x4.6 mm, Bio-Rad, Hercules, CA, USA) and coupled to a RI detector and an UV detector (λ=210 nm). The column was eluted with 2.5 mM H₂SO₄ as a mobile phase at 50°C at a flow rate of 0.5 ml/min.

Biomass growth was monitored by measuring the optical density at 600 nm (OD_{600nm}) using a visible spectrophotometer (Spectronic GENESYS 20 Visible Spectrophotometer) with a 1 cm path length absorption PS semi-micro cuvette (VWR, Radnor, PA, USA).

Enzymatic assay

Cell pellets after centrifugation of 5 mL culture broth (taken at 24 h of cultures) in a 15 mL Falcon tube (1,900 x g, 10 min, Centrifuge 5804R Eppendorf AG, Hamburg, Germany) were frozen at - 80°C until the time of enzymatic assays.

Cell pellets were thawed on ice and resuspended in 0.8 mL of the buffer associated with each assay. Then cells were lysed with beads (0.6 g of 0.1 mm zirconia beads, BioSpec Products, Bartlesville, OK, USA) in 2 mL screw top plastic vial at 4°C, using FastPrep-24 (MP Biomedicals, Solon, OH, USA) at 6 m.s^{-1} for 40 s. Three cycles of Fast-Prep with 5 min rest in between were carried out. Cell debris was removed by microcentrifugation (16,000 x g, 10 min, Microcentrifuge 1816, VWR, Radnor, PA, USA). Cell lysates were filtrated using 0.45 μm syringe filters (PES, VWR, Radnor, PA, USA) prior to enzyme activity assay. The protein content of the cell lysates was determined by the standard procedure of the Bio-Rad Protein Assay Kit (Bio-Rad, Hercules, CA, USA) with bovine serum albumin (BSA) as a standard. All measurements including standards were repeated three times.

All enzymatic assays were performed at 25°C with the Agilent 8453 spectrophotometer (Agilent 8453 UV-Visible Kinetic Mode, Agilent, Santa Clara, CA, USA). β -ketothiolase (THL) assay was performed according to Budde et al. 2010. CoA-transferase (CTF) assay was conducted according to Cary et al. 1990 with 0.15 M succinic acid disodium salt as the substrate. Acetoacetate decarboxylase (ADC) assay was performed by a method adapted from Yu et al. 2011. In brief, the buffer used for cell resuspension was 5 mM potassium phosphate buffer (pH 7.3). The assay buffer contained 20 mM acetate buffer (pH 4.8), 70 μM bromocresol green, and 10 mM lithium acetoacetate. Reaction was initiated with the addition of 50 μL of appropriately diluted cell extract and increase in absorbance at 620 nm was monitored. Alcohol dehydrogenase (ADH) assay was adapted from Ismaiel et al. 1993, Hanai et al. 2007 and Shen et al. 2011. Briefly, crude extracts were prepared in 130 mM of TrisHCl (pH 7.5). ADH activities were measured by following the reduction of acetone (200 mM) with NADPH ($OD_{340nm} = 6.2\text{ mM}^{-1}\cdot\text{cm}^{-1}$). The assay mixture (1 mL) contained 100 mM Tris-Cl buffer (pH 7.5), 5 mM dithiothreitol (DTT), and 0.2 mM NADPH. One enzyme unit is defined as 1 mmole of product formed per minute.

Yield calculations

All yields were expressed as carbon ratio. The theoretical isopropanol yield was calculated on a carbon basis considering the pathway shown in Figure 7.1. One mole of fructose is converted to 2 moles of acetyl-CoA and 2 moles of CO_2 . Then the two molecules of acetyl-CoA ligate into one acetoacetate, which is subsequently decarboxylated and reduced to form one mole of isopropanol. A 6-carbon molecule leads to a 3-carbon molecule, $Y_{S, \text{isopropanol}}^{\text{theo}} = 0.5\text{ Cmole/Cmole}$. The experimental isopropanol yield was the ratio of isopropanol produced and substrate consumed during a time interval (t_2-t_1): $Y_{S, \text{isopropanol}} = \left| \frac{\text{Isopropanol}_{t_2} - \text{Isopropanol}_{t_1}}{S_{t_2} - S_{t_1}} \right|$. All data are presented as means \pm SD from three independent experiments except when stated otherwise.

RESULTS

Coding sequence optimization

In order to redirect the carbon flow from PHB into isopropanol pathway, the strain Re2133 (Budde et al. 2011) was used as the parent strain since genes coding for acetoacetyl-CoA reductases (*phaB1B2B3*) and for the PHA synthase (*phaC1*) were deleted. Strain Re2133 transformed with the empty plasmid pBBR1MCS-2 was used as a reference strain during this study. This strain was cultivated on fructose as the sole carbon source, in a mineral medium designed to reach a biomass concentration of about 0.7 g/L once nitrogen was depleted. After nitrogen depletion, the carbon excess from fructose was directed towards pyruvate at concentration up to 2.61 ± 0.19 g/L (Figure 7.3 and Appendix 7.3).

The entire isopropanol production pathway from acetyl-CoA was inserted in the plasmid pBBR1MCS-2 to construct the plasmid pEG2. Plasmid pEG2 harbored the native *R. eutropha* genes *phaA* (H16_A1438) and *ctfAB* (H16_A1331 and H16_A1332), respectively coding for a β -ketothiolase A (THL) and the two subunits of a CoA-Transferase (CTF). Additionally, the plasmid also contained the heterologous genes from *Clostridium* species *adc* (CA_P0165) and *adh* (AF157307 nt 2351 to 3406), respectively coding for an acetoacetate decarboxylase (ADC) and an alcohol dehydrogenase (ADH) (Figure 7.2). The resulting strain Re2133/pEG2 produced 0.22 ± 0.07 g/L of isopropanol (Figure 7.3). The production titer reached was very low and up to 2.44 ± 0.14 g/L pyruvate byproduct was coproduced (Appendix 7.3), indicating that the expression of the isopropanol pathway genes was not significant enough to shunt all the PHB precursors towards isopropanol.

Cell extracts of Re2133/pEG2 were analyzed in terms of enzyme activities for the heterologous enzymes ADC and ADH. The activities of both heterologous enzymes were very low, respectively at 0.75 ± 0.84 U/mg and 0.05 ± 0.01 U/mg, while the activities of the native *R. eutropha* enzymes THL and CTF were 5.47 ± 0.62 U/mg and 9.89 ± 1.28 U/mg respectively (Table 7.1).

The poor expression of the heterologous genes from *Clostridium* species (*adc* and *adh*) necessary for isopropanol production in *R. eutropha* could be explained by differences in genome GC content between the *Clostridium* species (about 30% GC) and *R. eutropha* (about 66% GC) as depicted in Appendix 7.4. The differences in GC content between the two species could impact the transcriptional and translational efficiencies, since GC content is known to drive codon usage. Codon bias of the host organism has been reported as a major limiting factor in the production yield of a desired protein (Behura and Severson 2012). A comparative table of the codon usage in *R. eutropha*, *C. acetobutylicum*, and *C. beijerinckii* was constructed (Appendix 7.5) from the database <http://www.kazusa.or.jp/codon/> (Nakamura et al. 2000). Codon usage between these three organisms is very different. For instance, the codon UUA for Leucine, is not used at all by *R. eutropha*, whereas it is used 51-53% of the time by *C. acetobutylicum* and *C. beijerinckii*. Codon-optimization of the heterologous genes appears to be necessary to improve protein expression in *R. eutropha*.

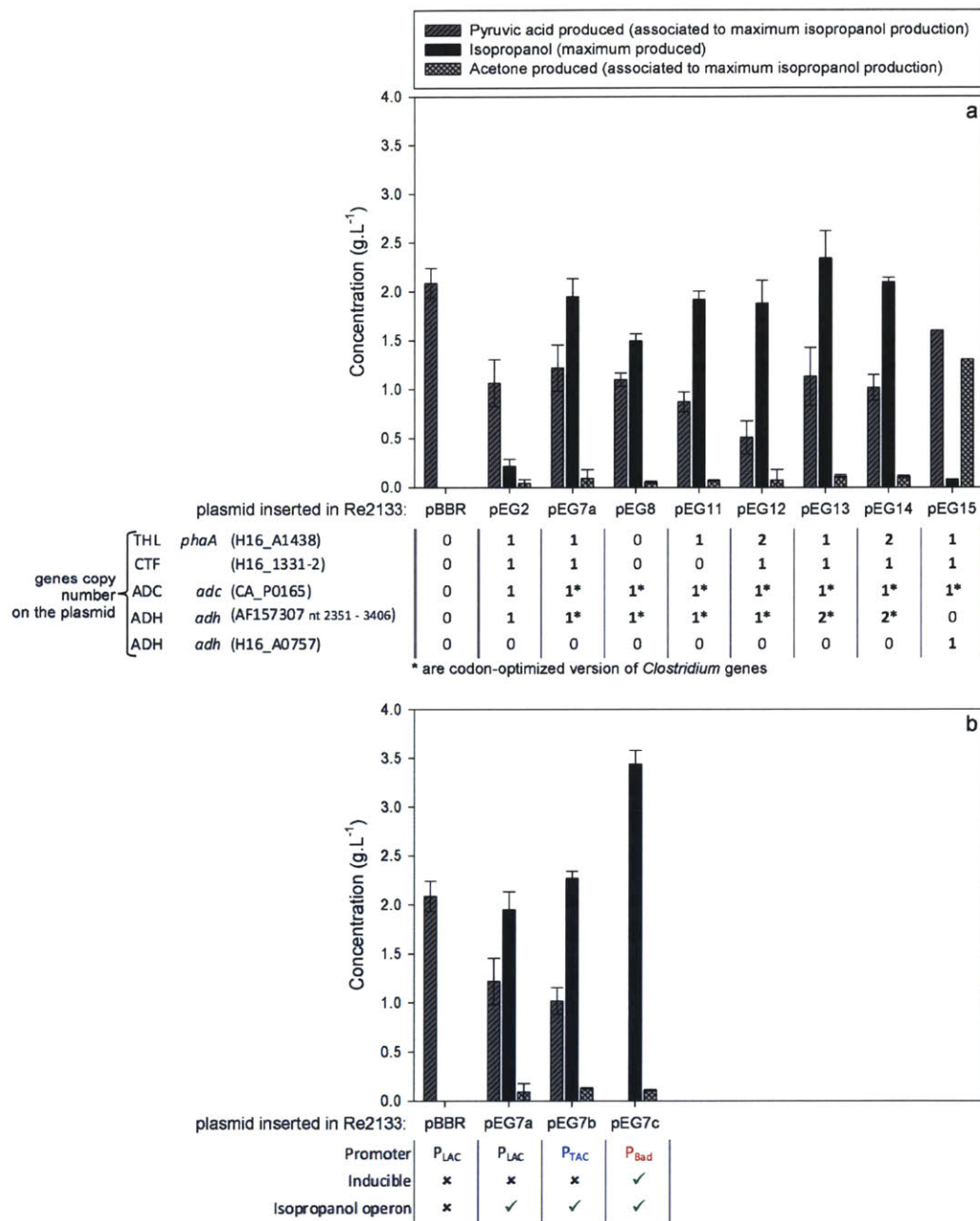


Figure 7.3: Time point in which maximum isopropanol concentration was produced. Concentrations of pyruvic acid and acetone detected at the same time point are also depicted. (a) Coding sequence evaluation with the plasmid pBBR1MCS-2 incorporated in the strain Re2133. Composition of the plasmid is indicated below each plasmid name. Experiment n=3 were performed, except for strains Re2133/pEG12 and Re2133/pEG14 where n=2 was performed, and Re2133/pEG15 where n=1 was performed. (b) Promoter evaluation with the same set of genes (*phaA* (H16_A1438), *ctfAB* (H16_A1331 H16_1332), codon-optimized *adc* (CA_P0165) and *adh* (AF157307 nt 2351 to 3406)). The promoter on the plasmid is indicated below each plasmid name. n=3, except for Re2133/pEG7c where n=2 was performed.

Codon-optimization to overcome the poor expression of heterologous genes from *Clostridium* species

The plasmid pEG7a was constructed with the codon-optimized version of the *adc* and *adh* heterologous genes of *Clostridium* species (Figure 7.2) and incorporated into Re2133. Utilization of codon-optimized genes successfully led to an increase in ADC and ADH activities in Re2133/pEG7a cell extracts. An activity of $8.89 \pm 1.30 \text{ U.mg}^{-1}$ and $0.72 \pm 0.04 \text{ U.mg}^{-1}$ were respectively determined for ADC and ADH (Table 7.1). As a result, the strain bearing pEG7a produced $1.95 \pm 0.18 \text{ g/L}$ isopropanol in 88 h (Figure 7.3), which corresponded to an 8.9 ± 3.0 fold increase compared to Re2133/pEG2. As indicated in Figure 7.4, there is a global increase in the carbon conversion ($0.17 \text{ Cmole.L}^{-1}$) to products (biomass, pyruvate, isopropanol, and acetone) in Re2133/pEG7a compared to Re2133/pEG2 ($0.10 \text{ Cmole.L}^{-1}$). This suggests that in the strain Re2133/pEG7a, more carbon was driven through the entire pathway instead of only the conversion of pyruvate to isopropanol. Cultivation time of 88h, the peak isopropanol production time, pyruvate concentration measured was $1.52 \pm 0.29 \text{ g/L}$ and acetone concentration measured was $0.09 \pm 0.09 \text{ g/L}$, suggesting that further redirection from pyruvate towards the production of isopropanol can be achieved.

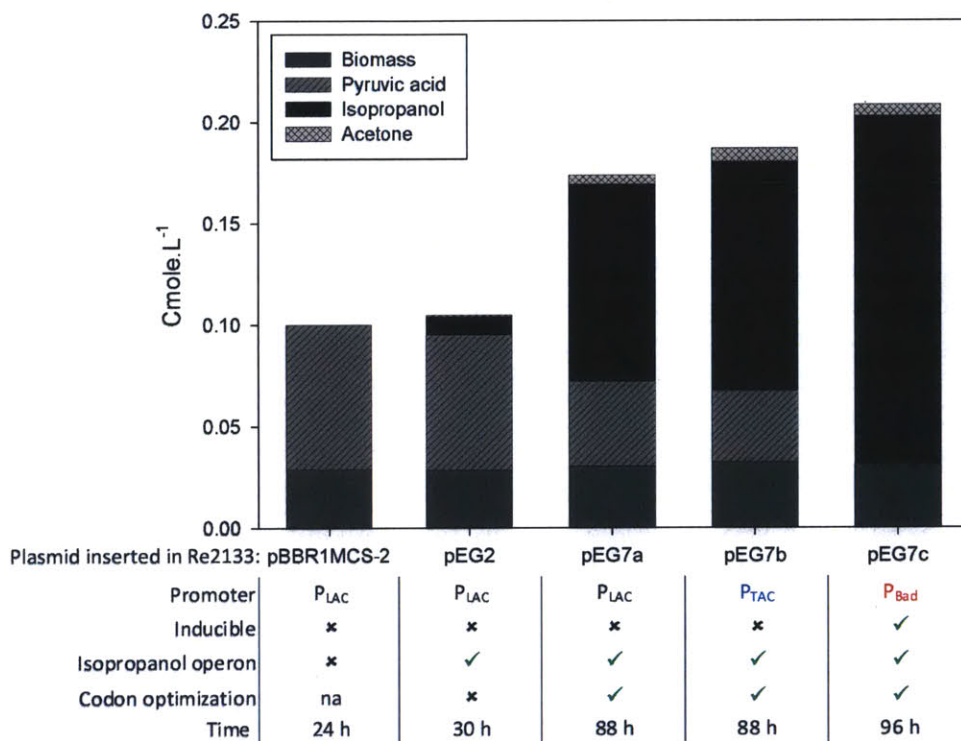


Figure 7.4: Carbon distribution in Cmole.L^{-1} of the products (biomass, pyruvic acid, isopropanol, and acetone) for the strains Re2133/pBBR1MCS-2, Re2133/pEG2, Re2133/pEG7a, Re2133/pEG7b, and Re2133/pEG7c. Cumulative data for the culture time point corresponding to the maximum concentration of total products.

Suitability of alcohol dehydrogenase (ADH) from *R. eutropha* for isopropanol production

An alternative to codon-optimization of heterologous ADH genes was to identify and use a native ADH gene from *R. eutropha* that is active towards acetone. One native ADH has been previously identified in *R. eutropha* and tested (Steinbüchel and Schlegel 1984; Lu et al 2012). This ADH was reported to be a very unspecific enzyme regarding to its substrates. Isopropanol was reported as one of its wide spectrum of substrates (Steinbüchel and Schlegel 1984). The sequence of *adh* has been published (Jendrossek, Steinbüchel et al. 1988) and by comparison to the whole genome sequence (Pohlmann et al. 2006), locus H16_A0757 was identified. In the wild type strain, this native ADH is only expressed under restricted supply of oxygen (Steinbüchel and Schlegel 1984). Nevertheless, mutant strains of *R. eutropha* with constitutive expression of *adh* have been isolated (Steinbüchel et al. 1987), indicating that *adh* expression under a constitutive promoter should lead to ADH enzyme activity even under aerobic conditions. Thus plasmid pEG15 was constructed with the native *R. eutropha adh* (H16_A0757) instead of the *C. beijerinckii adh* (Figure 7.2). The resulting strain Re2133/pEG15 produced a small amount of isopropanol (~0.8 g/L) compared to strain Re2133/pEG7a (1.95 ± 0.18 g/L) (Figure 7.3). Large amounts of acetone (~1.31 g/L) and pyruvate (~2.00 g/L) were detected in the supernatant of Re2133/pEG15. Although there was a slight ADH activity toward acetone, the expression of the ADH from *C. beijerinckii* led to 25 times higher isopropanol production. This indicates that ADH from *R. eutropha* is not specific towards acetone as a substrate, as a result, is not suitable for the production of isopropanol.

Influence of the pathway gene copy number on isopropanol production

In order to further direct carbon flow from pyruvate to isopropanol, copy numbers of three pathway genes (*phaA*, *ctfAB*, and *adh*) were investigated. An increase in gene copy number could result in an increase in protein expression level, and thus a higher enzymatic activity (Schendel *et al.* 1989). For this purpose, plasmids pEG8, pEG11, pEG12, pEG13, and pEG14 were constructed, which included various copy numbers of *phaA* (0 - 2), *ctfAB* (0 - 1), and *adh* (1 - 2) (Figure 7.2).

The activity of β -ketothiolase, encoded by *phaA*, in cell extracts increased with the plasmid gene copy number (Figure 7.5). Ketothiolase activity of 3.2 ± 2.2 U.mg⁻¹ in cell extract was found in strains with 0 copy of *phaA* on the plasmid. An addition of about 2.7 U/mg was detected with each additional copy of *phaA* on the plasmid. The increase in activity resulting from additional gene copies led to an increase in isopropanol production, although only for the addition of one gene copy (Re2133/pEG11 and Re2133/pEG8 shown in Figure 7.3). These results indicated that the reaction performed by the β -ketothiolase was no longer the limiting step when one copy of *phaA* was overexpressed on the plasmid.

The overexpression of native CoA-transferase (*ctfAB*) on the plasmid was not necessary since it did not improve the isopropanol production (Figure 7.3). Hence, the CoA-transferase was not a rate-controlling step when compared to the other enzymes in the pathway of interest. The addition of a second copy of the codon-optimized *adh* gene on the plasmid slightly increased the production of isopropanol by 1.11 ± 0.14 fold (Re2133/pEG14 vs Re2133/pEG12) and by 1.20 ± 0.18 fold (Re2133/pEG13 vs Re2133/pEG7a), depending on the plasmid construction (Figure 7.3). An additional copy of *adh* gene seemed to lead to a smaller increase in isopropanol production with the plasmid pEG14 than with the plasmid pEG13 (Figure 7.3). The difference

between these two constructions was the addition of a second *phaA* gene copy on the plasmid pEG14, thus increased the distance between the promoter and the second copy of *adh* from 4.4 to 5.6 kb. A previous study demonstrated that expression is greater for the gene that is closest to the promoter (Lim et al. 2011). To determine whether if such conclusion applied in this case, ADH specific activities obtained in the constructed strains were compared to the distance of the furthest *adh* gene from the promoter (Figure 7.5). In accordance with the findings of Lim et al. 2011, an inverse linear relationship between the distance from the promoter and the activity of the associated ADH was demonstrated (Figure 7.5). The addition of *adh* gene copies on the same plasmid did not seem to be an optimal strategy to increase ADH expression and activity for improved isopropanol production.

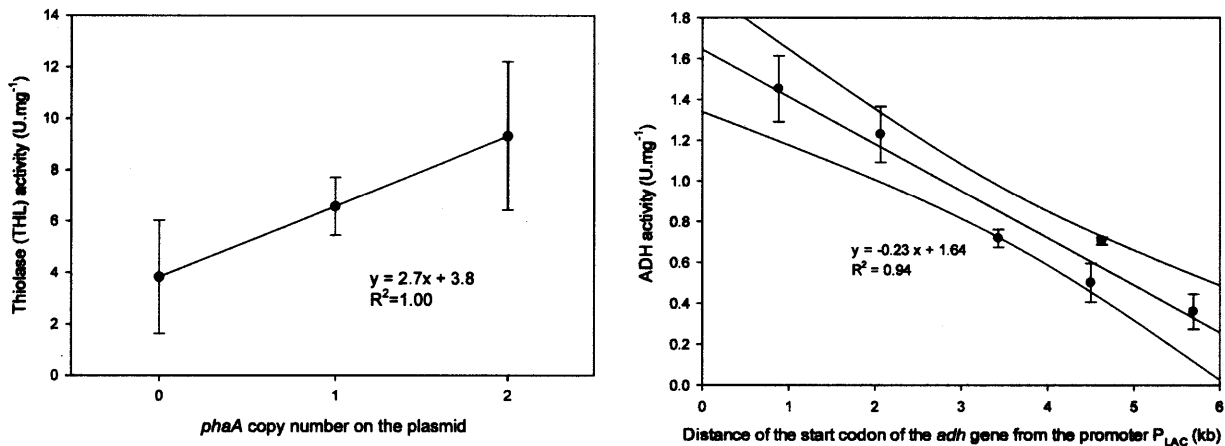


Figure 7.5: β -ketothiolase (THL) activity vs the copy number of *phaA* on the plasmid (left). For 0 copy of *phaA*, average of values from Re2133/pBBR1MCS-2 (n=3) and Re2133/pEG8 (n=3). For 1 copy, average of values get for Re2133/pEG2 (n=3), Re2133/pEG7a (n=3), Re2133/pEG11 (n=3), Re2133/pEG13 (n=3). For 2 copies, average of values get for Re2133/pEG12 (n=2) and Re2133/pEG14 (n=2). Alcohol dehydrogenase (ADH) activity associated to the expression of one *adh* gene copy vs the distance between the promoter and the *adh* gene start codon (right). The activity associated to the second *adh* gene (for the strains Re2133/pEG13 and Re2133/pEG14) was calculated by subtracting the activity of the cell extract measured for Re2133/pEG7a and Re2133/pEG13 respectively.

Promoter comparison

Promoter strength is another important parameter for pathway gene expression. We evaluated several promoter systems for isopropanol production, in which two are constitutively expressed promoters (P_{LAC} and P_{TAC}) and one of which is an inducible promoter (P_{BAD}). All three promoters were evaluated for the production of isopropanol in *R. eutropha*.

Comparison of the two constitutive promoters P_{LAC} and P_{TAC}

Fukui et al. 2010 evaluated several promoters to regulate gene expression in *R. eutropha*. Among the constitutive promoters identified (P_{LAC}, P_{TAC}, P_{phaC}, and P_{phaP}), P_{TAC} promoter was the strongest and demonstrated 1.5-2.0 fold higher read-through expression when compared with P_{LAC}. To test the effect of different promoter strength on isopropanol production, the P_{LAC}

promoter region (TTTACACTTTATGCTTCCGGCTCGTATGTTG) of the broad-host vector pBBR1MCS-2 was exchanged with the P_{TAC} promoter region (TTGACAATTAATCATCGGCTCGTATAATG) leading to the plasmid pBBR1MCS-2- P_{TAC} . Then the synthetic operon with four genes encoding for the isopropanol production pathway enzymes were digested from pEG7a and inserted into pBBR1MCS-2- P_{TAC} , resulting in plasmid pEG7b (Figure 7.2).

Strain Re2133 harboring pEG7b plasmid produced $2.27 \pm 0.07 \text{ g.L}^{-1}$ isopropanol (Figure 7.3), corresponding to a 1.16 ± 0.12 fold increase compared to the strain Re2133/pEG7a with the P_{LAC} promoter. In terms of total carbon titer, $0.19 \text{ Cmole.L}^{-1}$ were produced by the strain Re2133/pEG7b compared to the $0.17 \text{ Cmole.L}^{-1}$ produced by the strain Re2133/pEG7a (Figure 7.4). Constitutive expression of isopropanol pathway led to a growth-associated isopropanol production of $0.98 \pm 0.06 \text{ g per g}$ of biomass in the strain Re2133/pEG7a and $1.14 \pm 0.01 \text{ g.g}^{-1}$ in the strain Re2133/pEG7b. Consequently, a decrease in the maximal growth rate by 2.70 ± 0.07 times (Re2133/pEG7a) and by 3.19 ± 0.16 times (Re2133/pEG7b) compared to Re2133/pBBR1MCS-2 (0.17 h^{-1}) was observed. Low maximal growth rate of the strains harboring pEG7a and pEG7b (between 0.05 and 0.06 h^{-1}) is not attractive for an efficient cultivation strategy. To overcome the poor growth due to the growth-associated isopropanol production, an inducible promoter was evaluated to separate growth and production phases.

Study of an inducible promoter: P_{BAD}

Fukui et al. 2010 demonstrated that broad-host vector pBBad harboring P_{BAD} with *araC* regulator gene responding to the addition of L-arabinose was functional in *R. eutropha*. This system was utilized by inserting the synthetic isopropanol production pathway from pEG7a into the pBBad plasmid, which led to the plasmid pEG7c (Figure 7.2). Re2133/pEG7c flask cultures were induced with 0.1% L-arabinose at an $OD_{600\text{nm}}$ of 1.5, corresponding to 75% of the maximum $OD_{600\text{nm}}$ reached with the amount of nitrogen supplied. The maximal growth rate was $0.17 \pm 0.01 \text{ h}^{-1}$, which was the same as the strain with the empty plasmid pBBR1MCS-2. Isopropanol production by Re2133/pEG7c reached $3.44 \pm 0.14 \text{ g.L}^{-1}$ (Figure 7.3 and 7.6), which was an increase of 1.76 ± 0.18 fold compared to strain Re2133/pEG7a. The P_{BAD} promoter system with 0.1% L-arabinose induction allowed for a higher production of isopropanol than the two constitutive promoter systems tested (P_{LAC} and P_{TAC} with plasmids pEG7a and pEG7b respectively). Moreover no extracellular pyruvate was detected (Figure 7.3 and 7.6), indicating that the increase in promoter strength was sufficient to pull carbon through the isopropanol production pathway from fructose consumption. In Re2133/pEG7c, up to 0.21 mole.L^{-1} of total carbon (biomass with addition of isopropanol and acetone) were produced, which corresponded to a significant increase of carbon flow into the products formation comparatively to the other engineered strains (Figure 7.4). Slight promoter leakiness was detected which resulted in only 0.15 g of isopropanol produced per g of biomass in the absence of arabinose induction.

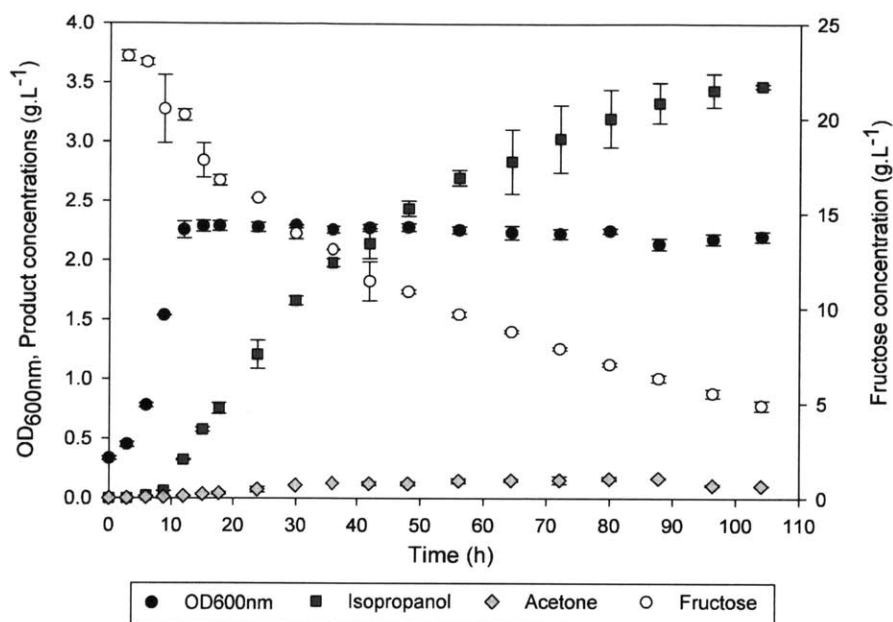


Figure 7.6: Evaluation of substrate (fructose) and products (biomass, acetone, and isopropanol) over cultivation time of Re2133/pEG7c.

DISCUSSION

This study presents the first demonstration of isopropanol production by *R. eutropha*. A rational design of isopropanol production plasmids and production evaluation in batch culture were performed. Codon usage differences between the host *R. eutropha* and *Clostridium* species was proven to be a critical design factor. Strain Re2133/pEG7a with codon-optimized version of the *Clostridium* genes *adc* and *adh* produced isopropanol that was 8.9 ± 3.0 folds higher ($1.95 \pm 0.18 \text{ g.L}^{-1}$) than Re2133/pEG2. Another strategy to avoid poor expression of heterologous genes was to directly use host gene coding for ADH. Although the expression of a native *adh* gene from *R. eutropha* was not appropriate for isopropanol production (Figure 7.3), an exploration of other potentially suitable ADHs from the *R. eutropha* genome could be fruitful. No native ADC encoding gene or ADC activity was reported in *R. eutropha* to date. However acetone excretion was reported by some mutant strains of *R. eutropha* partially or completely lacking the ability to synthesize PHB (Vollbrecht et al. 1978), indicating that a native decarboxylase gene may exist and could function to decarboxylate acetoacetate. Such gene or genes remain to be identified, evaluated, and tested for isopropanol production.

In order to further direct the carbon flow from pyruvate to isopropanol in strain Re2133/pEG7a, gene copy number and distance of the gene from the promoter were investigated. The addition of one copy of *adh* gene improved the isopropanol production. Considering that acetone was still detected in the culture broth, the alcohol dehydrogenase (ADH) may be the limiting step and may require a fine-tuning of expression to further increase isopropanol production. However, in order to enhance enzyme activity via an increase in gene dosage, the distance between the added-genes and the promoter should be reduced to a minimum (Figure 7.5).

Increasing the promoter strength further improved the isopropanol production. In accordance with Fukui et al. 2010, the use of P_{TAC} promoter instead of P_{LAC} promoter increased

the isopropanol concentration produced by 1.16 ± 0.12 fold (Figure 7.3). These two promoters led to a constitutive production of isopropanol. As a consequence, the growth rate is strongly reduced (0.05 h^{-1} to 0.06 h^{-1} instead of 0.17 h^{-1}) and such low growth rates were not realistic for scaled-up industrial production. The use of an inducible promoter P_{BAD} successfully overcame this problem. In addition, the constructed strain Re2133/pEG7c produced up to $3.44 \pm 0.14 \text{ g/L}$ isopropanol and no pyruvate after L-arabinose induction was detected (Figure 7.3 and 7.6), indicating that the increase in promoter strength was significant enough to increase the isopropanol pathway production to the level of the fructose consumption. One disadvantage of the inducible system P_{BAD} is the need to add an inducer molecule. It would be ideal to utilize a system that is auto-upregulated when a nutrient is depleted as it is for PHA production. Fukui et al. 2010 evaluated a vector system with P_{phaP} promoter along with the *phaR* gene coding for PhaR regulator, which was a useful expression vector enabling autoregulation of gene expression linked with PHB biosynthesis. However, this system relies on the presence of PHB in the cells (Pötter et al. 2002; York et al. 2002) and cannot be used for the production of other targeted molecules from PHB precursors with PHB⁻ mutants strains such as Re2133. Other inducible systems relay on nutrient depletion could also be employed here, such as the two-component signal transduction systems (Ninfa et al. 2007).

The key features for industrial production of isopropanol are high titer (to reduce recovery process costs), high yield (close to the theoretical production yield), high volumetric productivity, and cheap carbon source. To fulfill these requirements, the production strains must be selected for high specific productivity and high production yields. Titer and volumetric productivity will then depend on the cultivation monitoring. To assess the suitability of the best isopropanol production strain (Re2133/pEG7c) constructed in this study, the performances of this strain were compared to those of other engineered strains cultivated in similar conditions, i.e. batch cultures. The Re2133/pEG7c *R. eutropha* strain was able to produce up to $3.44 \pm 0.14 \text{ g/L}$ isopropanol. In batch mode, natural producers from the *Clostridium* family such as *C. isopropylicum* were able to produce titers up to 4.6 g/L with immobilized cells (Matsumura et al. 1992). Higher titer were reached with engineered strains: 4.9 g/L by *E. coli* (Hanai et al. 2007), 8.8 g/L by *Clostridium acetobutylicum* (Collas et al. 2012), and 9.5 g/L by *Candida utilis* (Tamakawa et al. 2013) (Table 7.1). Nevertheless in this work, the maximum titer of $3.44 \pm 0.14 \text{ g/L}$ of isopropanol was reached with only $0.82 \pm 0.02 \text{ g/L}$ of biomass under conditions of nitrogen depletion. Comparatively in *E. coli* batch culture (Hanai et al. 2007), nitrogen was not limiting which enabled a higher protein synthesis and biomass concentration considering the $\text{OD}_{600 \text{ nm}}$ reported (Dry Cell Weights were not estimated in the paper by Hanai et al.) (Table 7.1). The specific productivity and yields were calculated to better compare the performances of each strains. The overall specific productivity of Re2133/pEG7c was $0.044 \pm 0.006 \text{ g.g}^{-1}.\text{h}^{-1}$ ($0.016 \pm 0.001 \text{ g.L}^{-1}\text{OD}_{600\text{nm}}^{-1}\text{h}^{-1}$). The instantaneous maximal specific productivity of Re2133/pEG7c after induction by arabinose was $0.093 \text{ g.g}^{-1}.\text{h}^{-1}$, which corresponded to 62% of the maximum theoretical isopropanol production specific rate (Table 7.1). The maximum theoretical specific rate was calculated using the model developed by Grousseau et al. 2013, where the limiting rate of product formation was defined by the NADPH synthesis rate.

The overall yields of Re2133/pEG7c were respectively 1.3 and 1.8 times higher compared to the engineered isopropanol-producing *E. coli* strain (Hanai et al. 2007) and the engineered isopropanol-producing *C. acetobutylicum* strain (Dusséaux et al. 2013) (Table 7.1). The maximum yield reached by the strain Re2133/pEG7c corresponded to 64% of the theoretical yield ($0.5 \text{ Cmole.Cmole}^{-1}$). The strain Re2133/pEG7c will be further evaluated for the scale-up

production of isopropanol from various carbon sources. High cell density culture associated with a product recovery system with a controlled supply of nitrogen or any other limiting elements would be beneficial.

Table 7.1: Comparison of isopropanol producing-*R. eutropha* with other engineered isopropanol production organisms in batch culture.

References		Hanai et al., 2007	Tamakawa et al., 2013	This work		Theoretical maximum
Microorganism		<i>E. coli</i>	<i>Candida utilis</i>	<i>C. necator</i>		<i>C. necator</i>
Isopropanol	g.L ⁻¹	4.9	9.5	3.44	± 0.14	nc
Biomass	OD _{600nm}	20	nr	2.25	± 0.05	nc
Biomass	g.L ⁻¹	nr	nr	0.82 ^a	± 0.01	nc
Time	h	30.5	52	96.3		nc
Overall specific productivity	g.L ⁻¹ .OD _{600nm} ⁻¹ .h ⁻¹	0.008	nr	0.016	± 0.001	nc
Overall specific productivity	g.g ⁻¹ .h ⁻¹	nr	nr	0.044	± 0.006	nc
Maximum specific productivity	g.g ⁻¹ .h ⁻¹	nr	nr	0.093	± 0.004	0.15 ^b
Overall yield	Cmole.Cmole ⁻¹	0.18	nr	0.24	± 0.01	nc
Maximum Yield	Cmole.Cmole ⁻¹	0.22	nr	0.32	± 0.01	0.50 ^c

^a the CDW was calculated using the relationship: 1 OD_{600nm} = 0.363 g.L⁻¹

^b Calculated with kinetic modeling from Grousseau *et al.* 2013 considering a null growth rate

^c See Material and methods, 2.6. Yield calculation

nr: not reported, nc: not calculated

REFERENCES

- Aneja, K. K., R. D. Ashby and D. K. Solaiman (2009) "Altered composition of *Ralstonia eutropha* poly(hydroxyalkanoate) through expression of PHA synthase from *Allochromatium vinosum* ATCC 35206", *Biotechnol. Lett.* 31, (10), 1601-1612
- Aragao, G. M. F. (1996) "Production de poly-beta-hydroxyalkanoates par *Alcaligenes eutrophus*: caractérisation cinétique et contribution à l'optimisation de la mise en oeuvre des cultures", Institut National des Sciences Appliquées de Toulouse, Thèse n° d'ordre: 403
- Araki, S., H. Fukuhara, T. Isaka, F. Matsunaga and M. Yasuhara (1993), "Preparation of propylene by dehydration of isopropanol in the presence of a pseudo-boehmite derived gamma alumina catalyst", US5227563A
- Behura, S. K. and D. W. Severson (2012) "Codon usage bias: causative factors, quantification methods and genome-wide patterns: with emphasis on insect genomes", *Biol. Rev. Camb. Philos* 88, (1), 49-61
- Bruno, T. J., A. Wolk and A. Naydich (2009) "Composition-Explicit distillation curves for mixtures of gasoline with four-carbon alcohols (butanols)", *Energ. Fuels* 23, 2295-2306
- Budde, C. F., A. E. Mahan, J. N. Lu, C. Rha and A. J. Sinskey (2010) "Roles of multiple acetoacetyl Coenzyme A reductases in Polyhydroxybutyrate biosynthesis in *Ralstonia eutropha* H16", *J. Bacteriol.* 192, (20), 5319-5328
- Budde, C. F., S. L. Riedel, L. B. Willis, C. Rha and A. J. Sinskey (2011) "Production of Poly(3-Hydroxybutyrate-co-3-Hydroxyhexanoate) from plant oil by engineered *Ralstonia eutropha* strains", *Appl. Environ. Microbiol.* 77, (9), 2847-2854
- Cary, J. W., D. J. Petersen, E. T. Papoutsakis and G. N. Bennett (1990) "Cloning and expression of *Clostridium acetobutylicum* ATCC-824 acetoacetyl-Coenzyme A:acetate/butyrate:Coenzyme A transferase in *Escherichia coli*", *Appl. Environ. Microbiol.* 56, (6), 1576-1583
- Chen, J. S. and S. F. Hiu (1986) "Acetone-butanol-isopropanol production by *Clostridium beijerinckii* (Synonym, *Clostridium butylicum*)", *Biotechnol. Lett.* 8, (5), 371-376
- Collas, F., W. Kuit, B. Clement, R. Marchal, A. Lopez-Contreras and F. Monot (2012) "Simultaneous production of isopropanol, butanol, ethanol and 2,3-butanediol by *Clostridium acetobutylicum* ATCC 824 engineered strains", *AMB Express* 2, (1), 45
- Connor, M. R. and J. C. Liao (2009) "Microbial production of advanced transportation fuels in non-natural hosts", *Curr. Opin. Biotechnol.* 20, (3), 307-315
- Doi, Y., Y. Kawaguchi, Y. Nakamura and M. Kunioka (1989) "Nuclear magnetic-resonance studies of Poly(3-Hydroxybutyrate) and polyphosphate metabolism in *Alcaligenes eutrophus*", *Appl. Environ. Microbiol.* 55, (11), 2932-2938
- Dürre, P. (1998) "New insights and novel developments in clostridial acetone/butanol/isopropanol fermentation", *Appl. Microbiol. Biotechnol.* 49, (6), 639-648

Dusséaux, S., C. Croux, P. Soucaille and I. Meynial-Salles (2013) "Metabolic engineering of *Clostridium acetobutylicum* ATCC 824 for the high-yield production of a biofuel composed of an Isopropanol/Butanol/Ethanol mixture", *Metab. Eng.* 18, 1-8

Friedrich, C. G., B. Bowien and B. Friedrich (1979) "Formate and oxalate metabolism in *Alcaligenes eutrophus*", *J. Gen. Microbiol.* 115, (Nov), 185-192

Fukui, T., K. Ohsawa, J. Mifune, I. Orita and S. Nakamura (2010) "Evaluation of promoters for gene expression in polyhydroxyalkanoate-producing *Cupriavidus necator* H16", *Appl. Microbiol. Biotechnol.* 89, (5), 1527-1536

Fukui, T., M. Suzuki, T. Tsuge and S. Nakamura (2009) "Microbial Synthesis of Poly((R)-3-hydroxybutyrate-co-3-hydroxypropionate) from Unrelated Carbon Sources by Engineered *Cupriavidus necator*", *Biomacromol.* 10, (4), 700-706

Gibson, D. G., L. Young, R.-Y. Chuang, J. C. Venter, C. A. Hutchison and H. O. Smith (2009) "Enzymatic assembly of DNA molecules up to several hundred kilobases", *Nat. Methods* 6, (5), 343-345

Grousseau, E., E. Blanchet, S. Deleris, M. G. E. Albuquerque, E. Paul and J.-L. Uribealarea (2013) "Impact of sustaining a controlled residual growth on polyhydroxybutyrate yield and production kinetics in *Cupriavidus necator*", *Bioresource Technol.* 148, 30-38

Hanai, T., S. Atsumi and J. C. Liao (2007) "Engineered synthetic pathway for isopropanol production in *Escherichia coli*", *Appl. Environ. Microbiol.* 73, (24), 7814-7818

Inokuma, K., J. C. Liao, M. Okamoto and T. Hanai (2010) "Improvement of isopropanol production by metabolically engineered *Escherichia coli* using gas stripping", *J. Biosci. Bioeng.* 110, (6), 696-701

Ismail, A. A., C. X. Zhu, G. D. Colby and J. S. Chen (1993) "Purification and characterization of a primary-secondary alcohol dehydrogenase from two strains of *Clostridium beijerinckii*", *J. Bacteriol.* 175, (16), 5097-5105

Jang, Y. S., A. Malaviya, J. Lee, J. A. Im, S. Y. Lee, J. Lee, M. H. Eom, J. H. Cho and D. Y. Seung (2013) "Metabolic engineering of *Clostridium acetobutylicum* for the enhanced production of isopropanol-butanol-ethanol fuel mixture", *Biotechnol. Prog.* 29, (4), 1083-1088

Jendrossek, D., A. Steinbüchel and H. G. Schlegel (1988) "Alcohol dehydrogenase gene from *Alcaligenes eutrophus*: subcloning, heterologous expression in *Escherichia coli*, sequencing, and location of Tn5 insertions", *J. Bacteriol.* 170, (11), 5248-5256

Johnson, B. F. and R. Y. Stanier (1971) "Dissimilation of aromatic compounds by *Alcaligenes eutrophus*", *J. Bacteriol.* 107, (2), 468-483

Jojima, T., M. Inui and H. Yukawa (2008) "Production of isopropanol by metabolically engineered *Escherichia coli*", *Appl. Microbiol. Biotechnol.* 77, (6), 1219-1224

Kibby, C. L. and W. K. Hall (1973) "Studies of acid catalyzed reactions: XII. Alcohol decomposition over hydroxyapatite catalysts", *J. Catal.* 29, (1), 144-159

- Koller, M., A. Atlié, M. Dias, A. Reiterer and G. Brauneegg (2010) "Microbial PHA production from waste raw materials," in "Plastics from bacteria: natural functions and applications," Microbiology Monographs, G.-Q. Chen, 14: 85-119.
- Kovach, M. E., P. H. Elzer, D. S. Hill, G. T. Robertson, M. A. Farris, R. M. Roop, 2nd and K. M. Peterson (1995) "Four new derivatives of the broad-host-range cloning vector pBBR1MCS, carrying different antibiotic-resistance cassettes", Gene 166, (1), 175-176
- Krouwel, P. G., W. F. M. Vanderlaan and N. W. F. Kossen (1980) "Continuous production of normal-butanol and isopropanol by immobilized, growing *Clostridium butylicum* cells", Biotechnol. Lett. 2, (5), 253-258
- Kusakabe, T., T. Tatsuke, K. Tsuruno, Y. Hirokawa, S. Atsumi, J. C. Liao and T. Hanai (2013) "Engineering a synthetic pathway in cyanobacteria for isopropanol production directly from carbon dioxide and light", Metab. Eng. 20, 101-108
- Kusian, B., D. Sultemeyer and B. Bowien (2002) "Carbonic anhydrase is essential for growth of *Ralstonia eutropha* at ambient CO₂ concentrations", J. Bacteriol. 184, (18), 5018-5026
- Lee, S. Y., J. H. Park, S. H. Jang, L. K. Nielsen, J. Kim and K. S. Jung (2008a) "Fermentative butanol production by clostridia", Biotechnol. Bioeng. 101, (2), 209-228
- Lee, W. H., C. Y. Loo, C. T. Nomura and K. Sudesh (2008b) "Biosynthesis of polyhydroxyalkanoate copolymers from mixtures of plant oils and 3-hydroxyvalerate precursors", Bioresource Technol. 99, (15), 6844-6851
- Lim, H. N., Y. Lee and R. Hussein (2011) "Fundamental relationship between operon organization and gene expression", Proc. Natl. Acad. Sci. U. S. A. 108, (26), 10626-10631
- Lu, J., C. Brigham, C. Gai and A. Sinskey (2012a) "Studies on the production of branched-chain alcohols in engineered *Ralstonia eutropha*", Appl. Microbiol. Biotechnol. 96, (1), 283-297
- Lu, J., C. J. Brigham, C. Rha and A. J. Sinskey (2012b) "Characterization of an extracellular lipase and its chaperone from *Ralstonia eutropha* H16", Appl. Microbiol. Biotechnol. 97, (6), 2443-2454
- Matsumura, M., S. Takehara and H. Kataoka (1992) "Continuous butanol isopropanol fermentation in down-flow column reactor coupled with pervaporation using supported liquid membrane", Biotechnol. Bioeng. 39, (2), 148-156
- Nakamura, Y., T. Gojobori and T. Ikemura (2000) "Codon usage tabulated from international DNA sequence databases: status for the year 2000", Nucleic Acids Res. 28, (1), 292-292
- Ninfa, A. J., S. Selinsky, N. Perry, S. Atkins, Q. X. Song, A. Mayo, D. Arps, P. Woolf and M. R. Atkinson (2007) "Using two-component systems and other bacterial regulatory factors for the fabrication of synthetic genetic devices," in "Two-Component Signaling Systems, Pt A," Elsevier Academic Press Inc, M. I. Simon, B. R. Crane and A. Crane, San Diego, 422: 488-512
- Park, J. M., Y. S. Jang, T. Y. Kim and S. Y. Lee (2010) "Development of a gene knockout system for *Ralstonia eutropha* H16 based on the broad-host-range vector expressing a mobile group II intron", FEMS Microbiol. Lett. 309, (2), 193-200

- Park, J. S., H. C. Park, T. L. Huh and Y. H. Lee (1995) "Production of Poly-Beta-Hydroxybutyrate by *Alcaligenes eutrophus* transformants harboring cloned *phbcab* genes", *Biotechnol. Lett.* 17, (7), 735-740
- Peoples, O. P. and A. J. Sinskey (1989) "Poly-Beta-Hydroxybutyrate (PHB) biosynthesis in *Alcaligenes eutrophus* H16 - Identification and characterization of the PHB polymerase gene (*Phbc*)", *J. Biol. Chem.* 264, (26), 15298-15303
- Peralta-Yahya, P. P. and J. D. Keasling (2010) "Advanced biofuel production in microbes", *Biotechnol. J.* 5, (2), 147
- Pharkya, P., A. P. Burgard, E. Robin, M. J. Burk and J. Sun (2011), "Microorganisms and Methods for the co-production of isopropanol with primary alcohols, diols, and acids", US 2011/0201068 A1
- Pohlmann, A., W. F. Fricke, F. Reinecke, B. Kusian, H. Liesegang, R. Cramm, T. Eitinger, C. Ewering, M. Pötter, E. Schwartz, A. Strittmatter, I. Voss, G. Gottschalk, A. Steinbüchel, B. Friedrich and B. Bowien (2006) "Genome sequence of the bioplastic-producing "Knallgas" bacterium *Ralstonia eutropha* H16", *Nat. Biotechnol.* 24, (10), 1257-1262
- Pötter, M., M. H. Madkour, F. Mayer and A. Steinbüchel (2002) "Regulation of phasin expression and polyhydroxyalkanoate (PHA) granule formation in *Ralstonia eutropha* H16", *Microbiol.* 148, (Pt 8), 2413-2426
- Reinecke, F. and A. Steinbüchel (2009) "*Ralstonia eutropha* strain H16 as model organism for PHA metabolism and for biotechnological production of technically interesting biopolymers", *J. Mol. Microbiol. Biotechnol.* 16, (1-2), 91-108
- Repaske, R. and R. Mayer (1976) "Dense autotrophic cultures of *Alcaligenes eutrophus*", *Appl. Environ. Microbiol.* 32, (4), 592-597
- Schendel, F. J., E. J. Baude and M. C. Flickinger (1989) "Determination of protein expression and plasmid copy number from cloned genes in *Escherichia coli* by flow injection analysis using an enzyme indicator vector", *Biotechnol. Bioeng.* 34, (8), 1023-1036
- Schlegel, H. G. (1990) "*Alcaligenes eutrophus* and its scientific and industrial career", *NATO Adv. Sci. I. E.-App.* 186, 133-141
- Schwartz, E., A. Henne, R. Cramm, T. Eitinger, B. r. Friedrich and G. Gottschalk (2003) "Complete nucleotide sequence of pHG1: a *Ralstonia eutropha* H16 Megaplasmid encoding key enzymes of H₂-based lithoautotrophy and anaerobiosis", *J. Mol. Biol.* 332, (2), 369
- Shen, C. R., E. I. Lan, Y. Dekishima, A. Baez, K. M. Cho and J. C. Liao (2011) "Driving forces enable high-titer anaerobic 1-butanol synthesis in *Escherichia coli*", *Appl. Environ. Microbiol.* 77, (9), 2905-2915
- Simon, R., U. Prierer and A. Pühler (1983) "A broad host range mobilization system for in vivo genetic engineering: transposon mutagenesis in gram negative bacteria", *Nat. Biotech.* 1, (9), 784
- Slater, S., K. L. Houmiel, M. Tran, T. A. Mitsky, N. B. Taylor, S. R. Padgett and K. J. Gruys (1998) "Multiple beta-ketothiolases mediate poly(beta-hydroxyalkanoate) copolymer synthesis in *Ralstonia eutropha*", *J. Bacteriol.* 180, (8), 1979-1987

Steinbüchel, A., C. Fründ, D. Jendrossek and H. G. Schlegel (1987) "Isolation of mutants of *Alcaligenes eutrophus* unable to derepress the fermentative alcohol-dehydrogenase", Arch. Microbiol. 148, (3), 178-186

Steinbüchel, A. and H. G. Schlegel (1984) "A multifunctional fermentative alcohol-dehydrogenase from the strict aerobic *Alcaligenes eutrophus* - purification and properties", Eur. J. Biochem. 141, (3), 555-564

Survase, S. A., G. Jurgens, A. van Heiningen and T. Granstrom (2011) "Continuous production of isopropanol and butanol using *Clostridium beijerinckii* DSM 6423", Appl. Microbiol. Biotechnol. 91, (5), 1305-1313

Tamakawa, H., T. Mita, A. Yokoyama, S. Ikushima and S. Yoshida (2013) "Metabolic engineering of *Candida utilis* for isopropanol production", Appl. Microbiol. Biotechnol. 97, (14), 6231-6239

Tanaka, K., A. Ishizaki, T. Kanamaru and T. Kawano (1995) "Production of Poly(D-3-Hydroxybutyrate) from CO₂, H₂, and O₂ by high cell-density autotrophic cultivation of *Alcaligenes eutrophus*", Biotechnol. Bioeng. 45, (3), 268-275

Vollbrecht, D., M. A. Elnawawy and H. G. Schlegel (1978) "Excretion of metabolites by hydrogen bacteria.1. Autotrophic and heterotrophic fermentations", Eur. J. Appl. Microbiol. Biotechnol. 6, (2), 145-155

Wahl, A., N. Schuth, D. Pfeiffer, S. Nussberger and D. Jendrossek (2012) "PHB granules are attached to the nucleoid via PhaM in *Ralstonia eutropha*", BMC Microbiol. 12, (1), 262

Wilde, E. (1962) "Untersuchungen über wachstum und speicherstoffsynthese von *Hydrogenomonas*", Arch. Microbiol. 43, (2), 109

York, G. M., J. Stubbe and A. J. Sinskey (2002) "The *Ralstonia eutropha* PhaR protein couples synthesis of the PhaP phasin to the presence of polyhydroxybutyrate in cells and promotes polyhydroxybutyrate production", J. Bacteriol. 184, (1), 59-66

Yu, K., S. Hu, J. Huang and L.-H. Mei (2011) "A high-throughput colorimetric assay to measure the activity of glutamate decarboxylase", Enzyme Microb. Technol. 49, (3), 272-276

APPENDIX

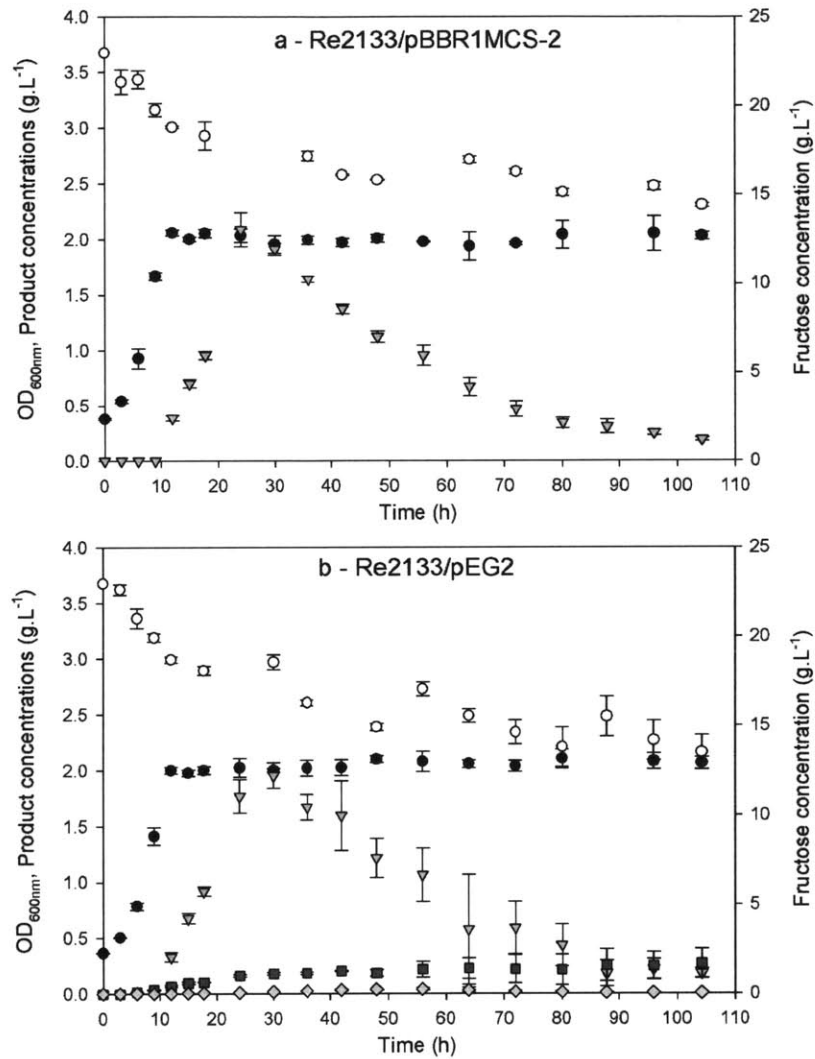
Appendix 7.1: Sequence of codon-optimized *adc* (CA_P0165) from *C. acetobutylicum*, encoding for an acetoacetate decarboxylase, followed by a synthetic Ribosome Binding Site and a six nucleotide linker, and of *adh* (AF157307) from *C. beijerinckii*, encoding for an alcohol dehydrogenase (GenScript USA Inc. (Piscataway, NJ, USA)).

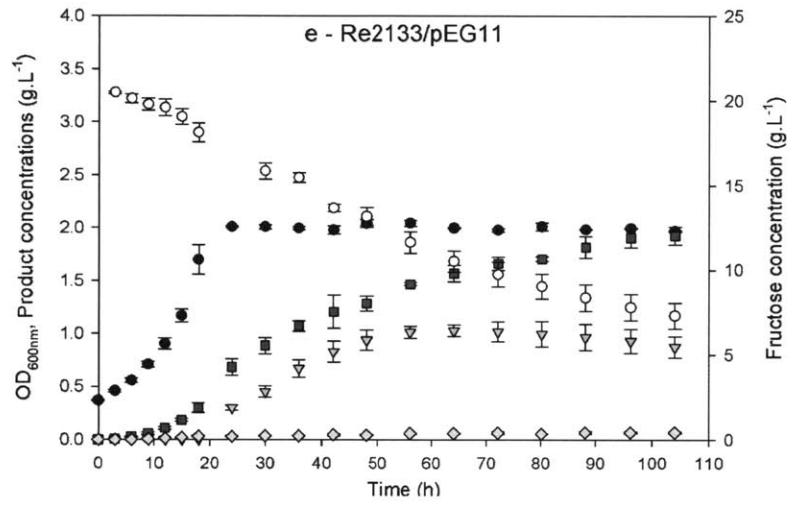
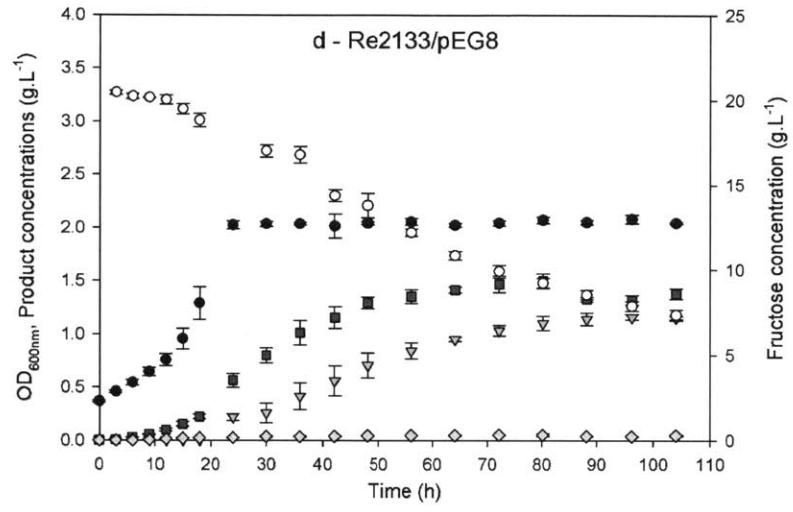
```
ATGCTGAAGGACGAAGTCATCAAGCAGATCTCGACCCCGCTGACGAGCCCGGCGTTCCCGC
GCGGCCCGTACAAGTTCACAACCGCGAATACTTCAACATCGTGTACCGCACCGACATGGAC
GCGCTGCGCAAGGTGGTCCCAGGAGCCGCTGGAAATCGACGAGCCGCTGGTCCGCTTCGAAA
TCATGGCGATGCACGACACCAGCGGCCTGGGCTGCTACACGGAGAGCGGCCAGGCCATCCC
GGTGTTCGTTCAACGGCGTCAAGGGCGACTACCTGCATATGATGTACCTGGACAACGAACCG
GCCATCGCGGTGGGCCGCGAGCTGAGCGCCTACCCGAAGAAGCTGGGCTACCCGAAGCTGT
TCGTGGACTCGGACACCCTGGTTCGGCACGCTGGACTACGGCAAGCTGCGCGTGGCCACCGC
GACGATGGGCTACAAGCACAAGGCCCTGGACGCGAACGAGGCCAAGGACCAGATCTGCCGC
CCGAACTACATGCTGAAGATCATCCCGAACTACGACGGCTCGCCGCGCATCTGCGAACTGAT
CAACGCGAAGATCACCGACGTCACGGTCCACGAGGCCTGGACCGGCCCGACGCGCCTGCAG
CTGTTTCGACCATGCCATGGCGCCGCTGAACGACCTGCCGGTGAAGGAAATCGTGTTCGTCGTC
GCATATCCTGGCGGACATCATCCTGCCGCGCGCAGAGGTGATCTACGACTACCTGAAGTGAA
AAGGAGGACAACCATGAAGGGCTTCGCCATGCTGGGCATCAACAAGCTGGGCTGGATCGAA
AAGGAACGCCCGGTTCGCCGGCTCGTACGACGCCATCGTGCGCCCGCTGGCCGTGTCGCCGTG
CACCAGCGACATCCACACGGTGTTCGAGGGCGCCCTGGGCGACCGCAAGAACATGATCCTG
GGCCATGAGGCGGTGGGCGAGGTGGTTCGAAGTCGGCAGCGAAGTGAAGGACTTCAAGCCGG
GCGACCGCGTCATCGTGCCGTGCACCACGCCGACTGGCGCTCGCTGGAGGTGCAGGCCGG
CTTCCAGCAGCACAGCAACGGCATGCTGGCGGGCTGGAAGTTCTCGAACTTCAAGGACGGC
GTCTTCGGCGAATACTTCCATGTGAACGACGCCGACATGAACCTGGCGATCCTGCCGAAGGA
CATGCCGCTGGAGAACGCCGTGATGATCACCGACATGATGACCACGGGCTTCCACGGCGCC
GAACTGGCGGACATCCAGATGGGCTCGTTCGGTGGTTCGTGATCGGCATCGGCGCCGTGGGCCT
GATGGGCATCGCCGGCGCGAAGCTGCGCGGCGCGGGCCGCATCATCGGCGTTCGGCAGCCGC
CCGATCTGCGTGGAGGCCGCGAAGTTCTACGGCGCGACCGACATCCTGAACTACAAGAACG
GCCACATCGTCGACCAGGTGATGAAGCTGACCAACGGCAAGGGCGTCGACCGCGTGATCAT
GGCCGGCGGCGGCTCGGAAACGCTGAGCCAGGCGGTCTCGATGGTGAAGCCGGGCGGCATC
ATCAGCAACATCAACTACCACGGCTCGGGCGACGCCCTGCTGATCCCGCGCGTGGAGTGGG
GCTGCGGCATGGCGCATAAGACCATCAAGGGCGGCCTGTGCCCGGGCGGCCCGCTGCGCGC
CGAAATGCTGCGCGACATGGTTCGTGTACAACCGCGTGGACCTGTCGAAGCTGGTGACCCAC
GTGTACCATGGCTTCGACCACATCGAGGAAGCCCTGCTGCTGATGAAGGACAAGCCGAAGG
ACCTGATCAAGGCGGTTCGTGATCCTGTGA
```

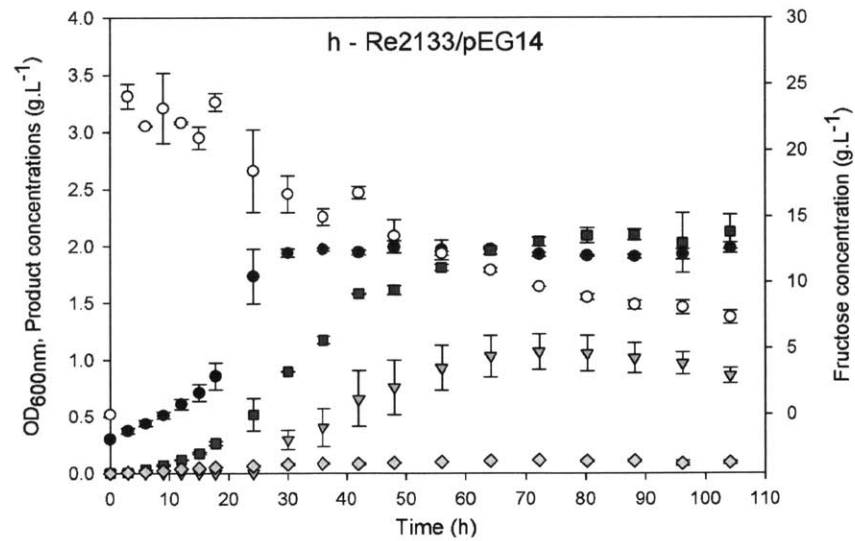
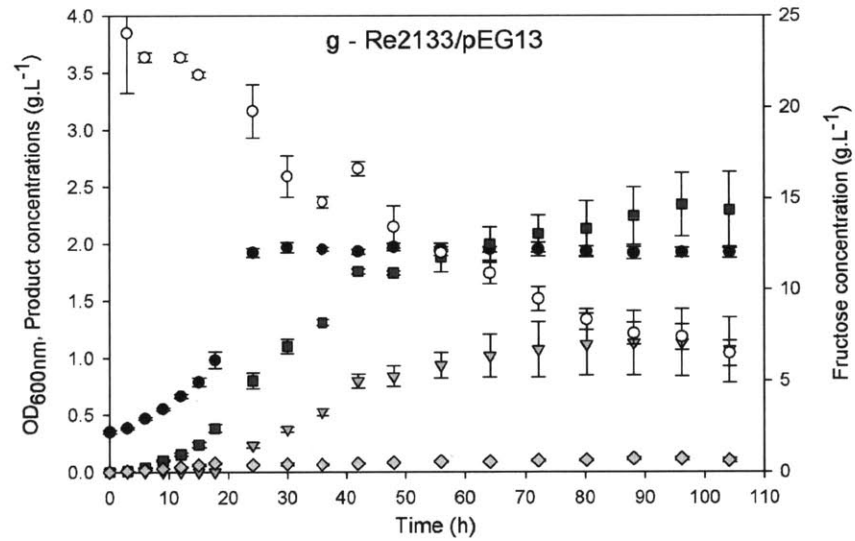
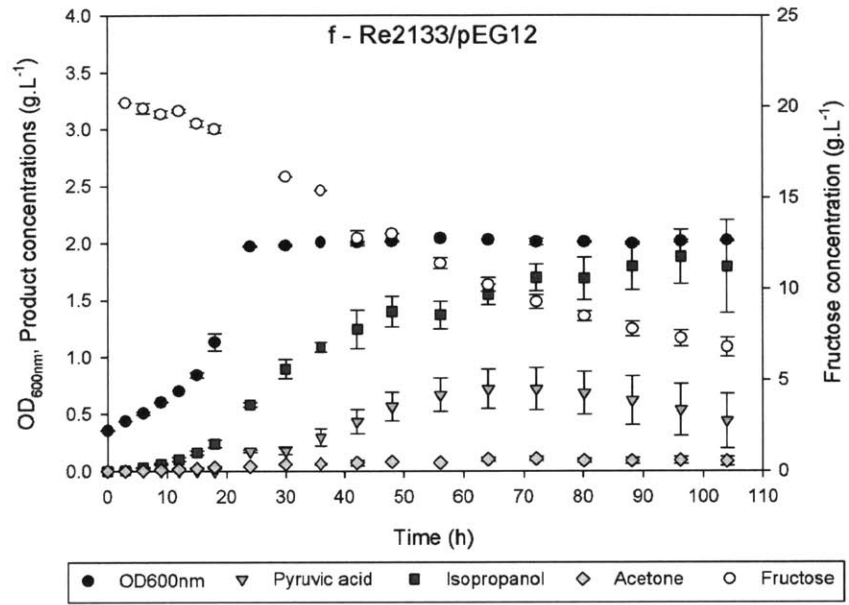
Appendix 7.2: Primers used in this study.

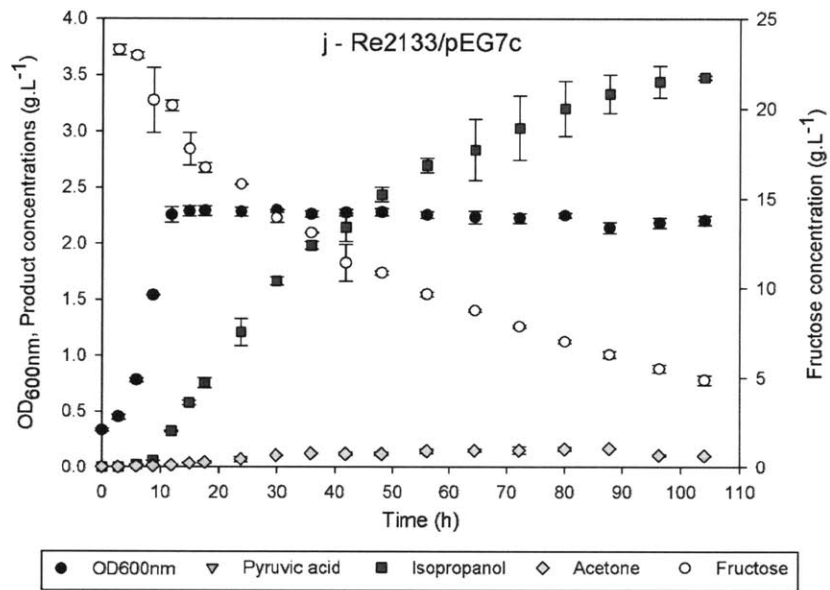
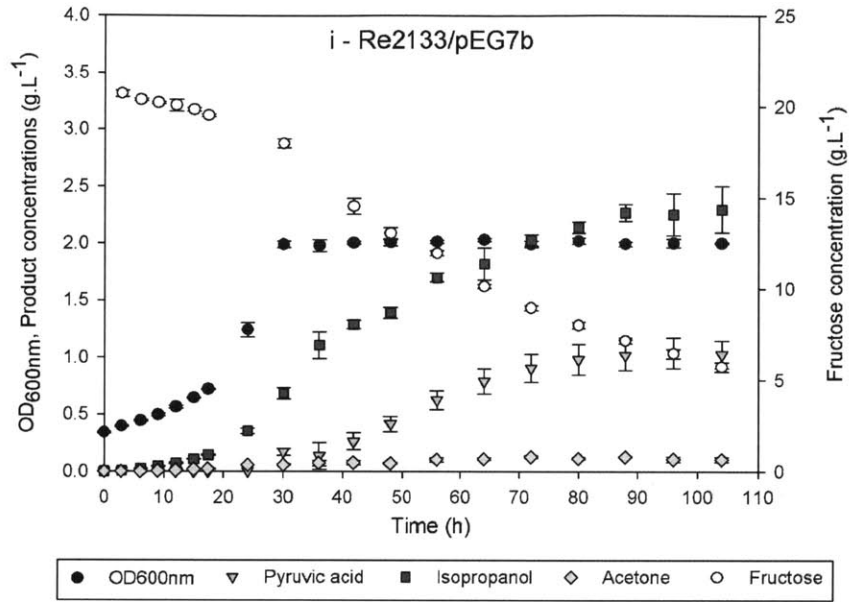
Primer name	Sequence
5'-OL pBBR1MCS-2 phaA	GGGTACCGGGCCCCCCTCGAGATGACTGACGTTGTCATCGTATCC
3'-OL ctfAB phaA	GCTGGCGTAGACCTTGTTTCATGGTTGTCCTCCTTTTTATTTGCGCTCGACTGCCAG
5'-OL phaA ctfAB	CTGGCAGTCGAGCGCAAATAAAAAGGAGGACAACCATGAACAAGGTCTACGCCAG C
3'-OL adc ctfAB	GTTTAATTACTTCATCCTTTAACATGGTTGTCCTCCTTTTTACAGCAGCGGAGCGCCA GTCTTGG
5'-OL ctfAB adc	CCAAGACTGGCGCTCCGCTGCTGTAAAAAGGAGGACAACCATGTTAAAGGATGAAG TAATTA AAC
3'-OL adh adc	CTAGCATTGCAAAACCTTTCATGGTTGTCCTCCTTTTTACTTAAGATAATCATATATA AC
5'-OL adc adh	GTTATATATGATTATCTTAAGTAAAAAGGAGGACAACCATGAAAGGTTT
3'-OL pBBR1MCS-2 adh	GCAGGAATTCGATATCAAGCTTATCGATTTATAATAACTACTGCTTTAATTAAGT C
3'-OL adc* ctfAB	GCTTGATGACTTCGTCCTTCAGCATGGTTGTCCTCCTTTTTACAGCAGCGGAGCGCC
5'-OL ctfAB adc*	GGCGCTCCGCTGCTGTAAAAAGGAGGACAACCATGCTGAAGGACGAAGTCATCAAG C
3'-OL pBBR1MCS-2 adh*	CCCGGGCTGCAGGAATTCGATATCAAGCTTATCGATTCACAGGATCACGACCGCC
5'-OL pBBR1MCS-2 adc*	CCGGGCCCCCCTCGAGAAAGGAGGACAACCATGCTGAAGGACGAAGTCATCAAG
3'-OL adc* phaA	GCTTGATGACTTCGTCCTTCAGCATGGTTGTCCTCCTTTTTATTTGCGCTCGACTGCC
5'-OL phaA adc*	GGCAGTCGAGCGCAAATAAAAAGGAGGACAACCATGCTGAAGGACGAAGTCATCA AGC
3'-OL phaA phaA	GGATACGATGACAACGTCAGTCATGGTTGTCCTCCTTTTTATTTGCGCTCGACTGCCA
5'-OL phaA phaA	TGGCAGTCGAGCGCAAATAAAAAGGAGGACAACCATGACTGACGTTGTCATCGTAT CC
3'-OL adh* adh*	GCATGGCGAAGCCCTTCATGGTTGTCCTCCTTTTTACAGGATCACGACCGCC
5'-OL adh* adh*	GGCGGTTCGTGATCCTGTGAAAAGGAGGACAACCATGAAGGGCTTCGCCATGC
3'-OL adh_reh adc*	GGCTTTCATCATTGCGGTCATGGTTGTCCTCCTTTTCACTTCAGGTAGTCGTAGATCA CC
5'-OL adc* adh_reh	GGTGATCTACGACTACCTGAAGTGAAAAGGAGGACAACCATGACCGCAATGATGAA AGCC
3'-OL pBBR1MCS-2 adh_reh	GCAGGAATTCGATATCAAGCTTATCGATTCAGTGCGGCTTGATGGC
5'-OL Ptac pBBR1MCS-2	TTGACAATTAATCATCGGCTCGTATAATGTGTGGAATTGTGAGCGGATAACAATTC
3'-OL Ptac pBBR1MCS-2	CATTATACGAGCCGATGATTAATTGTCAAGCCTGGGGTGCCTAATGAG

Appendix 7.3: Evaluation of substrate and products over cultivation time on strains Re2133/pBBR1MCS-2, Re2133/pEG2, Re2133/pEG7a, Re2133/pEG8, Re2133/pEG11, Re2133/pEG12, Re2133/pEG13, Re2133/pEG14, Re2133/pEG7b, and Re2133/pEG7c. Genotype of each plasmid can be found in Figure 7.2.

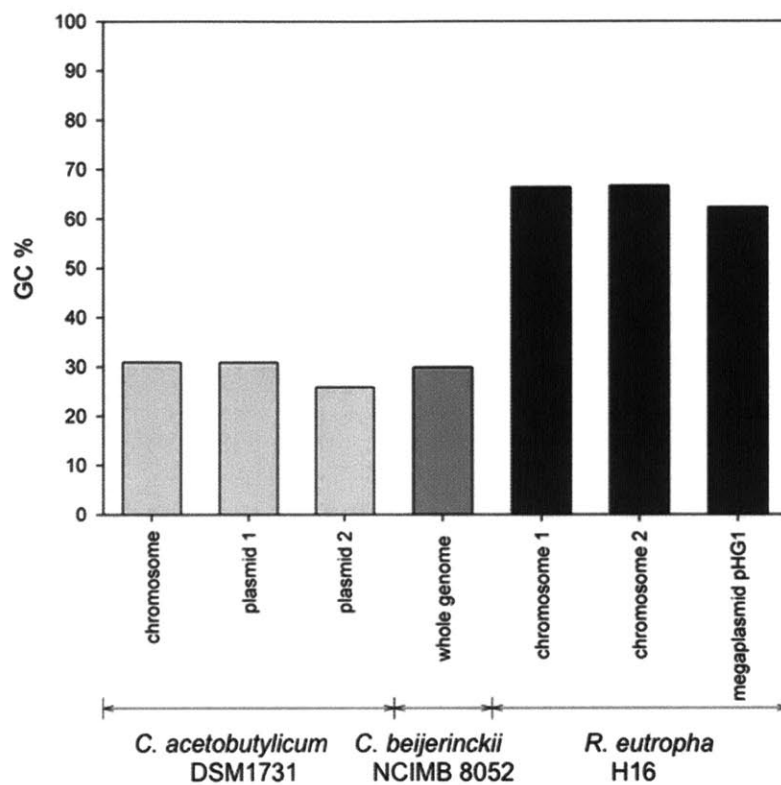








Appendix 7.4: GC content of *C. acetobutylicum* DSM 1731 genome, *C. beijerinckii* NCIMB 8052 genome, and *R. eutropha* H16 genome.



Appendix 7.5: Comparative table of codon usage in *R. eutropha*, *C. acetobutylicum*, and *C. beijerinckii*.

DNA Codon	SLC	% of usage			DNA Codon	SLC	% of usage		
		<i>C. necator</i> H16	<i>C. Beijerinckii</i> NCIMB 8052	<i>C. acetobutylicum</i>			<i>C. necator</i> H16	<i>C. Beijerinckii</i> NCIMB 8052	<i>C. acetobutylicum</i>
UUU	F			85%	UUU	F	18%	82%	74%
UUC	F			15%	UUC	F	82%	18%	26%
UUA	L			100%	UUA	L	0%	51%	53%
UUG	L			0%	UUG	L	6%	12%	14%
CUU	L			0%	CUU	L	5%	21%	19%
CUC	L			0%	CUC	L	14%	2%	0%
CUA	L			0%	CUA	L	1%	12%	10%
CUG	L			0%	CUG	L	74%	3%	3%
CAU	H	36%	83%	79%	AUU	I	12%	43%	31%
CAC	H	64%	17%	21%	AUC	I	85%	7%	5%
CAA	Q	14%	77%	86%	AUA	I	2%	50%	64%
CAG	Q	86%	23%	14%	AUG	M	100%	100%	100%
AAU	N	24%	84%	79%	GUU	V	5%	44%	48%
AAC	N	76%	16%	21%	GUC	V	32%	4%	1%
AAA	K	10%	70%	67%	GUA	V	4%	42%	39%
AAG	K	90%	30%	33%	GUG	V	59%	10%	12%
GAU	D	26%	87%	86%	UCU	S	3%	24%	25%
GAC	D	74%	13%	14%	UCC	S	18%	4%	7%
GAA	E	40%	79%	73%	UCA	S	4%	30%	29%
GAG	E	60%	21%	27%	UCG	S	37%	4%	0%
UGU	C	9%	70%	83%	AGU	S	3%	27%	31%
UGC	C	91%	30%	7%	AGC	S	35%	11%	8%
UGG	W	100%	100%	100%	CCU	P	6%	38%	36%
CGU	R	8%	8%	24%	CCC	P	27%	3%	4%
CGC	R	68%	2%	3%	CCA	P	6%	53%	52%
CGA	R	3%	4%	3%	CCG	P	61%	7%	8%
CGG	R	17%	1%	0%	ACU	T	5%	43%	42%
AGA	R	1%	71%	59%	ACC	T	57%	6%	4%
AGG	R	4%	15%	12%	ACA	T	4%	46%	47%
GGU	G	7%	29%	31%	ACG	T	34%	5%	7%
GGC	G	76%	9%	9%	GCU	A	5%	39%	37%
GGA	G	4%	52%	51%	GCC	A	47%	6%	11%
GGG	G	13%	10%	9%	GCA	A	9%	48%	45%
					GCG	A	39%	7%	7%

CHAPTER 8

Characterization of an extracellular lipase and its chaperone from *Ralstonia eutropha* H16

(This chapter was modified from a previously published article in Applied Microbiology and Biotechnology, 2013. 97: 2443-2454 'Characterization of an extracellular lipase and its chaperone from *Ralstonia eutropha* H16' Jingnan Lu, Christopher Bringham, ChoKyun Rha, and Anthony Siskey © Springer-Verlag)

INTRODUCTION

Lipases (triacylglycerol acylhydrolases) are ubiquitous enzymes in nature. They play a crucial role in fat metabolism by catalyzing the hydrolysis of triacylglycerol to free fatty acids and glycerol at the interface of lipid and water (Gupta et al. 2004; Jaeger and Reetz 1998). Although lipases are highly chemo-, regio-, and chiral- selective enzymes, they also process esterolytic activities for the carboxyl ester bond cleavage of water-insoluble esters (Jaeger and Reetz 1998; Reis et al. 2009; Treichel et al. 2010). Lipases can also catalyze the reverse reaction in the presence of a low water concentration (Franken et al. 2010; Park et al. 2005; Severac et al. 2011).

Lipases are serine hydrolases with a conserved catalytic triad: serine, aspartate or glutamate, and histidine. These three amino acid residues always appear in this order, but are distant from each other in the lipase primary sequence. In the lipase tertiary structure, the catalytic triads are positioned within a close distance to each other in order to catalyze the hydrolysis reaction (Arpigny and Jaeger 1999; Gupta et al. 2004; Jaeger and Reetz 1998; Jaeger et al. 1999). The mechanism of cleavage involves the deprotonated serine hydroxyl group nucleophilically attacking the carbonyl carbon of the lipid ester bond. A proton is then transferred from the triad residues to the substrate hydroxyl group resulting in the cleavage of the ester bond between the fatty acid and glycerol backbone. The intermediate fatty ester is then attacked by water to regenerate the catalytic triad and fatty acid (Reis et al. 2009). A characteristic α/β hydrolase fold was found in all lipase crystallographic structures solved to date, including bacterial *Pseudomonas* and *Bacillus* lipases, fungal *Rhizomucor* lipases, and horse and human pancreatic lipases (Arpigny and Jaeger 1999; Bourne et al. 1994; Derewenda et al. 1992; Jaeger and Reetz 1998; Noble et al. 1993; Roussel et al. 1999; Schrag and Cygler 1997; van Pouderoyen et al. 2001). Since lipase enzymes catalyze reactions at the interface of water and neutral water-insoluble ester substrates, the catalytic triad that is buried in the structure must surface in order to access the substrate (Cherukuvada et al. 2005; Reis et al. 2009; Wang et al. 2007). This major conformational change results in lipase activity being highly inducible by lipids, hydrolysable esters, Tween detergents, glycerol, or bile salts (Boekema et al. 2007; Franken et al. 2010; Gupta et al. 2004; Kim et al. 1996; Lotti et al. 1998; Mahler et al. 2000).

Due to the high stability, selectivity, and specificity of lipases, they have been used extensively in food, detergent, cosmetic, synthesis, and pharmaceutical industries (Jaeger and Reetz 1998; Park et al. 2005; Treichel et al. 2010). Bacterial lipases, especially enzymes from *Bacillus*, *Pseudomonas*, *Burkholderia*, and *Straphylococcus* species, have been extensively studied and used commercially (Gupta et al. 2004; Jaeger and Eggert 2002; Pandey et al. 1999; Rosenstein and Gotz 2000; Sanchez et al. 2002). These lipases are mostly extracellular which

makes bulk production straightforward. Although many efforts have been made to increase lipase production in heterologous hosts like *Escherichia coli*, only a few heterologously-produced lipases are enzymatically active, because lipase gene expression and secretion are strictly regulated in the host organism (Rosenau and Jaeger 2000).

The metabolically versatile betaproteobacterium *Ralstonia eutropha* strain H16 is able to grow on various carbon sources including lipids and some detergents (Tween) (Budde et al. 2011a; Riedel et al. 2012; Yang et al. 2010; Budde et al. 2011b; Kahar et al. 2004; Ng et al. 2010). Since bacteria can only transport free fatty acids into the cytoplasm and utilize them via the β -oxidation pathway for the generation of the cellular building block acetyl-CoA and energy, lipids such as triacylglycerol and Tween compounds must be processed first by a secreted lipase enzyme (Budde et al. 2011a; Budde et al. 2011b; Gupta et al. 2004; Treichel et al. 2010). Previous microarray analysis by Brigham et al. on global gene expression of *R. eutropha* H16 revealed two putative lipase genes (locus tags H16_A1322 and H16_A3742) that were upregulated during trioleate growth. Deletion of lipase H16_A1322 (GeneID, 4249488) in *R. eutropha* H16 resulted in strain Re2313, which, unlike the wild type strain, was unable to emulsify palm oil in flask cultures. This suggested that lipase H16_A1322 played a role in the breakdown of triacylglycerol molecules in palm oil, and this breakdown of oil provided diacylglycerol, monoacylglycerol, and free fatty acids for emulsification of palm oil remaining in the culture (Brigham et al. 2010).

In this study, the *R. eutropha* H16 extracellular lipase (encoded by H16_A1322; henceforth known as LipA) and its concomitant chaperone (henceforth known as LipB) were identified and characterized. The properties of this lipase including relevant physicochemical characteristics and substrate specificities were examined and reported here.

MATERIALS AND METHODS

Bacterial strains and plasmids

Experiments were performed with the strains and plasmids listed in Table 8.1 and 8.2 respectively. Mutants were derived from wild-type *Ralstonia eutropha* H16 (ATCC 17699).

Table 8.1: Strains used in this study.

Strains	Genotype	Reference
<i>R. eutropha</i>		
H16	Wild-type, gentamicin resistant (Gen ^r)	ATCC17699
Re2313	H16 Δ <i>lipA</i> Gen ^r	(Brigham <i>et al.</i> , 2010)
Re2314	H16 Δ (H16_A3742) Gen ^r	This work
Re2315	H16 Δ <i>lipA</i> & A3742 Gen ^r	This work
Re2318	H16 Δ <i>lipB</i> Gen ^r	This work
<i>E. coli</i>		
S17-1	Conjugation strain for transfer of plasmids into <i>R. eutropha</i>	(Simon <i>et al.</i> , 1983)

Table 8.2: Plasmids used in this study.

Plasmids	Genotype	Reference
pJV7	pJQ200Kan with Δ <i>phaC1</i> allele inserted into BamHI restriction site, confers kanamycin resistance (Kan ^r)	(Budde <i>et al.</i> , 2011a)
pJL31	pJV7 with Δ <i>phaC1</i> allele removed by XbaI and SacI digestion and replace with Δ <i>lipB</i> allele (Kan ^r)	This work
pBBR1MCS-2	Broad-host-range cloning vector (Kan ^r)	(Simon <i>et al.</i> , 1983)
pCJB201	pBBR1MCS-2 with <i>R. eutropha lipA</i> gene inserted into the multiple cloning site (Kan ^r)	(Brigham <i>et al.</i> , 2010)
pJL36	pBBR1MCS-2 with <i>R. eutropha lipB</i> gene inserted into the multiple cloning site (Kan ^r)	This work

Growth media and cultivation conditions

All *R. eutropha* strains were cultivated aerobically in rich and minimal media with an initial pH of 6.8 at 30°C. Rich medium consisted of 2.75% (w/v) dextrose-free tryptic soy broth (TSB) (Becton Dickinson, Sparks, MD). Minimal medium was produced with the following salts: 4.0 g/L NaH₂PO₄, 4.6 g/L Na₂HPO₄, 0.45 g/L K₂SO₄, 0.39 g/L MgSO₄, 0.062 g/L CaCl₂, 0.05% (w/v) NH₄Cl, and 1 ml/L of a trace metal solution. The trace metal solution was prepared with 15 g/L FeSO₄·7H₂O, 2.4 g/L MnSO₄·H₂O, 2.4 g/L ZnSO₄·7H₂O, and 0.48 g/L CuSO₄·5H₂O in 0.1 M HCl. Carbon sources used were 1% palm oil (Wilderness Family Naturals, Silver Bay, MN) or 0.5% Tween-60 (Sigma-Aldrich). For all *R. eutropha* cultures, 10 µg/mL final concentration gentamicin was added. Kanamycin at 300 µg/mL concentration was added to *R. eutropha* with plasmid.

A single colony of *R. eutropha* from a TSB agar plate was used to inoculate 5 mL of TSB medium. The culture was then incubated on a roller drum for 24 h before being used to inoculate a 100 mL minimal medium flask culture, containing carbon sources mentioned above, to an initial OD₆₀₀ of 0.05. The 100 mL minimal medium culture was continuously shaken in a 30°C incubator at 200 rpm. Aliquots were removed from the flask culture at intermittent time points for analysis. OD₆₀₀ of cultures of each strain were measured throughout the cultivation period.

Plasmid and strain construction

Gene deletions from *R. eutropha* H16 genome were carried out by a standard procedure described previously (Quandt and Hynes 1993; York *et al.* 2001). Standard molecular biology techniques were performed for all DNA manipulations (Chong 2001).

The plasmid for markerless deletion was constructed by first amplifying approximately 500 base pairs of DNA sequence upstream and downstream of the target deletion gene using primers with identical sequence overlap at the end (Appendix 8.1). Overlap PCR using these primers resulted in a DNA fragment that contained both the upstream and downstream region of the target deletion gene. The resulting DNA fragment and parent plasmid, pJV7 (Table 8.2), were digested with the restriction enzymes XbaI and SacI (New England Biolabs, Ipswich, MA) and then ligated together to create the gene deletion plasmid. The gene deletion plasmid was

transformed into *Escherichia coli* S17-1 (Simon et al. 1983), which was used as a donor for the conjugative transfer of mobilizable plasmids. A standard mating-procedure was performed to introduce the gene deletion plasmid into *R. eutropha* via conjugation (Slater et al. 1998). Deletion strains were screened via diagnostic PCR with pairs of internal and external primer sets (Appendix 8.1).

Lipids extraction and thin layer chromatography analysis

Lipids from palm oil culture supernatants were qualitatively analyzed by thin layer chromatography (TLC). A 10 mL aliquot of culture was taken at different time points during the growth of *R. eutropha* H16 and mutant strains on palm oil as the sole carbon source. Samples were spun down via centrifugation at $4,000 \times g$, room temperature to separate supernatant from cell pellets. The lipids in the supernatant were extracted with 5 mL of chloroform/methanol (2:1, v/v) for 1 min with continuous mixing by vortex. The chloroform layer was removed, allowed to dry, and re-dissolved in fresh chloroform to a final concentration of 5 mg/mL. Aliquots of 10 μ L (50 μ g lipids) were spotted on silica gel TLC plate (EMD Chemicals, Gibbstown, NJ; 250 μ m thickness). A mixture with 10 μ g each of triacylglycerol (TAG: 1,2-distearoyl-3-oleoyl-rac-glycerol), diacylglycerol (DAG: 1,2-dipalmitoyl-rac-glycerol), monoacylglycerol (MAG: 1-palmitoyl-rac-glycerol) and free fatty acid (FFA: palmitate) (Nu-check Prep, Inc., Elysian MN) was also spotted as a standard. The TLC plate was developed first with chloroform/methanol/water (60:35:5, v/v) to 5 cm above the origin and then with hexane/diethyl ether/acetic acid (69.5:29.5:1, v/v). To visualize TAGs and lipase products, a 3% (w/v) cupric acetate solution in 8% (v/v) phosphoric acid was sprayed lightly and evenly onto the plate. The plate was placed in an oven ($\sim 200^\circ\text{C}$) for 10 to 30 min to char and then imaged with a camera (Canon, PowerShot Digital SD1200 IS).

Lipase Activity assay

Extracellular lipase activity was estimated using a modified protocol from Ng *et al.* with *p*-nitrophenyl palmitate (*p*NP) as a substrate (Ng et al. 2010). The assay mixture contains 100 mM glycine-HCl buffer at pH 7.0 and 0.1% (w/v) polyvinyl alcohol. Cell-free supernatant was added to the assay mixture to a final volume of 900 μ L and incubated at room temperature for 5 min. The reaction was initiated by the addition of 0.19 mg *p*NP in 100 μ L dimethyl sulphoxide. The absorbance was recorded at OD₄₀₅ by a spectrophotometer (Agilent 8453 UV-visible). Control assay mixtures do not contain substrate or cell-free supernatant. One enzyme unit (U) was defined as one μ mol *p*-nitrophenol liberated per min using extinction coefficient of $1.78 \times 10^4 \text{ M}^{-1} \text{ cm}^{-1}$.

Effect of pH, temperature, metal ions, and detergents

The effect of pH on lipase activity was tested using 100 mM buffers at various pH values from 3 to 12. Glycine-HCl buffer was used for the pH range from 3 to 7; pH values from 7.5 to 9 were achieved using Tris buffer; and glycine-NaOH buffer was utilized for pH values from 9.5 to 12. Cell-free supernatant was incubated with the various pH buffers at room temperature for 15 min prior to initiation of the reaction with the *p*NP substrate.

Temperature effect on lipase activity was assayed using a circulating-bath system (VWR) coupled to the spectrophotometer. Assay mixture of glycine-HCl (pH 7.0) and supernatant were incubated at various temperatures from 0 to 80°C for 15 min prior to the start of the reaction.

To test the effect of metals and chelating agents on lipase activity, metal ions (ZnCl₂, MgCl₂, FeCl₂·4H₂O, CaCl₂·2H₂O, CuCl₂·2H₂O, MnCl₂·4H₂O, or NiCl₂·6H₂O) and chelators (EDTA, EGTA) at concentrations of 0.1 mM or 1 mM were added to the assay mixture with glycine-HCl (pH 7.0) buffer and assayed at room temperature. To determine the metal ion preference for the lipase, 1 mM chelators were first added to the assay mixture and supernatant to chelate metal ions from the solution. Following chelation, a 1 mM metal ion solution was added to help restore the activity of the lipase prior to activity assay.

To determine the effect of detergents on lipase activity, Tween 20 (polyoxyethylene (20) sorbitan monolaurate), Tween 40 (polyoxyethylene (20) sorbitan monopalmitate), Tween 60 (polyoxyethylene (20) sorbitan monostearate), Tween 80 (polyoxyethylene (20) sorbitan monooleate), sodium dodecyl sulfate (SDS), Triton X-100 (tetramethylbutyl phenyl-polyethylene glycol), or Triton X-305 (octylphenoxy polyethoxyethane) at final concentrations of 0.001, 0.01, or 0.05% (v/v) was added to the assay mixture with glycine-HCl (pH 7.0). The reaction was carried out at room temperature.

All experiments were carried out in triplicates and the values reported are averages of the three ± standard deviation.

RESULTS

Identification of LipA lipase and LipB chaperone pairs

Given the lack of evidence that *R. eutropha* H16 can directly uptake palm oil and utilize it for growth, TAGs in palm oil must first be hydrolyzed to free fatty acids (FFAs) by a secreted extracellular lipase and then taken up by the cells. TAG hydrolysis during cultivation of *R. eutropha* H16, Re2313, Re2314, and Re2315 (Table 8.1) in palm oil cultures were qualitatively analyzed by TLC (Fig. 8.1). At culture time points of 8, 24, 48, and 72 h, an increase in intensity of the spots corresponding to free fatty acids (FFA), diacylglycerol (DAG), and monoacylglycerol (MAG) with a concomitant decrease in the TAG spot intensity were detected from cultures of wild-type (H16) cells. These observations suggested the presence of an extracellular lipase produced by *R. eutropha* H16 cells for the hydrolysis of the TAGs in palm oil into DAGs, MAGs, and FFAs during growth. Strain Re2313, a $\Delta lipA$ derivative of H16, was unable to hydrolyze TAGs to the extent of wild-type cells, which resulted in unchanged TAG spot intensities on the TLC plate over the entire cultivation time. The same phenotype was observed for the mutant strain Re2315 with a deletion of both *lipA* and H16_A3742 (annotated as a putative lipase) genes. However a single deletion of the H16_A3742 gene (strain Re2314) had no defect in TAG cleavage and resulted in a similar phenotype as compared to the wild type. This suggested that only the *lipA* gene is responsible for the production of the extracellular lipase that is able to hydrolyze TAGs in palm oil and liberate FFAs for cellular usage in *R. eutropha* H16 cultures.

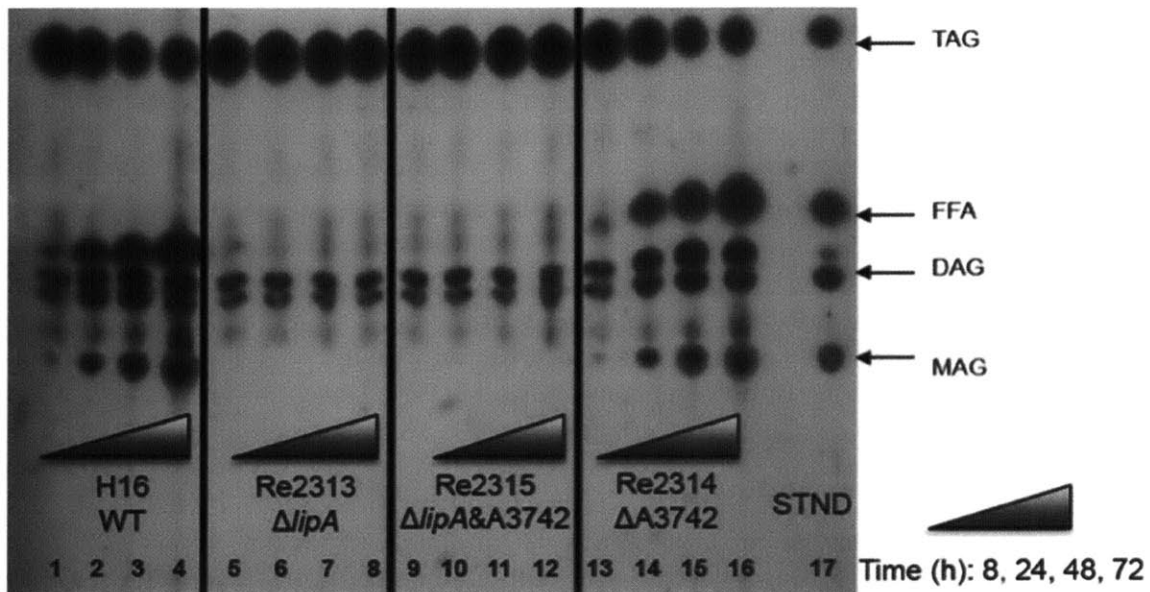


Figure 8.1: Thin layer chromatography (TLC) analysis of supernatants taken from the palm oil cultures of *R. eutropha* strains at 8, 24, 48, and 72 h. The TLC plate image shows the oil residue profile, including the presence of TAGs (triacylglycerols: 1,2-distearoyl-3-oleoyl-rac-glycerol), DAGs (diacylglycerols: 1,2-dipalmitoyl-rac-glycerol), MAGs (monoacylglycerols: 1-palmitoyl-rac-glycerol), and FFAs (free fatty acids: palmitate), during cultivation of *R. eutropha* strains H16 (WT), Re2313 ($\Delta lipA$), Re2314 ($\Delta A3742$), and Re2315 ($\Delta lipA \Delta A3742$) on palm oil (lanes 1 to 16). Standards were spotted and run on lane 17.

Introduction of the *lipA* gene into the mutant strain Re2313 via the overexpression plasmid pCJB201 was able to restore the TAG cleavage function of this strain (Fig. 8.2). Increasing the *lipA* gene dosage in both wild type and Re2313 resulted in more rapid TAG hydrolysis compared to just the wild type cell with vector alone (pBBR1MCS-2). The TAG spot intensity on the TLC plate decreased dramatically over the first 24 h and completely disappeared by 48 h when *lipA* was overexpressed. FFAs derived from TAGs built up in the media throughout cultivation time in the overexpression strains. This is likely the result of rapid FFA production outpacing FFA uptake and incorporation into the cell or accumulation of excess FFAs not needed for cell growth.

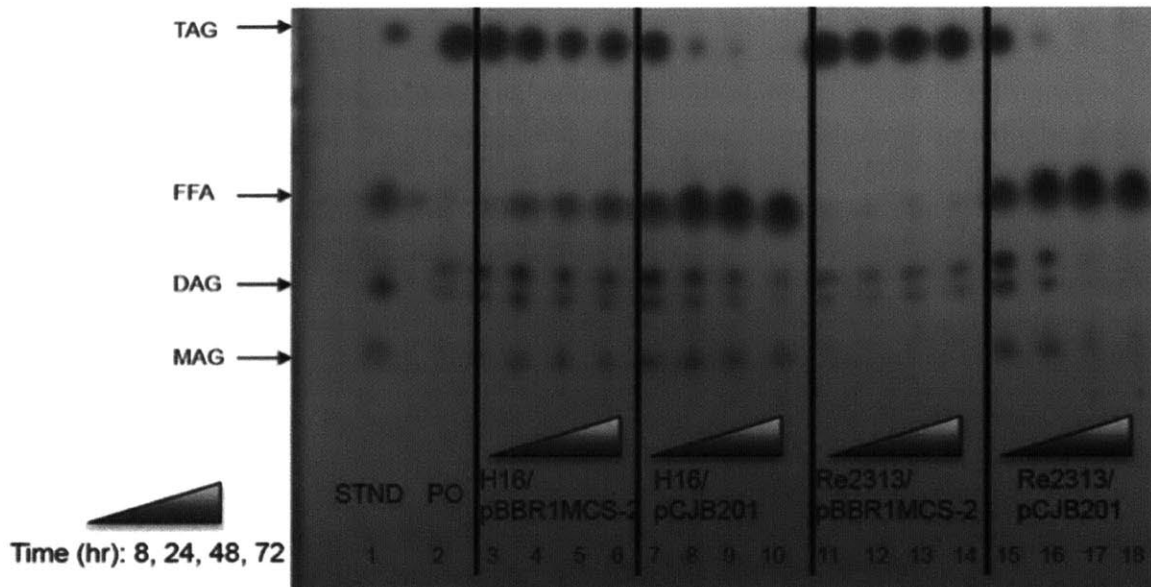


Figure 8.2: Overexpression of *lipA* in palm oil cultures. TLC plate image of oil residue profile during cultivation of H16/pBBR1MCS-2, H16/pCJB201, Re2313/pBBR1MCS-2, and Re2313/pCJB201 using palm oil as the sole carbon source. Lane 1 was spotted with standards and lane 2 with palm oil in initial culture media. Lanes 3 through 18 were spotted with supernatants removed from the *R. eutropha* cultures at 8, 24, 48, and 72 h.

Expression of *lipA* in heterologous hosts, such as *E. coli* and yeast, failed to produce an active lipase, which led us to the characterization of a lipase-specific foldase gene, *lipB* (H16_A1323), that is just downstream of *lipA*. Deletion of *lipB* (strain Re2318) showed the same growth phenotype in palm oil cultures as Re2313 (Appendix 8.2). Introduction of the plasmid-borne *lipA* gene to Re2318 did not restore TAG hydrolysis (data not shown), suggesting that LipA is a Class I lipase that requires its specific chaperone (i.e. LipB) for folding and secretion (Arpigny and Jaeger 1999; Frenken et al, 1993a; Frenken et al, 1993b; Hobson et al, 1993). LipA from *R. eutropha* H16 shares 48% and 44% sequence identity to the *Ralstonia* sp. M1 and *Pseudomonas* sp. lipases, respectively, while the chaperone LipB only had 45% and 27% sequence identity to chaperones of the same class (Gilbert 1993; Kim et al. 2001; Quyen et al. 2004; Quyen et al. 2005).

Further analysis of the secreted protein in supernatants of *R. eutropha* H16, H16/pCJB201 (*lipA* overexpression), Re2313 ($\Delta lipA$), and Re2318 ($\Delta lipB$) were grown in cultures containing palm oil. After 24 h, culture supernatants were harvested and subjected to SDS-PAGE analysis. The presence of a ~40 kDa protein on the gel was observed, but only for strains containing intact *lipA* and/or *lipB* genes (Appendix 8.3). The LipA enzyme H16_A1322 has a molecular weight of 38.6 kDa based on its primary amino acid sequence. H16/pCJB201 overexpressing *lipA* exhibited an increase in the amount of protein at ~40 kDa as compared to wild type. This observation suggests that LipA and LipB work together as an extracellular lipase/chaperone pair.

Growth and Lipase activity

Strains H16, Re2313, and Re2318 were individually cultivated in minimal media containing 1% palm oil as the sole carbon source (Figure 8.3A). Wild type H16 with an intact *lipA* gene reached an OD₆₀₀ of 15.0 by 48h. Strain Re2313 lacks *lipA* for the production of extracellular lipase, and not only was unable to hydrolyze TAGs in palm oil, but also did not grow significantly in the presence of unemulsified palm oil (Figure 8.1). Strain Re2318, which lacks lipase chaperone LipB, also was unable to grow on palm oil.

Activity of LipA was determined in the cell supernatants during palm oil cultivation of wild type, Re2313, and Re2318 strains (Figure 8.3B). Both Re2313 and Re2318 lack the gene for the production or secretion of active lipase, respectively, thus no lipase activity was detected (Figure 8.3B). In strain H16, lipase activity was determined to be ~47 mU/mL after 5 h of culture and remained active till after 24 h (Figure 8.3B). Reintroduction *in trans* of the *lipA* gene or the *lipB* gene into strains Re2313 or Re2318, respectively, restored growth of these strains on palm oil and also their lipase activities (Figure 8.4). Re2313/pCJB201 exhibited four times higher lipase activity than the wild-type strain, due to the increase of lipase gene dosage (Figure 8.4B). Strains Re2313/pCJB201 and H16/pCJB201 exhibit a decreased lag in growth in palm oil cultures as compared to the wild type, due to the increase in lipase activity (Figure 8.4A). Although the chaperone gene was overexpressed in the same way as the lipase gene in Re2318/pJL36, the growth rate and lipase activity was found to be similar to the wild-type strain (Figure 8.4). Reintroduction of the chaperone gene was able to restore the secretion mechanism of the lipase, but did not result in higher than wild-type levels of lipase activity. Lipase activity reached 1 U/mL when *lipA* was overexpressed in strain H16, thus explaining the rapid TAGs cleavage, compared to H16 with vector alone, as also detected by TLC (Figure 8.2).

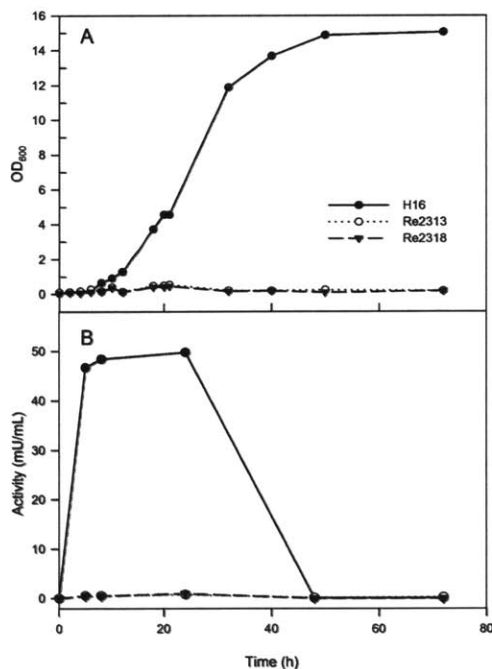


Figure 8.3: Growth (A) and lipase activities (B) of *R. eutropha* strains H16 (WT), Re2313 ($\Delta lipA$), and Re2318 ($\Delta lipB$) in 1% palm oil cultures. Culture OD₆₀₀ and lipase activity of H16 are indicated by the solid circles, Re2313 is shown with open circles, and Re2318 is represented by solid triangles.

LipA production by *R. eutropha* was induced by growth on various carbon sources (Table 8.3). Initial extracellular lipase activity was detected at 3 h after inoculation (data not shown). Lipase activity was dependant on the carbon source used; the activity at 10 h varied from 0.5 mU/mL in Tween 20 to 200 mU/mL in Tween 60. LipA was also produced and active with non-lipid carbon sources such as fructose. Of the carbon sources tested in this study, the LipA activity was observed in the following order (from highest to lowest activities): Tween 60> Tween 80>Palm Oil>Tween 40>Fructose> Tween 20 (Table 8.3).

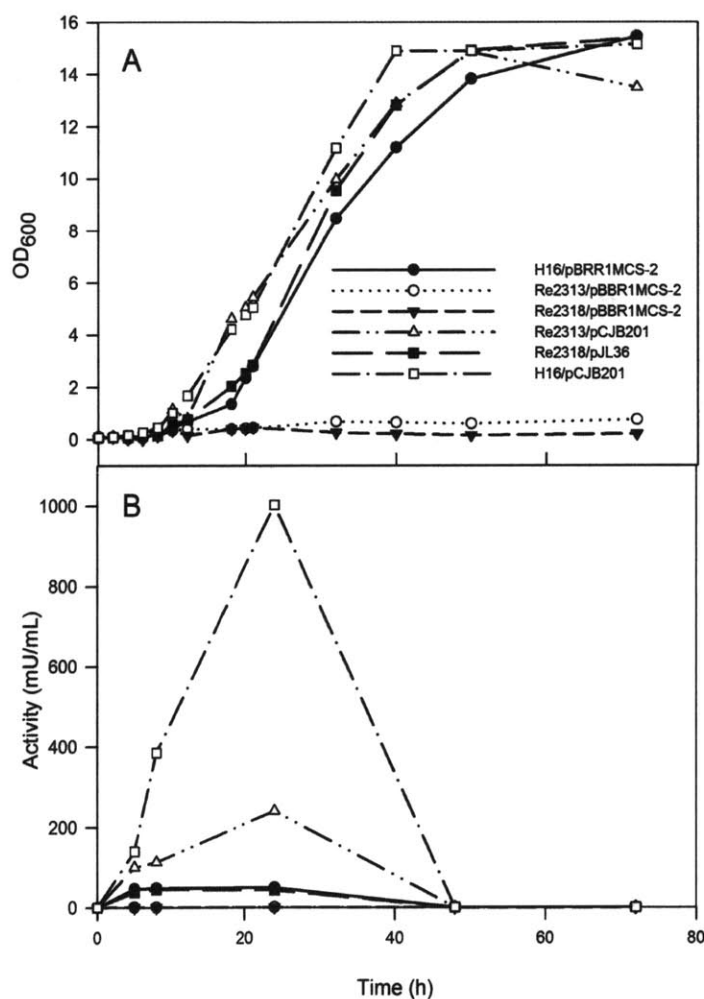


Figure 8.4: Growth (A) and lipase activities (B) of *R. eutropha* strains in 1% palm oil cultures. The culture OD₆₀₀ and activity profiles of H16, Re2313, Re2318, Re2313/pCJB201, Re2318/pJL31, and H16/pCJB201 are indicated by solid circles, open circles, solid triangles, open triangles, solid boxes, and open boxes, respectively.

Table 8.3: Effect of carbon sources on lipase production^a.

Carbon source	Lipase activity (mU/mL)
Fructose (0.5% w/v)	4.6±0.3
Palm Oil (0.5% v/v)	38.0±0.8
Tween 20 (0.5% v/v)	0.5±0.1
Tween 40 (0.5% v/v)	36.0±1.0
Tween 60 (0.5% v/v)	200.0±20.0
Tween 80 (0.5% v/v)	91.0±5.0

^aEach value represents the mean ± standard error on n = 3. Supernatants of *R. eutropha* strain H16 grown in various carbon sources were collected at 10 h of culture time for activity assays. Lipase activity was determined at room temperature, pH 7.0 in glycine-HCl buffer.

Decreased lag phase due to lipase overexpression

Growth of strain H16/pCJB201 in palm oil cultures not only resulted in quick TAG cleavage (Figure 8.2), but also shortened the lag phase of growth (Figure 8.4A and 8.5). Wild-type culture experienced a ~22 h lag phase when grown on palm oil as the sole carbon source. H16/pCJ201, on the other hand, reached exponential growth phase in less than 12 h. The increased amount of DAGs, MAGs, and FFAs liberated from TAG hydrolysis in the growth media acted as a natural surfactant and enhanced the oil emulsification during growth on palm oil (Appendix 8.4). Thus, the amount of time needed for the cells to adapt to the two-phase heterogeneity of the palm oil growth medium decreased significantly.

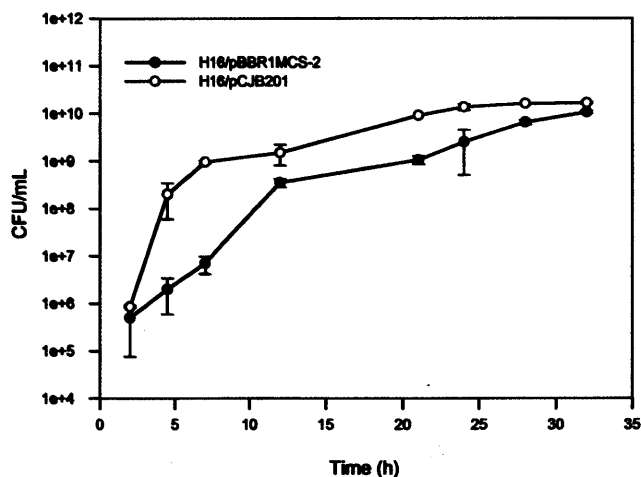


Figure 8.5: Viable colony counts of H16/pBBR1MCS-2 and H16/pCJB201 in palm oil cultures. Solid circles represent growth of strain H16 containing only empty vector (pBBR1MCS-2). Open circles indicate the colony-forming units of H16 with *lipA* overexpression (pCJB201). Data points represent the mean values of n = 3 ± standard deviation (error bars).

Substrate specificity

Substrate specificities of lipase enzymes classify them into one of the following categories: non-specific, regio-specific, or fatty acid-specific. Non-specific hydrolysis will result in complete breakdown of the TAG molecule into FFAs and glycerol, while regio-specific lipase will catalyze hydrolysis only at C1 and C3 position of the glycerol backbone. Fatty acid-specific lipase will only cleave fatty acid esters of certain chain lengths such as C12 lipids or C16 lipids (Arpigny and Jaeger 1999; Gupta et al. 2004; Treichel et al. 2010). The TLC analysis of H16/pCJB201 resulted in complete hydrolysis of TAGs, DAGs, and MAGs in the media into FFAs (Figure 8.2), suggesting that LipA is a non-specific lipase able to act at random for the complete breakdown of TAGs.

Effect of temperature, pH, metal ions, and detergents

The effects of temperature, pH, metal ions, and detergents on lipase activity were studied using culture supernatants of *R. eutropha* grown in Tween 60 for 10 h, since Tween 60 as the carbon source showed the highest induction of LipA activity compared to other carbon sources tested (Table 8.3). Lipase activity was measured at various temperatures from 0 to 80°C. LipA was active from 10 to 70°C (Figure 8.6A). The optimal activity was observed at a temperature of 50°C, in which the activity reached 27 U/mL at pH 7. Although *R. eutropha* prefers 30°C for growth, its extracellular lipase is quite thermostable and remained active even at high temperatures.

Buffers of pH 3 to 12 were used to determine the pH optimum for LipA activity. The pH for best growth and lipase production was shown to be pH 6.8 for *R. eutropha*. LipA showed maximum activity at pH 7.0 to 8.0, when the activity reached 3 U/mL at room temperature (Figure 8.6B). LipA was active in buffers ranging from pH 5 to pH 10 with a slight preference towards the alkaline pH buffers.

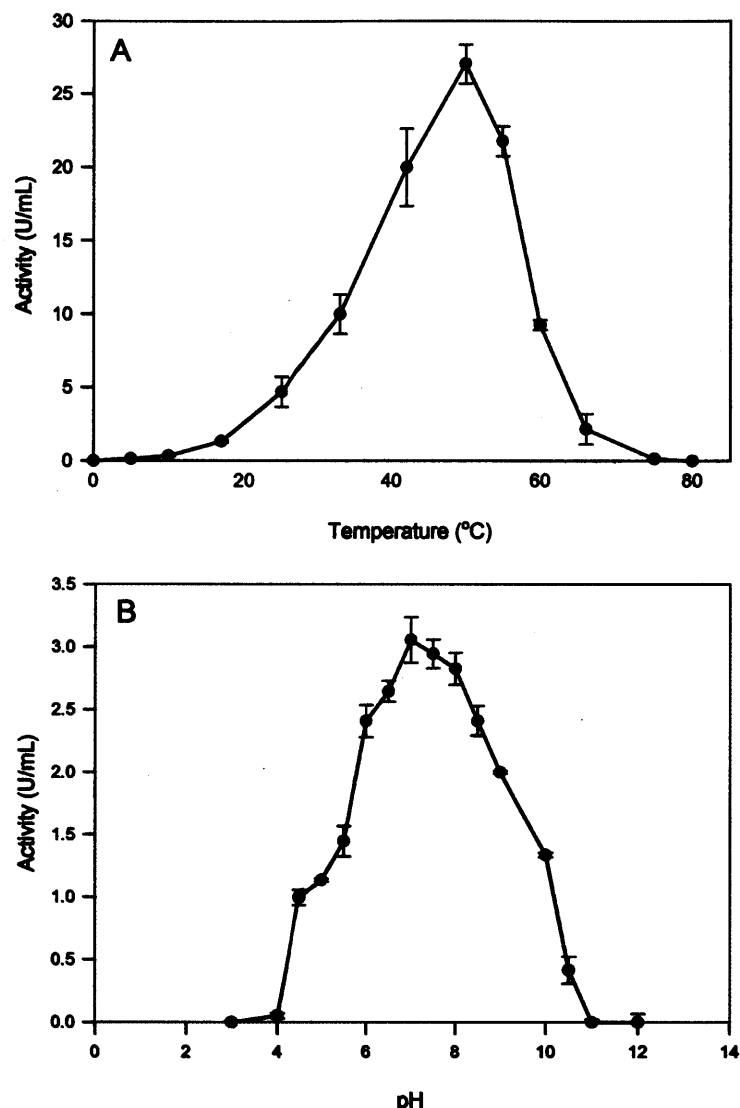


Figure 8.6: Effect of temperature (A) and pH (B) on LipA lipase activity. Average values from both experiments from three replications were plotted in solid circles with standard deviation values represented as error bars.

Although a metal cofactor is typically not involved in the mechanism of catalysis of lipases, divalent cations were reported to stimulate or inhibit lipase activity (El Khattabi et al, 2003; Gupta et al. 2004; Rosenstein and Gotz 2000). Divalent metal ions Zn^{2+} , Mg^{2+} , Fe^{2+} , Ca^{2+} , Cu^{2+} , Mn^{2+} , and Ni^{2+} , along with their chelators (EDTA and EGTA), were added at different concentrations to the assay mixture to examine their effect on LipA activity (Table 8.4). At concentrations of 0.1 mM, transition metal chelator EDTA and Ca^{2+} -chelator EGTA imparted little inhibition on LipA activity. At the same concentration, Zn^{2+} and Cu^{2+} inhibited LipA activity by ~50% while all other metal ions had little to no effect. The activity of LipA decreased dramatically to 3 - 18% of total activity when 1 mM of either chelators, Zn^{2+} , Fe^{2+} , Cu^{2+} , or Ni^{2+} were added. A 1 mM concentration of Mg^{2+} only inhibited LipA by 28%, while

Ca²⁺ and Mn²⁺ ions had no affect at all on lipase activity. This suggested that LipA activity could be inhibited by Zn²⁺, Fe²⁺, Cu²⁺, or Ni²⁺ but only slightly inhibited by Mg²⁺, while activity was not affected by Ca²⁺, and Mn²⁺ ions.

Table 8.4: Effect of various metal ions or chelating agents on lipase activity^a.

Metal ion	Relative activity (%) (0.1 mM metal ion or chelator)	Relative activity (%) (1 mM metal ion or chelator)
None	100	100
EDTA & EGTA	91	15
ZnCl ₂	43	3
MgCl ₂	94	72
FeCl ₂	86	18
CaCl ₂	98	99
CuCl ₂	68	11
MnCl ₂	115	99
NiCl ₂	90	7

^aEnzymatic assay was carried out at room temperature with pH 7.0 glycine-HCl buffer.

To test if Mg²⁺, Ca²⁺, and Mn²⁺ can reverse the inhibition caused by chelators, 1 mM of each ion was added separately to assay mixtures after the addition of 1 mM of both chelators (Figure 8.7). While chelators EDTA and EGTA inhibited the LipA activity by 83%, addition of Mg²⁺, Ca²⁺, or Mn²⁺ alleviated this inhibition and helped restore the LipA activity back to 80 to 95% of its original levels. Other metals had no affect on the inhibition caused by the addition of chelators. These results demonstrate that Mg²⁺, Ca²⁺, and Mn²⁺ divalent metal ions can stimulate lipase activity and alleviate chelator caused inhibition.

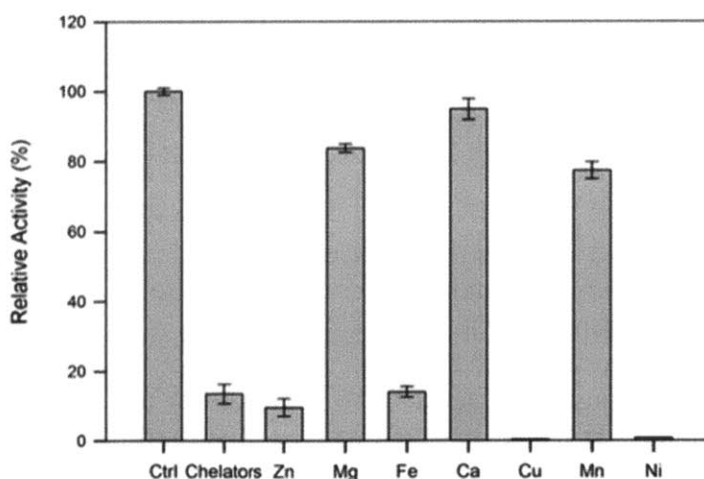


Figure 8.7: Metal ion alleviation of LipA lipase activity inhibition by chelators. Reactions were carried out at room temperature in pH 7.0 glycine-HCl buffer. Control was carried out without addition of chelators or metal ions. Metal ion solutions at a final concentration of 1 mM were added after the enzyme assay mixture was treated with 1 mM chelators. Average values from three experiments were plotted with error bars representing the standard deviation.

Detergents are known to either increase solubility of lipids (i.e. act as emulsifiers) or induce lipid aggregation, thus allowing lipase to better access the lipid substrate (Lin et al. 1995; Reis et al. 2009). To test the effect of detergents on LipA activity, 0.001, 0.01, and 0.1% (v/v) of Tween 20, Tween 40, Tween 60, or Tween 80, Triton X-100 or Triton 305, or SDS detergents was added to the enzymatic assay mixture at room temperature and pH 7.0 (Table 8.5). At low concentrations (0.001% v/v), Tween 40, Tween 60, Tween 80, and SDS all inhibited LipA activity by ~90%. However, an increase in the concentration to 0.01% (v/v) of Tween 40, Tween 60, Tween 80, and SDS helped restore the lipase activity. Interestingly Tween 40, which had restored LipA activity at 0.01% then again inhibited the activity at 0.1%. Addition of increasing concentration of Tween 20 resulted in LipA activity decrease by <90%. Triton X-100 was able to increase LipA activity by 586% at 0.001% and 333% at 0.1%. Increasing concentration of Triton X-305 reduced LipA activity by ~70%; however at 0.1% the LipA activity was restored to normal. This suggested that although some detergents could help stimulate LipA activity, the mechanism of detergent concentration to LipA activity is complex.

Table 8.5: Effect of detergents on lipase activity^a.

Detergent	Relative activity (%) (0.001% v/v detergent)	Relative activity (%) (0.01% v/v detergent)	Relative activity (%) (0.1% v/v detergent)
None	100	100	100
Tween 20	120	66	2
Tween 40	5	117	8
Tween 60	7	10	27
Tween 80	5	9	83
Triton X-100	686	543	433
Triton X-305	77	27	112
SDS	11	38	126

^aLipase assay was conducted with pH7.0 glycine-HCl buffer at room temperature.

DISCUSSION

In this study, we have characterized the extracellular triacylglycerol hydrolase from *R. eutropha* H16. This lipase, LipA, contains the conserved lipase catalytic triad Ser, His, and Asp in its primary structure (Appendix 8.5). Since LipA requires a lipase-specific foldase, LipB, to achieve its correct catalytic tertiary structure and be secreted outside of the cell, it belongs to the Class I lipase family (Arpigny and Jaeger 1999; Frenken et al, 1993b; Hobson et al, 1993). Protein sequence homology revealed that LipA and LipB, the lipase and chaperone pair of *R. eutropha* H16 were similar to those from *Ralstonia* sp. M1 (Quyen et al, 2004; Quyen et al, 2005). LipA primary sequence contains a signal peptide, which further support its function as a secreted lipase. Three cysteine residues were found in the primary sequence (Appendix 8.5) with the possibility of disulfide bond formation. Chaperone LipB could be required for this reduction *in vivo* (Kok et al. 1996).

LipA from *R. eutropha* H16 was determined to be a non-specific lipase, because it was able to completely hydrolyze TAGs into FFAs and glycerol. Non-specific lipases hold great importance in the field of biodiesel fuel production from TAGs, since they can act at random and

fully breakdown TAGs (Bajaj et al. 2010; Fjerbaek et al. 2009; Jegannathan et al. 2010; Singh and Singh 2010). Also, since LipA is a secreted lipase, its isolation process would be simplified, compared to intracellular lipases from other species, for lipase immobilization applications (Fjerbaek et al. 2009; Gupta et al. 2004; Jaeger and Reetz 1998). LipA can also catalyze a diverse range of substrates such as Tween 20, Tween 40, Tween 60, and Tween 80, due to its broad range of selectivity. The reaction rate of such catalysis varies directly and extensively with the chemical properties of the substrate. LipA favored Tween 60 as a substrate compared to other Tween compounds, with the least favored being Tween 20. LipA could favor long chain length linear fatty esters, since the hydrolysis of Tween 60 can only liberate stearic acid (18 carbon linear chain).

Overexpression of the *lipA* gene on a plasmid not only increased the TAG hydrolysis rate in culture but also resulted in a shortened *R. eutropha* lag phase when grow on palm oil. Biotechnological usage of LipA would reduce the dependence on surfactants, since more DAGs, MAGs, and FFAs, that act as natural surfactants, can be liberated from the rapid hydrolysis of TAGs in the initial growth stage (Jaeger and Eggert 2002; Skagerlind et al. 1992). The industrial fermentation time could be shortened, using a strain of *R. eutropha* that overexpresses *lipA*, because the cells can reach the stationary phase in half of the normal growth time, due to the increased amount of FFAs present in the culture for cell growth and biosyntheses.

Lipase activity can be affected not only by the carbon sources used, but also by physico-chemical factors such as temperature, pH, metal ion, and detergent. Although the optimal temperature and pH for lipase production correspond with the growth temperature and pH of the host microorganisms, most secreted lipases are active in a wide range of temperatures and pHs (Gupta et al. 2004). *R. eutropha* H16 LipA showed high activity at 50°C, which is similar to many other characterized bacterial lipases (Gupta et al. 2004). Most of the previously studied lipases have temperature optima in the range of 30 to 60°C, although some extreme lipases were also found that exhibited high activity even at low or high temperatures (Jeon et al. 2009; Joseph et al. 2008; Kulkarni and Gadre 1999; Nawani and Kaur 2007). Adjustment of the temperatures for optimal lipase performance, depending on application, can be achieved through the use of stabilizers such as ethylene glycol, sorbitol, or glycerol (Franken et al, 2010; Gupta et al, 2004). LipA had neutral to slightly alkaline pH optimum that is similar to most known bacterial lipases (Gupta et al, 2004; Kanwar et al, 2002; Lesuisse et al, 1993).

TAG hydrolysis by lipase does not require specific cofactors, although Ca^{2+} has been reported to stimulate the activity of lipases from *Bacillus*, *Pseudomonas*, *Chromobacterium*, and *Acinetobacter* species (Gupta et al. 2004; Kanwar et al. 2002; Rathi et al. 2001). The function of Ca^{2+} in lipase is highly debatable. It has been hypothesized that the released fatty acids associate with Ca^{2+} to form calcium salts, and thus relieve product (FFA) inhibition (Godtfredsen 1990; Macrae and Hammond 1985). Also, the role of Ca^{2+} was thought to stabilize the lipase tertiary structure. It has also been theorized that there is a direct involvement of Ca^{2+} in the catalysis for the activation of water molecules; however, this theory is highly unlikely since the calcium-binding site was found to be far from the active site in the *Burkholderia glumae* lipase crystal structure (Jaeger et al. 1999; Noble et al. 1993; Rosenstein and Gotz 2000; Verheij et al. 1980; Simons et al. 1999). The metal chelators EDTA and EGTA acted as inhibitors to all lipases, including LipA. Although the role of Ca^{2+} was not elucidated, it alleviated inhibition by chelation and stimulated LipA activity. Calcium ion could also be replaced by Mg^{2+} or Mn^{2+} without loss of activity in LipA. Reported in the literature, divalent cations Sr^{2+} or Ba^{2+} can also replace Ca^{2+} in lipase (Gupta et al. 2004). The LipA primary sequence contains several aspartate

residues that could be responsible for the binding of calcium (Appendix 8.5). To test the residues involved in potential Ca^{2+} binding, site-directed mutagenesis could be employed. Furthermore, like many reported lipases, LipA activity was inhibited by metal chelators (Table 8.4, Figure 8.7) and by various heavy metals (Gupta et al. 2004).

Lipase activity is highly inducible and the activity is dependent on substrate concentrations at the interface of water and lipid. Detergents, at a specific concentration, can cause non-polar substrates to aggregate or solubilize in water thus dramatically increasing the activity of lipase (Boekema et al. 2007; Reis et al. 2009). The addition of small amounts of Triton X-100 could cause a shift in the solubility equilibrium and cause substrate aggregation because the substrate concentration exceeded the solubility limit. Such change at the interface strongly activated LipA activity. Detergents such as Tween 20 could compete with the LipA active site, thus inhibiting the activity of LipA in our assay system. Thus, dependant on the type and concentration of detergents, LipA activity was either enhanced or inhibited. LipA characterized here had similar activity response to detergents as LipA from *Ralsonia* sp. M1 (Quyen et al. 2005). Since much is still unknown regarding lipase catalysis at the water-oil interface, the use of detergent-based inducers can only be determined experimentally at this time.

It has long been established that *R. eutropha* is the model organism for the production of polyhydroxyalkanoate (PHA), a polyester that can potentially replace current petroleum-based plastics in many applications. Palm oil is a promising carbon source because it is a readily available agricultural byproduct and has high density carbon content. Recently Riedel et al. were able to produce over 139 g/L of biomass using engineered *R. eutropha* with 74% of cell dry weight as PHA, using palm oil as the sole carbon source (Riedel et al. 2012). *R. eutropha* growth in palm oil, or any plant oil, presents challenges due to the heterogeneity between the oil feedstock and the aqueous media. Emulsifiers, such as the glycoprotein gum Arabic, were able to emulsify the palm oil in growth medium and make it more bioavailable without influencing *R. eutropha* growth (Budde et al. 2011a). In this work, overexpression of extracellular LipA in *R. eutropha* allowed for rapid TAGs hydrolysis (Figure 8.2) with liberated DAGs, MAGs, and FFAs acting as natural surfactants and ultimately resulted in a faster growth rate (Figure 8.4A and 8.5). Such properties could potentially make LipA an enzyme with important biotechnological usage, especially in the production of PHA from palm oil.

REFERENCES

- Arpigny JL, Jaeger KE (1999) Bacterial lipolytic enzymes: classification and properties. *Biochem J* 343: 177-183
- Bajaj A, Lohan P, Jha PN, Mehrotra R (2010) Biodiesel production through lipase catalyzed transesterification: An overview. *J Mol Catal B: Enzym* 62: 9-14
- Boekema BK, Beselin A, Breuer M, Hauer B, Koster M, Rosenau F, Jaeger KE, Tommassen J (2007) Hexadecane and Tween 80 stimulate lipase production in *Burkholderia glumae* by different mechanisms. *Appl Environ Microbiol* 73: 3838-3844
- Bourne Y, Martinez C, Kerfelec B, Lombardo D, Chapus C, Cambillau C (1994) Horse pancreatic lipase - the crystal structure refined at 2.3 angstrom resolution. *J Mol Biol* 238: 709-732
- Brigham CJ, Budde CF, Holder JW, Zeng QD, Mahan AE, Rha C, Sinskey AJ (2010) Elucidation of beta-oxidation pathways in *Ralstonia eutropha* H16 by examination of global gene expression. *J Bacteriol* 192: 5454-5464
- Budde CF, Riedel SL, Hubner F, Risch S, Popovic MK, Rha C, Sinskey AJ (2011a) Growth and polyhydroxybutyrate production by *Ralstonia eutropha* in emulsified plant oil medium. *Appl Microbiol Biotechnol* 89: 1611-1619
- Budde CF, Riedel SL, Willis LB, Rha C, Sinskey AJ (2011b) Production of poly(3-hydroxybutyrate-co-3-hydroxyhexanoate) from plant oil by engineered *Ralstonia eutropha* strains. *Appl Environ Microbiol* 77: 2847-2854
- Cherukuvada SL, Seshasayee ASN, Raghunathan K, Anishetty S, Pennathur G (2005) Evidence of a double-lid movement in *Pseudomonas aeruginosa* lipase: insights from molecular dynamics simulations. *Plos Comput Biol* 1: 182-189
- Chong L (2001) Molecular cloning - A laboratory manual, 3rd edition. *Science* 292: 446-446
- Derewenda ZS, Derewenda U, Dodson GG (1992) The crystal and molecular structure of the *Rhizomucor-Miehei* triacylglyceride lipase at 1.9 angstrom resolution. *J Mol Biol* 227: 818-839
- El Khattabi M, Van Gelder P, Bitter W, Tommassen J (2003) Role of the calcium ion and the disulfide bond in the *Burkholderia glumae* lipase. *J Mol Catal B: Enzym* 22: 329-338
- Fjerbaek L, Christensen KV, Norddahl B (2009) A review of the current state of biodiesel production using enzymatic transesterification. *Biotechnol Bioeng* 102: 1298-1315
- Franken LPG, Marcon NS, Treichel H, Oliveira D, Freire, DMG, Dariva C, Destain J, Oliveira JV (2010) Effect of treatment with compressed propane on lipases hydrolytic activity. *Food Bioprocess Technol* 3: 511-520
- Frenken LGJ, Bos JW, Visser C, Muller W, Tommassen J, Verrips CT (1993a) An accessory gene, *lipB*, required for the production of active *Pseudomonas glumae* lipase. *Mol Microbiol* 9: 579-589
- Frenken LGJ, Degroot A, Tommassen J, Verrips CT (1993b) Role of the *lipB* gene-product in the folding of the secreted lipase of *Pseudomonas glumae*. *Mol Microbiol* 9: 591-599

- Gilbert EJ (1993) *Pseudomonas* lipases - biochemical properties and molecular cloning. *Enzyme Microb Technol* 15: 634-645
- Godfredsen SE (1990) Application of lipases for synthesis of new chemicals. *Opp Biotransform* (1): 17-22
- Gupta R, Gupta N, Rathi P (2004) Bacterial lipases: an overview of production, purification and biochemical properties. *Appl Microbiol Biotechnol* 64: 763-781
- Hobson AH, Buckley CM, Aamand JL, Jorgensen ST, Diderichsen B, McConnell DJ (1993) Activation of a bacterial lipase by its chaperone. *Proc Natl Acad Sci USA* 90: 5682-5686
- Jaeger KE, Reetz MT (1998) Microbial lipases form versatile tools for biotechnology. *Trends Biotechnol* 16: 396-403
- Jaeger KE, Dijkstra BW, Reetz MT (1999) Bacterial biocatalysts: molecular biology, three-dimensional structures, and biotechnological applications of lipases. *Annu Rev Microbiol* 53: 315-320.
- Jaeger KE, Eggert T (2002) Lipases for biotechnology. *Curr Opin Biotechnol* 13: 390-397
- Jegannathan KR, Jun-Yee L, Chan ES, Ravindra P (2010) Production of biodiesel from palm oil using liquid core lipase encapsulated in kappa-carrageenan. *Fuel* 89: 2272-2277
- Jeon JH, Kim JT, Kim YJ, Kim HK, Lee HS, Kang SG, Kim SJ, Lee JH (2009) Cloning and characterization of a new cold-active lipase from a deep-sea sediment metagenome. *Appl Microbiol Biotechnol* 81: 865-874
- Joseph B, Ramteke PW, Thomas G (2008) Cold active microbial lipases: Some hot issues and recent developments. *Biotechnol Adv* 26: 457-470
- Kahar P, Tsuge T, Taguchi K, Doi Y (2004) High yield production of polyhydroxyalkanoates from soybean oil by *Ralstonia eutropha* and its recombinant strain. *Polym Degrad Stab* 83: 79-86
- Kanwar L, Gogoi BK, Goswami P (2002) Production of a *Pseudomonas* lipase in n-alkane substrate and its isolation using an improved ammonium sulfate precipitation technique. *Bioresour Technol* 84: 207-211
- Kim EK, Jang WH, Ko JH, Kang JS, Noh MJ, Yoo OJ (2001) Lipase and its modulator from *Pseudomonas* sp strain KFCC 10818: Proline-to-glutamine substitution at position 112 induces formation of enzymatically active lipase in the absence of the modulator. *J Bacteriol* 183: 5937-5941
- Kim SS, Kim EK, Rhee JS (1996) Effects of growth rate on the production of *Pseudomonas fluorescens* lipase during the fed-batch cultivation of *Escherichia coli*. *Biotechnol Prog* 12: 718-722
- Kok RG, Nudel CB, Gonzalez RH, NugterenRoodzant IM, Hellingwerf KJ (1996) Physiological factors affecting production of extracellular lipase (LipA) in *Acinetobacter calcoaceticus* BD413: Fatty acid repression of lipA expression and degradation of LipA. *J Bacteriol* 178: 6025-6035.
- Kulkarni N, Gadre RV (1999) A novel alkaline, thermostable, protease-free lipase from *Pseudomonas* sp. *Biotechnol Lett* 21: 897-899

- Lesuisse E, Schanck K, Colson C (1993) Purification and preliminary characterization of the extracellular lipase of *Bacillus subtilis* 168, an extremely basic pH-tolerant enzyme. *Eur J Biochem* 216: 155-160
- Lin SF, Chiou CM, Tsai YC (1995) Effect of Triton X-100 on Alkaline lipase production by *Pseudomonas pseudoalcaligenes* F-111. *Biotechnol Lett* 17: 959-962
- Lotti M, Monticelli S, Montesinos JL, Brocca S, Valero F, Lafuente J (1998) Physiological control on the expression and secretion of *Candida rugosa* lipase. *Chem Phys Lipids* 93: 143-148
- Macrae AR, Hammond RC (1985) Present and future applications of lipases. *Biotechnol Genet Eng Rev* 3: 193-217
- Mahler GF, Kok RG, Cordenons A, Hellingwerf KJ, Nudel BC (2000) Effects of carbon sources on extracellular lipase production and lipA transcription in *Acinetobacter calcoaceticus*. *J Ind Microbiol Biotechnol* 24: 25-30
- Nawani N, Kaur J (2007) Studies on lipolytic isoenzymes from a thermophilic *Bacillus sp.*: Production, purification and biochemical characterization. *Enzyme Microb Technol* 40: 881-887
- Ng KS, Ooi WY, Goh LK, Shenbagarathai R, Sudesh K (2010) Evaluation of jatropha oil to produce poly(3-hydroxybutyrate) by *Cupriavidus necator* H16. *Polym Degrad Stab* 95: 1365-1369
- Noble MEM, Cleasby A, Johnson LN, Egmond MR, Frenken LGJ (1993) The crystal structure of triacylglycerol Lipase from *Pseudomonas glumae* reveals a partially redundant catalytic aspartate. *FEBS Lett* 331: 123-128
- Pandey A, Benjamin S, Soccol CR, Nigam P, Krieger N, Soccol VT (1999) The realm of microbial lipases in biotechnology. *Biotechnol Appl Biochem* 29: 119-131
- Park Hyun Lee KS, Chi YM, Jeong SW (2005) Effects of methanol on the catalytic properties of porcine pancreatic lipase. *J Microbiol Biotechnol* 15: 296-301
- Quandt J, Hynes MF (1993) Versatile suicide vectors which allow direct selection for gene replacement in gram-negative bacteria. *Gene* 127: 15-21
- Quyen DT, Nguyen TT, Le TTG, Kim HK, Oh TK, Lee JK (2004) A novel lipase/chaperone pair from *Ralstonia sp* M1: analysis of the folding interaction and evidence for gene loss in *R. solanacearum*. *Mol Genet Genomics* 272: 538-549
- Quyen DT, Le TTG, Nguyen TT, Oh TK, Lee JK (2005) High level heterologous expression and properties of a novel lipase from *Ralstonia sp* M1. *Protein Expression Purif* 39: 97-106
- Rathi P, Saxena RK, Gupta R (2001) A novel alkaline lipase from *Burkholderia cepacia* for detergent formulation. *Process Biochem* 37: 187-192
- Reis P, Holmberg K, Watzke H, Leser ME, Miller R (2009) Lipases at interfaces: A review. *Adv Colloid Interface Sci* 147-48: 237-250

- Riedel SL, Bader J, Brigham CJ, Budde CF, Yusof ZAM, Rha C, Sinskey AJ (2012) Production of poly(3-hydroxybutyrate-co-3-hydroxyhexanoate) by *Ralstonia eutropha* in high cell density palm oil fermentations. *Biotechnol Bioeng* 109: 74-83
- Rosenau F, Jaeger KE (2000) Bacterial lipases from *Pseudomonas*: Regulation of gene expression and mechanisms of secretion. *Biochimie* 82: 1023-1032
- Rosenstein R, Gotz F (2000) Staphylococcal lipases: Biochemical and molecular characterization. *Biochimie* 82: 1005-1014
- Roussel A, Canaan S, Egloff MP, Riviere M, Dupuis L, Verger R, Cambillau C (1999) Crystal structure of human gastric lipase and model of lysosomal acid lipase, two lipolytic enzymes of medical interest. *J Biol Chem* 274: 16995-17002
- Sanchez M, Prim N, Randez-Gil F, Pastor FI, Diaz P (2002) Engineering of baker's yeasts, *E. coli* and *Bacillus* hosts for the production of *Bacillus subtilis* lipase A. *Biotechnol Bioeng* 78: 339-345
- Schrag JD, Cygler M (1997) Lipases and alpha/beta hydrolase fold. *Methods Enzymol* 284: 85-107
- Severac E, Galy O, Turon F, Monsan P, Marty A (2011) Continuous lipase-catalyzed production of esters from crude high-oleic sunflower oil. *Bioresour Technol* 102: 4954-4961
- Simon R, Priefer U, Puhler A (1983) A broad host range mobilization system for *in vivo* genetic-engineering - Transposon mutagenesis in gram negative bacteria. *Bio-Technology* 1: 784-791
- Simons JW, van Kampen MD, Ubarretxena-Belandia I, Cox RC, Alves dos Santos CM, Egmond MR, Verheij HM (1999) Identification of a calcium binding site in *Staphylococcus hyicus* lipase: generation of calcium-independent variants. *Biochemistry* 38: 2-10
- Singh SP, Singh D (2010) Biodiesel production through the use of different sources and characterization of oils and their esters as the substitute of diesel: A review. *Renewable Sustainable Energy Rev* 14: 200-216
- Skagerlind P, Jansson M, Hult K (1992) Surfactant interference on lipase catalyzed-reactions in microemulsions. *J Chem Technol Biotechnol* 54: 277-282
- Slater S, Houmiel KL, Tran M, Mitsky TA, Taylor NB, Padgett SR, Gruys KJ (1998) Multiple beta-ketothiolases mediate poly(beta-hydroxyalkanoate) copolymer synthesis in *Ralstonia eutropha*. *J Bacteriol* 180: 1979-1987
- Treichel H, de Oliveira D, Mazutti MA, Di Luccio M, Oliveira JV (2010) A review on microbial lipases production. *Food Bioprocess Technol* 3: 182-196
- van Pouderooyen G, Eggert T, Jaeger KE, Dijkstra BW (2001) The crystal structure of *Bacillus subtilis* lipase: a minimal alpha/beta hydrolase fold enzyme. *J Mol Biol* 309: 215-226
- Verheij HM, Volwerk JJ, Jansen EHJM, Puyk WC, Dijkstra BW, Drenth J, Dehaas GH (1980) Methylation of histidine 48 in pancreatic phospholipase-A2 - Role of histidine and calcium ion in the catalytic mechanism. *Biochemistry* 19: 743-750

Wang Y, Wei DQ, Wang JF (2007) Molecular dynamics studies on T1 lipase: insight into a double-flap mechanism. *J Chem Inf Model* 50: 875-878

Yang YH, Brigham CJ, Budde CF, Boccazzi P, Willis LB, Hassan MA, Yusof ZA, Rha C, Sinskey AJ (2010) Optimization of growth media components for polyhydroxyalkanoate (PHA) production from organic acids by *Ralstonia eutropha*. *Appl Microbiol Biotechnol* 87: 2037-2045

York GM, Stubbe J, Sinskey AJ (2001) New insight into the role of the PhaP phasin of *Ralstonia eutropha* in promoting synthesis of polyhydroxybutyrate. *J Bacteriol* 183: 2394-2397

APPENDIX

Appendix 8.1: List of primers used in this study. Restriction sites are underlined.

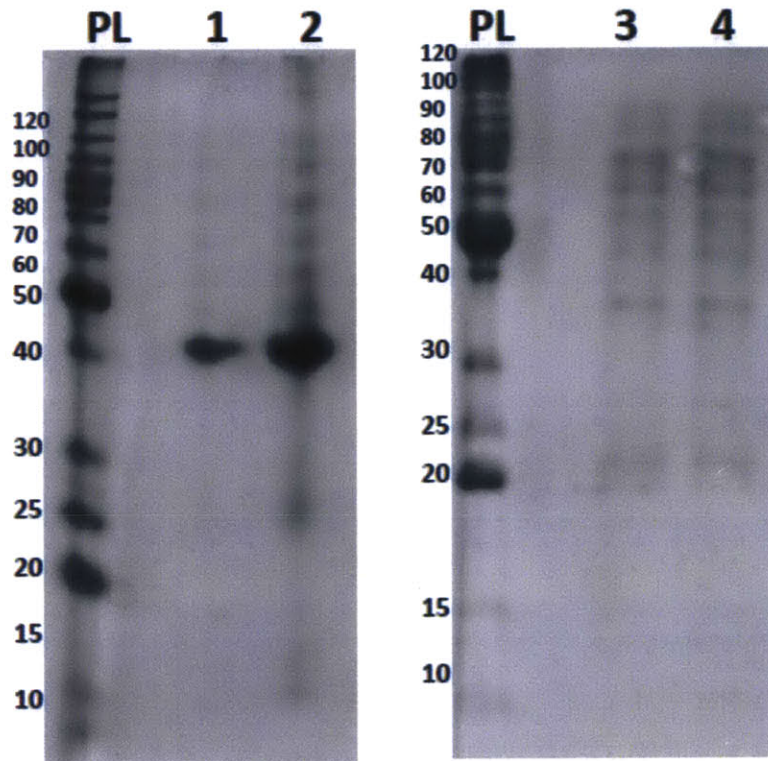
Name	Sequence ^a
ΔA3742 upstream F	5'-CATAGAGCTCTACCTGAAGGCCAGCGGC-3'
ΔA3742 upstream R	5'-AGACTTAATTAAGTTCACGGGCGCTCTCCCT-3'
ΔA3742 downstream F	5'-CACATTAATTAAGTAAATCCCCGCCGGCGCAA-3'
ΔA3742 downstream R	5'-AGTATCTAGATGCCGGTAGCCGGTCTCAGA-3'
ΔA3742 diagF	5'-CGGCAAGGATGAGTTCGA-3'
ΔA3742 diagR	5'-CGCGTTGATGAAATGGGTG-3'
ΔA1323 upstream F	5'-GCATTCTAGACGCTCAAGATCCTGACCACGCGTG-3'
ΔA1323 upstream R	5'- CTTTGGGCGATGCAGCGCGGCTACACCCGGCCGCCGCCGCGCCGGC-3'
ΔA1323 downstream F	5'- GCCGGCGCGGCGGCGGCGGCGGTGTAGCCGCGCTGCATCGCCCAAAG-3'
ΔA1323 downstream R	5'-GCCGGGATCCGCAACCCGCCATGGACCATCCAC-3'
ΔA1323 diagF	5'-GGACCGGCTGGTGTACGACGATATC-3'
ΔA1323 diagR	5'-GCCTGCGCCAACGCCGCACCGATGTC-3'
A1323 F	5'-GCATGGATCCGTGTACTGGCTGACGATGCCG-3'
A1323 R	5'-GCATGAGCTCCTATCGTGCCTGCCGCCGCGC-3'

^a Restriction sites are underlined

Appendix 8.2: Palm oil emulsification by H16, Re2313 (*lipA* deletion), and Re2318 (*lipB* deletion) after 24 h of growth.



Appendix 8.3: SDS-PAGE gel of extracellular protein in the concentrated supernatant of: H16 (WT, Lane 1); H16/pCJB201 (*lipA* overexpression, Lane 2); Re2313 ($\Delta lipA$, Lane 3); Re2318 ($\Delta lipB$, Lane 4). PL: BenchMark™ Protein Ladder (Invitrogen). Supernatants (100 mL total volume) of *R. eutropha* strains, grown on 1% palm oil at a culture time of 24 h, were lyophilized and concentrated to 1 mL. Concentrations of proteins in the concentrated supernatant determined by Bradford assay were as follows: H16, 640 $\mu\text{g/ml}$; H16/CJB201, 850 $\mu\text{g/ml}$; Re2313, 425 $\mu\text{g/ml}$; Re2318, 385 $\mu\text{g/ml}$. The concentrated supernatants are stained with Coomassie brilliant blue. 15 μl of concentrated supernatant and protein ladder were individually loaded onto the gel. Protein ladder molecular weight indicated in kDa. LipA has molecular weight of 38.6 kDa.



Appendix 8.4: Palm oil emulsification by H16/pBBR1MCS-2 (WT) vs. H16/pCJB201 (*lipA* overexpression) 5 h following inoculation.



Appendix 8.5: Nucleotide sequence and amino acid sequences of LipA. The conserved catalytic triad Ser, His, and Asp residues were bolded in red. The cysteine residues were in italicized green.

```

ATGGAGCACAGCGGACACCACGCGTGGCGACGACGACGCCCGCGCTACGCGAGCAGAAGGCCGGCAAGGCCTTGCGCAGGCTCGCAGGCACAGCCACGC < 100
M E H S G H H A C G R R T P A L R E Q K A G K A L R R L A G T A T L
    10      20      30      40      50      60      70      80      90

TGGTCGACGCGGCCATGCTGGCGCAGCCAGCACCAGCCCTGGCCGCGAGCGGCGACTACGCGAAGACGCGTTACCCGATCGTGGTCCACGGACTGAC < 200
V A A A M L A Q P A P A L A A S G D Y A K T R Y P I V L V H G L T
    110     120     130     140     150     160     170     180     190

CGGCGCGCCAGGATGGTGGTGTGCTCGACTACTGGTATGGCATCCCGAAGTGTGCGGGCCACGGCGCGCAAGTCTATGTGGCCACGGTGCCTGCG < 300
G A A R M G G V L D Y W Y G I P E V L R A N G A Q V Y V A T V P S
    210     220     230     240     250     260     270     280     290

TTCAACAGCGACGAAGAGCGCGCCCTGGCGCTGCAGGCCTATGTGCGCGCGGTCAAGCTGGAAGCGGCGCAGACAAGGTCAACCTGATCGGCCACAGCC < 400
F N S D E E R A L A L Q A Y V R A V K L E S G A D K V N L I G H S Q
    310     320     330     340     350     360     370     380     390

AGGCGGGCCGACCTCGCGCATGCTGGCGGCGATGTCGCGCAGGACGTGGCCCTCGGTACCACCATCGGCAGCCCGCATCGCGGCGAGCGAAGTGGCCGA < 500
G G P T S R M L A A M S P Q D V A S V T T I G S P H R G S E V A D
    410     420     430     440     450     460     470     480     490

CACCGTGTGGACCTGATCAATGGCGTCAACAGTATTCGATCGCCGGCGGCTACTCGTCCGCATCATCCAGGGCGTGTCTGATACAGTGGGTGGTTC < 600
T V L D L I N G V N S I P I A G P V L V G I I Q G V L D T V G W F
    510     520     530     540     550     560     570     580     590

AACGGCATCGGCAACGGGCGGCGCTGGACAGGATGCGCTGGCCCTCGCTCAAGATCCTGACCAGCGTGGCGCCCGGAGCAGAATGCGCGCCTCGATG < 700
N G I G N G Q A L D Q D A L A S L K I L T T R G A A E Q N A R L D A
    610     620     630     640     650     660     670     680     690

CCACGCTGGTGGCCCGCACGAAATCGGCACTGGGGCCGATTGCAATACTGCTGGCGCGGTGTCGAGCAACGGCAGGCGCGCGATGCCGCGGGCAACTT < 800
T L V P G T K S A L G P D C N T A G A V S E Q R Q A R D A A G N F
    710     720     730     740     750     760     770     780     790

CGTCACCCATACCCAGGCCGCTATTCCTGGACCGGCGAGGTGGCGGCTTCAGCCTGCTGCGCTCCAACCTGCTGGATCCGACCACGGTGTATGATGTCG < 900
V T H T Q A A Y S W T G Q G G P F S L L R S N L L D P T T V M M S
    810     820     830     840     850     860     870     880     890

GCGTCGCGCGGGCTGATGGACCTGAAGGGCGCGGCCCAATGACGGGCTGGTCTCGGTCTGCAGCAGCAAGTGGGGCCGGGTGCTGGCCACGGGCTACT < 1000
A S A G L M D L K G A G P N D G L V S V C S S K W G R V L A T G Y Y
    910     920     930     940     950     960     970     980     990

ACTGGAACCATCTCGACGAGGTGAACAGATGGCCGGCCTGTACCAGGACGCTCGATCCGCGCACGGTCATTCTCAGCCACGCCAACCGGCTGCGCAATGA < 1100
W N H L D E V N Q M A G L Y Q D V D P R T V I L S H A N R L R N D
    1010    1020    1030    1040    1050    1060    1070    1080    1090

CCAGCTCTGA < 1110
Q L *

```


CHAPTER 9

Production of biopolymer from common waste materials in *Ralstonia eutropha*

(Part of this chapter was previously published in Journal of Macromolecular Science, 2009. 49: 226-248 'Biosynthesis of poly(hydroxyalkanoates)' Jingnan Lu, Ryan Tappel, and Christopher Nomura © Taylor & Francis Group)

INTRODUCTION

Polyhydroxyalkanoates (PHAs) are polyesters that can be produced by a variety of native bacterial strains. These polyesters are produced as intracellular carbon storage compounds and energy reserves (Abe and Doi 2002; Anderson and Dawes 1990). The major property of these polyesters is its biodegradability, which has attracted much attention from single-use bulk, commodity plastics, to specialized medical applications (Bunger et al. 2007; Dvorin et al. 2003; Mendelson et al. 2007; Sodian et al. 2000; Sodian et al. 2002; Stock et al. 2000; Sudesh 2004; William and Martin 1999; Zinn et al. 2001). The physical properties of PHAs are based on the number of carbon atoms in the individual monomer units as well as on the physical structure of these monomers following their incorporation into polymer chains. In general, PHA monomers may be divided up into three main classes: short-chain-length (SCL) PHAs, which consist of monomers with chain lengths of 3-5 carbon units; medium-chain-length (MCL) PHAs, which consist of monomers with chain lengths between 6 and 14 carbon units; and long-chain-length (LCL) PHAs, which are composed of monomers with carbon chain lengths greater than 14 units (Figure 9.1). These monomers can be incorporated to form homopolymers or copolymers with variety physical properties. Polymers composed solely of SCL monomer units generally have thermoplastic properties, which polymers composed of MCL subunits generally have elastomeric properties (Abe and Doi 2002; Anderson and Dawes 1990; Braunegg et al. 1998; Gomez et al. 2012). The best-studied copolymer has composition of both SCL and MCL monomers. PHA copolymers with a relatively high mol% of SCL monomers and low mol% of MCL monomers have properties similar to the bulk commodity plastic polypropylene. One of such PHA copolymers is poly(3-hydroxybutyrate-*co*-3-hydroxyhexanoate), which is less brittle than poly(3-hydroxybutyrate) and has a lower Young's modulus and lower melting temperature. It is a flexible, but tough plastic with great industrial potential (Budde et al. 2011a; Budde et al. 2011b; Madision and Huisman 1999; Steinbuchel and Valentin 1995; Sudesh et al. 2000; Witholt and Kessler 1999). The monomeric composition of PHA polymers can be influenced by several factors, including the organism producing the PHA polymer, the carbon source on which cells are grown, how that carbon source is metabolized in the cells, the types of monomer-supplying enzymes used, and the type of PHA synthase used to synthesize the polymer (Abe and Doi 2002; Aragao et al 2009; Braunegg et al. 1998; Budde et al. 2011a; Bunger et al. 2007; Fiorese et al. 2009; Slater et al. 1998; Witholt and Kessler 1999).

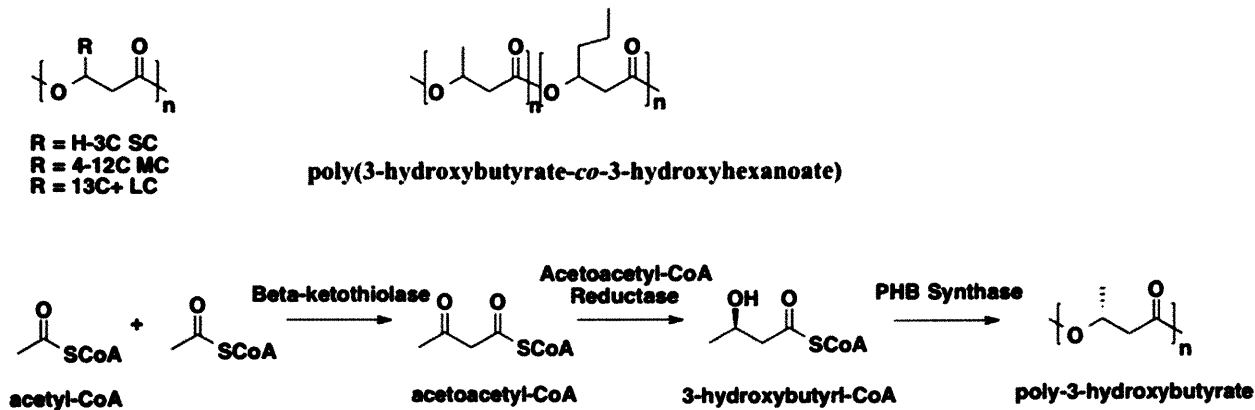


Figure 9.1: Structure of PHA with various monomer units (top left) and structure of poly(3-hydroxybutyrate-co-3-hydroxyhexanoate) (top right). PHB (poly-3-hydroxybutyrate) production pathway condensates two molecules of acetyl-CoA to acetoacetyl-CoA and subsequently reduce it to 3-hydroxybutyryl-CoA. PHB synthase then connects each monomer units into polymeric esters (bottom schematic).

Ralstonia eutropha is a hydrogen-oxidizing bacterium capable of growing in both anaerobic and aerobic environments. Both organic compounds and hydrogen can be used as sources of energy. *R. eutropha* is known to produce PHA when exposed to excessive amounts of carbon while in nitrogen or phosphate-limited environment. Up to 80% cell dry weight of PHA can be accumulated in wild type strains. For the past decades, *R. eutropha* has been the model organism for the study of PHA accumulation and has been engineered to produce PHAs with various monomer compositions (Bowien and Schlegel 1918; Brigham et al. 2012; Brigham et al. 2010; Budde et al. 2011a; Budde et al. 2011b; Pohlmann et al. 2006; Reinecke and Steinbuchel 2009; Riedel et al. 2014; Riedel et al. 2011; Steinbuchel and Schlegel 1989; Sugimoto et al. 1999; Volova et al. 2005; Yang et al. 2010). In one study, wild type *R. eutropha* was engineered to contain an enoyl coenzyme A hydratase from *Pseudomonas aeruginosa* and PHA synthase of *Rhodococcus aetherivorans* with broad substrate specificity that can incorporate both SC and MC monomers into the copolymers. This engineered strain was able to produce poly(3-hydroxybutyrate-co-3-hydroxyhexanoate) with 17 to 30 mol% hydroxyhexanoate (HHx) from palm oil (Budde et al. 2011a; Budde et al. 2011b; Riedel et al. 2011).

Palm oil is one of the most abundant plant oil and is a cheap carbon source. It consists mostly of triacylglycerols, in which three fatty acids are attached to a glycerol backbone, although a small amount of free fatty acids also exists. In order to utilize palm oil, *R. eutropha* secretes an extracellular lipase (LipA), which is able to cleave off and release fatty acids from triacylglycerols (Lu et al. 2013). Some bacteria also synthesize and secrete surfactants, which increases the surface area of fats for lipase catalysis. Acetyl-CoAs, resulting from beta-oxidation of these free fatty acids, are used for cellular growth, and can also be condensed and reduced to 3-hydroxybutyryl-CoA for the production of poly(3-hydroxybutyrate) (Figure 9.1). MCL acyl-CoA from oxidation of fatty acids can also be incorporated into PHA by the flexible PHA synthase to form PHA copolymers with both SC and MC monomers such as poly(3-hydroxybutyrate-co-3-hydroxyhexanoate) (Figure 9.1). Utilization of palm oil in large-scale fermentation processes faces the challenge of limited carbon source bioavailability. Palm oil is insoluble in growth media, which creates a heterogeneous mixture with the oils either concentrated at the top of the fermenter vessel or around the vessel walls. As a result, growth of *R. eutropha* experiences a

long lag phase, because the cells are unable to gain access to the oils, the sole carbon source (Budde et al. 2010a; Riedel et al. 2011). Various surfactants were reported to improve the emulsification of oils in growth media and improve the growth lag phase (Budde et al. 2010b). Addition of surfactants, however, can be time-consuming and costly in large-scale industrial fermentation processes. In this study, *R. eutropha* extracellular lipase LipA was overexpressed to increase the rate of triacylglycerides cleavage to free fatty acids, which acted as natural surfactants.

In a separate study, *R. eutropha* growth media was formulated to contain vinasse, the waste byproduct of ethanol fermentation. Due to increasing fuel demands, ethanol production has escalated in recent years. Vinasse is generated as a byproduct of the ethanol industry. For every liter of ethanol produced, nine to fourteen liters of vinasses are released into the environment. Studies have used vinasse as a source of biogas production, animal feed, or rich fertilizer, but this last usage can lead to ground waters contamination when vinasse is applied excessively on soils (Granato and Junior 1991; Pereira and Pereira 2008). Vinasse is rich in organic acids, phosphates and other components that could be used as nutrient sources for a biotechnological process to produce value-added products, such as PHAs. The presence of toxic phenol compounds and high salts limited its usage by most microorganisms; however the metabolic versatile *R. eutropha* can efficiently degrade phenol compounds and grow under harsh conditions (Santos et al. 2005). Here, the composition of vinasse was elucidated and reformulated to achieve optimal *R. eutropha* growth and PHA production.

MATERIALS AND METHODS

Chemicals, bacterial strains and plasmids

Chemicals were purchased from Sigma-Aldrich unless indicated otherwise. Experiments were performed with strains listed in Table 9.1.

Table 9.1: Strains used in this study.

<i>R. eutropha</i> Strains	Genotype	Reference
H16	Wild-type, gentamicin resistant (Gen ^r)	ATCC17699
H16/pBBR1MCS-2	Wild-type containing broad-host-range cloning vector (Gen ^r Kan ^r)	(Brigham et al., 2010)
Re2313	H16 Δ <i>lipA</i> Gen ^r	(Brigham et al., 2010)
Re2313/pBBR1MCS-2	H16 Δ <i>lipA</i> containing broad-host-range cloning vector (Gen ^r Kan ^r)	(Lu et al. 2013)
H16/CJB201	Wild-type containing pBBR1MCS-2 with <i>R. eutropha lipA</i> gene inserted into the multiple cloning site (Gen ^r Kan ^r)	(Lu et al. 2013)

Growth media and cultivation conditions

R. eutropha were cultivated aerobically in rich and minimal media at 30°C. Rich medium consisted of 2.75 % (w/v) dextrose-free tryptic soy broth (TSB) (Becton Dickinson, Sparks, MD). Minimal medium used to cultivate *R. eutropha* was formulated as described previously (Lu et al. 2012). For all *R. eutropha* cultures, 10 µg/mL final concentration of

gentamicin was added. Kanamycin at 300 µg/mL concentration was added to *R. eutropha* with plasmid.

A single colony of *R. eutropha* from a TSB agar plate was used to inoculate 5 mL of TSB medium. The culture was then incubated on a roller drum for 24 h at 30°C before being used to inoculate a flask culture of 100 mL minimal medium, containing 2% (w/v) fructose as carbon source, to an initial OD₆₀₀ of 0.1. The minimal medium culture was continuously shaken in a 30°C incubator at 200 rpm for 24 h before transferred into the fermenters. In the vinasse culture studies, minimal medium was substituted with 100% vinasse. pH of vinasse culture was adjusted to 6.8 with 1 M NaOH. The cultures were inoculated as described above and aliquots of culture were removed periodically for carbon and nitrogen source analysis.

Batch fermentation conditions

A Sixfors proportional–integral–derivative (PID) controller system (Infors, Switzerland) was used for fermentation studies. The Sixfors bioreactor system contains six bench-scale bioreactors. Each fermentation glass vessel is 500 ml in volume with a working volume of 400 ml. The operating temperature of the cultures was kept at 30°C. The pH was maintained with 2mM NaOH at 6.8±0.1 throughout the cultivation period. Initial culture OD₆₀₀ is diluted to 0.1. Fermentation culture media contains minimal media with 4% (v/v) palm oil and 0.4% (w/v) NH₄Cl as carbon and nitrogen source respectively. Dissolved oxygen (pO₂) was measured with an Ingold polarographic probe and maintained at above 40% O₂ saturation by automatically adjusting the flow of a mixture of air and pure oxygen via flow controllers while maintaining an air flow of 500 ml/min and also by automatically adjusting the agitation speed from 200 to 900 rpm. Foam during cultivation was mechanically eliminated with a pair of cable ties attached to the shaft of the impellor.

Polymer quantification

Fermentation cultures of 5 ml aliquots were sampled throughout the cultivation period. Aliquots were added to pre-weighted polypropylene test tubes and centrifuged at 6,500 x g for 10 min at 4°C. The pellets were washed first with 5 ml sterile water kept at 4°C and then 2 ml hexanes to remove salts and residual oils. Lastly the pellets were resuspended in 2 ml cold water, frozen overnight at -80°C, and lyophilized for cell dry weight (CDW) determination. PHB content were measured as described previously (Karr et al. 1983; York et al. 2003).

Carbon and nitrogen analysis

Culture supernatants were filtered and injected into HPLC to determine concentrations of fructose, sucrose, lactose, glycerol, acetate, and ethanol. The HPLC was equipped with an ion exchange column, and the detection methods used were previously described (Kurosawa et al. 2010). Ammonium concentrations in vinasse were measured using an ammonium assay kit (Sigma-Aldrich) following the manufacturer's instructions.

Enzymatic activity assays

Extracellular lipase activity was determined using a modified protocol with *p*-nitrophenyl palmitate (*p*NP) as a substrate (Ng et al. 2010). The assay mixture contains 100 mM glycine-HCl buffer at pH 7.0 and 0.1% (w/v) polyvinyl alcohol. Cell-free supernatant was added to the assay mixture to a final volume of 900 μ L and incubated at room temperature for 5 min. The reaction was initiated by the addition of 0.19 mg *p*NP in 100 μ L dimethyl sulphoxide. The absorbance was recorded at OD₄₀₅ by a spectrophotometer (Agilent 8453 UV-visible). Control assay mixtures do not contain substrate or cell-free supernatant. One enzyme unit (U) was defined as one μ mol *p*-nitrophenol liberated per min using extinction coefficient of $1.78 \times 10^4 \text{ M}^{-1} \text{ cm}^{-1}$.

RESULTS

Cellular growth and PHA production on palm oil

Production of poly(3-hydroxybutyrate-*co*-3-hydroxyhexanoate) in engineered *R. eutropha* on palm oil was a success (Budde et al. 2011a); however in order for this process to become economically viable at industrial fermentation scales, cultivation lag phase must be reduced and the use of surfactants should be eliminated. *R. eutropha* LipA is an extracellular lipase and is crucial for the metabolism of lipids. LipA catalyzes the non-specific hydrolysis of triacylglycerol into diacylglycerol, monoglycerol, glycerol, and free fatty acids at the interface of lipid and water. The triacylglycerol molecules, together with their cleavage products, form an emulsion within the aqueous media and therefore become bioavailable for cell growth. LipA was overexpressed in wild type *R. eutropha* previously and was able to reduce growth lag phase on palm oil in batch flask cultures (Lu et al. 2013). Here, the *R. eutropha* LipA overexpression strain was cultivated in fermentation settings in hope to achieve the same result.

Wild type *R. eutropha* (H16/pBBR1MCS-2), *R. eutropha* LipA overexpression strain (H16/pCJB201), and mutant *R. eutropha* with *lipA* deletion (Re2313/pBBR1MCS-2) were cultivated in Sixfors bioreactor system. This system contains six bench-scale reactors, so each strain were cultivated in duplicates. H16/pCJB201 shown minimal lag phase when grown in culture with 4% (v/v) palm oil and reached maximum cell dry weight at 48h. Whereas the wild type *R. eutropha* experienced ~24 h lag phase before reaching maximum cell dry weight of 24 g/L at 72 h. Strain lacking *lipA* gene encoding the extracellular lipase did not grow on palm oil, because *R. eutropha* is unable to update triacylglycerol directly. Presence of excess LipA in cultures reduced the lag phase in palm oil fermentation by at least 24 h while achieving same overall cell dry weight (Figure 9.2).

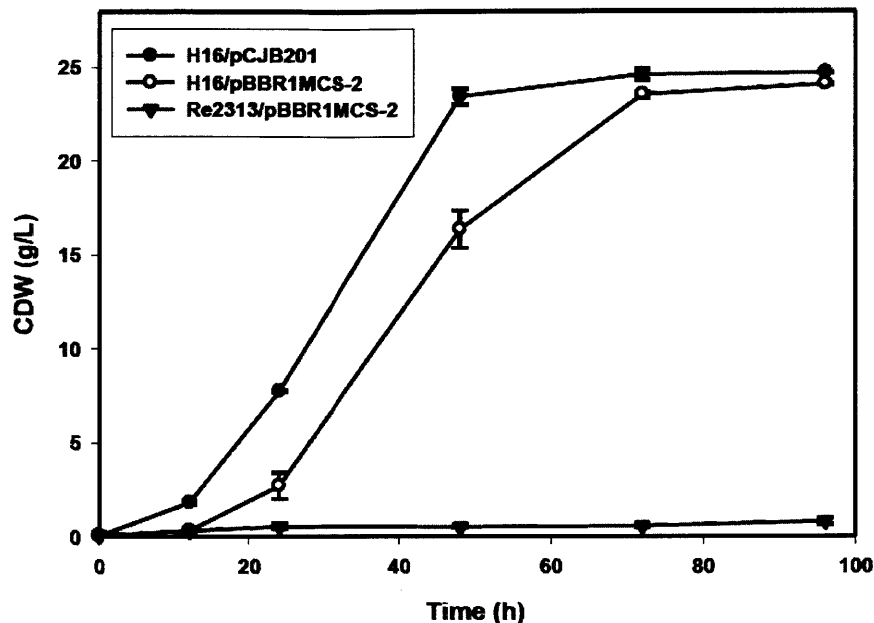


Figure 9.2: Cell dry weight (CDW) profile of strains H16/pCJB201 (solid circles), H16/pBBR1MCS-2 (open circles), and Re2313/pBBR1MCS-2 (solid triangles) on 4% (v/v) palm oil over fermentation cultivation time of 96 h. Error bar represents standard deviation of duplicate experiments and data here are average of two experiments.

The amount of PHA polymers produced by each strain was analyzed. Since these strains were not engineered with broad substrate specificity thiolase, reductase, or polymerase, poly-3-hydroxybutyrate was solely produced as the PHA polymer. Both H16/pCJB201 and H16/pBBR1MCS-2 accumulated the same amount of PHA over 96 h cultivation period on palm oil as the sole carbon source. Similar to cell growth, strain H16/pCJB201 reached such production level ~24 h prior to H16/pBBR1MCS-2. Since Re2313/pBBR1MCS-2 was unable to grow in palm oil, only a small amount of PHA was accumulated from the few free fatty acids in palm oil (Figure 9.3).

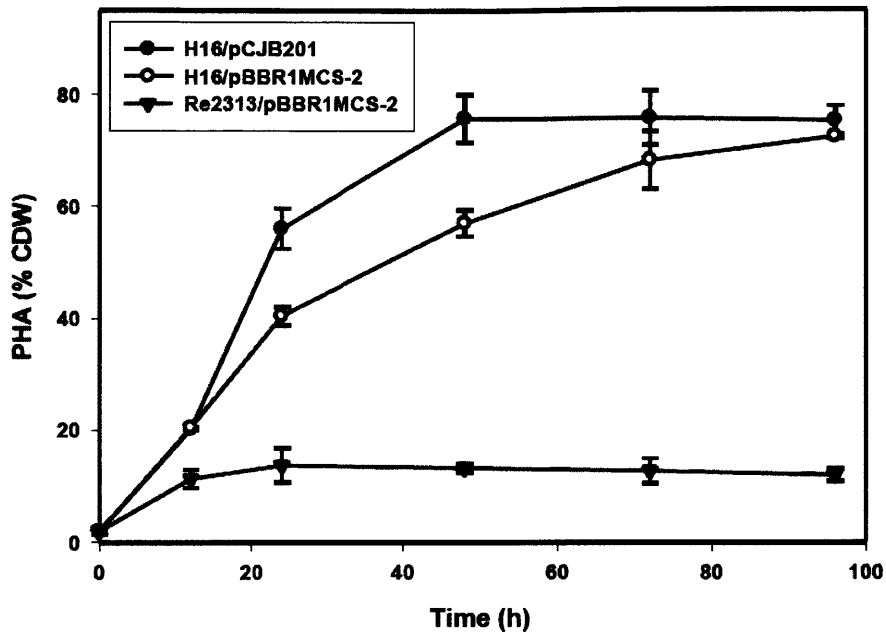


Figure 9.3: Amount of PHA, specifically poly-3-hydroxybutyrate, accumulated in H16/pCJB201 (solid circles), H16/pBBR1MCS-2 (open circles), and Re2313/pBBR1MCS-2 (solid triangles). Data represent average of two experiments on 4% (v/v) palm oil and error bars are the standard deviations.

The Re2313/pBBR1MCS-2 has the *lipA* gene deleted from the genome, therefore it does not express any secreted lipase and has no lipase activity in its culture supernatant. H16/pBBR1MCS-2, however, had moderate lipase activity in its supernatant throughout the fermentation period. Lipase activity increased slowly in the first 12 hours and stayed constant until the end of fermentation. Compared to the lipase activity in batch flask culture, activity of lipase detected in fermentation process is much lower. This is surprising, since more palm oil or specifically more triacylglycerol is present in the fermentor vessels and therefore should have activated lipase transcription and activity. Another theory could be that since lipase catalyzes the hydrolysis reaction at the lipid water interface, the excess lipase is associated with the lipids and not the aqueous supernatant used in the current lipase activity assay. H16/pCJB201 has *lipA* overexpressed under a constitutively expressed promoter, thus showed higher lipase activity for 24 h and activity stayed at ~170 mU/ml till the end of fermentation (Figure 9.4).

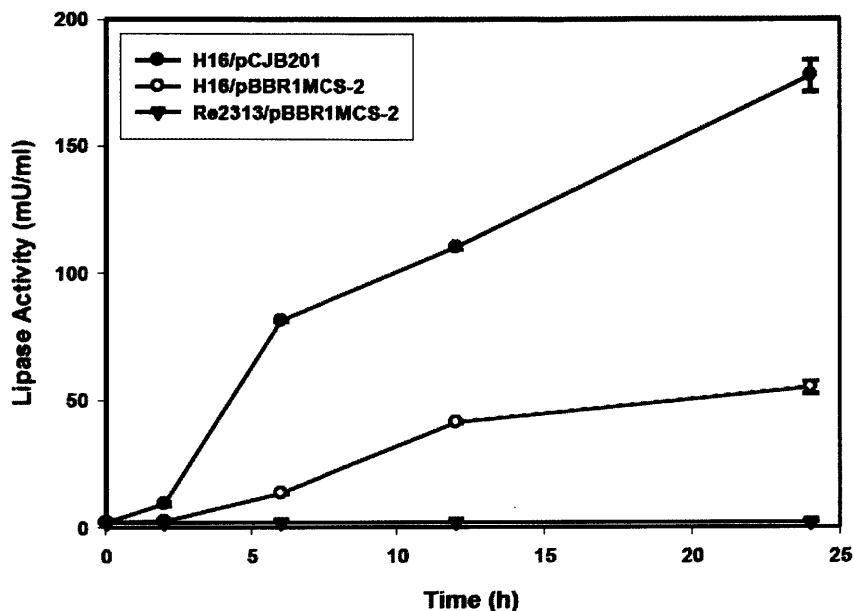


Figure 9.4: Lipase activities of *R. eutropha* strains in 4% (v/v) palm oil fermentation cultures. The average of H16/pCJB201 (solid circles), H16/pBBR1MCS-2 (open circles), and Re2313/pBBR1MCS-2 (solid triangles) strain activities were indicated by solid circles, open circles, and solid triangles respectively.

Additional LipA in the fermentation culture shortens cultivation times without compromising cellular growth and PHA production. It also eliminated the usage of surfactants, since the rapidly cleaved free fatty acids can act as cell's natural surfactants. Overexpression of *lipA* did not affect cell dry weight and PHA concentration. Overall, increased LipA activity shortened fermentation culture time by at least 24 h.

Cellular growth and PHA production on vinasse

Approximately 60 billion liters of ethanol are produced annually for gasoline additives. The ethanol produced can be from fermentation of corn or sugar cane. For each liter of ethanol produced, nine to thirteen liters of vinasse byproduct is also produced. Such a large volume of vinasse effluent has generated many environmental concerns due to its impact on soil and ground water resources. Studies have indicated that the main impact of vinasse infiltration in soil and groundwater resources is increased concentration of salts, such as nitrate, nitrite, ammonium, magnesium, phosphate, aluminum, iron, manganese, chloride, and organic carbons (Granato and Junior 1991; Pereira and Pereira 2008). Here, vinasse is evaluated for its carbon and nitrogen composition, in addition to its potential as a nutrient source for PHA production by *R. eutropha*.

Vinasse harvested directed from an ethanol fermentation facility in Brazil is used in this study. The vinasse effluent appears as a clear dark brown mixture. Centrifugation at 13,000 x g eliminated ~5% solid particles from vinasse. The remaining liquid is referred to as vinasse liquid. The vinasse liquid is slightly acidic with pH of 6.2. Analysis of the vinasse liquid revealed sucrose, fructose, lactic acid, glycerol, acetic acid, and ethanol as carbon sources (Table 9.2). The carbon sources and their perspective concentrations determined here are different from what's reported in the literature. The organic acid composition reported is mainly lactic acid (20

g/L), acetic acid (12 g/L), butyric acid (11 g/L), malic acid (0.3 g/L), isobutyric acid (2 g/L), and glycerol (4 g/L) (Granato and Junior 1991; Pereira and Pereira 2008). The difference between the reported value and the ones determined here could be due to difference in ethanol fermentation facilities and batches.

Table 9.2: Carbon and nitrogen source composition and concentration in vinasse liquid.

Carbon source	Concentration (g/L)
Sucrose	7.2
Fructose	3.3
Lactic acid	2.5
Glycerol	4.0
Acetic acid	0.6
Ethanol	1.2
Nitrogen source	Concentration (mg/L)
Urea	Not detectable
Ammonia	178.2

R. eutropha accumulates PHA biopolymers when the cells are cultivated in high carbon, but low nitrogen or phosphorus conditions. The most widely used media composition for PHA production has carbon to nitrogen molar ratio of 73. In 100% vinasse, the carbon to nitrogen ratio is much lower, at a calculated value of 11. Therefore, in order for *R. eutropha* to switch to PHA production mode, more carbon source is needed in the growth culture. Wild type *R. eutropha* H16 was cultivated under three different media compositions, minimal media (MM) with 2% (w/v) fructose and 0.05% (w/v) NH₄Cl, 100% vinasse, and 100% vinasse with 1% (w/v) fructose. Pure vinasse liquid is capable of supporting *R. eutropha* growth and PHA production (Table 9.3 and Figure 9.5). Since carbon to nitrogen ratio is low in 100% vinasse liquid, the media did not support PHA production. OD₆₀₀ on pure vinasse liquid was ~3.2 lower than in minimal media with 2% fructose. The difference in OD₆₀₀ is the accumulation of PHA, which makes the cells larger in size. On the other hand, vinasse liquid supplemented with 1% fructose resulted in similar final OD reading as *R. eutropha* grown in media with 2% fructose (Table 9.3). Production of PHA reached ~80% CDW when *R. eutropha* was cultivated in minimal media with 2% fructose and 0.05% NH₄Cl. Cultivation using 100% vinasse only resulted in ~10% PHA production due to its low carbon to nitrogen ratio. When 1% fructose was added to 100% vinasse liquid, carbon to nitrogen ratio reached approximately 46. Such culture medium was optimal for PHA production as shown in Figure 9.5.

Table 9.3: Growth of *R. eutropha* H16 in minimal media (MM) with 2% (w/v) fructose (fruc.) and 0.05% (w/v) NH₄Cl, 100% vinasse (vin.), and 100% vinasse with 1% (w/v) fructose.

Media composition	OD ₆₀₀ :	0 h	6 h	24 h	48 h	72 h
MM 2% fruc. 0.05% NH ₄ Cl		0.04	0.25	7.82	12.90	13.56
100% vin.		0.03	0.54	4.44	4.10	4.24
100% vin. 1% fruc.		0.03	0.56	10.62	14.72	13.14

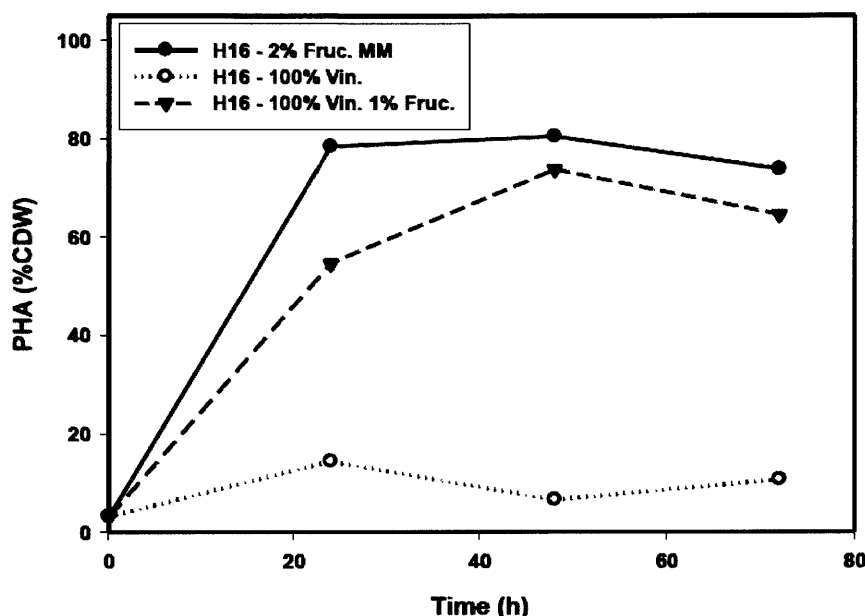


Figure 9.5: Production of PHA by *R. eutropha* H16 in minimal media with 2% fructose and 0.05% NH₄Cl (solid circles), 100% vinasse liquid (open circles), and 100% vinasse liquid with 1% fructose (solid triangles).

In order to understand carbon source utilization and preference, the concentration of fructose, sucrose, lactose, glycerol, acetate, and ethanol were monitored throughout the cultivation time. Fructose is a preferred carbon source by *R. eutropha*. In both the control and vinasse liquid with fructose cultures, strain H16 utilized ~7 to 8 g/L fructose for growth and PHA production. Fructose concentration stayed constant when *R. eutropha* is cultivated in 100% vinasse (Figure 9.6). Although *R. eutropha* is capable of using sucrose as a carbon source, in the presence of other carbon sources such as fructose, sucrose was not utilized (Figure 9.7). Lactose and ethanol can be easily taken up by cells, thus are favorable carbon sources by *R. eutropha*. Both lactose and ethanol were completely utilized from vinasse regardless of fructose supplementation (Figure 9.8, Figure 9.11). Glycerol and acetate utilization profiles were expected to be the same for both vinasse media compositions; however when *R. eutropha*'s growing in 100% vinasse supplemented with 1% fructose, both glycerol and acetate in vinasse were used to near-depletion after 72 h of growth, while these carbon sources were not utilized in 100% vinasse culture (Figure 9.9, Figure 9.10). This difference in carbon utilization could be the result of PHA production, which requires additional carbon source. In 100% vinasse culture,

carbon to nitrogen ratio did not support optimal production of PHA; therefore cells did not need extra the carbon source from glycerol and acetate (Figure 9.9, Figure 9.10).

Vinasse, the byproduct of ethanol fermentation, contains various salts, carbon, and nitrogen sources capable of supporting *R. eutropha* growth and PHA production. *R. eutropha* did not experience any toxic effects when cultivated on 100% vinasse. In order to achieve optimal production of PHA, 100% vinasse can be used with the supplementation carbon source such as fructose.

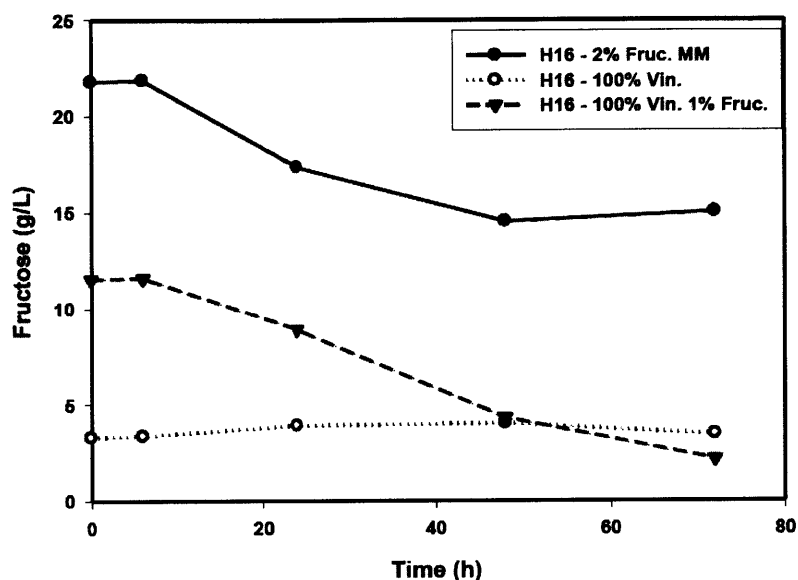


Figure 9.6: Fructose utilization profile of *R. eutropha* H16 in minimal media with 2% fructose and 0.05% NH_4Cl (solid circles), 100% vinasse liquid (open circles), and 100% vinasse liquid with 1% fructose (solid triangles).

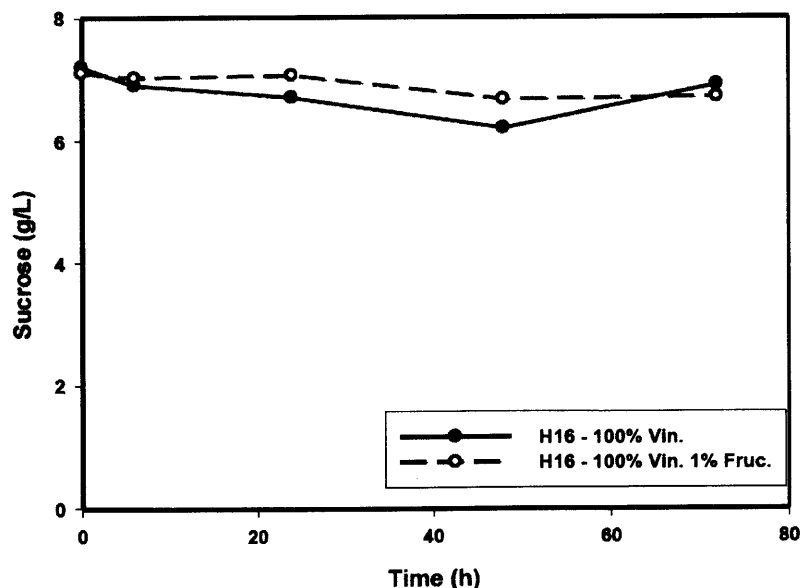


Figure 9.7: Sucrose utilization profile of *R. eutropha* H16 in 100% vinasse liquid (solid circles), and 100% vinasse liquid with 1% fructose (open circles).

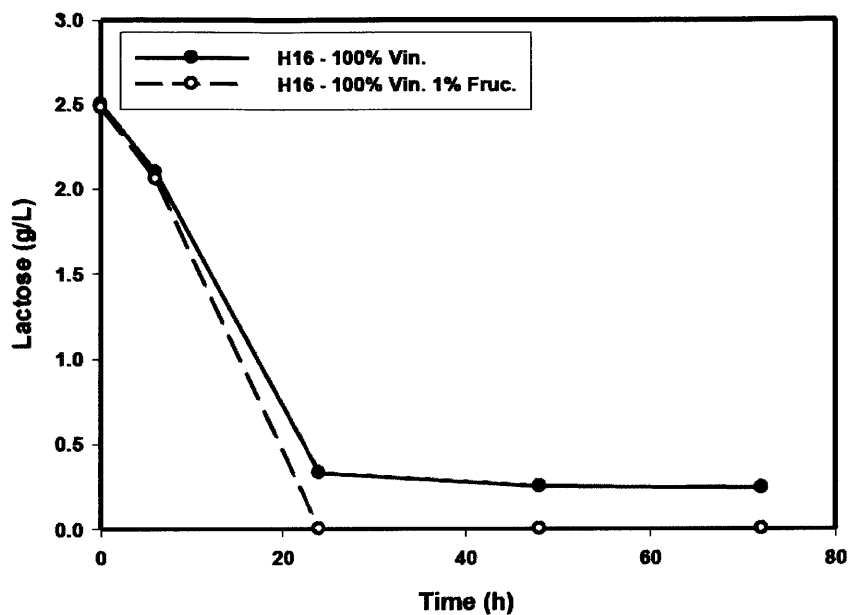


Figure 9.8: Lactose utilization profile of *R. eutropha* H16 in 100% vinasse liquid (solid circles), and 100% vinasse liquid with 1% fructose (open circles).

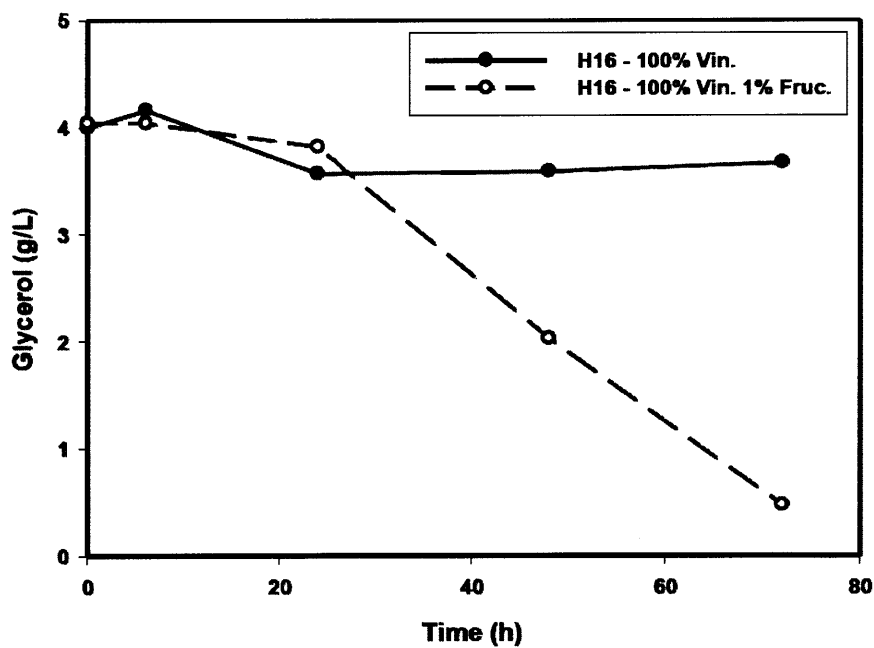


Figure 9.9: Glycerol utilization profile of *R. eutropha* H16 in 100% vinasse liquid (solid circles), and 100% vinasse liquid with 1% fructose (open circles).

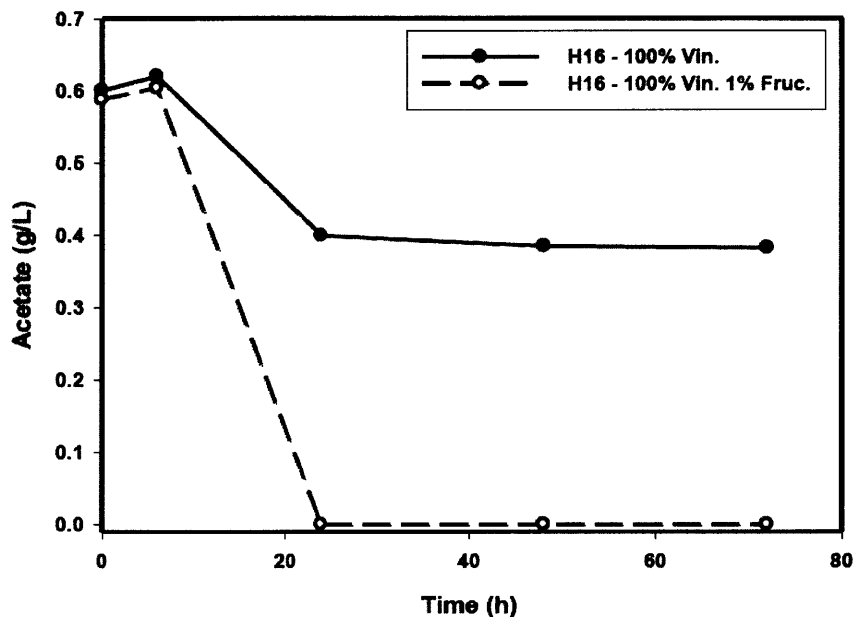


Figure 9.10: Acetate utilization profile of *R. eutropha* H16 in 100% vinasse liquid (solid circles), and 100% vinasse liquid with 1% fructose (open circles).

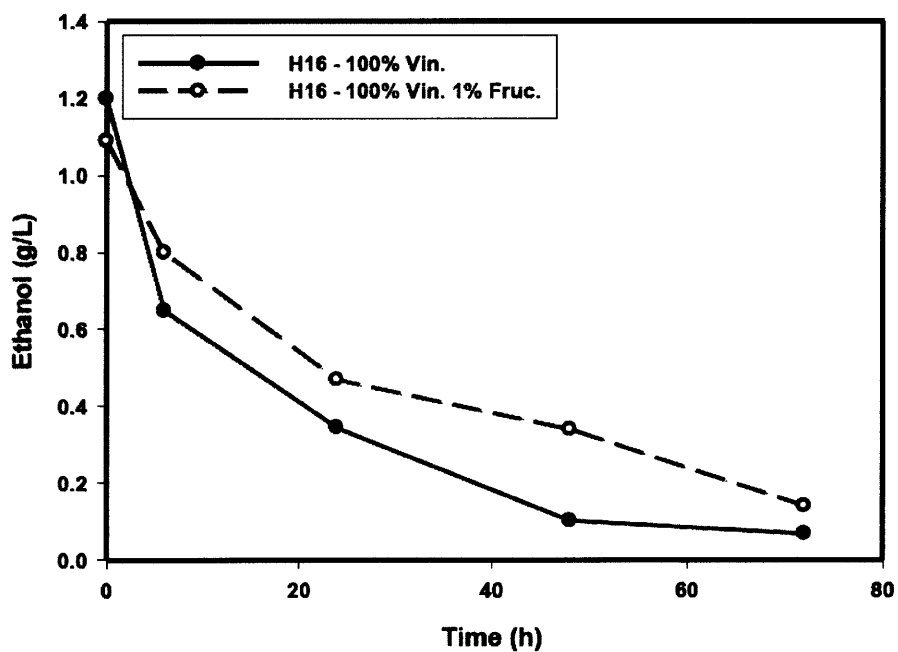


Figure 9.11: Ethanol utilization profile of *R. eutropha* H16 in 100% vinasse liquid (solid circles), and 100% vinasse liquid with 1% fructose (open circles).

DISCUSSION

PHA polymers are produced via a series of enzymatic reactions in wild type *R. eutropha* strain. The properties of PHA polymers are dependent on the starting carbon feedstocks, the

metabolic pathways for the conversion of those feedstocks into precursors for PHAs, and the specific activities and substrate specificities of the enzymes involved in the process (Aragao et al. 2009; Budde et al. 2011a; Hassan et al. 2002; Keenan et al. 2006; Peschel et al. 2008; Solaiman et al. 2004; Solaiman et al. 2006; Yang et al. 2010). In *R. eutropha*, PHAs are accumulated as granules and are surrounded by specific lipids and proteins. The granules in native polyhydroxybutyrate-producing organisms act as organelles that are involved in a process of simultaneous production and degradation via biosynthetic activity of PHA synthases and the thiolytic activities of PHA depolymerases.

Intracellular PHAs can be isolated by disruption of the cells and proteins surrounding the granules by both chemical and mechanical mechanisms. Isolated PHAs has been utilized as bulk commodity plastics, fishing lines, and medical products (Riedel et al. 2012). In order to reduce production cost, various common carbon sources have been studied and utilized for PHA production (Aragao et al. 2009; Budde et al. 2009a; Sugimoto et al 1999; Solaiman et al. 2000; Solaiman et al. 2006; Yang et al. 2010). In this study, two common and abundant carbon sources, palm oil and vinasse, were analyzed for *R. eutropha* growth and PHA production.

Conversion of palm oil to PHA has attracted much attention, because *R. eutropha* can utilize palm oil and produce valuable copolymers with both SCL and MCL monomers. Triacylglycerol, the main component in palm oil, is hydrolyzed to free fatty acids by an extracellular lipase, LipA (Lu et al. 2013). *R. eutropha* cells can then directly uptake these free fatty acids and break them down via the β -oxidation pathway for growth and PHA production. The physiological role of the β -oxidation pathway is to catabolize fatty acids for the production of reducing equivalents, the energy from respiratory electron transport chain. A fatty acid is activated by an acyl-CoA synthase and ATP to produce a substrate that will pass through a series of enzymes to produce acetyl-CoA and reduce the number of carbons in the fatty acid by two in a cyclic nature (Riedel et al. 2014). In *R. eutropha*, there are two sets of fully functional β -oxidation pathways, which is important for the production of acetyl-CoA and MCL-CoA moieties for PHA copolymers (Brigham et al. 2010). The most common PHA is poly-3-hydroxybutyrate, which consists 3-hydroxybutyrate as the monomer units. Poly-3-hydroxybutyrate is produced in wild type *R. eutropha*. However, when the strain is engineered to contain broad-substrate reductase and polymerase, poly(3-hydroxybutyrate-co-3-hydroxyhexanoate) can be produced from palm oil (Budde et al. 2011a).

Increasing the amount of extracellular LipA activity through *lipA* overexpression on a constitutively expressed vector in *R. eutropha* eliminated both the lag phase and use of surfactant in fermentation batch cultures with palm oil as the sole carbon source. This strategy could also be used in engineered *R. eutropha* strains for the production of poly(3-hydroxybutyrate-co-3-hydroxyhexanoate). Based on previous fermentation study on the production of poly(3-hydroxybutyrate-co-3-hydroxyhexanoate) from palm oil (Budde et al. 2011a; Riedel et al. 2011), theoretical yield calculated for wild type *R. eutropha* H16 growth with the same amount of carbon and nitrogen sources are 37.5 g/L cell dry weight and ~80% CDW PHB. Although PHB production was at the theoretical yield level, cell dry weight produced in this study was only ~68%. This could be the result of palm oil over-emulsification during fermentation process. It is likely that the rapid cleavage of triacylglycerol caused over-emulsification, since increased LipA also increased concentration of free fatty acids in the culture media. If the cellular fatty acid uptake and utilization are not as fast as triacylglycerol hydrolysis, free fatty acids will build up in the culture and act as natural surfactants, thus over emulsify the culture media. To overcome

this, an inducible promoter can be used to control the expression of *lipA*. Moreover, fatty acid uptake and utilization enzymes can be modified to rapidly break down the fatty acids.

Vinasse is generated as a byproduct of ethanol production. The typical method to dispose vinasse is by applying it to soils as a fertilizer. Although vinasse is rich in nutrients, too much vinasse in soil causes ground water contamination and soil runoffs. In this study, the carbon and nitrogen composition of vinasse were elucidated. Pure vinasse liquid is capable of supporting *R. eutropha* growth and did not cause any growth inhibition. However, for optimal PHA production, additional carbon source is needed in the vinasse liquid. A major challenge facing vinasse utilization is the inconsistency in nutrient components between ethanol fermentation facilities and batches. An industrial-wide effort is needed to standardize vinasse composition in order to utilize this waste byproduct for the production of value-added materials.

The promising potential of PHA biopolymers, combined with *R. eutropha*'s unique ability to utilize various carbon sources, made this cellular factory system an attractive candidate for industrial large scale production of biopolymers at low cost. In this study, *R. eutropha* was assessed for palm oil and vinasse utilization. The cells were able to grow and produce up to 80% CDW of PHAs from both common waste carbon sources.

REFERENCES

- Abe H, Doi Y (2002) 'Side-chain effect of second monomer units on crystalline morphology, thermal properties, and enzymatic degradability for random copolyesters of (R)-3-hydroxybutyric acid with (R)-3-hydroxyalkanoic acids'. *Biomacromolecules* 3: 133–138
- Anderson AJ, Dawes EA (1990) 'Occurrence, metabolism, metabolic role, and industrial uses of bacterial polyhydroxyalkanoates'. *Microbiol Rev* 54: 450–472
- Aragão GMF, Schimidell WN, Lutz IJ (2009) 'Preparation of PHA (polyhydroxyalkanoates) from a citric residue'
- Bowien B, Schlegel HG (1981) 'Physiology and biochemistry of aerobic hydrogen-oxidizing bacteria'. *Annual rev microbiology* 35: 405–452
- Braunegg G, Lefebvre G, Genser KF (1998) 'Polyhydroxyalkanoates, biopolyesters from renewable resources: physiological and engineering aspects'. *J Biotechnol* 65: 127–161
- Brigham CJ, Speth DR, Rha C, Sinskey AJ (2012) 'Whole genome microarray and gene deletion studies reveal regulation of the polyhydroxyalkanoate production cycle by the stringent response in *Ralstonia eutropha* H16'. *Applied and environmental microbiology*
- Brigham CJ, Budde CF, Holder JW, Zeng Q, Mahan AE, Rha C, Sinskey AJ (2010) 'Elucidation of β -oxidation pathways in *Ralstonia eutropha* H16 by examination of global gene expression' *J Bacteriol* 192: 5454–5464
- Budde CF, Riedel SL, Willis LB, Rha C, Sinskey AJ (2011) 'Production of poly(3-hydroxybutyrate-co-3-hydroxyhexanoate) from plant oil by engineered *Ralstonia eutropha* strains' *Appl Environ Microbiol* 77: 2847–2854
- Budde CF, Riedel SL, Hubner F, Risch S, Popovic MK, Rha C, Sinskey AJ (2011) 'Growth and polyhydroxybutyrate production by *Ralstonia eutropha* in emulsified plant oil medium' *Appl Microbiol Biotechnol* 89: 1611–1619
- Bunger CM, Grabow N, Sternberg K, Goosmann M, Schmitz KP, Dreutzer HJ, Ince H, Kische S, Nienaber CA, Martin DP, Williams SF, Klar E, Schareck W (2007) 'A biodegradable sent based on poly(L-lactide) and poly(4-hydroxybutyrate) for peripheral vascular application: preliminary experience in the pig'. *J Endovasc Ther* 14: 725–733
- Dvorin EL, Wylie-Sears J, Kaushal S, Martin DP, Bischoff J (2003) 'Quantitative evaluation of endothelial progenitors and cardiac valve endothelial cells: proliferation and differentiation on poly glycolic acid/poly-4-hydroxybutyrate scaffold in response to vascular endothelial growth factor and transforming growth factor beta1'. *Tissue Eng* 9: 487–493
- Fiorese ML, Freitas F, Pais J, Ramos AM, de Aragão GMF, Reis MM (2009) 'Recovery of polyhydroxybutyrate (PHB) from *Cupriavidus necator* biomass by solvent extraction with 1,2-propylene carbonate'. *Engineering in Life Sciences* 9(6): 454–461

Gomez JGC, Méndez BS, Nickel PI, Pettinari MJ, Prieto MA, Silva LF (2012) 'Making Green Polymers Even Greener: Towards Sustainable Production of Polyhydroxyalkanoates from Agroindustrial By-Products'. *Advances in Applied Biotechnology*

Granato EF, Junior JDL (1991) 'Anaerobic Digestion of Vinasse as Alternative Source of Electricity,' 1979: 1–5.

Hassan MA, Nawata O, Shirai Y, Rahman NAA, Yee PL, Ariff AB, Karim MIA (2002) 'A Proposal for Zero Emission from Palm Oil Industry Incorporating the Production of Polyhydroxyalkanoates from Palm Oil Mill Effluent'. *Journal of Chemical Engineering of Japan* 35(1): 9–14

Karr DB, Waters JK, Emerich DW (1983) Analysis of Poly- β -Hydroxybutyrate in *Rhizobium japonicum* Bacteroids by Ion-Exclusion High-Pressure Liquid Chromatography and UV Detection. *Appl Environ Microbiol* 46:1339-1344

Keenan TM, Nakas JP, Tannenbaum SW (2006) 'Polyhydroxyalkanoate copolymers from forest biomass'. *J Ind Microbiol Biotechnol* 33: 616–626

Kurosawa K, Boccazzi P, de Almeida NM, Sinskey AJ (2010) High-cell-density batch fermentation of *Rhodococcus opacus* PD630 using a high glucose concentration for triacylglycerol production. *J Biotechnol* 147:212-218

Lu J, Brigham CJ, Rha C, Sinskey AJ (2013) Characterization of an extracellular lipase and its chaperone from *Ralstonia eutropha* H16. *Appl Microbiol Biotechnol*.

Madison LL, Huisman GW (1999) 'Metabolic engineering of poly(3-hydroxyalkanoates): from DNA to plastic'. *Microbiology and molecular biology reviews MMBR* 63(1): 21–53

Mendelson K, Aikawa E, Mettler BA, Sales V, Martin D, Mayer JE, Schoen FJ (2007) 'Healing and remodeling of bioengineered pulmonary artery patches implanted in sheep'. *Cardiovasc Pathol* 16: 277–282

Ng KS, Ooi WY, Goh LK, Shenbagarathai R, Sudesh K (2010) Evaluation of jatropha oil to produce poly(3-hydroxybutyrate) by *Cupriavidus necator* H16. *Polym Degrad Stab* 95: 1365-1369

Nickzad A, Mogharei A, Monazzami A, Jamshidian H, Vahabzadeh F (2012) 'Biodegradation of Phenol by *Ralstonia eutropha* in a Kissiris-Immobilized Cell Bioreactor'. *Water Environment Research*

Peschel G, Dahse HM, Konrad A, Wieland GD, Mueller PJ, Martin DP, Roth M (2008) 'Growth of keratinocytes on porous films of poly(3-hydroxybutyrate) and poly(4-hydroxybutyrate) blended with hyaluronic acid and chitosan'. *J Biomed Mater Res A* 85: 1072–1081

Pohlmann A, Fricke WF, Reinecke F, Kusian B, Liesegang H, Cramm R, Eitinger T, Ewering C, Potter M, Schwartz E, Strittmatter A, Voss I, Gottschalk G, Steinbuchel A, Friedrich B, Bowien B (2006) 'Genome sequence of the bioplastic-producing "Knallgas" bacterium *Ralstonia eutropha* H16' *Nat Biotechnol* 24: 1257–1262

Pereira SY, Pereira P (2008) 'Environmental aspects in ethanol production related to vinasse disposal and groundwater'. *International Geological Congress*

Reinecke F, Steinbuchel A (2009) '*Ralstonia eutropha* strain H16 as model organism for PHA metabolism and for biotechnological production of technically interested biopolymers'. *J Microbiol Biotechnol* 16: 91-108

Riedel SL, Lu J, Stahl U, Brigham CJ (2014) 'Lipid and fatty acid metabolism in *Ralstonia eutropha*: relevance for the biotechnological production of value-added products' *Appl Microbiol Biotechnol*

Riedel SL, Bader J, Brigham CJ, Budde CF, Yusof ZAM, Rha C, Sinskey AJ (2011) 'Production of poly(3-hydroxybutyrate-co-3-hydroxyhexanoate) by *Ralstonia eutropha* in high cell density palm oil fermentations'. *Biotechnology and Bioengineering* 109: 74-83

Riedel SL, Brigham CJ, Budde CF, Bader J, Rha C, Stahl U, Sinskey AJ (2012) 'Recovery of poly(3-hydroxybutyrate-co-3-hydroxyhexanoate) from *Ralstonia eutropha* cultures with non-halogenated solvents'. *Biotechnology and Bioengineering* 110: 461-470

Steinbüchel A, Schlegel HG (1989) 'Microbiology Biotechnology Applied Excretion of pyruvate by mutants of *Alcaligenes eutrophus*, which are impaired in the accumulation of poly(3-hydroxybutyric acid) (PHB) under conditions permitting synthesis of PHB' 168-175.

Sugimoto T, Tsuge T, Tanaka K, Ishizaki (1999) 'A Control of Acetic Acid Concentration by pH-Stat Continuous Substrate Feeding in Heterotrophic Culture Phase of Two-Stage Cultivation of *Alcaligenes eutrophus* for Production of P(3HB) from CO₂, H₂, and O₂ under Non-Explosive Conditions. *Biotechnol and Bioeng* 62: 625-631

Santos MM, Venceslada BJ, Martin MA, Garcia GI (2005) 'Estimating the selectivity of ozone in the removal of polyphenols from vinasse'. *Journal of Chemical Technology & Biotechnology* 80(4): 433-438

Slater S, Houmiel KL, Tran M, Mitsky TA, Taylor NB, Padgett SR, Gruys KJ (1998) 'Multiple beta-ketothiolases mediate poly(beta-hydroxyalkanoate) copolymer synthesis in *Ralstonia eutropha*'. *J Bacteriol* 180: 1979-1987

Sodian R, Hoerstrup SP, Sperling JS, Martin DP, Daebritz S, Mayer JE, Vacanti JP (2000) 'Evaluation of biodegradable, three-dimensional matrices for tissue engineering of heart valves'. *ASAIO J* 46: 107-110

Sodian R, Loebe M, Hein A, Martin DP, Hoerstrup SP, Potapov EV, Hausmann H, Lueth T, Hetzer R (2002) 'Application of stereolithography for scaffold fabrication for tissue engineered heart valves'. *ASAIO J* 48: 12-16

Solaiman DKY, Ashby RD, Foglia TA, Marmer WN (2004) 'Poly(hydroxyalkanoates) from agricultural lipids and coproducts'. *Abstracts of Papers of the ACS* 227: U308-U308

Solaiman DKY, Ashby RD, Foglia TA, Marmer WN (2006) 'Conversion of agricultural feedstock and coproducts into poly(hydroxyalkanoates)'. *Appl Microbiol Biotechnol* 71: 783-789

Steinbuchel A, Valentin HE (1995) 'Diversity of bacterial polyhydroxyalkanoic acids'. *FEMS Microbiol Lett* 128: 219-228

Stock UA, Sakamoto T, Hatsuoka S, Martin DP, Nagashima M, Moran AM, Moses MA, Khalil PN, Schoen FJ, Vacanti JP, Mayer JE (2000) 'Patch augmentation of the pulmonary artery with bioabsorbable polymers and autologous cell seeding'. *J Thorac Cardiovasc Surg* 120: 1158-1168

Sudesh K, Abe H, Doi Y (2000) 'Synthesis, structure and properties of polyhydroxyalkanoates: biological polyesters'. *Prog Polym Sci* 25: 1503-1555

Sudesh K (2004) 'Microbial polyhydroxyalkanoates: an emerging biomaterial for tissue engineering and therapeutic applications'. *Med J Malaysia* 59: 55-56

Volova TG, Kozhevnikov IV, Yu B, Dolgoplova M, Yu, Trusova G, Kalacheva S, Yu V (2005) 'Physiological and Biochemical Characteristics and Capacity for Polyhydroxyalkanoates Synthesis in a Glucose-Utilizing Strain of Hydrogen-Oxidizing Bacteria, *Ralstonia eutropha* B8562'. *Microbiology* 74: 684-689

Williams SF, Martin DP (2002) 'Applications of PHAs in medicine and pharmacy'. In *Biopolymers*, Doi Y, Steinbuechel A, Eds Wiley-VCH: Weinheim, Germany 91-127

Witholt B, Kessler B (1999) 'Perspectives of medium chain length poly(hydroxyalkanoates), a versatile set of bacterial bioplastics'. *Curr Opin Biotechnol* 10: 279-285

Yang YH, Brigham CJ, Budde CF, Boccazzi P, Willis LB, Hassan MA, Yusof ZAM, Rha C, Sinskey AJ (2010) 'Optimization of growth media components for polyhydroxyalkanoate (PHA) production from organic acids by *Ralstonia eutropha*' 87: 2037-2045

York GM, Lupberger J, Tian J, Lawrence AG, Stubbe J, Sinskey AJ (2003) *Ralstonia eutropha* H16 encodes two and possibly three intracellular poly[D-3-hydroxybutyrate] depolymerase genes. *J Bacteriol* 185:3788-3794

Zinn M, Witholt B, Egli T (2001) 'Occurrence, synthesis and medical application of bacterial polyhydroxyalkanoates'. *Adv Drug Deliv Rev* 53: 5-21

CHAPTER 10

Conclusions and future work

SUMMARY OF AIMS AND ACHIEVEMENTS

Two principal aims of this thesis work were to redirect the native *R. eutropha* carbon storage system into the production of biofuel and to generate value-added materials from common waste carbon sources.

Wild type *Ralstonia eutropha* H16 produces polyhydroxybutyrate (PHB) as an intracellular carbon storage material during nutrient stress in the presence of excess carbon. Chapter 2 described a system by which, the excess carbon was redirected in engineered strains from PHB storage to the production of isobutanol and 3-methyl-1-butanol (branched-chain higher alcohols). These branched-chain higher alcohols can directly substitute for fossil-based fuels and be employed within the current infrastructure. Various mutant strains of *R. eutropha* with isobutyraldehyde dehydrogenase activity, in combination with the overexpression of plasmid-borne, native branched-chain amino acid biosynthesis pathway genes and the overexpression of heterologous ketoisovalerate decarboxylase gene, were employed for the biosynthesis of isobutanol and 3-methyl-1-butanol. Production of these branched-chain alcohols was initiated during nitrogen or phosphorus limitation in the engineered *R. eutropha*. One mutant strain not only produced over 180 mg/L branched-chain alcohols in flask culture, but also was significantly more tolerant of isobutanol toxicity than wild type *R. eutropha*. After elimination of genes encoding three potential carbon sinks (*ilvE*, *bkdAB*, and *aceE*), the production titer improved to 270 mg/L isobutanol and 40 mg/L 3-methyl-1-butanol. Semi-continuous flask cultivation was utilized to minimize the toxicity caused by isobutanol while supplying cells with sufficient nutrients. Under this semi-continuous flask cultivation, the *R. eutropha* mutant grew and produced more than 14 g/L branched-chain alcohols over the duration of 50 days. These results demonstrate that *R. eutropha* carbon flux can be redirected from PHB to branched-chain alcohols and that engineered *R. eutropha* can be cultivated over prolonged periods of time for product biosynthesis.

Branched-chain alcohols hold great potential as the next generation drop-in fuel. Not only can they be produced from renewable resources, their energy contents are higher than bioethanol and are more compatible with the current fuel distribution infrastructure than bioethanol. Described in Chapter 2, *R. eutropha* has been engineered to produce branched-chain alcohols, mainly isobutanol and 3-methyl-1-butanol. Productivity in this engineered strain is very low, partially due to poor growth in flask batch culture conditions. In order to increase cell density and branched-chain alcohols production, batch, fed-batch, and two-stage fed-batch fermentation cultures were carried out in Chapter 3. Concentrations of nitrogen and carbon sources needed to reach both maximum growth and production were investigated. A maximum production of 380 g/L was observed when NH_4Cl initial concentration is at 2 g/L. A maximum cell dry weight of 36 g/L was reached with 10 g/L carbon source, using a strain of *R. eutropha* that is incapable of producing polyhydroxyalkanoate or branched-chain alcohols. Branched-chain alcohol production titer reached 790 mg/L with a yield of 0.03 g g^{-1} and a maximum productivity of 8.23 mg/L/h in a two-stage fed-batch culture system with pH-stat control.

Ketoisovalerate is an important cellular intermediate for the synthesis of branched-chain amino acids, as well as other important molecules, such as pantothenate, coenzyme A, and glucosinolate. This ketoacid can also serve as a precursor molecule for the production of biofuels, pharmaceutical agents, and flavor agents in engineered organisms, such as the betaproteobacterium *R. eutropha*. The biosynthesis of 2-ketoisovalerate from pyruvate is carried out by three enzymes: acetohydroxyacid synthase (AHAS, encoded by *ilvBH*), acetohydroxyacid isomeroreductase (AHAIR, encoded by *ilvC*), and dihydroxyacid dehydratase (DHAD, encoded by *ilvD*). In Chapter 4, enzymatic activities and kinetic parameters were determined for each of the three *R. eutropha* enzymes as heterologously-purified proteins. AHAS, which serves as a gate-keeper for the biosynthesis of all three branched-chain amino acids, demonstrated the tightest regulation through feedback inhibition by L-valine ($IC_{50} = 1.2$ mM), L-isoleucine ($IC_{50} = 2.3$ mM), and L-leucine ($IC_{50} = 5.4$ mM). Intermediates in the valine biosynthesis pathway also exhibit feedback-inhibitory control of the AHAS enzyme. In addition, AHAS has a very weak affinity for pyruvate ($K_M = 10.5$) and is highly selective towards 2-ketobutyrate ($R = 140$) as a second substrate. AHAIR and DHAD are also inhibited by the branched-chain amino acids, although to a lesser extent when compared to AHAS. Experimental evolution and rational site-directed mutagenesis revealed mutants of the regulatory subunit of AHAS (*IlvH*) (N11S, T34I, A36V, T104S, N11F, G14E, and N29H), which, when reconstituted with wild type *IlvB*, lead to AHAS having reduced valine, leucine, and isoleucine sensitivity. Study of the kinetics and inhibition mechanisms of *R. eutropha* AHAS, AHAIR, and DHAD has shed light on interactions between these enzymes and the products they produce; therefore can be used to engineer *R. eutropha* strains with optimal production of 2-ketoisovalerate for value-added materials.

Isobutanol, as the next generation drop-in biofuel, has attracted much attention from both academia and industry. *R. eutropha* is a Gram-negative bacterium that stores carbons and energy as polyhydroxyalkanoates (PHAs), and has been engineered to repurpose these carbon and energy sources from PHA to isobutanol. Similar to other microorganisms, *R. eutropha* experiences toxicity from branched-chain alcohols and is unable to grow in the presence of 0.2% (v/v) isobutanol. Such low tolerance greatly limited *R. eutropha*'s ability to grow and produce isobutanol as mentioned in Chapter 2 and Chapter 3. In order to decrease isobutanol toxicity to the cells, isobutanol-tolerant strains were developed via experimental evolution. Mutations were detected in *acrA6* and *acrA* of these evolved strains. The effect of in-frame deletion of each gene from wild type and engineered isobutanol-producing *R. eutropha* strains on the physiology of the cells were assessed in Chapter 5. The mutant strains' ability to tolerate, consume, and produce isobutanol were also analyzed. Although single or double deletions of *acrA6* and *acrA* did not significantly improve the growth of *R. eutropha* in the presence of isobutanol, single and double deletions improved cell survival in the presence of high concentration of isobutanol. Moreover, *acrA* deletion in engineered isobutanol-producing *R. eutropha* slightly enhanced the strain's ability to produce isobutanol.

Carbonic anhydrase (CA) enzymes catalyze the interconversion of CO_2 and bicarbonate. These enzymes play important roles in cellular metabolism, CO_2 transport, ion transport, and internal pH regulation. Chemolithotrophic organism *Ralstonia eutropha* H16 is capable of growing on CO_2 as its sole carbon source via the Calvin-Benson-Bassham cycle. Genome sequencing revealed four putative CA genes in *R. eutropha*. In Chapter 6, the importance of all four CAs: Can, Can2, Caa, and Cag were examined via growth and activity analysis of strains with individual and combinatorial CA gene deletion, complementation, and overexpression. All four CAs are capable of performing the interconversion of CO_2 and HCO_3^- , although the

equilibrium towards the formation of CO_2 or HCO_3^- differs for each individual CA. Can, a β -CA was characterized thus far and was found to be essential for *R. eutropha* growth in air. Adding CO_2 to the culture could compensate growth defect due to deletion of *can*. Deletion or overexpression of the *caa* gene, which encodes for an α -CA, had the strongest deleterious influence on cell growth. Both Can2 and Cag exhibited similar behavior and had no effect on growth when deleted or overexpressed. Caa was further studied in detail and was confirmed to be located in the periplasm. Its periplasmic localization was confirmed via microscopy with RFP-fused Caa and growth study in the absence of periplasmic signal sequence. Understanding the metabolic role of CA enzymes in the chemolithoautotrophic bacterium *R. eutropha* is important for the development of high performance fermentation processes on CO_2 .

Since the production of isobutanol has been greatly limited by the feedback inhibition and substrate specificity of the pathway enzymes, in addition to product toxicity, Chapter 7 described the production of another biofuel, isopropanol, utilizing precursors of the PHA biosynthesis pathway to bypass tightly controlled branched-chain amino acid pathway. Isopropanol has attracted research and industrial attention as a promising biofuel alternative to ethanol and biodiesel for the replacement of petroleum. Isopropanol can be produced through biological conversion of renewable waste carbon streams such as carbohydrates, fatty acids, or CO_2 . In this study, for the first time, the heterologous expression of engineered isopropanol pathways were demonstrated and evaluated in a *Ralstonia eutropha* strain Re2133, which was incapable of producing polyhydroxyalkanoate (PHA). The synthetic production pathways were rationally designed through codon optimization, gene placement, and gene dosage in order to efficiently divert carbon flow from PHA precursors towards isopropanol. Among the constructed pathways, Re2133/pEG7c overexpressing native *R. eutropha* genes encoding a β -ketothiolase, a CoA-transferase, and codon-optimized *Clostridium* genes encoding an acetoacetate decarboxylase and an alcohol dehydrogenase, produced up to 3.44 g/L isopropanol in batch culture, with only 0.82 g/L of biomass. The intrinsic performance of 0.093 $\text{g}\cdot\text{g}^{-1}\cdot\text{h}^{-1}$ maximum specific production rate and 0.32 $\text{Cmole}\cdot\text{Cmole}^{-1}$ yield corresponded to more than 60% of the respective theoretical performance. Moreover, the overall isopropanol production yield of 0.24 $\text{Cmole}\cdot\text{Cmole}^{-1}$ and the specific productivity of 0.044 $\text{g}\cdot\text{g}^{-1}\cdot\text{h}^{-1}$ were higher than values reported in the literature to date for heterologously engineered isopropanol production strains in batch cultures. Re2133/pEG7c presents good potential for scale up microbial production of isopropanol from various substrates in high cell density cultures.

Lipase enzymes catalyze the reversible hydrolysis of triacylglycerol to fatty acids and glycerol at the lipid-water interface. The metabolically versatile *Ralstonia eutropha* strain H16 is capable of utilizing various molecules containing long carbon chains such as plant oil, organic acids, or Tween as its sole carbon source for growth. Global gene expression analysis revealed an upregulation of two putative lipase genes during growth on trioleate. Through analysis of growth and activity using strains with gene deletion and complementation in Chapter 8, the extracellular lipase (encoded by the *lipA* gene, locus tag H16_A1322) and lipase-specific chaperone (encoded by the *lipB* gene, locus tag H16_A1323) produced by *R. eutropha* H16 was identified. Increase in gene dosage of *lipA* not only resulted in an increase of the extracellular lipase activity, but also reduced the lag phase during growth on palm oil. LipA is a non-specific lipase that can completely hydrolyze triacylglycerol into its corresponding free fatty acids and glycerol. Although LipA is active over a temperature range from 10 to 70°C, it exhibited optimal activity at 50°C. While *R. eutropha* H16 prefers a growth pH of 6.8, its extracellular lipase LipA is most active between pH 7 and 8. Cofactors are not required for lipase activity,

however EDTA and EGTA inhibited LipA activity by 83%. Metal ions Mg^{2+} , Ca^{2+} , and Mn^{2+} were found to stimulate LipA activity and relieve chelator inhibition. Certain detergents are found to improve solubility of the lipid substrate or increase lipase-lipid aggregation; as a result SDS and Triton X-100 were able to increase lipase activity by 20 to 500%. *R. eutropha* extracellular LipA activity can be hyper-increased, making the overexpression strain a potential candidate for commercial lipase production or in fermentations using plant oils as the sole carbon source.

Polyhydroxyalkanoates (PHAs) are biologically produced polyesters, which can consist of a diverse set of repeating unit structures. These biologically produced polyesters have many attractive properties and have been produced for use as bulk commodity plastics, fishing lines, and medical products. PHAs have also attracted much attention as biodegradable polymers that can be produced from biorenewable resources. Wild type *Ralstonia eutropha* is capable of producing polyhydroxybutyrate under nutrient stress high in carbon. When engineered, the cellular machinery can incorporate specific monomers into PHA polymers from different type of carbon sources, which could result in various tailored PHAs with interesting properties. In Chapter 9, waste carbon sources such as palm oil and vinasse were utilized for the production of PHAs in *R. eutropha*. Palm oil, the most abundant plant oil, consists mainly of triacylglycerol. In palm oil fermentation, wild type *R. eutropha* experiences a long lag phase due to limited availability of free fatty acids for cellular growth. To overcome this challenge, an extracellular lipase was overexpressed in *R. eutropha*, which accelerated the conversion of triacylglycerol into free fatty acids and reduced fermentation lag phase. Vinasse, a major byproduct of the ethanol industry, is a major environmental concern due to its acidic organic acids composition, which causes soil runoffs and ground water contaminations. For the first time, vinasse was analyzed for its carbon and nitrogen content, and formulated for *R. eutropha* growth and PHA production.

OPPORTUNITIES FOR FUTURE WORK

In silico pathway construction and cofactor balance

Engineered pathway decreases the overall fitness of the cells and subsequently production yield through unbalanced pathway precursors and reducing-cofactors (Dawes and Senior 1973). Stoichiometric modeling of *R. eutropha* metabolism (Grousseau et al. 2013) for the production of isobutanol was conducted using 54 reactions. Considering parameters such as carbon, energy, and coenzymes, the isobutanol production system was found to be limited in cofactor NADPH (data not shown). To improve the strain for the production of isobutanol using CO_2 as the carbon source, the production pathway could be engineered to utilize NADH-dependent enzymes instead of NADPH-dependent enzymes. In the current design, both acetohydroxyacid isomeroreductase (AHAIR) and alcohol dehydrogenase (ADH) are NADPH-specific, which causes major cofactor unbalance. Variant of AHAIR and ADH can be used to unbiased NADPH utilization.

Alternatively, a transhydrogenase, such as the *E. coli* pyridine nucleotide transhydrogenase (UdhA), can be expressed in the *R. eutropha* production strain to replenish the NADPH pool (Figure 10.1) (Sauer et al. 2004). UdhA was tested via overexpression of the enzyme to increase NADPH availability and PHA production in heterologous *E. coli* system. The increased intracellular NADPH concentration that resulted from UdhA overexpression allowed greater cofactor availability for the acetoacetyl-CoA dehydrogenase reaction, therefore

more PHA production (Sanchez et al. 2006). In most organisms, the redox cofactor NADPH is generated via the pentosephosphate pathway by glucose-6-phosphate dehydrogenase and 6-phosphogluconate dehydrogenase. Proteomic studies of *R. eutropha* revealed no active 6-phosphogluconate dehydrogenase under heterotrophic growth conditions, suggesting that *R. eutropha* synthesizes its cofactor NADPH from other pathway(s) during organoheterotrophic growth. One potential pathway involves the malic enzyme. The malic enzyme catalyzes the conversion of malate to pyruvate and is part of a metabolic cycle that also includes pyruvate carboxylase and malate dehydrogenase (Figure 10.1). An increase in transcription of the malic enzyme gene also upregulates the transcription of both pyruvate carboxylase and malate dehydrogenase (Sauer and Eikmanns 2005). Another enzyme, nonphosphorylating glyceraldehyde 3-phosphate dehydrogenase (GapN) bypasses 1,3-bisphospho-D-glycerate in Entner-Doudoroff pathway and generates an additional NADPH from NADH, at the expense of one ATP (Figure 10.1) (MacEachran and Sinskey 2013). In order to increase the intracellular NADPH pool, *udhA* and *gapN* can be heterologously expressed in *R. eutropha* or *maeA* could be overexpressed to increase isobutanol production.

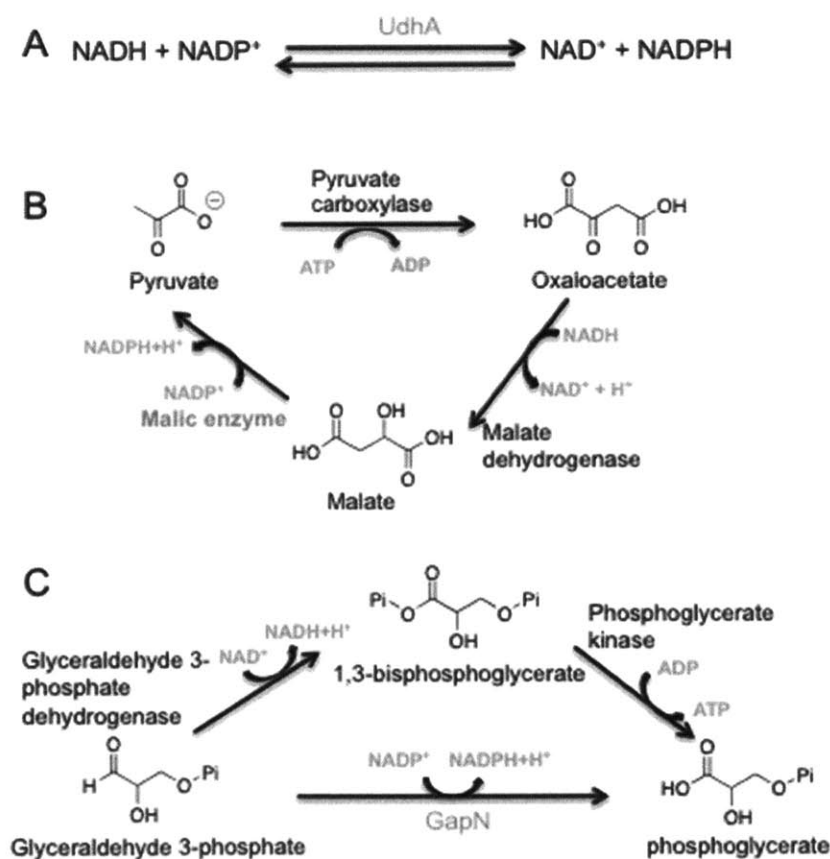


Figure 10.1: Schemes for alteration of NADH/NADPH pool sizes in *R. eutropha* isobutanol production strains. A) the use of soluble pyridine nucleotide transhydrogenase (UdhA) can directly perform transhydrogenation to increase NADPH pool levels. B) Malic enzyme (encoded by *maeA* and/or *maeB* in *R. eutropha*) can increase the NADPH pool at the expense of ATP. C) The nonphosphorylating glyceraldehyde-3-phosphate dehydrogenase (GapN) produces NADPH by conversion of glyceraldehyde-3-phosphate to phosphoglycerate.

Genes *udhA*, *maeA*, and *tadD* (*gapN* homolog) were separately cloned from *E. coli*, *R. eutropha*, and *Rhodococcus opacus* respectively into vector pBBR1MCS-2. Initial expression in *R. eutropha* wild type and Re2061 resulted in overall reduction of NADH level and increasing NADPH level (Figure 10.2). These cofactor-recycling systems could be further evaluated for isobutanol production.

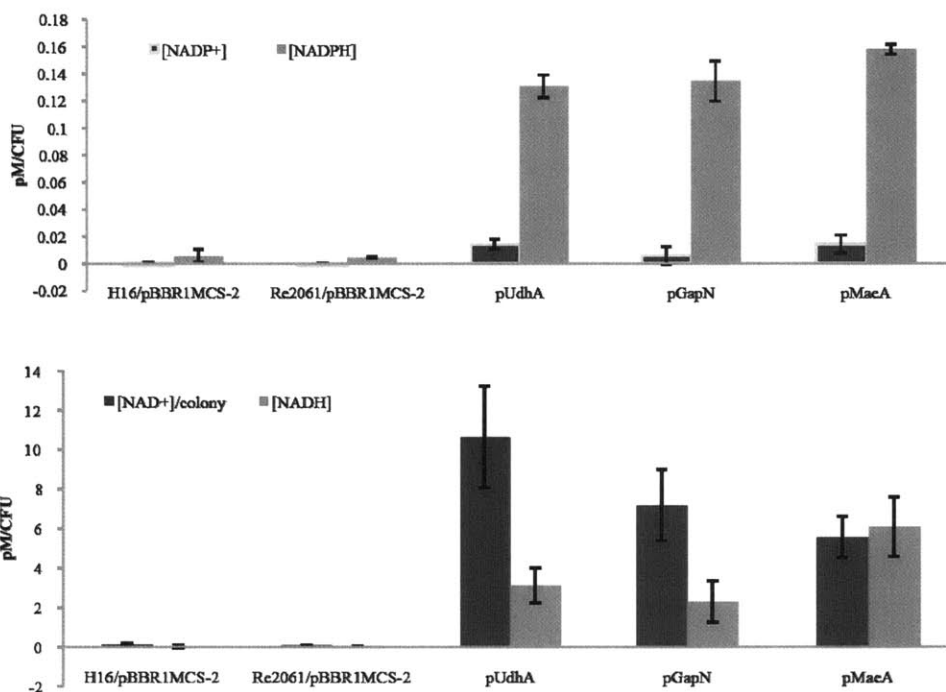


Figure 10.2: Concentration of NADP⁺, NADPH, NAD⁺, and NADH in pM per colony. The assay used for cofactor measurement was described in Chapter 2. Error bar represents standard deviation of n = 3.

Utilization of synthetic metabolons to improve substrate channeling

Metabolic conversion requires multiple complex reaction steps. Nature uses metabolic channeling, a process in which enzymes of the same pathway come together physically and forms a metabolon in order to efficiently transfer intermediates from one catalytic site to another. Such natural phenomenon has inspired engineers to bring biocatalysts together physically via covalent co-immobilization linkers, non-covalent encapsulations, or scaffolds (Schoffelen and Hest 2011). Isobutanol production enzymes can be linked together via amino acid linkers or deposited on scaffolds to increase efficiency, specificity, and regulation of this engineered metabolic pathway (Figure 10.3).

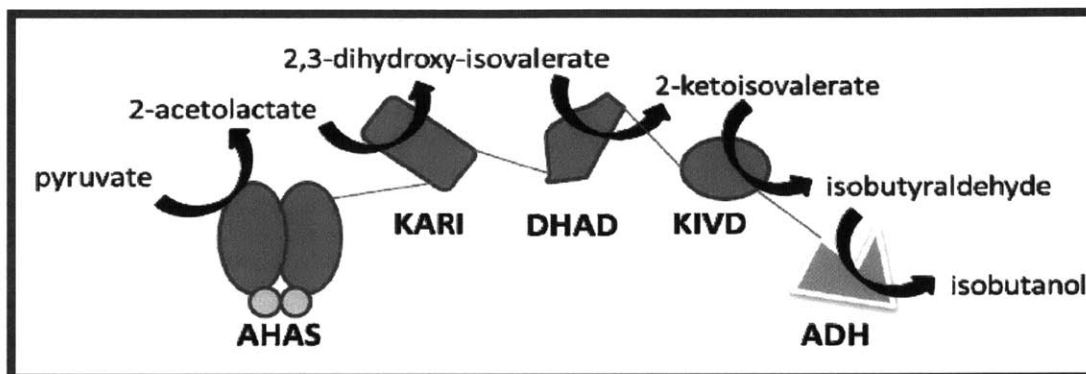
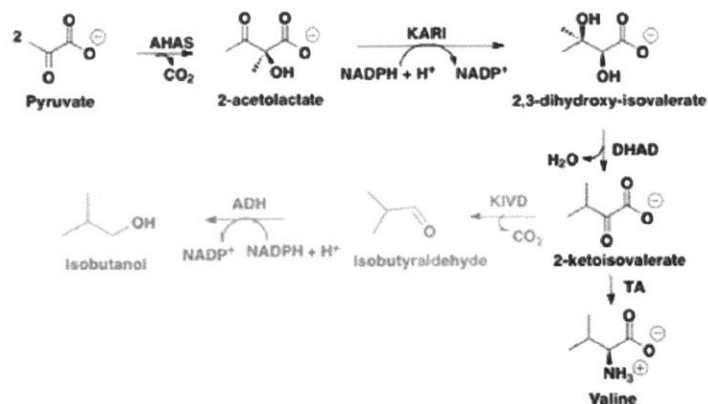


Figure 10.3: Life is crowded, so nature groups pathway enzymes in an assembly line, in order to increase substrate-channeling efficiency between enzymes. Isobutanol production enzymes can be linked together as depicted here to efficiently channel substrates between enzymes.

Establish an addiction system to eliminate antibiotic usage on plasmid-borne genes

Genetically engineered organisms often contain plasmids harboring production pathway genes. To ensure plasmid stability in the recombinant hosts, antibiotics are usually used. The use of antibiotics can be expensive in large fermentative processes. For these reasons, an additional system is often established to eliminate antibiotic usage while retaining plasmid stability. The plasmid addiction system functions in a way so the plasmid-free cells are killed or severely reduced in growth. A plasmid addiction system can be employed to eliminate antibiotic usage in the isobutanol and isopropanol production fermentation. Proline biosynthesis is essential for the survival of *R. eutropha*. Gene *proC*, encodes pyrroline-5-carboxylate reductase (ProC), was deleted from the *R. eutropha* chromosome. ProC catalyzes the last reduction step in proline biosynthesis. Since there is no other natural synthesis route to proline, without ProC the cells cannot survive (Budde et al. 2011). *R. eutropha* Δ *proC* strain constructed was unable to grow in minimal media without supplemented proline (Figure 10.4). Gene *proC* was then cloned and inserted upstream of the MCS (multiple-cloning site) in expression plasmid pBBR1MCS-2 (Figure 10.4). Even in the absence of antibiotic, *R. eutropha* Δ *proC* must retain the pBBR1MCS-2 with *proC* expression plasmid, thus genes in the isobutanol or isopropanol production pathway cloned in the MCS will be constitutively expressed during the entire fermentation.

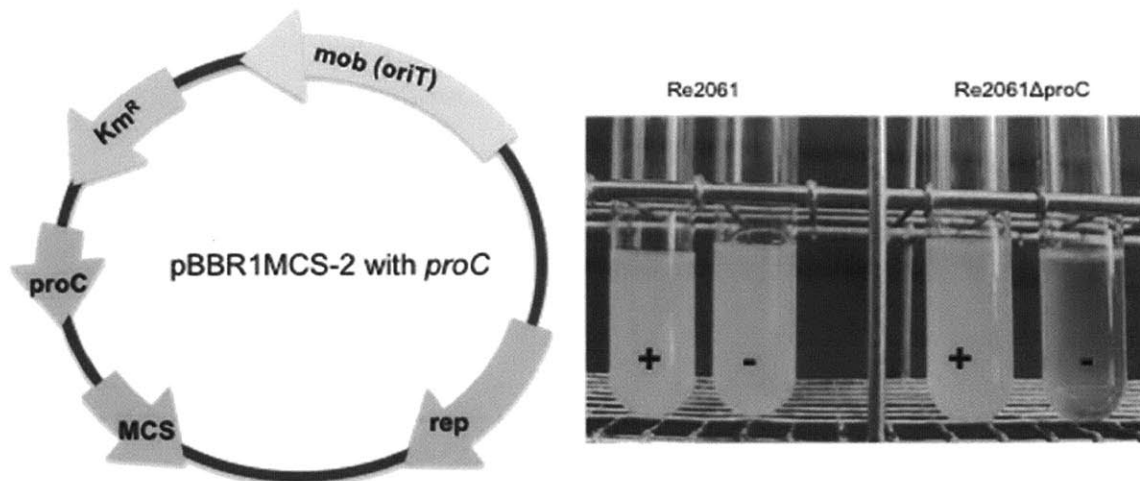


Figure 10.4: Expression plasmid addition system. Gene *proC* was cloned into expression plasmid pBBR1MCS-2 upstream of its MCS (left). *R. eutropha* Re2061 Δ *proC* growth in minimal media after 24 h. (+), addition of 0.3% proline; (-) minimal media without proline (right).

Overcoming the codon bias of *R. eutropha* for enhanced protein expression

Condon-usage bias is a phenomenon when synonymous codons are used with different frequencies and it is a defining characteristic of each genome. Codon biases vary dramatically between organisms. It is generally accepted that the speed at which ribosomes decode a codons depends on the cellular concentration of the tRNA that recognize it. Also, it is important to note that the most abundant codons correspond with the most abundant tRNAs, and vice versa. As a result, codon bias strongly correlates with gene expression levels in organisms (Behura and Severson 2012; Nakamura et al. 2000; Gustafsson et al. 2004; Plotkin and Kudla G 2011; Hershberg and Petrov 2008).

When heterologous genes are overexpressed in *R. eutropha*, differences in codon usage can impede translation due to the demand for one or more tRNAs that may be rare or lacking in the population. Consequently, the insufficient tRNAs pools can lead to translational stalling, premature translation termination, translation frame shifting, and amino acid misincorporation, which ultimately result in the depression of the target protein synthesis (Behura and Severson 2012; Nakamura et al. 2000; Gustafsson et al. 2004; Plotkin and Kudla G 2011; Hershberg and Petrov 2008). This is especially true when a gene encodes clusters of numerous rare *R. eutropha* codons. As stated in the case of isopropanol production in Chapter 7, codon bias was one of the major challenge and has limited the cell's production capability.

Among other possibilities to enhance the expression yield of protein are by assembling various combinations of rare tRNA gene to optimize the expression of genes isolated from organisms with genomes that have corresponding codon usage bias. These actually have been tested for example in the experiment to overcome the codon bias in *E. coli*. In this experiment, an overexpression plasmid encodes various rare tRNA genes. This system is reported to significantly enhance the expression of several genes derived from an AT-rich Plasmodium genome (Novy et al. 2001). Accordingly, this idea could be implemented to overcome the codon bias of *R. eutropha* for enhanced protein expression.

In order to improve the expression of heterologous proteins, the number of codons that are underrepresented in *R. eutropha* genome should be identified and overexpressed. As shown

in Figure 10.5, twenty underused triplet codons were identified in wild type *R. eutropha*. Of which, only 50% have identified tRNAs in the genome. There is a high probability that by elevating the cognate tRNA levels in *R. eutropha*, the expression yields of heterologous proteins whose genes contain rare codons can be remarkably improved.

Triplet	AA	Frequency	Usage	Triplet	AA	Frequency	Usage
UUA	Leu	0.3	0	CUU	Leu	4.9	0.05
CUA	Leu	1.2	0.01	GUU	Val	3.8	0.05
GUA	Val	3	0.04	ACU	Thr	2.3	0.05
UCA	Ser	1.9	0.04	GCU	Ala	6	0.05
ACA	Thr	2.1	0.04	AUA	Ile	0.8	0.02
AGA	Arg	0.7	0.01	UCU	Ser	1.4	0.03
AGG	Arg	2.7	0.04	AGU	Ser	1.8	0.03
GGA	Gly	3.8	0.04	CGA	Arg	2	0.03
CCA	Pro	3.2	0.06	CCU	Pro	3.2	0.06
AAA	Lys	2.9	0.1	UGU	Cys	0.9	0.09

Figure 10.5: Rare codons identified in wild type *R. eutropha*. Codons with identified tRNAs are shown on the left, while codons with unidentified tRNAs are presented on the right.

In order to elevate the tRNA levels, all rare tRNA gene copy number need to be increased. The rare codons with identified tRNAs were directly cloned and overexpressed from *R. eutropha* genome. The rare codons without any identified tRNA were engineered from existing tRNAs by single nucleotide mutagenesis at the triplet anticodon site of tRNA as depicted in Figure 10.6. Once all the tRNAs were cloned and linked together, the rare codon sequence can be either inserted into the expression vector or inserted in the genome of the host organism (Figure 10.7). Both systems could allow for enhanced expression of heterologous genes in *R. eutropha*, and subsequently increased production titer of desired compounds.

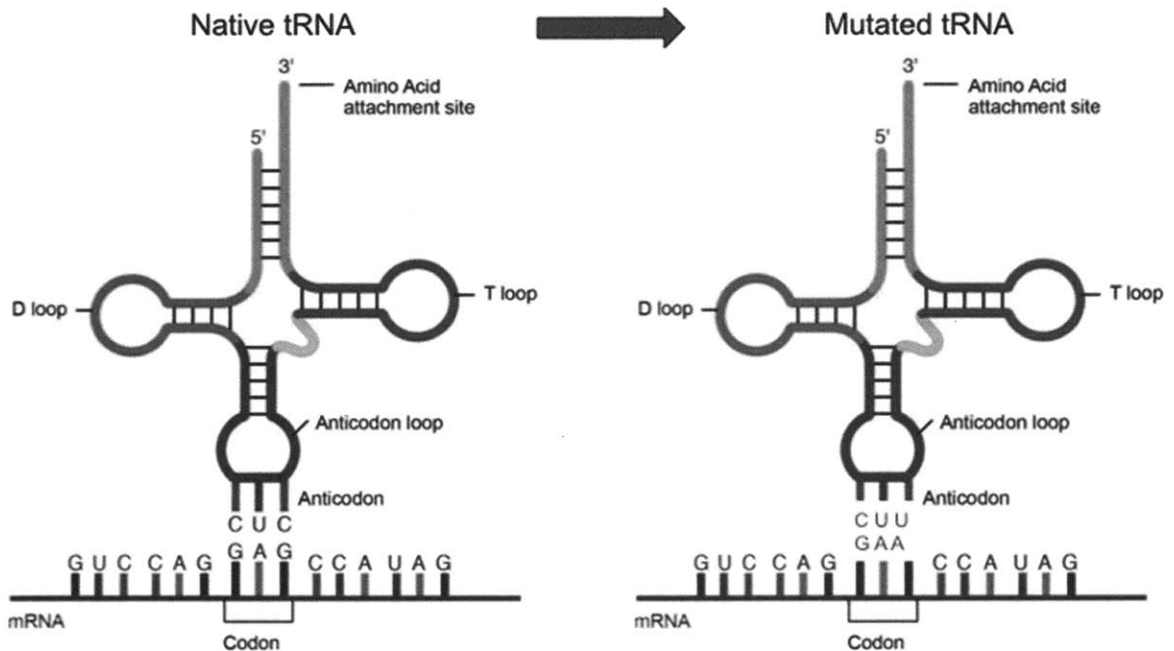
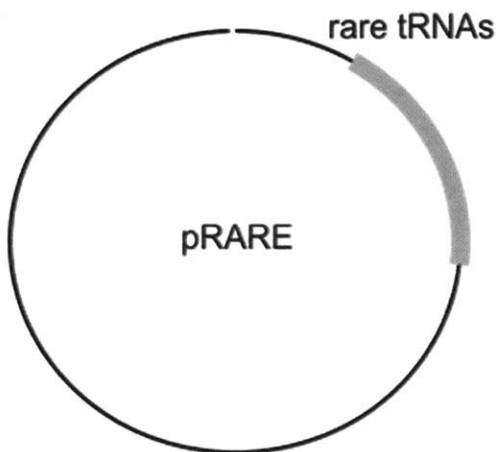


Figure 10.6: Site-directed mutagenesis on native tRNA for the making of rare tRNA that's absent from the *R. eutropha* genome.

Option 1:



Option 2:



Figure 10.7: The two possible usages of rare tRNA overexpression system. Option 1 depicts the utilization of rare tRNA on an overexpression plasmid. This system allows for a controlled tRNA expression at desired growth time period. Option two has rare tRNAs inserted in the genome of *R. eutropha* Re2061, under the constitutively expressed *phaC* promoter.

FINAL THOUGHTS

Two of the main concerns facing the world are fossil fuel shortages and increasing green house gas emissions. The current solution is supplementing gasoline with ~10% bioethanol. The production and utilization of bioethanol is nearly carbon neutral. CO₂ emitted from vehicles

was uptake by crops through carbon fixation, processed crops are used for bioethanol fermentation, bioethanol can then be used to run the vehicles. Bioethanol production, however, is not sustainable. It competes with the food source and is not compatible with the car engines and the current gasoline distribution infrastructures. Mostly importantly, its production byproduct vinasse has lead to soil runoffs and ground water contaminations. In this thesis, several solutions were implemented to overcome these challenges.

R. eutropha, a soil bacterium with a tendency to store carbon in the form of complex polyesters was engineered to convert CO₂ into biofuels, specifically isobutanol and isopropanol. Isobutanol or isopropanol is >15% more energy efficient than bioethanol, and can be directly substituted for or blended with, gasoline. Unlike biofuel production in algae, isobutanol and isopropanol produced in engineered *R. eutropha* are directly secreted and isolated via distillation, allowing these engineered bacteria systems to grow continuously for a long period of time while producing biofuels.

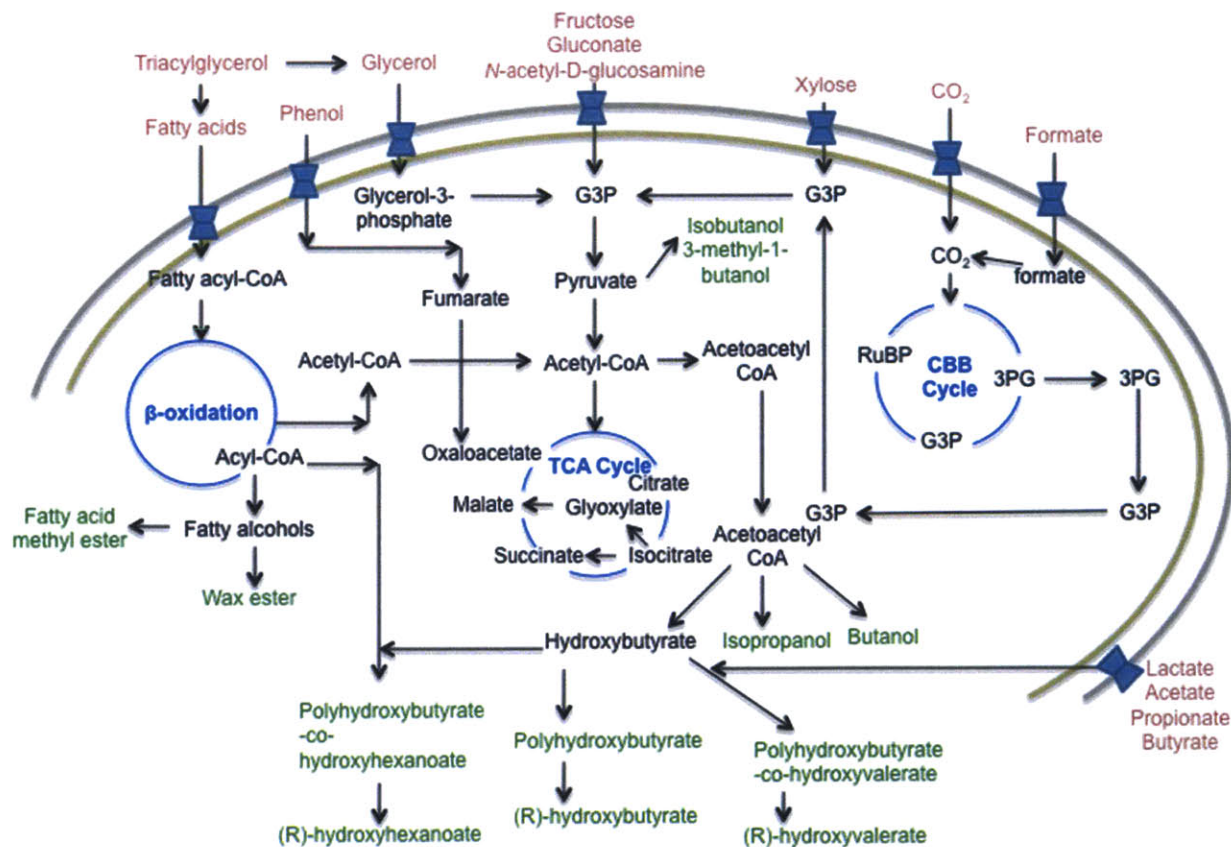


Figure 10.8: Schematic demonstrating *R. eutropha*'s metabolic versatility and its ability to produce value-added materials.

The common industrial waste products, palm oil and vinasse, were assessed and utilized for bioplastic production in engineered *R. eutropha*. These bioplastics can be engineered with various properties and can be converted into commodity plastics for everyday use, thus could eliminate or reduce fossil-based plastics. Utilizing the genetically tractable and metabolically versatile bacterium *R. eutropha* for the production of value-added materials from common waste

carbon sources has the potential to affect the two high-priority environmental concerns.

Studies of *R. eutropha* metabolic processes have demonstrated that it is a model microbial factory. Specifically, *R. eutropha* is very versatile in the metabolic processes that it can run. Taking advantage of the organism's ability to move large quantities of carbon for PHA biosynthesis, metabolism can be rerouted to produce a variety of useful bio-based commodity products. Figure 10.8 gives an overview of the many production pathways that were demonstrated in wild type and engineered *R. eutropha* strains. Undoubtedly, more useful pathways remain to be constructed and streamlined in *R. eutropha*.

Much of the focus in *R. eutropha* bioengineering has been on optimizing the yields and productivities of compounds the organism can synthesize. Future directions include optimization of utilization and conversion of different carbon sources to be used in the synthesis of value-added products. This aspect of cellular metabolism is especially critical given the role of *R. eutropha* as a bioremediator and the trend towards usage of unrefined, waste carbon as feedstock for production of value-added compounds. As much of the metabolic potential of *R. eutropha* is untapped, there may be no limit in sight of which natural products can be synthesized and subsequently marketed.

REFERENCES

- Behura SK, Severson DW (2012) Codon usage bias: causative factors, quantification methods and genome-wide patterns: with emphasis on insect genomes. *Biol Rev Camb Philos* 88(1):49–61
- Budde C, Riedel S, Willis L, Rha C, Sinskey AJ (2011) Production of poly(3-hydroxybutyrate-co-3-hydroxyhexanoate) from plant oil with engineered *Ralstonia eutropha*. *App Environ Microbiol* 77: 2847-2854
- Dawes EA, Senior PJ (1973) The role and regulation of energy reserve polymers in microorganisms. *Adv Microb Physiol* 10: 135-266
- Grousseau E, Blanchet E, Deleris S, Albuquerque MGE, Paul E, Uribelarrea JL (2013) Impact of sustaining a controlled residual growth on polyhydroxybutyrate yield and production kinetics in *Cupriavidus necator*. *Bioresour Technol* 148: 30-38
- Gustafsson C, Govindarajan S, Minshull J (2004) Codon bias and heterologous protein expression. *Trends in Biotechnol* 22: 346-353
- Hershberg R, Petrov DA (2008) Selection on Codon Bias. *Annual Review of Genetics* 42: 287-299
- MacEachran DP, Sinskey AJ (2013) The *Rhodococcus opacus* TadD protein mediates triacylglycerol metabolism by regulating intracellular NAD(P)H pools. *Microbial Cell Fact* 12: 104-116
- Nakamura Y, Gojobori T, Ikemura T (2000) Codon usage tabulated from international DNA sequence databases: status for the year 2000. *Nucleic Acids Res* 28(1): 292-304
- Novy R, Drott D, Yaeger K, Mierendorf R, Novagen, Inc. (2001) Overcoming the codon bias of *E. coli* for enhanced protein expression. In *Novations* June: 12
- Plotkin JB, Kudla G (2011) Synonymous but not the same: the causes and consequences of codon bias. *Nature Review Genetics* 12: 32-42
- Sauer U, Canonaco F, Heri S, Perrenoud A, Fischer E (2004) The soluble and membrane-bound transhydrogenases UdhA and PntAB have divergent functions in NADPH metabolism of *Escherichia coli*. *J Biol Chem* 279: 6613-6619
- Sauer U, Eikmanns BJ (2005) The PEP-pyruvate-oxaloacetate node as the switch point for carbon flux distribution in bacteria. *FEMS Microbiol Rev* 29: 765-794
- Sanchez AM, Andrews J, Hussein I, Bennett GN, San KY (2006) Effect of overexpression of a soluble pyridine nucleotide transhydrogenase (UdhA) on the production of poly(3-hydroxybutyrate) in *Escherichia coli*. *Biotechnol Prog* 22: 420-425
- Schoffelen S, van Hest JCM (2012) Multi-enzyme systems: bringing enzymes together *in vitro*. *Soft Matter* 8: 1736-1746

CURRICULUM VITAE

Jingnan Lu

229 Vassar St, Cambridge MA 02139
(315) 383-9156 jlu5189@mit.edu

EDUCATION

Massachusetts Institute of Technology, Cambridge MA- GPA: 4.6/5.0 **September 2014**
Ph.D. Candidate in Biological Chemistry Thesis Advisors: Anthony Sinskey

Relevant courses: Strategic Decision Making in Life Sciences; Case Studies and Strategies in Drug Discovery and Development; Principles and Practice of Drug Development, Enzymology, Human Biochemistry & Metabolic Diseases; Protein Folding & Human Diseases; Case Studies in Biomedical Engineering

State University of New York in association with Syracuse University, Syracuse NY-GPA: 4.0 (major) 3.8
(overall)/4 **May 2009**
B.Sc. in Chemistry Upper Division Honor Thesis Advisor: Christopher Nomura

PROFESSIONAL EXPERIENCE

Student Consultant, Consulting Club at MIT **2012-2014**

- Analyzed the market size for the treatment of Duchene Muscular Dystrophy; examined 60+ drug candidates, created and pitched a \$100M investment portfolio based on scientific performance, correlation between drugs, NPV, and IRR assessments. As a result, the client (private equity firm) was able to receive several rounds of investments to pursue this portfolio.
- Surveyed the market of bioenergy production and storage products; analyzed and compared the client's new technologies based on LCOE and competitive landscape; created a market entry strategy. Based on the recommendations, the client entered the bioenergy market and received over \$10M in funding.

Residential Assistant, MIT Undergraduate Dorm **2012-2014**

- 24/7 support for the undergraduate community, hosted programs to enrich the living environment

Mediator, MIT Resources to Ease Friction and Stress **2012-2014**

- Offering confidential consultations of difficult conversations, people, and conflicts

Technology Specialist Intern, Fish & Richardson P.C. **2013**

- Drafted patents for pharmaceutical companies and prepared amendments to the patent office

Head Teaching Assistant, MIT Biochemistry I & II **2009-2013**

- Created recitation materials, supported other TAs, and taught 150+ undergraduate students

LEADERSHIP EXPERIENCE

Vice President/Advisor, Consulting Club at MIT **2012-2014**

- Organized and lead biweekly discussions on business news, manage internal relations

Engagement Manager, Consulting Club at MIT **2013**

- Brought in new clients for the club and engaged in client relations
- Mentored and supported a team of 7 Ph.D. students on an industry analysis and product acquisition case

President, Women in Chemistry, MIT **2012-2013**

- Hosted professional development, social, and networking events to encourage, promote, recognize and advocate for female chemists in the Boston area

Graduate Student Representative, MIT Subject Evaluation Committee **2012-2013**

- Drafted and launched a new subject evaluation survey for all 30 MIT departments and programs

PUBLICATIONS (Articles, Book chapters, & Patent)

Jingnan Lu, Christopher Brigham, Sophia Li, Anthony Sinskey (2015) 'Chapter 12: *Ralstonia eutropha* as a platform for the production of biofuels, biodegradable plastics, and fine chemicals from diverse carbon sources' *Biotechnologies for Biofuel Production and Optimization*. Submitted

Jingnan Lu, Christopher Brigham, Jens Plassmeier, Anthony Sinskey (2014) 'Characterization and modification of enzymes in the 2-ketoisovalerate biosynthesis pathway of *Ralstonia eutropha* H16' Applied Microbiology and Biotechnology, accepted for publication

Estelle Grousseau, **Jingnan Lu**, Nathalie Gorret, Stephan Guillouet, Anthony Sinskey (2014) 'Isopropanol production with engineered *Cupriavidus necator* as bioproduction platform' Applied Microbiology and Biotechnology 98: 4277-4290

Claudia Gai, **Jingnan Lu**, Christopher Brigham, Amanda Bernardi, Anthony Sinskey (2013) 'Insights into bacterial carbon dioxide metabolism revealed by the characterization of four carbonic anhydrases in *Ralstonia eutropha* H16' Applied Microbiology and Biotechnology Express

Sebastian Riedel, **Jingnan Lu**, Christopher Brigham (2013) 'Lipid and fatty acid metabolism in *Ralstonia eutropha*: relevance for the biotechnological production of value added products' Applied Microbiology and Biotechnology

Qiang Fei, Christopher Brigham, **Jingnan Lu**, Rongzhan Fu, Anthony Sinskey (2013) 'Production of branched-chain alcohols by recombinant *Ralstonia eutropha* in fed-batch cultivation' Biomass and Bioenergy 56: 334-341

Jingnan Lu, Christopher Brigham, ChoKyun Rha, Anthony Sinskey (2013) 'Characterization of an Extracellular Lipase and its Chaperone from *Ralstonia eutropha* H16' Applied Microbiology and Biotechnology

Jingnan Lu, Christopher Brigham, Claudia Gai, Anthony Sinskey (2012) 'Studies on the production of branched-chain alcohols in engineered *Ralstonia eutropha*' Applied Microbiology and Biotechnology 96: 283-297

Christopher Brigham, Claudia Gai, **Jingnan Lu**, Daan Speth, Mark Worden, Anthony Sinskey (2012) 'Chapter 38: Engineering *Ralstonia eutropha* for the Production of Isobutanol Motor Fuel from CO₂, H₂, and O₂' Advance Biofuels and Bioproducts. Springer: ISBN 978-1-4614-3347-7

Charles Budde, Alison Mahan, **Jingnan Lu**, ChoKyun Rha, Anthony Sinskey (2010) 'The Roles of Multiple Acetoacetyl-CoA Reductases in Polyhydroxybutrate Biosynthesis in *Ralstonia eutropha* H16' Journal of Bacteriology, 192: 5319- 5328

Jingnan Lu, Ryan Tapple, Christopher Nomura (2009) 'Mini-Review: Biosynthesis of Poly(hydroxyalkanoate)' Polymer Reviews, 29: 226-248

Christopher Nomura, **Jingnan Lu** (2009) 'Hydrophobic Compound Capture-Apparatus Made From Biodegradable Polymers and Methods Based Thereon' U.S. Patent Application US2010/0041159A1

SKILLS

Languages: fluent in English and Mandarin Chinese

Research: molecular biology, protein characterization, enzymatic assay, small molecule synthesis, analytical analysis, microbial cell culture, bioinformatics

Certificate: Harvard TIPS; MIT Mediation Certificate; MIT Graduate Student Teaching Certificate; MIT Teaching Assistant Certificate; Level One Tutoring Certificate

FELLOWSHIP and AWARDS

- MIT Graduate Women of Excellence-group and individual awards (2013)
- Best of MIT News (2012)
- NIH Chemical Biology Interface Fellowship (2009)
- MIT Chapin Fellowship (2009)
- Chancellor's Award for Student Excellence (2009)
- John A. Meyer Award for Environmental Chemistry (2007-2008)
- Chemistry Citizen's Award (2006-2007)
- University Foundation Award (2005-2009)